Interaction of Silver Nanoparticles and Silver Ions with Soil, Plant and Earthworm *Aporrectodea caliginosa*

A dissertation
submitted in partial fulfilment
of the requirements for the Degree of
Doctor of Philosophy

at
Lincoln University
by
Nadir Saleeb

Lincoln University
2019

Abstract of a thesis submitted in partial fulfilment of the
requirements for the Degree of Doctor of Philosophy

Interaction of Silver Nanoparticles and Silver Nitrate with Soil, Plant and Earthworm *Aporrectodea caliginosa*

by
Nadir Saleeb

Silver nanoparticles (AgNPs) are frequently synthesised for use in consumer products and appliances because of their antimicrobial properties and ease of incorporation into plastics, industrial materials and solutions. Currently, there are no regulations for the use of AgNPs in consumer products or their disposal. Therefore, there is a need to evaluate the impact of AgNPs in the environment. Because of their chemistry and slow dissociation to reactive Ag ions (Ag^+) over time, AgNPs have been shown in both prokaryote and eukaryote models to be cytotoxic. Ionic Ag could bio-accumulate in the environment, thereby causing toxic effects on soil microbes and other organisms, plants, and animals.

This thesis examined (1) the mobility of AgNPs and Ag^+ (as silver nitrate, $AgNO_3$) in soil and (2) the uptake of Ag by various plants. In particular, it evaluated (3) the chronic toxic effects on sunflower plants, and (4) the acute and chronic toxic effects on *Aporrectodea caliginosa* earthworms.

In the soil mobility study, at a specific pH, the K_D value (distribution of Ag between solid and solution phases) for AgNPs was 10-fold higher than for Ag^+, indicating that Ag+ is more mobile and more toxic than AgNPs. This could be due to saturation of binding sites in soil. K_D increased at higher pHs because of increased sorption to variable charged surfaces in soil. In soil incubation studies conducted at 20°C and 35°C, the solubility of AgNPs/Ag^+ was greater at the higher soil temperature. The sorption of AgNPs to soil decreased over time, because all AgNPs were transformed into Ag^+ due to degradation over time.

Plant uptake of Ag in different parts (root cf. shoot) of perennial ryegrass (*Lolium perenne* L.) grown in soil amended with different concentrations (ranging from 0.0019% to 1%) of AgNPs and Ag+ indicated that Ag^+ was 10-fold more soluble than AgNPs. Soil pH had a significant effect on sorption of AgNPs/Ag^+ by plants, with sorption increasing with increased pH. Exposure of ryegrass to various

AgNPs/Ag$^+$ concentrations showed that concentrations < 10 mg/kg (dry matter) had a stimulatory effect on plant growth but >200 mg/kg of AgNPs/Ag$^+$ reduced plant growth.

In an Ag uptake study of nine vegetables (spinach, parsley, radish, lettuce, rocket, carrot, silver beet, leek, beetroot) grown in Templeton Silt Loam soil amended with 70 mg/kg AgNPs/Ag+, Ag uptake by control plants from naturally present Ag in soil was low (0.5 mg/kg) compared to a 3.5 to 3.8 mg/kg concentration in plants grown in soils spiked with AgNPs/Ag$^+$ respectively. The highest concentration factor (5–9) occurred in carrot, silverbeet and spinach.

A more detailed study on Ag concentrations in sunflower following 53-days' exposure to soil amended with 150 mg/kg AgNPs/Ag$^+$ showed that Ag accumulated in the roots > leaves. In the sunflower, Ag$^+$ > AgNPs increased the activity of the antioxidant enzymes superoxide dismutase (SOD), catalase (CAT), glutathione peroxidase (GPx) and glutathione S-transferase (GST) in a dose- and time dependent manner and also increased the lipid peroxides, ascorbate oxidase, pyrogallol peroxidase and guaiacol peroxidase. Total carotenoids were lower only in the plants exposed to Ag+. Chlorophyll A but not chlorophyll B was significantly inhibited ($P<0.05$) in plants exposed to AgNP/Ag+. Total protein and total soluble carbohydrate significantly declined in sunflower exposed to the two Ag compounds, but the total phenolic compounds, urease enzyme activity and vitamins A, E and C were increased.

The LD_{50} of AgNPs and Ag+ on earthworms was determined as 2,649 and 305 mg/kg soil respectively (unpublished data). A short-term (24 and 48 h) filter paper study and a more extensive long-term (4-week) soil sub-chronic toxicity study in earthworms on the effects of AgNPs and Ag+ showed a dose- and time-dependent enhancement of lipid peroxidation, and several-fold increase in the activities of a range of antioxidant enzymes (including SOD, CAT, GPx and GST), with Ag+ more toxic than AgNPs. A study comparing the toxicity of AgNPs and Ag+ to earthworms by measuring pharmacokinetic parameters showed that when exposed to soil amended with 20 mg/kg AgNPs/Ag$^+$, Ag+ was more toxic than AgNP as shown by terminal half-life, mean residence time, area under the curve, maximum concentration, bio-concentration factor, and the rate of elimination. Thus, Ag+ > AgNPs caused dose- and time-dependent growth inhibition and oxidative stress in both *A. caliginosa* earthworms and plants, with resultant increases in lipid peroxidation and antioxidant enzymes.

In conclusion, this study of AgNPs and Ag$^+$ effects on Ag mobility in soil, accumulation of Ag in nine vegetable types, and effects on two plants (sunflower, ryegrass) and an earthworm (*A. caliginosa*) showed accumulation of Ag, increased lipid peroxidation, and elevation of antioxidant enzyme (CAT, SOD, GPx, GST) activities, in addition to changes in a series of other parameters in sunflower and ryegrass that correlated with their adverse effects. The multi-level effect approach adopted in this study, including an earthworm pharmacokinetic study, provided a better understanding of the potential risk of AgNPs to non-target plants and earthworms, although Ag+ proved to be more toxic than AgNPs. This study shows that evaluating several lower tier biomarkers offered a meaningful and an informative assessment of potential effects of AgNPs on plants and earthworms.

Keywords: AgNPs, Ag+, toxicity, soil, plant, sunflower, earthworms, *A. caliginosa*, Ag distribution in plant, chlorophyll, total soluble protein, total soluble carbohydrates, total phenolic compounds, antioxidant enzymes,antioxidant vitamins, AgNPs mobility, K_D value, incubation, vegetables trace element.

Acknowledgements

It is a great honour to thank my main supervisor, Professor Ravi Gooneratne, for his valuable advice and continuous support throughout my PhD programme. During this period Prof. Ravi was more than a supervisor to me, always advising me, and suggesting valuable solutions to any problems I faced in my practical work. Because of his interest in my PhD research and his extraordinary patience to read and correct my writing, I was able to finish my PhD study. I will remain forever grateful to him.

My deep respect and appreciation go to Professor Brett Robinson, my co supervisor, for his design and planning of the experiments concerning the effect of AgNPs on plants and their mobility in soil. His analytical advice and follow-up of the results of the plant work taught me to solve some analytical problems I faced during laboratory work.

I also thank my associate co-supervisor, Dr Jo Cavanagh from Manaaki Whenua Landcare Research, for her funding a part of my PhD project and for her valuable scientific opinions.

My thanks are extended to Associate Professor Craig Bunt for his help in determining silver nanoparticle size and for his support in the pharmacokinetics work.

I would like to express my deep thanks to Dr James Ross for his explanations and guidance on how to use different statistical programmes.

I thank Mr Martin Welby for his assistance in my practical work by supporting me with items I required ranging from chemicals, scientific instruments, to soil and earthworms. I also like to thank Dr Kiran Munir who helped me with an experiment during a short period I was ill.

For Mr Karl Gately, I would like to express my deep respect and appreciation for his strong help and for supplying the chemical supplies that I required from the laboratories.

My earnest thanks to the analytical service team in Burns building at Lincoln University, especially Roger Cresswell, for his help and support when I needed it. Special thanks to Lynne Clucas and Lean Hassell for helping me in stores and analysing samples in the lab, which helped this research succeed. Thanks to Lynne Clucas for analysing my samples by ICP-OES in a short time.

My thanks and appreciation to my friend Mr A K M Mofasser Hossain for his help and discussion about the problems I faced during the preparation of this dissertation.

Finally, my deep thanks to my dear colleague Mrs Abby Bate for her advice and guidance at the beginning of my research work.

Declaration

Some aspects of this thesis have been submitted for publication in refereed international journals and or in final stages of preparation for publication.

● Manuscripts submitted:

1- Mobility of silver nanoparticles and silver ions in the soil- plant system. *Journal of Environmental Quality*.
2- Toxicity of silver nanoparticles and silver ions to sunflower plant (*Helianthus annuus* L.). *SDRP Journal of Food Science & Technology.*
3- Comparative Pharmacokinetics analysis of silver in earthworm Aporrectodea caliginosa exposed to AgNPs and Ag+. *Journal of Environmental Modeling & Assessment*.

● Manuscripts in preparation:

1- Antioxidant enzyme activity and lipid peroxidation in *Aporrectodea caliginosa* earthworms exposed to AgNPs and Ag^+. *Environmental Chemistry and Toxicology.*
2- Silver accumulation in different parts of sunflower (*Helianthus annuus L.*). *Plant, Cell and Environment.*

● Oral Presentations:

1. Biochemical toxicity studies in earthworm *Aporrectodea caliginosa*, exposed to AgNPs / $AgNO_3$. Thesis proposal presentation, Lincoln University, Lincoln, 14 August.

2. Interaction of AgNPs/AgNO3 with soil, plant and earthworm *A. caliginosa* in contaminated soil (2016). Lincoln University Postgraduate Conference, Lincoln, 24 August.

3. Biochemical- & neuro- toxicity of silver nanoparticle and silver nitrate in soil to *Aporrectodea calginosa* earthworms (2017). Presented at the Congress of the European Societies of Toxicology, Bratislava, Slovakia, 10 September.

Table of Contents

Abstract ii

Acknowledgements v

Declaration..vi

Table of Contents vii

List of Tables xiii

List of Figures xiiiv

[redacted] **Chapter 1 Introduction** 1

1.1 Background 1

1.2 Research aims 2

1.3 Objectives 3

1.4 Hypotheses 3

[redacted] **Chapter 2 Literature Review** 4

2.1 Nanoparticles..4

2.2 Naturally occurring nanoparticles..4

2.3 Silver nanoparticles..5
  2.3.1 Synthesis of AgNPs..5
  2.3.2 Silver nanoparticle properties..6
  2.3.3 Silver nanoparticle characterisation 7

2.4 Mobility and fate of silver nanoparticles in soil..8

2.5 Sorption of AgNPs and Ag+ by soils at different pHs 9

2.6 Chemical speciation of silver nanoparticles..9

2.7 Toxicity of silver nanoparticles in terrestrial ecosystems.. 11

2.8 Earthworms – *Aporrectodea caliginosa* (*A. caliginosa*) 12

2.9 Toxicity of silver nanoparticles to aquatic ecosystems.. 13

2.10 Tolerance and uptake of AgNPs and Ag+ by plants 14
  2.10.1 Effect of heavy metals on sunflower 16

2.11 Antioxidant enzymes.. 17

[redacted] **Chapter 3 Materials and Methods** 19

3.1 Synthesis of silver nanoparticles.. 19

3.2 Quantitation of synthesised silver nanoparticles 19

3.3 Morphology of synthesised AgNPs 20

3.4 Charge and particle size of AgNPs (using zetasizer).. 20

3.5 Soil parameters 21
  3.5.1 Soil pH measurement..21
  3.5.2 Determination of soil chloride concentration..21
  3.5.3 Determination of soil carbon and nitrogen concentrations 22
  3.5.4 Determination of soil moisture content 22
  3.5.5 Determination of field capacity 22

3.6 Sample preparation for ICP-OES analysis 23
  3.6.1 Plant material..23

3.6.2 ICP-OES analysis 23
3.7 Determination of some physical properties of synthesised AgNPs 23

[redacted] **Chapter 4 Mobility of Silver Nanoparticles and Silver Ions in the Soil–Plant System .24**
4.1 Abstract 24
4.2 Introduction 24
4.3 Materials and methods 26
4.3.1 Soils 26
4.3.2 Nanoparticle preparation and zeta potential 26
4.3.3 Preliminary experiments to determine the optimal extraction method 26
4.3.4 Ag sorption as a function of concentration and pH 27
4.3.5 Extractable Ag in incubated soils 27
4.3.6 Response of *Lolium perenne* to Ag$^+$ and AgNPs 27
4.3.7 Uptake of Ag$^+$ and AgNPs by a selection of vegetables 28
4.3.8 Chemical analyses 28
4.4 Data analysis 29
4.5 Results and discussion 29
4.6 Conclusions 36
4.7 Supplementary data 36

[redacted] **Chapter 5 Silver Accumulation in Different Parts of Sunflower (*Helianthus annuus L.*) 37**
5.1 Abstract 37
5.2 Introduction 37
5.3 Materials and methods 39
5.3.1 Preparation of AgNPs 39
5.3.2 Soil 39
5.3.3 Experimental design 39
5.3.4 Other analyses 40
5.4 Statistical analysis 40
5.5 Results 40
5.6 Discussion 47
5.6.1 Effect of Ag on macro- and micro-nutrients 48
5.7 Conclusion 49

[redacted] **Chapter 6 Toxicity of Silver Nanoparticles / Silver Ions to Sunflower 50**
6.1 Abstract 50
6.2 Introduction 50
6.3 Materials and methods 52
6.3.1 Silver nanoparticles synthesis and quantification 52
6.3.2 Charge measurement and particle size using zetasizer 52
6.3.3 Experimental design 52
6.3.4 Chemicals and reagents 52
6.3.5 Soil pH 52
6.3.6 Soil total carbon and nitrogen 52
6.3.7 Soil chloride and moisture content in soil 52
6.3.8 Soil field capacity measurement 52
6.3.9 Sunflower leaf homogenisation 53
6.3.10 Leaf preparation to measure antioxidant enzymes 53

6.4 Statistical analysis 57

6.5 Results 57
    6.5.1 Catalase 57
    6.5.2 Superoxide dismutase 58
    6.5.3 Glutathione-S-transferase 58
    6.5.4 Glutathione peroxidase 59
    6.5.5 Lipid peroxidation 59
    6.5.6 Ascorbate oxidase 60
    6.5.7 Pyrogallol peroxidase 60
    6.5.8 Guaiacol peroxidase 61
    6.5.9 Chlorophyll A and B and total carotenoids 61
    6.5.10 Total soluble protein 62
    6.5.11 Total phenolic compounds 63
    6.5.12 Total soluble carbohydrates 63
    6.5.13 Urease 64
    6.5.14 Vitamins A and E 64
    6.5.15 Vitamin C 65

6.6 Discussion 65
    6.6.1 Antioxidant enzymes 65
    6.6.2 Lipid peroxidation (LPO) or thiobarbituric acid reactive species (TBARS) 68
    6.6.3 Chlorophyll and total carotenoids 69
    6.6.4 Total soluble protein 70
    6.6.5 Total phenolic compounds 71
    6.6.6 Total soluble carbohydrates 71
    6.6.7 Urease 72
    6.6.8 Vitamins A, E and C 72

6.7 Conclusions 73

[redacted] **Chapter 7 Biochemical Toxicity of Silver Nanoparticles and Ag^+ (as $AgNO_3$) to *Aporrectodea caliginosa Earthworm,* Using Filter Paper as a Matrix 74**

7.1 Abstract 74

7.2 Introduction 74

7.3 Materials and methods 75
    7.3.1 Chemicals and reagents 75
    7.3.2 Experiments 75

7.4 Statistical analysis 78

7.5 Results 78
    7.5.1 Superoxide dismutase 78
    7.5.2 Catalase 79
    7.5.3 Glutathione peroxidase 80
    7.5.4 Glutathione-S-transferase 81
    7.5.5 Lipid peroxidation (LPO) 82

7.6 Discussion 83

7.7 Conclusion 85

[redacted] **Chapter 8 Antioxidant enzyme activity and lipid peroxidation in *Aporrectodea caliginosa* earthworms exposed to AgNPs and Ag+ (as $AgNO_{3)}$ 86**

8.1 Abstract 86

8.2 Introduction 86

8.3 Materials and methods 88

- 8.3.1 Chemicals and reagents 88
- 8.3.2 Silver nanoparticles synthesis and quantification 88
- 8.3.3 Silver nanoparticles charge measurement and particle size 88
- 8.3.4 LD$_{50}$ study of AgNPs and Ag$^+$ (Described in Appendix G) 89
- 8.3.5 Experimental design (earthworm soil studies*)* 89
- 8.3.6 Earthworm homogenisation 89
- 8.3.7 Total protein in earthworm homogenate 90
- 8.3.8 Silver concentration in earthworms 90
- 8.3.9 Calculation of enzymes activity (described in Appendix F) 90
- 8.3.10 Assay of antioxidant enzymes 90

8.4 Statistical analysis 91

8.5 Results 91
- 8.5.1 Silver nanoparticles 91
- 8.5.2 Ag accumulation in earthworms 92
- 8.5.3 Superoxide dismutase 92
- 8.5.4 Catalase 94
- 8.5.5 Glutathione peroxidase 94
- 8.5.6 Glutathione-S-transferase **95**
- 8.5.7 Lipid peroxidation 96

8.6 Discussion 97

8.7 Conclusion 101

[redacted] **Chapter 9 Comparative Pharmacokinetics Analysis of Silver in Earthworm *Aporrectodea caliginosa* Exposed to AgNPs/Ag$^+$(as AgNO$_3$) 102**

9.1 Abstract 102

9.2 Introduction 102

9.3 Materials and methods 104
- 9.3.1 Soil 104
- 9.3.2 Earthworms *A. caliginosa* 104
- 9.3.3 Nanoparticle preparation 104
- 9.3.4 Silver nanoparticles characterisation 104
- 9.3.5 Experimental design 105
- 9.3.6 Silver analysis 105

9.4 Pharmacokinetic analysis 105

9.5 Statistical analysis 105

9.6 Results 105

9.7 Discussion 107

9.8 Conclusion 109

[redacted] **Chapter 10 General Discussion, Conclusions and Future Research 110**

10.1 General discussion 110

10.2 Impact of silver nanoparticles / silver nitrate in soil on earthworms 111

10.3 Impact of silver nanoparticles / silver nitrate in soil on plants 114

10.4 Conclusions 119

10.5 Future research 120

Appendix A: Stability tests 122

A.1 Effect of AgNPs strage at different temperature…………………………………………………………..
124**Error! Bookmark not defined.**
A.2: Effect of pH on AgNP spectra .... 124.
A.3: Effect of 70 °C on stability of AgNPs……………………………………………………………………………….125.
A.4: Effect of Ultraviolet radiation……………………………………………………………………………………………126.

Appendix B: Distribution coeffecient comparison **of different extractable solutions 125**

Appendix C: Rate of sorption of AgNPs and Ag+ by soil as a function of time........................... 126

Appendix D: Determination of silver (Ag) and selected elements in soil used for ryegrass cultivation, using aqua regia and 0.5-g sample (n = 3) (mg/kg) 127

Appendix E: Determination and recovery of AgNPs and silver nitrate (Ag^+) (added to soil)......130

Appendix F: Determination of elements in nine vegetables exposed to 0 and 70 mg/kg AgNPs or Ag^+ 131

Appendix G: Calculation of antioxidant enzymes activity in earthworm (µM min^{-1} mg $protein^{-1}$) and sunflower (U/g) 133

Appendix H Determination of 72-h LD_{50} of AgNPs and Ag^+ in earthworm *A. caliginosa* (n = 6/dose) 134
H.1 Determination of LD_{50} of *A. caliginosa* exposed to Ag+ 134
H.2 Determination of LD_{50} of *A. caliginosa* exposed to Ag+ 134

References 136

List of Tables

Table 4.1: Properties of the soils used in the extraction experiments and pot trials. Values in brackets represent the standard error of the mean (n = 3). 32

Table 4.2: Mass required (dry matter) to exceed the tolerable daily intake of 0.005 mg/kg/day for a 70-kg person. 35

Table 5.1: Determination of (Ca) calcium, (Cu) cupper, (K) potassium on sunflower exposed to 150 mg/kg AgNPs/ Ag+. Results expressed as mean ±SE (n= 4). Letters on the SE are significantly different.

Table 5.2: Determination of magnesium (Mg), manganese (Mn), and sodium (Na) in sunflower exposed to 150 mg/kg AgNPs/Ag^+. Results expressed as mean ± SE (n = 4). Letters on the SE are significantly different ($P < 0.05$). 43

Table 5.3: Phosphorus (P), sulphur (S), and zinc (Zn) concentrations in different parts of the sunflower plant exposed to 150 mg/kg AgNPs/Ag^+. Result expressed as Mean ± SE (n=4). Superscript letters shown for each plant segment are significantly different ($P < 0.05$)..46

Table 8.1: Comparison of mean enzyme activity, lipid peroxidation (LPO), and associated statistical data of *A. caliginosa* exposed to the two Ag concentrations (0.3, 3 mg/kg) common to both AgNPs and Ag^+. All enzyme results are expressed as µmol/mg protein. LPO is expressed as mg MDA / mg protein..93

Table 8.2: Lipid peroxidation measured as malondialdehyde (MDA) equivalents normalised to total earthworm *A. caliginosa* homogenate protein (mean + SEM) following exposure to different concentrations of AgNPs or Ag^+ over 4 weeks. 96

Table 9.1: Values for pharmacokinetic parameters following exposure of *A. caliginosa* earthworm to TSL soil amended with 20 mg/kg AgNP or Ag^+. Ag+. Results presented as mean ± standard error means (n = 4). 107

Table A2.1.1: Incubation of prepared AgNPs for 4 weeks at different temperatures (22°C and 4°C). 122

List of Figures

Fig. 2.1: Flow chart of defence mechanisms against damage caused by ROS. 17
Fig. 3.1: UV spectrum of synthesised AgNPs (5 µg/ml in water). Maximum absorbance was at 400 nm. 20
Fig. 3.2: Zeta potential of AgNPs. Zeta potential = −41 mV (zeta deviation = −18.4 mV). 21
Fig. 4.1: Distribution coefficients (K_D = sorbed / solution concentration quotients) as a function of pH for Ag-nanoparticles in the Templeton Silt Loam (A), ionic silver in the Templeton Silt Loam (B), and both nanoparticles (NP) and ionic silver (Ag^+) in the Pukekohe granular soil (C). The legend indicates the initial concentrations in the ambient solution (mg/l). For A & B, bars indicate the standard error of the mean (n = 3). 30
Fig. 4.2: Change in the distribution coefficient (K_D = sorbed / solution concentration quotients) as a function of incubation time at 4, 20, and 35°C for nanoparticles (A) and ionic silver (B) in Templeton Silt Loam. Error bars represent the standard error of the mean (n = 3). 33
Fig. 4.3: (A) Plant biomass index (treatment / control mass quotient) as a function of Ag concentration in soil. (B) Leaf Ag concentration as a function of Ag concentration in soil. 34
Fig.4.4: Silver concentration in the edible portions of plants grown in Templeton Silt Loam either without silver or spiked with 70 mg/kg either nanoparticles or ionic. Bars represent the standard error of the mean (n = 5). 35
Fig. 5.1: Sunflower seeds grown in three different media (TSL control soil, and soil mixed with 150 mg/kg AgNPs or Ag^+ at 25 days from cultivation. All the plants appeared to be in good health and there was no difference in plant morphology between the three groups. 41
Fig. 5.2: Sunflower plants just before harvest (53 days after sowing). Those exposed to AgNPs/Ag^+ had become weak, stunted and fallen down ~~b~~ecause the stems were too weak. 41
Fig. 5.3: Sunflower root growth at harvest 53 days after seed planting. 42
Fig. 5.4: Accumulation of silver (Ag) in roots and root hairs of sunflower plants exposed to control, AgNPs, or Ag+ amended soils. 42
Fig. 5.5: Distribution of Ag in in different parts of sunflower plants exposed to AgNPs/Ag^+ for 53 days. (S1, S2, S3, S4 refer to stem sections 1, 2, 3, and 4.) 43
Fig. 6.1: Leaf catalase enzyme activity (CAT) in leaves of sunflower plants grown in soil containing 150 mg/kg Ag as AgNPs or Ag^+. Results are presented as mean ± SE of four replicates. Means with different letters on the bars are significantly different ($P < 0.05$). 57
Fig. 6.2: Superoxide dismutase (SOD) enzyme activity in leaves of sunflower plants grown in soil containing 150 mg/kg Ag as AgNPs or Ag^+. Results are presented as mean ± SE of four replicates. Means with different letters on the bars are significantly different ($P < 0.05$). 58
Fig. 6.3: Glutathione S-transferase (GST) enzyme activity in the leaves of sunflower plants exposed to 150 mg/kg Ag as AgNPs or Ag^+. Results are presented as mean ± SE of four replicates. Means with different letters on the bars are significantly different ($P < 0.05$). 58
Fig. 6.4: Glutathione peroxidase (GPx) enzyme activity in leaves of sunflower plants grown in soil containing 150 mg/kg Ag as AgNPs or Ag^+. Results are presented as mean ± SE of four replicates. Means with different letters on the bars are significantly different ($P < 0.05$). 59
Fig.6.5: Malondialdehyde (MDA) concentration (ug/g wet wt) in leaves of sunflower plants grown in soils containing 150 mg/kg Ag as AgNPs or Ag^+. Results are presented as mean ± SE of four replicates. Means with different letters on the bars are significantly different ($P < 0.05$). 59

Fig. 6.6: Ascorbate oxidase activity in the leaves of sunflower plants grown in soil containing 150 mg/kg Ag as AgNPs or $AgNO_3$ (Ag^+). Results are presented as mean ± SE of four replicates. Means with different letters on the bars are significantly different ($P < 0.05$). 60

Fig. 6.7: Pyrogallol peroxidase activity in leaves of sunflower plants grown in soil containing 150 mg/kg Ag as AgNPs or $AgNO_3$ (Ag^+). Results are presented as mean ± SE of four replicates. Means with different letters on the bars are significantly different ($P < 0.05$). 60

Fig. 6.8: Guaiacol peroxidase activity in the leaves of sunflower plants grown in soil containing 150 mg/kg Ag as AgNPs or $AgNO_3$ (Ag^+). Results are presented as mean ± SE of four replicates. Means with different letters on the bars are significantly different ($P < 0.05$). 61

Fig. 6.9: Chlorophyll A & B and total carotenoid concentration in leaves of sunflower plants grown in soil containing 150 mg/kg Ag as AgNPs or $AgNO_3$ (Ag^+). Results are presented as mean ± SE of four replicates. Means with different letters on the bars are significantly different ($P < 0.05$). 62

Fig. 6.10: Total protein in leaves of sunflower plants grown in soil containing 150 mg/kg Ag as AgNPs or $AgNO_3$ (Ag^+). Results are presented as mean ± SE of four replicates. Means with different letters on the bars are significantly different ($P < 0.05$). 62

Fig. 6.11: Total phenolic compounds (TPC) in leaves of sunflower plants grown in soil containing 150 mg/kg Ag as AgNPs or $AgNO_3$ (Ag^+). Results are presented as mean ± SE of four replicates. Means with different letters on the bars are significantly different ($P < 0.05$). 63

Fig. 6.12: Total soluble carbohydrate concentration in leaves of sunflower plants grown in soil containing 150 mg/kg Ag as AgNPs or $AgNO_3$ (Ag^+). Results are presented as mean ± SE of four replicates. Means with different letters on the bars are significantly different ($P < 0.05$). 63

Fig. 6.13Uurease concentration in leaves of sunflower plants grown in soil containing 150 mg/kg Ag as AgNPs or $AgNO_3$ (Ag^+). Results are presented as mean ± SE of four replicates. Means with different letters on the bars are significantly different ($P < 0.05$). 64

Fig. 6.14: Vitamin A and E in the leaves of sunflower plants grown in soil containing 150 mg/kg Ag as AgNPs or $AgNO_3$ (Ag^+). Results are presented as mean ± SE of four replicates. Means with different letters on the bars are significantly different ($P < 0.05$). 65

Fig. 6.15: Vitamin C in leaves of sunflower plants grown in soil containing 150 mg/kg Ag as AgNPs or $AgNO_3$ (Ag^+). Results are presented as mean ± SE of four replicates. Means with different letters on the bars are significantly different ($P < 0.05$). 65

Fig. 7.1: Superoxide dismutase (SOD) enzyme activity (mean ± SE) in *A. caliginosa* exposed to AgNPs or Ag^+ ($AgNO_3$) in filter paper for 24 h (A, B) and 48 h (C, D). 79

Fig.7.2: Catalase (CAT) enzyme activity (mean + SD) in *A. caliginosa* exposed to AgNPs or Ag^+ ($AgNO_3$) in filter paper for 24 h (A, B) and 48 h (C, D). 80

Fig. 7.3: Glutathione peroxidase enzyme activity (mean + SD) in *A. caliginosa* exposed to AgNPs or $AgNO_3$ (Ag^+) in filter paper for 24 h (A, B) and 48 h (C, D). Means with different letters on the bars are significantly different ($P < 0.05$). 81

Fig. 7.4: Glutathione-S-transferase enzyme activity (mean + SD) in *A. caliginosa* exposed to AgNPs or $AgNO_3$ (Ag^+) in filter paper for 24 h (A, B) and 48 h (C, D), with no significant differences observed. 82

Fig. 7.5: Lipid peroxidation (as MDA) enzyme activity (mean + SD) in *A. caliginosa* exposed to AgNPs and Ag^+ in filter paper for 24 h (A, B) and 48 h (C, D). Mean with different letters on the bar (Ag^+ at 24 h) is the only significant difference ($P < 0.05$). 83

Fig. 8.1: Silver concentration (mean ± SEM) in homogenates of *A. caliginosa* (n = 5) exposed to (A) Ag^+ ($AgNO_3$; 0, 0.03, 0.3, 10 mg/kg) or (B) AgNPs (0, 0.3, 30, 300 mg/kg) for 1, 2, 3 and 4 weeks. Means with different letters on bars are significantly different ($P < 0.05$) from the controls. 92

Fig. 8.2: Superoxide dismutase (SOD) enzyme activity (mean ± SEM) in *A. caliginosa* (n = 5) exposed to (A) Ag^+ ($AgNO_3$; 0, 0.03, 0.3, 10 mg/kg) or (B) AgNPs (0, 0.3, 30, 300 mg/kg) for 1, 2, 3 and 4 weeks. Means with different letters on bars are significantly different ($P < 0.05$) from the controls..93
Fig. 8.3: Catalase (CAT) enzyme activity (mean ± SEM) in *A. caliginosa* (n = 5) exposed to (A) Ag^+ ($AgNO_3$; 0, 0.03, 0.3, 10 mg/kg) or (B) AgNPs (0, 0.3, 30, 300 mg/kg) for 1, 2, 3 and 4 weeks. Means with different letters on bars are significantly different ($P < 0.05$) from the controls..94
Fig. 8.4: Glutathione peroxidase (GPx) enzyme activity (mean ± SEM) in *A. caliginosa* (n = 5) exposed to (A) Ag^+ ($AgNO_3$; 0, 0.03, 0.3, 10 mg/kg) or (B) AgNPs (0, 0.3, 30, 300 mg/kg) for 1, 2, 3 and 4 weeks. Means with different letters on bars are significantly different ($P < 0.05$) from the controls..........................**.......................................95**
Fig. 8.5: Glutathione-S-transferase (GST) enzyme activity (mean ± SEM) in *A. caliginosa* (n = 5) exposed to (A) Ag^+ ($AgNO_3$; 0, 0.03, 0.3, 10 mg/kg) or (B) AgNPs (0, 0.3, 30, 300 mg/kg) for 1, 2, 3 and 4 weeks. Means with different letters on bars are significantly different ($P < 0.05$) from the controls..96
Fig. 9.1: Mean silver (Ag) concentration in *A. caliginosa* earthworm homogenate following exposure to Ag in soil at 20 mg/kg in the form of AgNP (●) or Ag^+ (○). The bars are standard error of the mean (n = 4) at each time point. 106
Fig. A1.1: Distribution coefficients (K_D = sorbed / solution concentration quotients) as a function of extractant type (*x*-axis). The soils were spiked with 1000 mg/kg Ag either as AgNPs or Ag^+. The error bars are the standard error of the mean (n = 3). 122

Fig. A2.2.1: Spectral changes observed at different pHs recorded at 398 nm. (a) is pH 6.5, (b) pH 9.23, and (c) pH 4.1. At pH 9.23 the spectrum became broad with a decrease in absorption intensity compared to pH 65. At pH 4.1 also the spectrum became broad with a marked decrease in absorption intensity. The concentration used was 5 µg/ml AgNPs...123
Fig. A2.3.1: Absorbance decreased 30% after incubation of AgNPs solution for 5 h at 70°C.........123
Fig. A2.3.2: Decrease in absorbance when incubated under UV light. (a) 0 h, (b) 1 h, (c) 2 h, (d) 3 h, (e) 4 h. The absorbance intensity decreased with time when exposed to UV radiation at 254 nm. The strength of ultraviolet light was 300 mW/cm^2. 124
Fig. B1.1: Determination of equilibrium time of AgNPs/Ag^+ (mg/l) as a function of agitation time, 20 rpm with 0.1 M KNO_3 for AgNPs/Ag^+. Values are average of three replicates......126
Fig. G.1.1: LD_{50} of AgNPs (n = 6). 134
Fig. G.2.1: LD_{50} of $AgNO_3$ (Ag^+) (n = 6)...135

Chapter 1

Introduction

1.1 Background

Silver nanoparticles (AgNPs) are efficient antimicrobial agents (Dakal *et al*., 2016) and thus have become one of the most widely used nanomaterials in commercial products. The special characteristics of AgNPs that have led to their extensive use in a variety of consumer products are the same characteristics that raise concern. Nanoparticles are generally highly mobile in their free state and have a very large surface area (Abdul, 2010). Nanoparticle (NP) sizes vary, but by definition they are particles sized between 1 and 100 nm in all three dimensions (Graf *et al*., 2003). Nanoparticles, therefore, generally have a high surface to volume ratio, which increases their reactivity with biological fluids (Beer *et al.*, 2012). However, there are concerns that their widespread use in various industries could result in release into the environment (soil, water). The increased use of NPs may cause toxic effects on environmental organisms because of discharge of discharge of wastes from these industries into landfills and waterways, and via sewage sludge (when used as a fertiliser) to land, with potential to cause soil, fresh water, and estuarine pollution.

Nanoparticles exhibit a range of compositions and can be classified as either organic, inorganic or carbon-based particles of nanometric scale. Because of their unique characteristics, NPs can be used as a catalyst, in sensoring, and in imaging (Bogart *et al*., 2014). Hence NPs have varied applications in engineering, biotechnology, magnetic separation and re-concentration of target analytes – and in biomedical sciences such as in target drug delivery and diagnostic imaging, for example Magnetic Resonance Imaging (MRI), Cat scans (CT) and ultrasound (Mody *et al*., 2010).

The shape and size of the NPs have important roles in different applications (Khan *et al*., 2017). One of the main properties of metal NPs is that they absorb small molecules at their large surface area (Chen *et al*., 2017). It is reported that metals solutions are thermodynamically unstable and hence need to be kinetically stabilised to prevent aggregation (Pappas *et al*., 2007). Some metals NPs, because of their functionality, high sensitivity, and size-dependent optical properties and photo-stability, have been used in environmental and bio-analytical fields as a probe to study biomolecular interactions. The strong interaction of NPs towards analyte molecules and/or aggregation of them in the presence of an analyte can result in spectral changes, which form non-functionalised NPs

(Krajczewski *et al*., 2017). Colloidal metals NPs possess specific properties not found in the original molecules (Mishra, 2015).

In this study, the focus was on AgNPs. Silver nanoparticles have major application in medical therapy as antibacterial agents for wound healing and in other industries because of their catalytic, optic, electric and magnetic properties. However, AgNPs could enter waste streams and bio-accumulate in soil, fresh water and estuarine environments where their toxicity could affect many organisms including earthworms (Meyer *et al*., 2010). Therefore, this thesis sought to determine the impact of exposure to AgNPs in the environment by, among other things, examining antioxidant enzyme activity in the earthworm as a signature of chronic toxicity.

Silver nanoparticles were synthesised in our laboratory by reduction of Ag+ and the product was stabilised using tri-sodium citrate (Carey, 1889). The concentration of the AgNPs thus produced was measured using flame atomic absorption, followed by study of a range of their physical properties.

This thesis consists of two parts. (1) Plant study: The mobility of AgNPs in soil, accumulation of Ag and also selected essential macro (Ca, P, S, K, Mg) and micro (B, Cu, Zn, Fe, Mn) elements were studied in a range of plants – sunflower, ryegrass, carrot, radish, leek, lettuce, parsley, rocket (arugula), beetroot silverbeet and spinach). (2) Animal study: The effect of exposure to Ag was studied in an environmentally relevant organism, the earthworm. More detailed studies were then conducted on the sunflower (plant) and the earthworm (animal). The emphases in the sunflower and earthworm studies were on Ag accumulation, lipid peroxidation (LPO) and enzyme responses [superoxide dismutase (SOD), catalase (CAT), glutathione peroxidase (GST), glutathione peroxidase (GPx), and total protein (TP), and chlorophyll in sunflower] to oxidative stress caused by AgNP/Ag^+. Results obtained revealed that Ag+ was more toxic to the earthworms and plants than AgNPs. This result led us to perform a pharmacokinetic analysis to determine why Ag+ may be more toxic than AgNP.

1.2 Research aims

This project aimed to investigate the mobility of AgNPs and Ag^+ (in the form of $AgNO_3$) in soil; uptake of Ag by plants (sunflower, ryegrass, carrot, radish, leek, lettuce, parsley, rocket, beetroot, silverbeet, and spinach); and by an environmentally relevant organism, the earthworm *(Aporrectodea caliginosa)*. Specifically, the thesis investigated the effects of AgNPs on antioxidant enzyme (SOD, CAT, GPx, GST) responses in *A. caliginosa* and sunflower (*Helianthus*), and compared these with the effects caused by Ag^+.

1.3 Objectives

1. To investigate the mobility of AgNPs and Ag^+ ($AgNO_3$) in soil.

2. To compare Ag accumulation, LPO (marker of oxidative stress) and effect on antioxidant enzyme (SOD, CAT, GPx, GST) activities in *A. caliginosa* earthworms exposed to AgNPs/Ag^+ in soil and filter paper.

3. To study the pharmacokinetics of *A. caliginosa* exposed to AgNPs/Ag^+ in soil.

4. To compare the uptake of Ag and the effects on antioxidant enzyme activities in sunflower plants exposed to AgNPs and Ag^+.

5. To determine the concentration of Ag in different parts of sunflower and morphological changes that occurred when exposed to AgNPs/Ag^+.

1.4 Hypotheses

1. Silver nitrate (Ag^+) is more toxic than AgNP to *A. caliginosa*.

2. Induction of LPO and antioxidant enzymes (SOD, CAT, GPx, GST) is markedly higher in *A. caliginosa* exposed to Ag+ than in earthworms exposed to AgNPs.

3. The pharmacokinetic profile of Ag in *A. caliginosa* is different between those exposed to AgNPs and Ag+.

4. Mobility of Ag added to soil as AgNPs and Ag+ are different.

5. Silver is concentrated in root > leaves > stem > flower.

6. Silver nitrate is more toxic than AgNPs to sunflower and ryegrass plants.

7. Uptake and morphological changes are more marked in sunflower plants exposed to Ag+ than in those exposed to AgNPs.

Chapter 2

Literature Review

2.1 Nanoparticles

Nanoparticles are particles between 1 and 100 nanometres (nm) in size with a surrounding interfacial layer (Batista *et al.*, 2015). The interfacial layer consists of ions, and inorganic and organic molecules (Batista *et al.*, 2015). Organic molecules coating inorganic nanoparticles are known as stabilisers or capping agents. Nanoparticles exhibit behaviour and characteristics that are not associated with the substance as a whole (bulk material) (Schwirn *et al.*, 2014); for example, Cu^{+2} NPs < 50 nm are considered super hard material that does not exhibit the malleability and ductility of bulk Cu. Nanoparticles possess a high surface area to volume ratio, which provides a greater driving force for diffusion. The large surface area to volume ratio also reduces the incipient melting temperature of NPs (Amsh, 2012). Some of these nanoparticles occur naturally, for example in volcanic ash. Some occur by accident, for example during the combustion of fuels. Others by human activities. Many occur by design.

2.2 Naturally occurring nanoparticles

Natural phenomena such as volcanic eruptions and many industrial and domestic activities, such as welding, smelting, cooking, and manufacturing of road and air transport, release NPs into the atmosphere (Tripathi *et al.*, 2017b). NPs can be formed in liquid phase, gas phase or be air borne. In liquid and gas phases, NPs can be formed by chemical reactions. In the gas phase, the reactions that generate NPs occur either naturally in the atmosphere, are caused by human activities or are formed during volcanic eruptions. Airborne NPs in rural areas are the result of chemical reactions such as the oxidation of volatile compounds of biogenic or anthrobiogenic origin, while in urban areas NPs are released from the exhausts of diesel engines and cars with defective catalytic converters (Tripathi *et al.*, 2017b).

It is well established that NPs intentionally engineered for advanced technologies and consumer products have become a new source of exposure (Yokel and MacPhail, 2011). And smaller sized NPs may be more toxic because of their larger surface area (Zhang *et al.*, 2016).

2.3 Silver nanoparticles

2.3.1

There are two main approaches for manufacturing of nanomaterial. The first is top-down, which involves breaking down of large pieces of material to generate the required nanostructure. The second is bottom up, where atoms and molecules are assembled into larger nanostructure (Su and Chang, 2018).

Many methods have been developed for AgNP synthesis using different preservatives and reducing agents. Zhang *et al.* (2016) reported that AgNPs can be prepared by physical, chemical or biological methods. In the Carey (1889) colloidal Ag method, a mixture of iron Fe^{2+} sulphate heptahydrate and tri-sodium citrate solution are added dropwise to $AgNO_3$ solution with vigorous shaking, centrifuged, and decanted. The supernatant and the pellet formed are washed four times with sodium tri-citrate solution, centrifuged, and the supernatant decanted. Finally, the pellet is re-suspended in Milli-Q water to yield a dark brown reddish solution of AgNPs of particles sized 10–14 nm. Solomon *et al.* (2007) and Kandarp and Mihir (2013)) synthesised AgNPs sized 10–12 nm diameter by a chemical reduction method of Ag salt (such as $AgNO_3$) using ice-cold sodium borohydride to reduce the ionic Ag and adding 0.1% of PVP to stabilise AgNPs. Xiong *et al.* (2013) described a method to synthesise soluble stable AgNPs sized 22–30 nm based on reduction of Ag^+ ions (in $AgNO_3$) with hydrazine hydrate in the presence of polyacrylamide (PAM) at pH 10. Gudikandula and Maringanti (2016) prepared AgNPs using chemical reduction and biological methods. The chemical reduction method involved heating 10^{-3} M $AgNO_3$ to boiling, followed by addition of 5 ml of 1% sodium tricitrate dropwise and continued heating until the colour changes to pale brown. The biological method by the same authors involved growth of *Pycnoporus* fungi in malt extract and glucose medium for 5 days followed by filtration. An aliquot of the filtrate is mixed with 1 mM $AgNO_3$ as a reducing agent and incubated at 32°C for 20 min. In a method developed by Suriati *et al.* (2014), $AgNO_3$ is reduced by tri-sodium citrate and ascorbic acid in varied concentrations to produce AgNPs of different sizes and morphologies. Gusman *et al.* (2009) used $AgNO_3$ as the metal salt precursor and two stabilising agents, sodium dodecyl sulphate (SDS) and Na citrate, for AgNP synthesis. Hydrazine hydrate and Na citrate solutions were used as reducing agents. Silver nanoparticles have also been prepared using bacterial strain *Escherichia coli* with $AgNO_3$ where *E. coli* acted as the reducing agent (Gandhi and Khan, 2016).

Plants have been used in AgNP synthesis. Lotus aqueous extract acted as the reducing and stabilising agent in AgNP synthesis using $AgNO_3$ as the precursor (He *et al.*, 2018). Water extract of *Coriandrum* was added to 0.01 M $AgNO_3$ in the ratio of 1 ml of plant extract to 75 ml $AgNO_3$ solution to prepare AgNP (Khan *et al.*, 2018). Grapefruit peel has also been used to synthesise AgNPs. The fried peel was ground and extracted by hot water and filtered, 20 ml of filtrate was added to 80 ml 1 mM $AgNO_3$ and the solution kept in sunlight for 30 min, then centrifuged, the upper layer discharged and the sedimented AgNP dried for 2 h at 60°C (Faghihi *et al.*, 2017). Aloe vera plant extract was boiled to 80°C, cooled and filtered, then 10 ml of the extract was added to 90 ml of 1 mM $AgNO_3$ and incubated in the dark overnight to produce AgNPs (Asharaf *et al.*, 2016). *Cinnamomum zeylanicum* bark has also been used in AgNP synthesis with the bark acting as a reducing and stabilising agent to $AgNO_3$ (Gauthami *et al.*, 2015).

2.3.2 Silver nanoparticle properties

Many physical and chemical properties of AgNPs – including surface chemistry, particle sizes and their distribution, shape, particle morphology and composition, coating, capping, agglomeration, dissolution rate, reactivity in solution, efficiency of ion release, cell type, and type of reducing agent used for synthesis – have been described in the literature, but they vary with the synthesis method used.

Silver nanoparticles are extraordinarily efficient at absorbing and scattering light. The interaction between AgNPs and light depends on the conduction electrons on the metal surface, which can collectively oscillate when excited by light at a specific wavelength. This is known as surface plasmon resonance (SPR) and can lead to strong scattering and absorption of light. Spherical AgNPs when examined in dark field microscopy appear as bright blue peaking at 450 nm (violet colour) to 530 nm (green colour) (Théoret and Wilkinson, 2017). The colour depends on the size and shape of the particles. Changing of particle size causes a shifting of the SPR of the electromagnetic wavelength towards the infra-red region of the electromagnetic spectrum, producing AgNPs with rod or plate shape (Peng *et al.*, 2010).

The biological effects of AgNPs depend on the different surface charges of their coating. Agglomeration occurs with most of the engineered NPs, with agglomeration of AgNPs occurring within the cytoplasm and nuclei HepG2 cell (Akter *et al.*, 2018). It has been shown that dissolution of NPs in the long-term may result in surface oxidation leading to the production of ionic Ag (Akter *et al.*, 2018). Jiang *et al.* (2005) studied the effects of electrolytes and surfactants on the catalytic properties of AgNPs on silica. It was found that the presence of a surfactant depressed the catalytic activity by inhibiting the adsorption of the reactants onto the surface of the particles. Electrolytes either increase the immigration rate of the reactants in the solution, which can result in an increase in catalytic reaction rate, or inhibit the adsorption on the surface of Ag particles leading to a loss in the activity of metal particles.

2.3.3 Silver nanoparticle characterisation

In order to determine the safety, efficiency and behaviour of AgNPs, and to evaluate their impact on the environment, it is important to characterise AgNPs. Characterisation of AgNPs can be performed using different analytical techniques, namely (in alphabetical order), Atomic Force Microscopy (AFM), Dynamic Light Scattering (DLS), Fourier Transform Infrared Spectroscopy (FTIR), Localised Surface Plasmon Resonance (LSPR), Scanning Electron Microscopy (SEM), Transmission Electron Microscopy (TEM), UV-Visible Spectroscopy (UV-VIS), X-ray Diffraction (XRD), and X-ray Photoelectron Spectroscopy (XPS).

Atomic Force Microscopy: AFM is used to investigate the dispersion and aggregation of NPs, in addition to determining their size, shape, sorption and structure. This method can be used in three modes: contact mode, non-contact mode, and intermittent sample contact mode. One disadvantage of AFM is overestimation of the lateral dimension of the sample due to cantilever; also it needs much attention in sample preparation and choice of operating mode (Pletikapić *et al.*, 2012).

Dynamic Light Scattering: This technique is used for physiochemical characterisation of synthesized nano-materials. DLS can probe the size distribution of small particles scaled from submicron down to 1 nm in solution or suspension (de Kanter *et al.*, 2016).

Fourier Transform Infrared Spectroscopy: This technique has been widely used to measure organic polymers and inorganic compounds, in addition to detection of small changes in spectra. FTIR provides accurate and reproducible measurements and also a favourable signal to noise ratio (Zhang *et al*., 2016) With FTIR, it is possible to detect small absorbance change in the order of 10^{-3} (Kumar, 2010).

Localised Surface Plasmon Resonance: LSPR involves a coherent, collective, spatial oscillation of the conduction electrons in metallic NPs, which could be excited by near-visible light. This technique is used to define several parameters including electronic properties, size, and shape of NPs. It is also used to investigate the fundamental properties and processes of NPs in bio-molecular detection and can provide thermodynamic and real-time kinetic data for the binding process (Anandalakshmi *et al.*, 2016; Goudarzi *et al.*, 2016; Zhang *et al.*, 2016).

Scanning Electron Microscopy: SEM uses a beam of highly energetic electrons to probe objects on a very fine scale. It is a surface imaging method capable of identifying different particles sizes, size distribution, particle shape and surface morphology (Buhr *et al.*, 2009).

Transmission Electron Microscopy: This is a technique used for characterisation and quantitation of NPs, determining grain size, size distribution and morphology. One of the disadvantages is that it requires a high vacuum, thin sample section and is time consuming. Careful sample preparation for TEM analysis is extremely important in order to obtain high quality images (Su, 2017).

UV-Visible Spectroscopy: UV-VIS is very useful for primary characterisation of synthesised NPs. It can be used to monitor synthesis and stability and analyse spectral properties of AgNPs. The spectral response of AgNP is a function of its diameter. As the diameter increases, the peak plasmon resonance shifts to a longer wavelength and broadens. At diameters > 80 nm, a second peak of a shorter wavelength appears (Deepa and Suryaprakash, 2016). This secondary peak is due to a quadrupole resonance that has a different electron oscillation pattern than the primary dipole resonance. The peak width and the effect of the secondary resonance yield a unique spectral fingerprint for a plasmonic NP with a specific size and shape. This technique is mostly used for analysis of both molecular and crystal structure, and qualitative identification of various compounds and quantitative resolution of chemical species (Deschamps, 2010).

X-ray Diffraction: used to detect sample crystal structure using a beam of x-ray diffracting through the crystal by specific angel. It is utilized to identify synthesised AgNPs crystal structure (Nogueira *et al*. 2014).

X-ray Photoelectron Spectroscopy: This surface-sensitive technique is used for quantitative chemical analysis to estimate spatial distribution of ions at the vapour–electrolyte interface (Olivieri *et al.*, 2016).

2.4 Mobility and fate of silver nanoparticles in soil

Sagee *et al.* (2012) reported that AgNPs are highly mobile in soil. This mobility is reduced when soil particle aggregates are large. To study the fate of AgNPs in soil Coutris *et al.* (2012) used $AgNO_3$ and uncoated and citrate-coated AgNPs in two soils of contrasting organic matter, radiolabelled for quantification by gamma spectrometry, and followed the changes in binding strength over time. The authors found that AgNPs can act as a continuous source of bioaccessible Ag, while Ag^+ from $AgNO_3$ is rapidly released into soil. Contamination of soil by AgNPs and Ag+ causes significant inhibition of soil enzyme activity, but addition of organic matter can reverse this. Chemical speciation of Ag suggests that AgNPs can induce greater toxic effects on soil enzymes at low Ag concentration (Shin *et al.*, 2012; Peyrot *et al.*, 2014).

2.5 Sorption of AgNPs and Ag^+ ($AgNO_3$) by soils at different pHs

The sorption of AgNPs/Ag^+ (from $AgNO_3$) is dependent on the pH of the medium and the partitioning between AgNPs and Ag^+ (Oromieh, 2011). Silver nanoparticles are oxidised and transformed to Ag^+ in soil slowly with time (McShan *et al.*, 2014). At constant pH, the extent of aggregation of AgNPs/Ag^+ depends on the concentrations and can be viewed using TEM and XRD (Phanjom and Ahmed, 2017). Klitzke *et al.* (2015) found that soil interacts with AgNPs to increase colloidal stability due to dissolved organic matter (DOM) inhibiting aggregation. Dissolved organic matter reduces Ag oxidation and inhibits Ag^+ release from the solution, but surface charge does not appear to control the sorption of AgNPs (Klitzke *et al.*, 2015)**.** The classical sorption isotherm is used to describe the sorption of engineered AgNPs from both stable and unstable suspensions (Abraham *et al.*, 2013). The Langmuir isotherm suggests monolayer sorption, as explained by the blocking effect due to electrical repulsion of individual NPs. For *n*Ag sorption from an unstable suspension, the sorption isotherm does not follow classical sorption models, suggesting interplay between aggregation and sorption. In unstable suspensions, aggregates are instead formed in suspension and then sorbed (Abraham *et al.*, 2013).

Sepúlvida (2014) constructed a wetland matrix as an alternative to conventional wastewater treatment plants and applied many processes to remove chemical pollutants in the wetland such as adsorption, chemical reactions, uptake by biofilm and plants, and filtration to evaluate their efficacy in the removal of AgNPs. To investigate adsorption processes in a solid wetland, the author used sand, gravel and zeolite as substrates. The effect of biofilm was evaluated by measuring adsorption and uptake over 24 hours. To assess adsorption and uptake by wetland plants (*Phragmites australis*), the experiment was performed for 4 weeks and a mass balance carried out of the total amount of Ag. The results showed that adsorption was higher on sand and zeolite than on gravel. However, the presence of an active biofilm on the gravel enhanced the removal of AgNPs from wastewater by adsorption and uptake processes. It was also found that *P. australis* plants were able to adsorb/uptake AgNPs from wastewater to some extent with uptake by plant roots contributing to the removal of Ag^+.

2.6 Chemical speciation of silver nanoparticles

The investigation of physiochemical properties such as pH, ionic strength, ligands, concentration and soil–water interface chemistry are good tools to predict the environmental fate and reactivity of

AgNPs (VandeVoort and Arai, 2012). Benoit *et al.* (2013) reported that soil organic matter and pH determine the longevity of AgNPs in soil. They evaluated the chemical speciation of Ag by means of Ag electrodes and total solution measurements to help differentiate what fraction of NPs are dissolved and are in a free ionic (Ag^+) state and what portion would remain as NPs. In acidic soil, more free Ag^+ ions occur, but in the presence of organic matter ions were tightly bound as complexes. In a study of the chemical speciation of AgNPs in soil over 6 months, it was found that most of the Ag would be either bound to colloidal particles sized between 10 and 200 nm or dissolved in the soil (Benoit *et al*., 2013). The transport of Ag in soil is affected by several rate-limiting processes, including adsorption and release reactions (Zhang, 2012). This study assessed the adsorption-desorption of Ag in different soils, and in particular looked at how zinc (Zn) influences Ag retention and transport in soil, using kinetic batch adsorption-desorption and column experiments. It was evident that in all soils the adsorption isotherms were highly nonlinear with great affinity to the Webster soil. Zn reduced Ag adsorption, suggesting competitive behaviour. Column experiments revealed highest Ag mobility in the Olivier soil and least in the Webster soil. The study concluded that the presence of Zn enhances Ag mobility (Zhang, 2012).

Speciation and mobility of $AgNO_3$, Ag chloride (AgCl), and Ag sulphide (Ag_2S) NPs were investigated using X-ray absorption and Nano Diffusive Gradient in Thin Film (DGT) devices (Sekine *et al.*, 2015). This study also examined the aging profile and stability of the three Ag forms ($AgNO_3$, Ag_2S, AgCl) at three different soil pHs. The transformation of $AgNO_3$, Ag_2S and AgCl NPs was dependent on the pH. Silver chloride formation and persistence were seen under acidic conditions. Sulphur-bound Ag was observed in neutral to alkaline media. Silver sulphide NPs were found to be stable under all conditions tested and remained sulphur-bound even at 7 months. The mobility of Ag was low in soil containing Ag_2S NPs, with results indicating that Ag_2S NPs are chemically stable and have profoundly low Ag mobility over an extended period (Sekine *et al.*, 2015). Settimio *et al.* (2014) developed an isotopic dilution method for simultaneous determination of the partitioning (K_D value) and mobility *(E*-value) of Ag in soil, using the Ag 110-m isotope and 10 mM calcium nitrate along with cation exchange resin to correct possible interference from non-isotopically exchangeable forms. They reported that labile Ag in soils spiked with soluble Ag salt and aged for 2 weeks, there was rapid conversion of soluble Ag into non-isotopically exchangeable forms either irreversibly or adsorbed as a precipitate in soil. Results showed that measurement of labile Ag is an important factor in evaluating the toxicity risk of AgNPs to soil organisms or to predict bioaccumulation through the food chain.

The soil sorption of Ag, uncoated and coated with 0.3% polyvinylpyrrolidone (PVP), applied at concentrations of 1, 10 and 100 mg/l AgNPs onto soil, in a microbial-facilitated soil denitrification process using native bacteria in soil showed that AgNPs exhibited less toxicity to the denitrifying bacteria than expected. Toxicity was linked to the AgNPs' affinity for soil surfaces (K_D), where the particles with low K_D values were the only toxic AgNPs (VandeVoort and Arai, 2012).

2.7 Toxicity of silver nanoparticles in terrestrial ecosystems

The main route by which AgNPs enter the environment is as industrial effluent and/or as a by-product of sewage treatment plants. The NPs are too small to be filtered out, so they and other materials end up in the resulting wastewater treatment sludge, which is spread on the land surface as a fertiliser in some countries (CEINT, 2013). This can result in toxicity to terrestrial organisms including earthworms and also to aquatic organisms via rainfall runoff. Silver accumulates in soil, water, terrestrial animals, plants and aquatic animals (Hoke *et al*., 2015) and as a majority of AgNPs react with sulphur and oxygen thus the structure and function of AgNPs is changed. Such newly created Ag compounds can be more stable and less toxic than AgNPs (Jesmer *et al*., 2017). Peyrot *et al.* (2014) studied how AgNPs affect enzyme activities in soil with and without added organic matter and found that Ag inhibited the activity of phosphomonoesterase, arylsulfatase, β-D glucosidase and leucin- amino-peptidase as a function of soil Ag concentration. They also found that adding organic matter to the soil enhanced enzyme activities. Schlich *et al.* (2013a) reported that 90% of AgNPs bind to sewage sludge, while Colman *et al.* (2013) showed that the addition of AgNPs to biosolids increased N_20 fluxes and changed microbial community composition, biomass, and extracellular enzyme activity, as well as having species-specific effects on above-ground plant biomass. Geisler-Lee *et al.* (2014) investigated the phytotoxicity of AgNPs to important crop plants. (They selected AgNPs because of the OECD designation of Ag as a priority NP.) On evaluation of the toxicity and bioavailability of AgNPs in agar and soil media, they found that seedling growth is adversely affected by exposure to AgNPs. Biosolids containing AgNPs, when applied as a fertiliser to soil, exert adverse effects on soil organisms, inhibit plant growth (Colman *et al.*, 2013) and reduce the number of soil microbes(Linares, 2016).

Evidence of the toxicity of AgNPs to earthworms include growth inhibition, decrease in cocoon productivity and a lower biomass (Colman *et al*., 2013). Khalil (2016) exposed *Aporrectodea caliginosa* earthworms to different concentrations of AgNPs for 28 days and no mortality was observed, but the biomass, cellulase levels and number of hatched cocoons were reduced in a concentration-dependent manner compared to the controls. The effects of AgNP size and surface coating (which affects the charge) on the bioaccumulation and toxicity (survival, growth, cocoon production) of the earthworm *Lumbricus rubellus* were investigated by Makama *et al.* (2016). Silver nanoparticles were synthesised and coated using either of three coating agents: bovine serum albumin (AgNP-BSA), chitosan (AgNP-Chit) or PVP (AgNP-PVP), with negative, positive and neutral charges respectively. Total tissue Ag concentration was highest in the AgNP-BSA group especially at low AgNP exposure concentrations, whereas reproduction was impaired at high concentrations. The authors reported that the toxicity of AgNP-BSA (negative) > AgNP-PVP (neutral) > AgNP-Chit (positive). Silver nanoparticles reduced the length and body width of *Caenorhabditis elegans* nematodes incubated in a microfluidic chip, but enabled the roundworm to travel longer distances compared to the controls (J.H. Kim *et al.*, 2016).

A study of the effects of AgNPs and Ag+ on bioavailability and their toxicity to *Eisenia fetida* juvenile earthworms, investigated for 1, 9, 30 and 52 weeks, showed that (Ag^+) ($AgNO_3$) is toxic and caused deaths, but that AgNPs were relatively less toxic but this changed with time, apparently by the slow conversion of AgNPs to ionic Ag^+ in soil over time (Diez-Ortiz *et al*., 2015). In addition, exposure of *E. fetida* to 5-nm-sized PVP-PE1-coated AgNPs in soil resulted in high Ag accumulation, weight loss and mortality of the earthworms due to disruption of the tegument, possibly caused by dermal absorption of Ag ions, but that Ag uptake was mostly localised in the digestive tract epithelium (García-Velasco *et al*., 2016). In contrast, when *E. fetida* was exposed to Ag+ and AgNPs coated with PVP or oleic acid during standard reproduction tests, no significant effects on growth or mortality were observed (Wilson *et al.*, 2010), suggesting that Ag^+ ions released from AgNPs may be responsible for the reduction in growth and development caused by AgNPs (William *et al.,* 2011). AgNPs and Ag+ reduced growth and reproduction of *Lumbricus rubellus* and this was most marked at the higher exposure concentrations; and juvenile mortality, in addition to tissue pathology, was observed on long-term exposure (van der Ploeg *et al.*, 2014).

Rani *et al.* (2009) reported cytotoxicity and genotoxicity of AgNPs to human cells. AgNPs reduced the ATP content, damaged mitochondria, and increased the production of reactive oxygen species (ROS) (Rani *et al.*, 2009). The ROS generated can interact with biomolecules such as protein, enzymes and DNA. This was confirmed by Kim *et al*. (2009) who showed that cytotoxicity and genotoxicity induced by AgNPs is oxidative stress related.

2.8 Earthworms – *Aporrectodea caliginosa* (*A. caliginosa*)

Earthworms play important roles in agroecosystems. Their feeding and burrowing activities incorporate organic residues into the soil, enhancing decomposition, and promoting humus formation, nutrient cycling, and soil structural development (Kladivko *et al*., 1986). The earthworm chosen for this study was *A. caliginosa*, an endogeic (burrowing) earthworm that lives in and feeds on the soil, because it is widespread in New Zealand agricultural soils. *A. caliginosa* earthworms have the ability to preserve and contribute to the overall productivity of the soil ecosystem by promoting organic matter decomposition and regulating the turnover of organic matter. Earthworm activity also enhances mineralisation and humification of soil organic matter. In addition, there is a positive relationship between earthworm activity, soil respiration and nutrient cycling. Earthworm activity can stimulate microbiological activity in casts and the presence of earthworms can modify soil microbial activity (Amaral *et al.*, 2006; Roh *et al.*, 2009).

Earthworms are important soil macro-invertebrates and are non-target soil organisms often used in assessing the general impact on soil of chemical pollution such as by pesticides and heavy metals. In addition, *A. caliginosa* has the potential to reduce upward losses of water, increase water retention and increase dispersion of agricultural chemicals applied to the soil surface (McDaniel *et al.*, 2015). The biochemical responses in *A. caliginosa* have been used as biomarkers to provide an early-warning signal of exposure to soil contamination. Booth and O'Halloran (2009) measured three biomarkers – acetyl cholinesterase and glutathione-S-transferase (GST) enzyme activities and lysosmal neutral red retention – in *A. caliginosa* to detect exposure to organophosphate insecticides. Gooneratne *et al*. (2011) used electrophysiological changes in *A. caliginosa* as a biomarker of exposure when undertaking an ecotoxicological assessment of acid mine drainage.

2.9 Toxicity of silver nanoparticles to aquatic ecosystems

The widespread use of AgNPs in consumer products especially textiles has resulted in transfer to and distribution of NPs within soil and waterways (lakes and streams) (Colman *et al*., 2013). Major chemical transformations of AgNPs occur in the presence of various aqueous forms, particularly the transformation of metallic Ag caused by reactions with inorganic ligands like sulphide, with effects on physical and chemical stability and also toxicity, which can result in less toxic compounds such as Ag_2S. Suggestions have been made to prohibit the release of AgNPs into the environment or their direct application as an anti-microbial agent in aquaculture, because of their effects on aquatic systems.

For example, exposure of the aquatic plant *Lemna gibba* for over 7 days to different concentrations of AgNPs resulted in inhibition of growth as demonstrated by a significant decrease of frond numbers. This effect was highly correlated with an increase in the production of intracellular ROS (Abdallah *et al.*, 2013). The AgNPs ingested by *Daphnia magna* accumulated under the carapace on the external body surface causing abnormal swimming and this effect was dose related (Saba *et al.*, 2012). Ronny *et al.* (2013) examined the effects of Ag in nano, bulk, and ionic forms on zebra fish embryos using a next-generation-sequencing approach and found significant alteration in the expression of many genes. These changes were associated with oxidative phosphorylation of protein synthesis pathways in the zebra fish exposed to AgNPs. In a study of the toxicity of colloidal AgNPs to various life stages of rainbow trout, the embryos, larvae and juveniles were found to be the most sensitive (Johari *et al*., 2012). In addition to a dose-dependent reduction in blood chloride and potassium, increases in cortisol and cholinesterase enzyme levels were observed in the juveniles exposed to AgNPs. Kalbassi (2011) reported how salinity can reduce the toxic effect of AgNPs on rainbow trout. They concluded that the release of AgNPs into freshwater ecosystems can lead to more biological, physical and chemical irrecoverable impacts on these ecosystems, including on aquatic organisms such as rainbow trout and other fish, in comparison with saline water ecosystems.

2.10 Tolerance and uptake of AgNPs and Ag^+ ($AgNO_3$) by plants

The phytotoxicity of AgNPs was studied in *Phaseolus radiatus* and *Sorghum bicolor* in soil and agar media and AgNPs were found to inhibit seedling growth in both media (Lee *et al.*, 2012). Uptake of AgNPs by the plants was examined under an electron microscope, which showed that AgNPs were less toxic to plants grown in the soil because of reduced bioavailability in soil (Lee *et al.*, 2012). The geochemical reactivity and human bio-accessibility of AgNPs can be determined in soil by a method commonly used for other elements. Lee *et al*. (2012) used five pots containing urban soil with Ag content equivalent to 6.8 mg/kg and incubated these for 45 days for stabilisation. Geochemical reactivity was determined by extraction using 0.43 M or 2 M nitric acid, which yielded 8% and 50% Ag recovery respectively. The authors used four methods to assess bio-accessibility, namely the Simplified Bio accessibility Extraction Test, the Unified Barge Method, artificial lysosmal fluid, and modified Gamb's solution. Among these methods, artificial lysosmal fluid was found to yield the least Ag bio-accessibility (17%) and the Simplified Bio accessibility Extraction Test the highest (99%). The results suggested that all Ag can be released from soil over time under specific conditions.

Koontz *et al*. (1980) studied the effect of Ag on calcium (Ca), phosphorus (P) and sulphur (S) uptake by tomatoes, beans and corn grown in nutrient solutions labelled with ^{33}P, ^{34}S and ^{46}Ca with varying concentrations of $AgNO_3$. It was shown that 50 mM $AgNO_3$ inhibited shoot uptake of all three ions investigated. In the roots, Ca uptake increased whereas that of P and S decreased. An autoradiogram of beans and corn, using ^{110m}Ag, showed uniform distribution of Ag ions in the shoot, and corn showed high Ag concentration along leaf margins and at the tip where exudation of xylem (also called guttation) had occurred. In addition, the roots showed a high Ag concentration. The authors believed that Ag is phloem mobile.

Addition of AgNPs to *Arabidopsis thaliana* resulted in vegetative development being prolonged by 2–3 days and new plant growth shortened by 3-4 days (Geisler-Lee *et al.*, 2014). In addition, the germination rate decreased drastically over three generations. This finding proved that AgNPs induced abiotic stress causing reproductive toxicity in *A. thaliana*. The movement of AgNPs in *A. thaliana* followed three pathways. At 7 days after planting, AgNP was attached to the primary surface roots and then entered the root tips. At around 14 days, the AgNPs moved into the roots, entering the primordial lateral root and root hairs. At 17 days AgNPs were found in vascular tissues and throughout the plant from root to shoot (Geisler-Lee *et al.*, 2014).

El-Temsah and Joner (2010) used seed germination tests to investigate the effect of the heavy metal iron (Fe) at 0–5000 mg/l on uptake of 0–100 mg/l AgNPs in three plants, ryegrass, barley and flax. Germination was completely inhibited by high Fe concentrations (2000–5000 mg/l). However, Fe at low concentrations (250 mg/l) can be used without detrimental effects. Seed germination was inhibited but not completely by AgNPs. It appears that seed germination is not an accurate measure of the environmental impact of AgNPs (El-Temsah and Joner, 2010).

The effects of AgNP on germination and early growth were studied in 11 species of wetland plants (Yin *et al.*, 2012). Plants were exposed to AgNPs (10 or 40 mg/l Ag) coated with PVP or gum Arabic (GA), and Ag+ in two exposure scenarios: simple pure culture (direct exposure) and seed planted in soils in a greenhouse (soil exposure). Results showed that direct exposure to PVP-AgNP had no effects, but that 40 mg/l GA- AgNP exposure significantly reduced the germination rate in three species (*Scirpus cyperinus, Juncus effusus, Phytolacca americana*) and enhanced the germination of one species (*Eupatorium fistulosum*). In contrast, Ag+ at 40 mg/l enhanced germination of five species (*Carex scoparia, Juncus effusus, Panicum virgatum, Eupatorium fistulosum, Phytolacca americana*). Silver nanoparticles affected root growth more than leaf growth. *Lolium multiflorum* was the only one out of 11 plants that grew rapidly on exposure to Ag+ and GA-coated AgNPs. In all other plants, growth was significantly reduced. PVP-coated AgNPs inhibited only one plant species.

On exposure of the aquatic plant *Lemna gibba* to AgNPs, its growth was inhibited in a concentration-dependent matter. Silver accumulated intracellularly due to the slow release of free Ag from AgNPs, and the subsequent increased formation of intracellular ROS led to damage of plant cells (Oukarroum *et al.*, 2013).

Onions, a widely consumed food throughout the world, contain a high concentration of flavonoids. The effect of Ag on onions was studied using a nutritive solution (containing Ag at 0, 20, 40, and 80 mg/l as $AgNO_3$) and foliar spray at Ag concentrations of 0, 20 and 40 mg/l, also as $AgNO_3$, with samples taken at 30, 60 and 90 days following exposure (Juarez-Maldonado *et al.*, 2013). The total antioxidant capacity was determined along with Ag accumulation and AgNP formation. Silver nitrate improved the total antioxidant capacity, and the accumulation of Ag in different tissues of the plant was highest following the foliar spray (Ahmed *et al*. 2016; Lakshmaanan *et al*., 2018).

The absorption of Ag by watermelon plants and its effect on lycopene (a carotenoid in that protects against oxidative damage) and antioxidant status were measured following the application of 0, 30, 60 90 and 200 mg/l Ag^+ as $AgNO_3$ at 8-day intervals throughout the crop cycle (De La Fuente *et al.*, 2014). Accumulation of Ag in the plant root and tissues and antioxidant status of the plant increased three-fold. There was no significant difference between the treated groups, but the lycopene concentration was too low compared to other reports (2.73 ug/g vs 47.8 ug/g) (Perkin *et al.*, 2001). This could be due to exogenous application of $AgNO_3$ and temperatures > 30°C, which inhibited lycopene synthesis in the plants exposed to 30 mg/l $AgNO_3$.

In a study of English oak by Olchowik *et al.* (2017), which evaluated the effects of a foliar spray of AgNPs and CuNPs, four times during a vegetation season at four concentrations (0–50 ppm), on growth parameters, extent of leaves infected by powdery mildew, and spontaneous ectomycorrhizal colonisation, neither AgNPs nor CuNPs had any effect on the growth parameters of the oak seedlings. However, TEM studies showed malformations in the shape of plastids and disturbance to plastoglobuli, and sand starch content of oak leaves in the 50 mg/kg AgNP- and CuNP-treated groups.

2.10.1 Effect of heavy metals on sunflower

When 65-day-old sunflowers were subjected to foliar spray containing AgNPs at three concentrations (0, 25, 50 mg/l of 1 g/l), organic fertiliser (0, 0.75, 1.5 g/l) or salicylic acid (0, 60, 120 mg/l), increases in leaf and branch numbers and carbohydrate concentration were detected at the highest concentrations of foliar spray, that is, at 50 ml/l AgNPs, 1.5 g/l organic fertiliser and 120 mg/l of salicylic acid (Yaseen *et al.*, 2016).

When the roots of sunflower plants (18 days old) were subjected to salt stress by treating them with 50 mM NaCl, and the foliage sprayed with potassium (K) salts (sulphate, dihydrogen phosphate, carbonate, chloride, hydroxide (1.25% K+ in Tween 20)) twice at weekly intervals, application of NaCl alone adversely affected sunflower growth (Akram *et al.*, 2009). However, the application of different K salts reversed the effects and in general improved plant health.

Azevedo *et al.* (2005) investigated the effect on sunflower growth of cadmium (Cd) at 5, 50, and 500 uM in the soil, for 21 days. The Cd application significantly decreased plant root and shoot growth, and there were marked declines in chlorophyll A & B concentrations in the plant, which dramatically affected photosynthesis.

The exposure of sunflowers to high lead (Pb) concentrations resulted in marked Pb uptake by the plant, inhibition of and a decrease in leaf numbers, chlorophyll, seed germination and weight of dry matter, but had no effect on the height of the 40-day-old sunflowers (Paliwal *et al.*, 2013).

2.11 Antioxidant enzymes

Oxidation is a chemical reaction that can produce free radicals, thereby leading to chain reactions that may damage the cells of organisms. Antioxidants are compounds that inhibit this oxidation. Reactive oxygen species (ROS) are generated as by-products during mitochondrial electron transport and as intermediates of metal-catalysed oxidation reactions. The ROS oxidise DNA, lipids, and proteins. Formation of ROS can result in the general phenomenon of oxidative stress, which can lead to inflammation, aging and, if severe, even death. To balance the oxidative state, plants and animals maintain complex systems of overlapping antioxidants, such as glutathione and enzymes (e.g. catalase, superoxide dismutase, glutathione peroxidase). There are also other antioxidants such as vitamins A, C, and E.

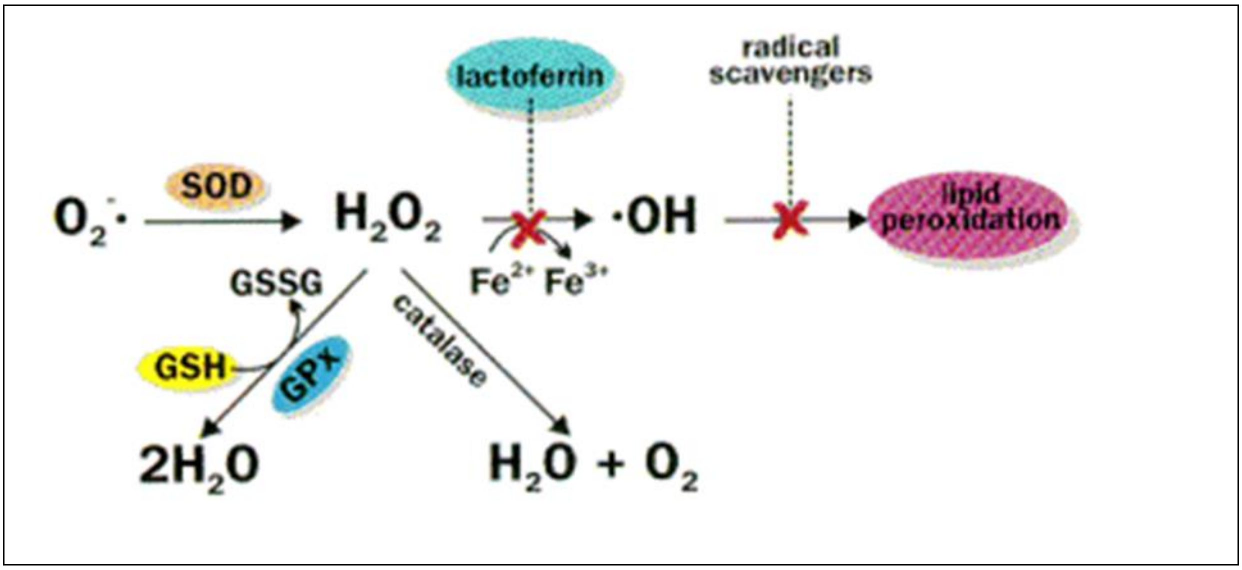

Fig. 2.1: Flow chart of defence mechanisms against damage caused by ROS.

Figure 2.1 shows the defence mechanisms whereby antioxidant enzymes operate against the damage caused by ROS. Superoxide dismutase (SOD) catalyses the dismutation of superoxide radicals to hydrogen peroxide (H_2O_2). The H_2O_2 is toxic and hence is removed in one of three ways. It can be converted to two molecules of water, catalysed by GPx in the presence of reduced glutathione (GSH) as a substrate, which converts to oxidised glutathione (GSSG). The second route is conversion of H_2O_2 to water and oxygen, catalysed by the enzyme catalase. The third pathway is conversion to hydroxyl ions (´OH). This latter problem could be overridden by minimising the concentration of the metal due to binding to a storage and transport protein (e.g. lactoferrin) (Somasundaram *et al.*, 2018).

Chapter 3

Materials and Methods

All the chemicals used in this study were purchased from Sigma-Aldrich, Sydney, Australia.

Spectrophotometric analyses were performed using a Shimadzu UV-visible spectrophotometer, model 1200 (Tokyo, Japan) Flame atomic absorption spectroscopy (FAAS) (Shimadzu, model 6400, Tokyo) was used for determination of trace elements, using inductively coupled plasma - optical emission spectrometry (ICP-OES) for multi-elemental analysis.

3.1 Synthesis of silver nanoparticles

The AgNPs were synthesised using a modified Carey (1889) method. The method was based on the reduction of $AgNO_3$ using ferrous sulphate heptahydrate, with trisodium citrate to cap the particles so that agglomeration does not occur. In this method 0.256 g of $AgNO_3$ was dissolved in 2.5 ml of deionised water to make a 0.603 M solution. A mixture of 2.5 ml of 1.076 M ferrous sulphate heptahydrate and 3.5 ml of 1.368 M trisodium citrate dihydrate was next added dropwise to the $AgNO_3$ solution with vigorous mixing using a magnetic stirrer. The colourless solution forms a dark brown precipitate, which was mixed for 2 min to produce a homogeneous brown-black AgNP suspension. The AgNP suspension was next transferred to a 50-ml Falcon™ tube and centrifuged at 1865 x g RCF for 10 min. The supernatant was discarded, and the pellet formed was re-suspended in 10 ml of 0.68 M trisodium citrate and re-centrifuged at 1.865 x g RCF for 10 min, the supernatant removed, and the pellet re-suspended in 10 ml of 0.68 M trisodium citrate. The last step was repeated four more times. Finally, the pellet was re-suspended in 10 ml of deionised water. The synthesised AgNPs were kept at 4°C pending quantification. The AgNP suspension was diluted with deionised water before use.

3.2 Quantitation of synthesised silver nanoparticles

The synthesised AgNPs (diluted with deionised water) were quantified by FAAS using the Merck certiPUR multi-elements standard (Merck, Dharmstadt). The linearity range used was 1.25, 2.5, 5 and 10 µg/ml. The concentration of the synthesised AgNPs varied between 12 and 13 mg/ml. The maximal absorbance of AgNPs was 400 nm (Fig. 3.1).

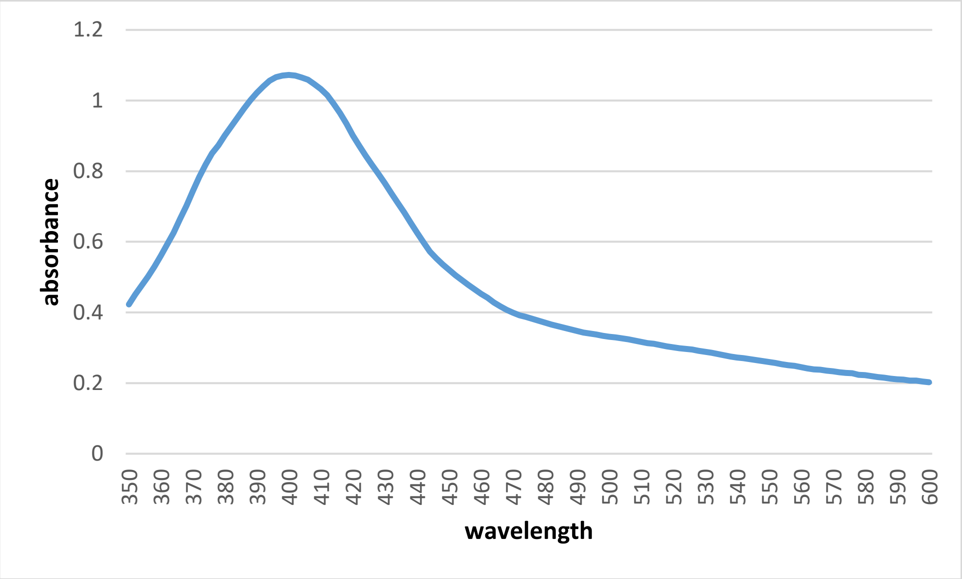

Fig. 3.1: UV spectrum of synthesised AgNPs (5 µg/ml in water). Maximum absorbance was at 400 nm.

3.3 Morphology of synthesised AgNPs

A transmission electron microscope (Philips CM 200 high resolution analytical TEM, Amsterdam, The Netherlands) fitted with a Gatan digital camera was used to characterise the morphology of AgNPs. The sample was diluted 1:1000 with deionised water before analysis to obtain a more uniform distribution. Approximately 10 µl of diluted sample was deposited onto each grid and left to dry under a fume hood. The citrate-coated AgNPs were spherical in shape and the diameter varied between 10 and 50 nm with the majority between 30 and 40 nm and an average of 35 nm.

3.4 Charge and particle size of AgNPs (using zetasizer)

Zeta potential is a measure of the magnitude of electrostatic forces between particles. Zeta potential determines the surface charge of NPs, which is an indicator of NP stability. The zetasizer can also measure the size distribution within a sample, usually performed with Dynamic Light Scattering (DLS). Both zeta potential and size distribution were performed by Dr Craig Bunt (Lincoln University) in the Otago University laboratory.

The average mean particle size and zeta potential of the synthesised AgNPs were determined using a Zetasizer Nano ZS (Malvern Instruments, Worcestershire, UK) at 25°C. The conditions of measurement were: He/Ne laser (wavelength 633 nm), scattering angle 90°, refractive index 1.33, and viscosity 0.887 mPa. Before measurement, the stock AgNP solution was diluted 200-fold with water. The average zeta potential of my synthesised AgNPs was −41 mV (Fig. 3.2).

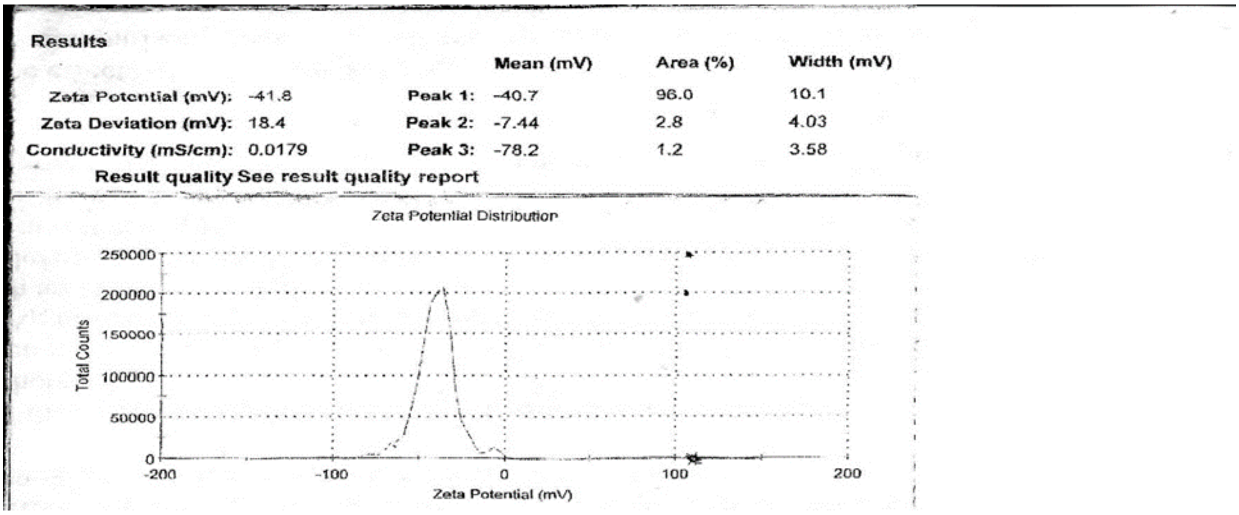

Results

			Mean (mV)	Area (%)	Width (mV)
Zeta Potential (mV):	-41.8	Peak 1:	-40.7	96.0	10.1
Zeta Deviation (mV):	18.4	Peak 2:	-7.44	2.8	4.03
Conductivity (mS/cm):	0.0179	Peak 3:	-78.2	1.2	3.58

Result quality See result quality report

Fig. 3.2: Zeta potential of AgNPs. Zeta potential = −41 mV (zeta deviation = −18.4 mV).

3.5 Soil parameters

Templeton silt loam (TSL) was used in the soil, plant and earthworm studies. The soil was air dried and passed through a 2-mm sieve prior to determination of pH, chloride, carbon and nitrogen concentrations. TLS was obtained from a non-grazed section of the Lincoln University commercial dairy farm, New Zealand.

3.5.1 Soil pH measurement

One gram of dried soil was mixed with 10 ml of deionised water in a 25-ml bottle (in triplicate) and placed on a shaker for 30 min, allowed to stand at room temperature on the work bench overnight, and the pH of the supernatant measured with a pH meter calibrated with pH buffers 4 and 7.

3.5.2 Determination of soil chloride concentration

Soil supernatants from 3.5.1 were filtered through a 0.2-µm membrane prior to analysis and 2 ml of the sample filtrate were used. Soil chloride concentration was determined using ion exchange chromatography (Dionex DX-2100 fitted with a Dionex AS-AP autosampler and integrated by Chromeleon Peaknet 6.8). The system has an Anion Self-Regenerating Suppressor (Dionex AERS 500) and detection was by conductivity. Samples were water extracts from plant or soil origin and were separated with a weak sodium carbonate / sodium bicarbonate eluent on a Dionex AS9-SC column (Dionex Corporation, Sunnyvale, California 940-3603, USA). The chloride concentration was 146.6 mg/l. The calibration curve was from 0.1 to 100 ug/ml. The result are presented as Mean ± SE (146.6 ± 25.97) from triplicates.

3.5.3 Determination of soil carbon and nitrogen concentrations

Combustion of soil at 900°C in an oxygen atmosphere converts elemental carbon (C) and nitrogen (N) into CO_2, N_2 and NO_x (Elementar, HmbH, Hnaa, Germany). NO_x was subsequently reduced to N_2, then passed through a thermal conductivity cell to determine CO_2 and N_2. The concentrations of C and N were 2.62% and 0.26% respectively.

3.5.4 Determination of soil moisture content

Soil samples (5 g) (in triplicate) were placed in a crucible and the weight recorded. The crucibles were kept in an oven maintained at 105°C for 24 h. The crucibles were covered and kept in a dissector to cool. The crucibles were reweighed and the weight recorded. The percentage of moisture content was calculated from the equation:

$$\text{Moisture content} = \frac{\text{fresh soil weight} - \text{dry soil weight x 100}}{\text{fresh soil weight}}$$

The soil moisture content was 22.5%.

3.5.5 Determination of field capacity

Field capacity is the amount of water held in soil after excess water has drained away after rain or irrigation, usually taking 2–3 days. Field capacity (expressed symbolically as Θ_{fc}) is defined as the bulk water retained in soil at −0.33 J/kg or −0.33 bar of hydraulic head or suction pressure (Grewal *et al.*, 1990). To determine the field capacity of soil, a metal column of 2 cm height was filled with 100 g of fresh soil. The volume of soil was determined using the equation $(7.3/2)^2 \text{ x } \Pi \text{ x } 2$, where 7.3 is column diameter, 2 is column height in cm, Π is a constant equal to 3.14 and 2 is fresh soil height. The value obtained was 83.7. Then the weight of the fresh soil was calculated using the equation 83.7 x 100 + 19/100 = 99.6 g, where 100 g is the fresh soil weight and 19% the moisture content of the fresh soil. The experiment was performed in triplicate. The columns containing 99.6 g of fresh soil were kept in a tank of 2 cm height filled with water to 2 cm height and transferred to a tension table (which provided the required suction pressure to remove the excess water) for 2–3 days to achieve equilibrium, followed by measuring the weight of each column. The columns were then incubated in an oven maintained at 105°C for 24 h. The column was re-weighed after drying. Finally, the soil was removed from the column and the weight of each empty column recorded. The field capacity was calculated using the following equation:

(Fresh soil weight after equilibrium − dry soil weight) x 100/(dry soil weight − empty column weight). The average field capacity recorded was 41%.

3.6 Sample preparation for ICP-OES analysis

3.6.1 Plant material

Plants were harvested and the different parts incubated at 65°C for 72 h to dryness and made into a powder using a tissue lyser (Tissuelyser II Qiagen, USA), for ICP-OES analysis for determination of Ag concentration.

3.6.2 ICP-OES analysis

Plant powder, soil or earthworms were digested using concentrated nitric acid and hydrochloric acid (3:1) aqua regia in a microwave (CEM MARS Xpress operating in selectable output of 0–1600 watts ± 15%; CEM Corporation, North Carolina, USA). The Ag concentration was determined using an ICP-OES (Varian 720, Australia). The calibration curve was constructed by serially diluting the Merck ICP standard (1 mg/ml) (Rahway, New Jersey, USA).

3.7 Determination of some physical properties of synthesised AgNPs

The physical properties of AgNPs measured included effect of pH, storage, temperature and UV radiation and these are explained in more detail in Appendix A.

Chapter 4

Mobility of Silver Nanoparticles and Silver Ions in the Soil–Plant System

4.1 Abstract

The widespread use of silver nanoparticles (AgNPs) as a bactericide will ultimately result in their increased concentration in soils. I measured the solubility, toxicity and plant uptake of both AgNPs and silver ions (Ag^+) in an immature pallic soil, Templeton loamy silt (pH = 5.1), and a Granular silt loam (pH = 6.0). The soil sorption of AgNPs was significantly greater than for Ag^+, and both moieties were more strongly sorbed at lower concentrations and higher pHs. From pH <4 to pH 8, K_D values increased from <10 up to c. 500 for Ag^+, and 100–10 000 for AgNPs. There was strong evidence that our citrate-coated AgNPs were transformed into Ag^+ during the course of the plant growth experiments and plant responses were similar for both the Ag^+ and AgNPs treatments. Soil concentrations >100 mg/kg significantly reduced the biomass of *Lolium perenne* and resulted in foliar concentrations of up to 10 mg/kg dry matter. At a soil concentration of 70 mg/kg, silverbeet and spinach accumulated 5–10 mg/kg Ag, which may present a human health risk. Regarding citrate-coated AgNPs, the environmental impact of environmental release is largely determined by the equivalent mass concentration of Ag^+, into which they will ultimately transform. Given the widespread interest in AgNPs, there has been a lack of basic research into Ag^+. This should be the subject of future research.

4.2 Introduction

Silver nanoparticles (AgNPs) are increasingly used due to their antimicrobial activity. As of 2015, >410 products on the global market contained AgNPs, with an annual global production >550 tonnes (Hedberg *et al*., 2015). Household and industrial waste may enter soil via the land application of treated municipal effluent or sewage sludge (Colman *et al*., 2013) or via industrial emissions. Potentially, AgNPs may accumulate in soil leading to reduced soil fertility (Shin *et al*. 2012; Peyrot *et al*. 2014), entry into food chains via plant uptake (Anjum *et al*. 2013), or leaching of Ag into groundwater.

Silver nanoparticles are insoluble, forming a colloidal solution when coated with citrate (Howe and Dobson, 2002). The behaviour of AgNPs in soil depends on their size and surface coating (Dong *et al*. 2009). Citrate coated AgNPs are more soluble and more persistent than their PVP-coated counterparts (McGillicuddy *et al*., 2017).

Through their surface coating, AgNPs may bind to soil colloids via specific adsorption (Pallavicini *et al*., 2014). As AgNPs may have a surface charge, they may also interact electrostatically with soil colloids, although Klitzke *et al.* (2015) reported that the surface charge had minimal effect on AgNPs' sorption. The degree of AgNPs sorption in soil is affected by pH, ionic strength and the organic matter content (Kleja *et al*. 2016), and fraction of dissolved organic matter (Van Koetsem *et al*. 2018). As with other moieties, AgNPs and Ag^+ sorption is higher in clay-rich soil than in sandy soil (Jacobson *et al*., 2005).

Ultimately, AgNPs will transform into Ag^+ in the environment (Liu and Hurt, 2010) and Ag^+ could enter soil solution from the oxidation of NPs or dissociation of adsorbed Ag from the soil (Benoit *et al*., 2013). Geochemically, Ag is classed as a chalcophile, often associated with sulphur (McLennan, 1998). The solubility and hence mobility of Ag^+ is limited by precipitation with chloride (Sagee *et al*. 2012), as well as the normal sorption processes affecting metal cations.

In soil, AgNPs concentrations as low as 0.14 mg/kg Ag can adversely affect soil biota (Colman *et al*., 2013). Cox *et al*. (2016) reported that AgNPs were more toxic than Ti_2O, resulting in higher oxidative stress and genotoxicity as well as lower seed germination and root elongation in *Arabidopsis thaliana, Oryza sativa, Lemna gibba* (duckweed), *Ricinus communis, Vigna radiata,* and *Cucurbita pepa* (zucchini). Exposure to >25 mg/kg of AgNPs and Ag^+ induces oxidative stress, similar to other trace elements (Kumari *et al*., 2009). The toxicity of AgNPs is size dependent, with smaller AgNPs (< 20 nm in diameter) being more penetrative and toxic than larger particles (Scherer *et al*., 2019).

AgNPs are deposited on the surface of the cell and organelles, resulting in growth inhibition in some plants such as radish sprouts (*Raphanus sativa*) (Zuverza-Mena *et al*., 2016), and lettuce (*Lactuca sativa*) at solution concentrations c. 10 mg/l (Gruyer *et al*., 2014). Paradoxically, other studies have shown that low concentrations of AgNPs increase the growth of *Brassica* spp. and *Eruca sativa* (Sharma *et al*., 2012a; Yin *et al*., 2012; Vannini *et al*., 2013), possibly through hormesis (Mattson and Calabrese, 2009).

Most previous work on plant uptake has focused on hydroponic cultures, which enables the precise measurement of soluble Ag and AgNPs, which can be used as a proxy for bioavailable Ag. There is a lack of information comparing AgNPs and Ag^+ on plant uptake from soil and relating this Ag in soil solution, as estimated using a dilute-salt extraction. I hypothesise that as AgNPs and Ag^+ will be retained by soil, manifold higher concentrations will be required to induce plant toxicity or significant plant-uptake.

I aimed to determine the solubility, toxicity and plant uptake of both AgNPs and Ag^+ in two distinct soil types and elucidate the risk of AgNPs accumulating in soil, leaching to groundwater or entering the food chain via plant uptake. I selected *Lolium perenne* (L.) for detailed investigation at several concentrations of Ag^+ and AgNPs, because this is one of the most commonly-occurring pasture species (Cunningham *et al.*, 1993). Nine edible plants (carrot, radish, leek, lettuce, parsley, rocket, beetroot, silverbeet, and spinach) were screened for Ag uptake when grown on soils spiked with AgNPs or Ag^+.

4.3 Materials and methods

4.3.1 Soils

Some 500 kg of soil of a typic immature pallic soil, a Templeton Loamy Silt (TLS), were collected from a non-grazed section of the Lincoln University commercial dairy farm, New Zealand (43°38’11.35” S, 172°26’17.00” E). A Granular Silt Loam (GSL) was collected from a commercial vegetable growing area in Pukekohe, New Zealand (37°13’18.92”S 174°52’5.94”E). After removing non-decomposed plant material, soils were collected from the top 0.25 m depth. The soil was homogenised using a spade, air dried and passed through a 7-mm sieve to remove large stones and roots. The soil was homogenised using a spade. A subsample (20 kg) of soil for the laboratory experiments was dried at 60°C until a constant weight was obtained and sieved to < 2 mm using a nylon sieve. The properties of the two soils are given in Table 4.1.

4.3.2 Nanoparticle preparation and zeta potential

Silver nanoparticles (AgNPs) were freshly prepared on the day of the experiments. Citrate-coated AgNPs were synthesised as described in Chapter 3, section 3.1. The zeta potential of AgNPs was determined as described in Chapter 3, section 3.1, 3.4

4.3.3 Preliminary experiments to determine the optimal extraction method

Batch experiments were used to determine the sorption of Ag^+ and AgNPs as a function of pH and Ag concentration. Preliminary experiments to determine the rate of sorption by the soil as a function of time revealed that there was little change in solution concentration after 120 min (Appendix C). Comparing different extractants revealed that 0.1 M KNO_3 resulted in measurable partitioning of Ag between the solid and solution phases (Appendix A). Thereafter, all experiments used 0.1 M KNO_3 agitated with soil for 120 min.

4.3.4 Ag sorption as a function of concentration and pH

Centrifuge tubes (50 ml) were filled with 5 g of soil. Solutions (30 ml of 0.1 M KNO_3) were added containing Ag at concentrations of 0 (control), 9, 19, 38, 75, 150, and 300 mg/l. Silver was added as either Ag^+ (as $AgNO_3$) or AgNPs. The solution pH was adjusted to values ranging from 2.8 to 8.3 after addition of the sorbent by adding 0, 0.1, 0.2, and 0.3 ml of HNO_3 (BDH ARISTAR nitric acid 70%, diluted 1:10) or 0.05, 0.1, 0.2, 0.4 ml KOH (BDH AnalaR KOH 2 M) to decrease or increase pH, respectively. Tubes were placed on an end-over-end agitator (20 rpm) for 2 h, then centrifuged for 20 min at 4700 rpm (4577 RCF). The supernatants were separated and centrifuged again using Ependorff tubes at 13 400 rpm (9,050 RCF) for 30 min and acidified using 1 ml of concentrated HNO_3.

4.3.5 Extractable Ag in incubated soils

Soil was spiked with 1000 mg/kg Ag, as either Ag^+ (added as $AgNO_3$) or AgNPs, and 2.5-g portions weighed into 45 centrifuge tubes (50 ml). The moisture content of the soils was adjusted to 30% (w/w). The soil in three tubes was extracted immediately with 15 ml of 0.1 M KNO_3, using the aforementioned methods. The remaining tubes were divided into three lots (21 tubes each) and placed either in a refrigerator at 4°C, in a laboratory cupboard at room temperature (20°C), or in an incubator at 35°C. The Ag in the soil from three tubes from each treatment was extracted deparately using KNO_3 after 1, 2, 4, 8 and 16 days.

4.3.6 Response of *Lolium perenne* to Ag^+ and AgNPs

Some 200 kg of soil was divided into 5-kg portions that were spiked with either Ag^+ ($AgNO_3$) or AgNPs to give concentrations of approximately 19, 39, 78, 156, 312, 625, 1250, 2500, 5000, or 10 000 mg/kg. Control soil without spiking was set aside. The spiking was achieved by preparing the 10 000 mg/kg using the silver salts and then diluting the mixture with unspiked soil. Subsamples were taken for chemical analyses to determine actual concentrations of Ag and other trace elements (Appendix D), and recovery of Ag from soil was determined (Appendix E). Each concentration was placed into three 1.5-L pots, moistened to field capacity, and left for 6 weeks to equilibrate in the greenhouse facility at Lincoln University. Some 50 seeds of *Lolium perenne* were sown into each pot and allowed to grow for 45 days. Pots were watered once daily to field capacity. The day/night temperatures during the experimental period were 12°C and 22°C respectively. The above-ground portions of the *L. perenne* plants were removed from 2 cm above the soil to reduce the risk of contamination with soil particles. Leaf, tiller, stem and seed material was thoroughly rinsed in deionised water then dried at 65°C until a constant weight was obtained. The dry weights were measured, and then the dried plant material was ground using a Retch ZM200 grinder and stored in sealed plastic vials for chemical analysis.

4.3.7 Uptake of Ag^+ and AgNPs by a selection of vegetables

Portions (100 kg each) of soil were spiked to 70 mg/kg with either Ag^+ (as $AgNO_3$) or AgNPs. A further 100 kg was set aside as a control. The control and spiked soils (~ 1.5 kg soil) were put into 1.5L pots (n = 135) and placed in a glasshouse at Lincoln University for 6 weeks to equilibrate. In December 2016, the pots were planted with either *Daucus carota* subsp. *sativus* (carrot), *Raphanus raphanistrum* subsp. *sativus* (radish), *Allium ampeloprasum* (leek), *Lactuca sativa* (lettuce), *Petroselinum crispum* (parsley), *Eruca vesicaria* subs. *sativa* (rocket), *Beta vulgaris* subsp. *vulgaris* (beetroot), *Beta vulgaris* subsp. *maritima*) (silverbeet/chard), or *Spinacia oleracea* (spinach). There were five replicates for each treatment (control, AgNPs or $AgNO_3$), giving a total of 15 pots for each of the nine species in the 2 test and 1 control group. Pots were watered daily to field capacity. When mature, the plants were harvested, and the edible portions excised and weighed. The harvest dates were: carrot (Feb 2017), radish (Jan 2017), leek (May 2017), lettuce (March 2017), parsley (April 2017), rocket (Jan 2017), beetroot (Feb 2017), silverbeet (Feb 2017), and spinach (Jan 2017). The edible portions were washed thoroughly in deionised water. Root vegetables (carrot, radish, and beetroot) were peeled first to remove any Ag-contaminated dust. The edible portions were dried, weighed again, ground using a Retch ZM200 grinder, and stored in sealed plastic vials for chemical analysis.

4.3.8 Chemical analyses

For both plants and soils, pseudo-total elemental analyses were carried out using microwave digestion in 8 ml of Aristar^{TM} nitric acid (± 69%), diluted with milli Q water to a volume of 25 ml and filtered using Whatman no. 52 filter paper (pore size 7 µm). The concentrations of Cd together with other elements (Ag, Ca, Mg, K, P, S, Cu, Zn, and Mn) were determined (Appendix D) using inductively coupled plasma optical emission spectrometry (ICP-OES Varian 720 ES – USA), as described in Chapter 3, section 3.6.2. For the batch extraction experiments, the solution Ag concentration was determined using a Shimadzu 6400 Flame Atomic Absorption Spectrophotometer (FAAS). A parallel ICP-OES analysis was carried out on randomly selected samples from the bulk samples to confirm the results of the AAS.

4.4 Data analysis

The distribution of Ag between the solid and solution phase, K_D, was calculated from batch experiments following the method of Simmler *et al*. (2013), shown in Eq 1:

$$K_D = \frac{Ag\ adsorbed\ (mg/kg)}{Ag\ in\ solution\ (mg/L)} = \frac{(C_{Ag\ Y/SO} - (C_{Ag\ Y/pH\ X} - C_{no\ Ag/pH\ X}))\ (mg/L)\ x\ \frac{0.03\ L}{0.005\ kg}}{(C_{Ag\ Y/pH\ X} - C_{no\ Ag/pH\ X})\ (mg/L)} \quad \text{Eq. 1}$$

where $C_{Ag\ Y/pH\ X}$ is the Ag solution concentration in the treatment in which the sorption is assessed. $C_{no\ Ag/pH\ X}$ is the Ag solution concentration measure in the treatment with the corresponding pH, without Ag spiking and $C_{Ag\ Y/SO}$ is the Ag solution concentration in the corresponding spiked treatment without addition of sorbent. K_D values can be considered dimensionless as 1 L of aqueous solution equals approximately 1 kg thereof.

Data were tested for normality before analysis. Log-normal data were log-transformed. Significant differences were determined using ANOVA with Fisher's Least Significant-Difference post-hoc test to compare means using Minitab® 17 (Minitab Inc., State College, Pennsylvania, USA). The level of significance was 0.05.

4.5 Results and discussion

The sorption of AgNPs and Ag^+ by the Templeton Silt Loam (TSL) and Granular Silt Loam (GLS) soils is shown in Fig. 4.1. The results show that at a given pH, the K_D value (sorbed / solution concentration coefficient) was some 10-fold higher for the AgNPs compared to the Ag^+. This indicates that Ag^+ is likely to be more mobile and therefore more toxic than AgNPs. These findings are in contrast to those of Wang *et al*. (2018), who reported that the sorption of AgNPs onto 10 soils was generally lower than the corresponding sorption of Ag^+ ions. These differences may be due to the type of coating of the AgNPs; my study used trisodium citrate, whereas Wang *et al*. (2018) used polyvinylpyrrolidone (PVP). Similarly, Rahmatpour *et al.* (2017) reported that PVP-AgNPs had similar sorption properties to Ag^+ ions in four calcareous soils. Differences in the surface chemistry of the AgNPs may have led to differences in specific adsorption processes. This highlights the importance of the type of surface coating when determining the environmental fate of NPs (Klitzke *et al*., 2015).

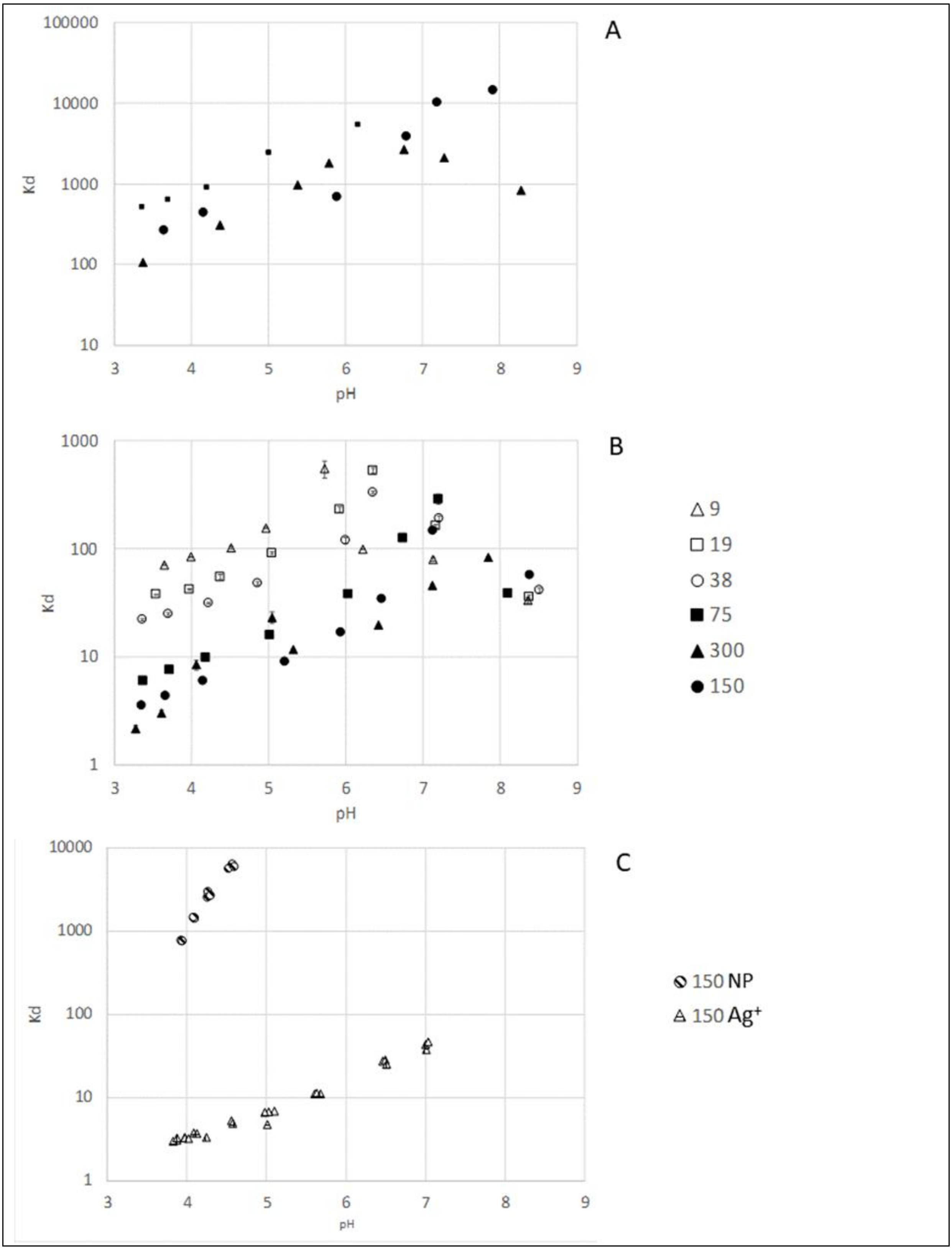

Fig. 4.1: Distribution coefficients (K_D = sorbed / solution concentration quotients) as a function of pH for Ag-nanoparticles in the Templeton Silt Loam (A), ionic silver in the Templeton Silt Loam (B), and both nanoparticles (NP) and ionic silver (Ag^+) in the Pukekohe granular soil (C). The legend indicates the initial concentrations in the ambient solution (mg/l). For A & B, bars indicate the standard error of the mean (n = 3).

The reduced sorption of both AgNP and Ag^+ ions at higher concentrations is consistent with other studies (Klitzke *et al*., 2015; Rahmatpour *et al*., 2017; Wang *et al*., 2018) and is likely due to saturation of binding sites in soil (Robinson *et al*., 2009). This mechanism may explain the significantly higher sorption of AgNPs compared to Ag^+ ions in my study. While the concentrations of AgNPs and Ag^+ ions were similar on a mass ratio concentration (i.e. mg/l in solution), the *molar* concentration of AgNPs is manifoldly lower than Ag^+ ions at a similar mass ratio concentration. The nanoparticles used in this study had an average radius of 12.5 nm, some 73 times larger than Ag^+ ions (0.172 nm). Therefore, the molar concentration of AgNPs will be some 300 000 times lower than Ag^+ ions at the same mass ratio concentration. Were AgNPs and Ag^+ ions compared on a molar basis, the sorption of AgNPs would be manifoldly lower than Ag^+ ions.

For both AgNPs and Ag^+, K_D increases with increasing pH. The behaviour of Ag^+ ions is similar to other cations in soil solution, where sorption increases at high solution pHs due to increasing sorption to variable-charged surfaces, increasing specific adsorption and decreasing the stability of precipitated salts (Robinson *et al*., 2009). The reason for the increase in AgNPs' sorption at higher pH values is less clear. Given that the AgNPs in this experiment were coated with citrate, which acquires a negative charge, I hypothesised that sorption may have been reduced at higher pHs. This increase in sorption may be explained if the citrate coating was removed, e.g. during the extraction process, or if the citrate coating itself became positively charged due to the sorption of cations. While I did not aim to elucidate the sorption mechanisms in this study, my findings are consistent with those of Wang *et al*. (2018), who reported that PVP-AgNPs primarily bound to Fe-oxides. In my results, the GSL, which is rich in Fe oxides (Table 4.1), sorbed some 5-fold more AgNPs than the TLS at similar pH values.

Fig. 4.2 shows the effect of incubation on the solubility of AgNPs and Ag^+ ions at 4°, 20°, and 35°C. For Ag^+ ions, sorption over 16 days significantly increased, with the largest increases occurring at the highest temperature. This is consistent with many studies that have demonstrate that trace elements become less soluble over time as a function of age (Mclaughlin *et al*., 1996), and occur due to increasing specific adsorption, occlusion by Fe and Al oxides, as well as sorption into soil colloids (Robinson *et al*., 2009). In contrast, incubation of AgNPs decreased their sorption for soil, with the largest decreases in sorption occurring at the highest incubation temperature (35^{o}C). This is consistent with the degradation of AgNPs into Ag^+ ions over time, a result also reported by McShan *et al*. (2014). Given that there was a significant decrease in sorption, even in the AgNPs incubated at 4^{o}C, it may be that over the course of several months all the AgNPs will transform into Ag^+ ions. Therefore, the potential for leaching and environmental toxicity of soils contaminated with AgNPs may increase with time. These findings indicate that the results of other studies may change dramatically if they are conducted on aged, rather than freshly spiked, soil.

Table 4.1: Properties of soils used in the extraction experiments and pot trials. Values in brackets represent the standard error of the mean (n = 3).

	Templeton Loamy Sand (TLS)[1]	**Granular Sandy Loam (GSL)[2]**
Sand/silt/clay (%)	76/20/4	15/60/25
pH (H_2O)	5.1	6.0
CEC (meq / 100 g)	12.3	22
C (%)	3.3 (0.03)	2.1
N (%)	0.3 (0.00)	0.2
P (mg/kg)	732 (11)	3414 (26)
S (mg/kg)	383 (6)	491 (6)
Ca (mg/kg)	3329 (58)	4147 (117)
Mg (mg/kg)	3426 (71)	2400 (95)
K (mg/kg)	2541 (279)	1951 (59)
Cd (mg/kg)	0.13 (0.00)	1.5 (0.03)
Zn (mg/kg)	70 (2)	173 (10)
Cu (mg/kg)	5 (0)	65 (1)
B (mg/kg)	7.3 (1.0)	33 (0)
Fe (mg/kg)	17727 (353)	44606 (96)
Mn (mg/kg)	357 (20)	1226 (12)
Ag (mg/kg)	<2	<2

[1]Data from Simmler *et al*. (2013). [2]Data from Al Mamun *et al*. (2016).
CEC is cation exchange capacity.

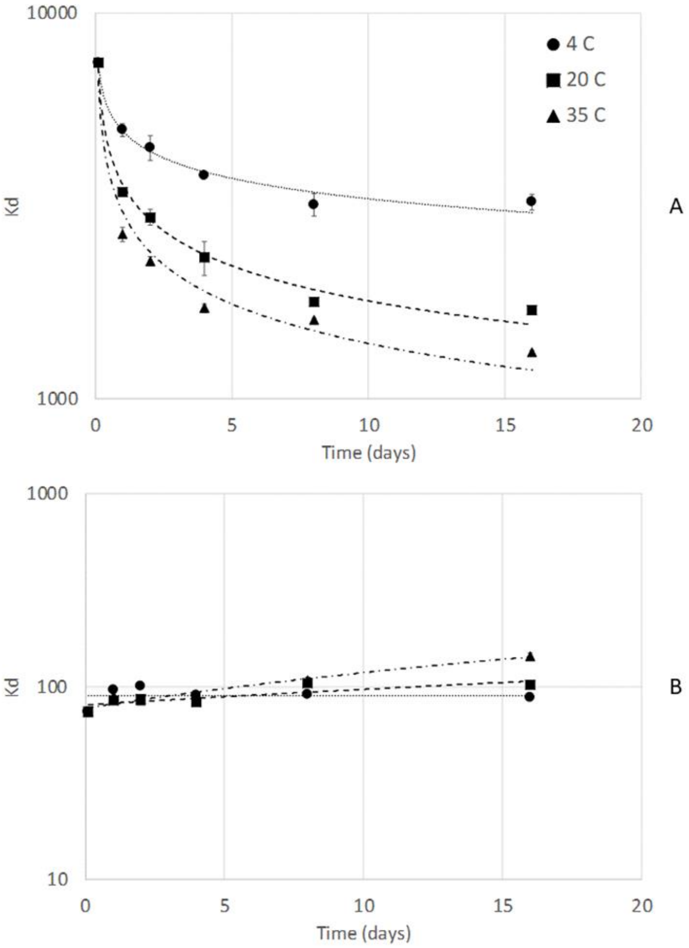

Fig. 4.2: Change in the distribution coefficient (K_D = sorbed / solution concentration quotients) as a function of incubation time at 4, 20, and 35°C for nanoparticles (A) and ionic silver (B) in Templeton Silt Loam. Error bars represent the standard error of the mean (n = 3).

Fig. 4.3A shows the effect of AgNPs and Ag^+ on the biomass index (treatment / control biomass quotient) of *L. perenne*. At soil concentrations < 100 mg/kg Ag, the Ag^+ ion treatment had a significantly higher biomass index compared to the AgNPs. Given that at Ag^+ ion concentrations of <10 mg/kg, the treatments were higher than the controls (i.e. biomass index > 1) these lower treatments had a stimulatory effect on plant growth. This is likely due to the nitrate that was added as a counter ion to the Ag^+ ions, rather than the Ag^+ itself. At concentrations > 625 mg/kg there was no growth in the Ag^+ ion treatments, whereas there was small but measurable growth of the *L. perenne* in the AgNPs treatments. Fig. 4.3B shows that there were no differences between the AgNPs treatment and the Ag^+ treatment with regard to Ag uptake by *L. perenne.* Given the transformation of AgNPs into Ag^+ ions (Fig. 4.2), it is likely that there were few material differences in the treatments during the experimental period as the soils were incubated for 6 weeks at 20°C prior to planting. The results show that at Ag concentrations (AgNPs and Ag^+ ions) of <100 mg/kg (where the biomass was not significantly different from the control) there was measurable plant uptake, with a bioaccumulation coefficient (plant / soil concentration quotient) of 0.01 – 0.1, with the maximum plant concentration c. 5 mg/kg occurring in soils with c. 100 mg/kg Ag.

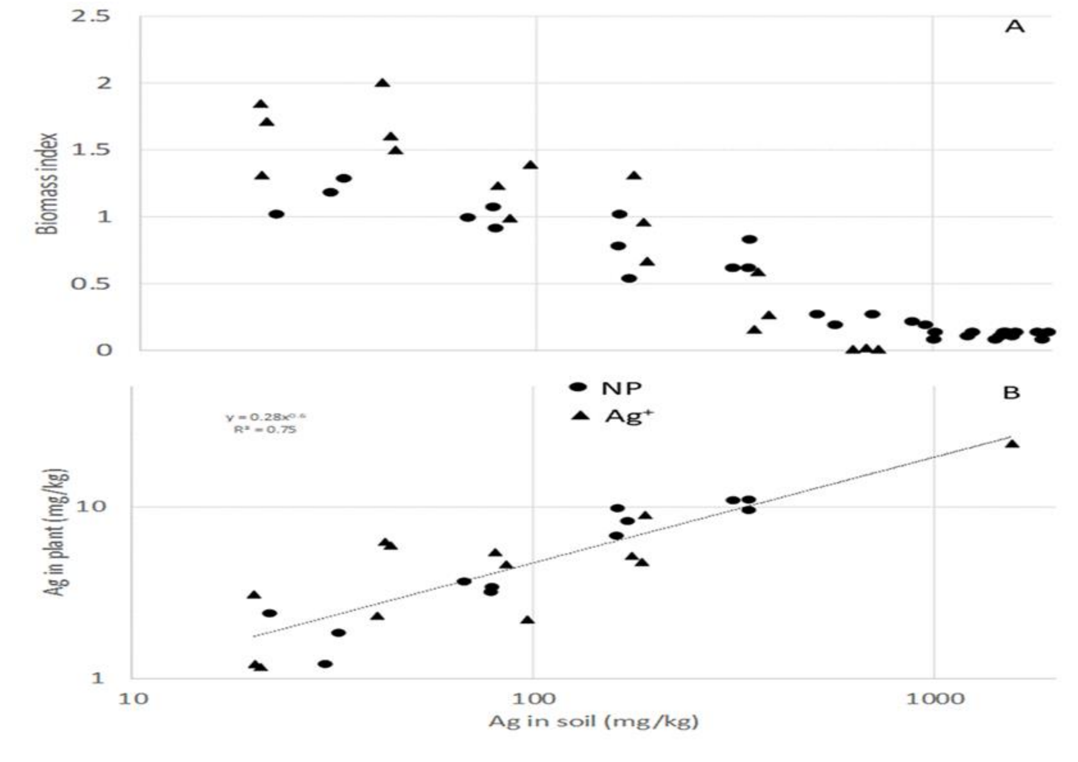

Fig. 4.3: (A) Plant biomass index (treatment / control mass quotient) as a function of Ag concentration in soil. (B) Leaf Ag concentration as a function of Ag concentration in soil.

Fig.4.4 shows the Ag uptake of nine vegetables grown in the TLS spiked with AgNPs or Ag^+ ions (at 70 mg/kg) and incubated for 48 h before planting. Except for lettuce, all the treatments accumulated significantly more Ag than the control. On average, the control plants took up 0.5 mg/kg Ag, and plants grown in soils spiked with AgNPs or Ag^+ ions took up an average of 3.8 and 3.5 mg/kg respectively. There were significant differences in Ag uptake between species, with the highest concentrations (5–9 mg/kg) occurring in carrots, silverbeet and spinach. There were no significant differences in plant Ag uptake between the AgNPs and Ag^+ ions treatments, except for radish and silverbeet, where there were small but significant differences.

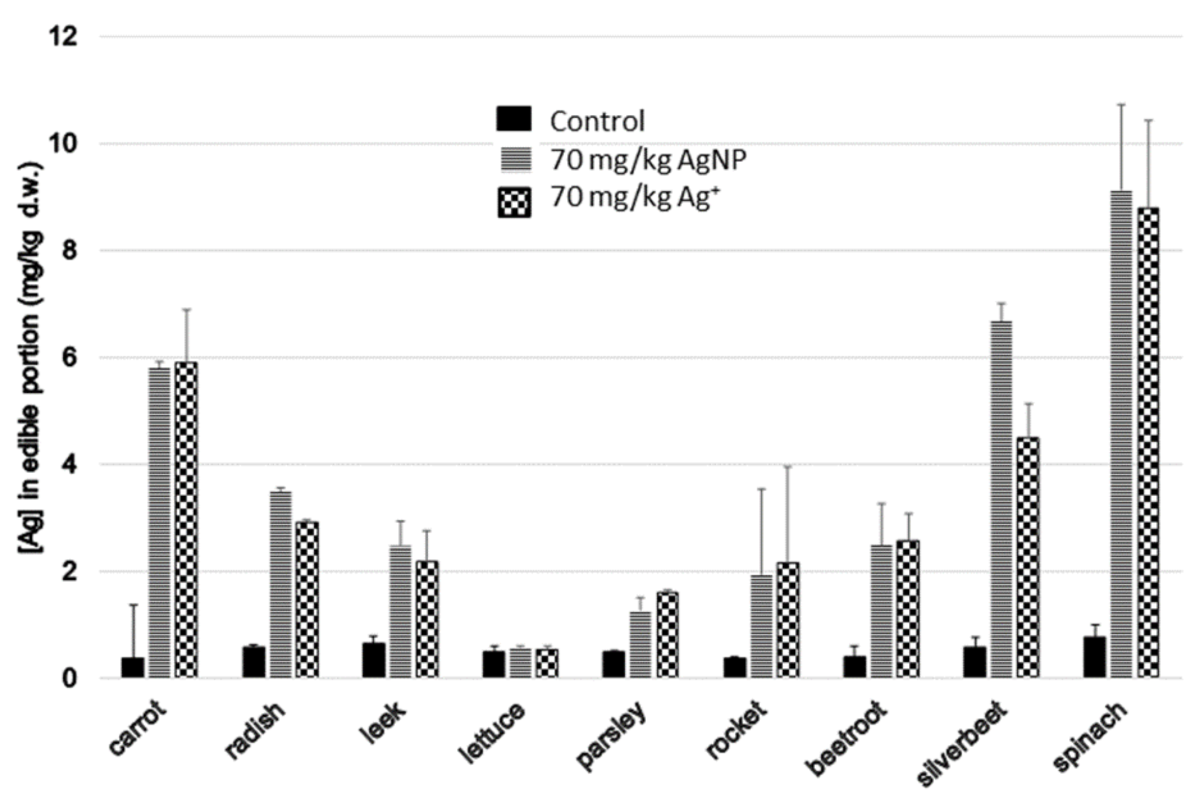

Fig.4.4: Silver concentration in the edible portions of plants grown in Templeton Silt Loam either without silver or spiked with 70 mg/kg either nanoparticles or ionic. Bars represent the standard error of the mean (n = 5).

Table 4.2 shows the mass of each vegetable that a 70-kg individual would need to consume to exceed the Tolerable Daily Intake (TDI) for Ag, which is set at 0.005 mg/kg/day USEPA 2018). For all vegetables except carrots, silverbeet, and spinach in the silver treatments, an individual is unlikely to exceed the TDI when following a normal diet. For spinach, the TDI may be exceeded by consuming as little as 38 g (dry matter).

Table 4.2: Mass required (dry matter) to exceed the tolerable daily intake of 0.005 mg/kg/day for a 70-kg person.

	Control	AgNPs	Ag^+
Carrot	921	60	59
Radish	603	100	120
Leek	538	141	161
Lettuce	714	603	648
Parsley	700	273	219
Rocket	921	179	162
Beetroot	875	141	136
Silverbeet	603	52	78
Spinach	449	38	40

These results indicate that there is a potential human health risk through consuming vegetables grown in Ag-contaminated soil. The vegetables in these experiments were peeled and washed. It is likely that more Ag would be consumed on unpeeled or poorly washed vegetables as significant amounts of Ag may be consumed via dust particles that are attached to the plant (Al Mamun *et al.*, 2017).

4.6 Conclusions

The soil sorption of AgNPs was significantly greater than for Ag^+, and both moieties were more strongly sorbed at lower concentrations and higher pHs. Similarly, at equal mass concentrations Ag^+ was some 10-fold more toxic than AgNPs, while the reverse was true if molar concentrations were compared. There was strong evidence that AgNPs were transformed into Ag^+ during the course of these experiments. Therefore, regarding citrate-coated AgNPs, the environmental impact of environmental release is largely determined by the equivalent mass concentration of Ag^+, into which they will ultimately transform. There is a large variation between plant species in Ag uptake, with some members of the Amaranthaceae (spinach & silverbeet) accumulating sufficient Ag to present a risk to human health. Given the widespread interest in AgNPs, there has been a lack of basic research into Ag^+; this should be the subject of future research.

4.7 Supplementary data

APPENDIX B: Comparison between different extractable solutions.

APPENDIX C: Rate of sorption by soil as a function of time.

APPENDIX D: Determination of trace elements in ryegrass exposed to AgNPs/Ag^+

APPENDIX E: Determination of recovery percent of AgNPs/Ag^+ from soil

APPENDIX F: Determination of elements in nine vegetables exposed to 70 mg/kg AgNPs/Ag^+

Chapter 5

Silver Accumulation in Different Parts of Sunflower

(*Helianthus annuus L.)*

5.1 Abstract

Silver ions (Ag^+) and silver nanoparticles (AgNPs) are increasingly entering the environment through the use and disposal of products impregnated with Ag for bactericidal purposes. The aim of this study was to investigate the distribution and concentration of Ag (from AgNPs/Ag^+) in plants (from root to shoot) with the sunflower (*Helianthus annuus* L.) used as a model plant. The distribution and concentration of Ag in the sunflower plant was studied following its exposure to 150 mg/kg AgNPs/Ag^+ in soil for 53 days. Both forms of Ag accumulated in roots>leaves>stem>flower>seed. In the control plant, the Ag concentrations were ~1.5 and 1.8 mg/kg in the root and leaf respectively. In the sunflower plants exposed to 150 mg/kg AgNPs, the Ag concentrations were 17.8 and 2.75 mg/kg in the root and leaf respectively and the corresponding values in plants exposed to Ag^+ were 15.6 and 9.3 mg/kg, possibly due to greater translocation of Ag^+ to leaves on exposure to $AgNO_3$. Exposure of sunflower to both AgNPs and Ag^+ caused growth inhibition and reduction in root size and this was most prominent in the plants exposed to Ag^+ although the Ag accumulation in these roots was relatively less than in the plants exposed to AgNPs but not significantly different.

5.2 Introduction

Silver nanoparticles comprise metallic Ag [Ag (0)], vary in size between 1 and 100 nm in diameter, and are usually spherical shaped with a negative or positive surface charge depending on the coating material used. These AgNPs can enter the soil mainly through sewage sludge (Schlich *et al.*, 2013a), released by such industries as medical and pharmaceutical, textile and socks, kitchenware and toothpaste producers. Therefore, AgNPs can enter the environment via industrial effluent and when these products are used or disposed of (McGillicuddy *et al.*, 2017). Additional anthropogenic sources of Ag in soil include atmospheric deposition (especially from ore processing), landfills with household refuse, industrial wastes, and leaching of metal tailings (Smith and Carson, 1977). Boyle (1968) estimated that the average Ag content of soils (except for mineralised zones such as mining areas) is ~ 0.30 mg/kg and the average abundance in the Earth's crust is 0.10 mg/kg. Silver concentrations in soils classified by land use are ~ 0.13 kg/mg (residential), 0.19 mg/kg (agricultural), and 0.37 mg/kg (industrial) (Klein, 1972).

Silver can be phytotoxic to plants, causing cellular damage by disrupting a plant's metabolic processes. Tolerance to Ag toxicity may involve similar mechanisms as for other plant stressors, including other toxins and climatic extremes (Sharma *et al.*, 2012b). The effects of AgNPs on vascular plants are of particular concern. Since plants closely interact with soil, water and the atmosphere, Ag could transfer from contaminated environments, including from soil, to food plants, exposing consumers in the food chain to Ag (Miralles and Tamara, 2012). Silver has been found in some plants, such as up to 40 mg/kg in *Lolium multiflorum*, and 1 mg/kg in *Arabidopsis thaliana, Oryza sativa,* and *Vicia faba* (Mazumdar and Ahmed, 2011; Yin *et al.*, 2011; Patlolla *et al.*, 2012; Wang *et al.*, 2013).

Sunflower (*Helianthus annuus* L.) was used in this study as an example to examine the distribution and accumulation of Ag from AgNPs/Ag^+ in different parts of the plant, because it is an important oil seed crop (Murthy and Seshaiah, 1974). It is used for energy production, biogas and biodiesel, medical applications, as a food, and also in rhizo-filtration to remove heavy metals from soil (Dushenkov *et al.*, 1995; Putt, 1997; Singh and Singh, 2010).

Because AgNPs are used in many products, including pesticides used in some greenhouse crops grown hydroponically, Ag may accumulate in the rhizosphere (San and Don, 2013). Gruyer *et al.* (2014) investigated the effect of AgNPs on plants and found that the root length was increased in barley but inhibited in lettuce and radish. Generally, the toxicity of AgNPs/Ag^+ on the plants depends on plant species, growth medium, concentration of AgNPs/Ag^+ used, and the exposure time (Tripathi *et al*. 2017a).

Thuesombat *et al.* (2014) investigated the effect of particle size of AgNPs on *Oryza sativa* L. using particle sizes of 20, 30, 60, 70, 120 and 150 nm at different concentrations (0.1, 1, 10, 1000 mg/l). They found that seed germination and seedling growth were inhibited at lower particle sizes and at higher AgNPs concentrations.

Garcia *et al.* (2006) irrigated sunflower cultivated in soils amended with 500 mg/l of heavy metals Cd, Pb, Zn, and Cu separately and also as a mixture in soil for 40 days, with daily irrigation. The sunflower plants grown in such amended soil decreased in mass and height by 35–40% respectively. The leaves became more fragile, and the plants possessed fewer roots. Plants exposed to Cd showed stem necrosis closer to the root, and those exposed to Pb and Zn showed twisted stems.

Silver nanoparticles affect several plant growth parameters including leaf surface area, chlorophyll, and carbohydrate concentration (Krizkova *et al.*, 2008). Salama (2012) studied the effect of AgNPs on the growth of common bean (*Phaseolus vulgaris* L.) and corn (*Zea mays* L.). Fifteen millilitres from five concentrations of AgNPs (20, 40, 60, 80, 100 mg/kg) in triplicates were added daily to fertile loam soil in pots (14 x 18 x ¾ cm) for 12 days. The concentration of AgNPs < 60 mg/kg promoted plant growth while high concentrations (80–100 mg/kg) caused phytotoxicity. Silver nanoparticles generally induce ROS and thereby cause oxidative stress in plant species, and affect gene expression, genotoxicity, and inhibit seed germination and root size (Cox *et al*., 2016).

Qian *et al*. (2013) studied the impact of both AgNPs and Ag^+ at 0.2, 0.5, and 3 mg/l concentrations on *Arabidopsis thaliana* in Murashige and agar media at physiological, ultrastructural and molecular levels. The authors reported, first, that at 3 mg/l AgNPs, germination was unaffected. As seedlings grew, however, both AgNPs and Ag^+ had an inhibitory effect on root length and fresh weight of the plant, with AgNPs having a stronger inhibitory effect than Ag^+ in a dose-dependent manner. The root inhibition of plants exposed to 3 and 0.5 mg/l AgNPs were 74.4% and 34.5% that of control plants after a week, and 91.7% and 58.6% after 2 weeks' exposure. Second, transmission electron microscope study and metal content determination showed that AgNPs could accumulate in the leaves and disrupt the thylakoid membrane structure and decrease chlorophyll content. The authors concluded that AgNPs (10-nm particle size) were more toxic than Ag^+. Yin *et al*. (2011) reported that AgNPs' toxicity to *Lolium multiflorum* may be direct or through AgNPs delivering dissolved Ag to critical biotic receptors, with smaller particles (6 nm) causing more toxic effect than larger ones (25 nm). This study investigated the distribution and concentration of Ag throughout the sunflower plant (from root to shoot), on exposure to 150 mg/kg AgNPs/Ag^+ in soil for 53 days.

5.3 Materials and methods

5.3.1 Preparation of AgNPs

The synthesis of the AgNPs used in this study and their size (30 nm) determination are described in Chapter 3, sections 3.1and 3.3 respectively.

5.3.2 Soil

The test soils are described in Chapter 3, section 3.5.

5.3.3 Experimental design

About 100 kg of TSL soil was collected (coordinates 43°38'44.67"S and 172°27'3.19"E), sieved and dried. The soil was divided into three portions of about 33 kg each. One portion was mixed with

AgNPs to an Ag concentration of 150 mg /kg, and a second for an equivalent amount of Ag with $AgNO_3$. The third portion was the control soil. The test soils with AgNPs or Ag^+ were first mixed in a container, using a pestle, and then were transferred to a second container for more mixing, and then back to the first container again for a thorough mixing. This process was repeated 10 times for each soil to achieve complete mixing. Then 20 kg of each mixed soil was distributed between four 8-L pots (5 kg in each) and the moisture adjusted to field capacity. Three sunflower seeds were planted in each pot, followed by water addition to approximate field capacity as described in Chapter 4. On day 25, two sunflower plants were removed from each pot and disposed of, leaving one test plant per pot. These plants were harvested on day 53, and the different plant parts collected separately: roots, root hairs, the stem divided into four equal parts, leaves, flower, seed base, and seed. The different plant parts were divided into two portions. The contents of one portion were put into an oven bag, dried at 65°C for 72 h for complete drying, and then powdered in a tissue analyser (Tissuelyser II Qiagen, USA). The powder was then subjected to aqua regia digestion to determine the concentration of Ag and those of several other elements (Ca, Cu, K, Mg, Mn, Na, P, S, Zn) using ICP-OES as described in Chapter 3, section 3.6.2. The other portion was kept in plastic bags and stored at −20°C for analysis of antioxidant enzymes, lipid peroxidation, peroxidation, chlorophyll A and B and total carotenoids, total soluble protein, total phenolic compounds, total soluble carbohydrates, urease enzyme, and antioxidant vitamins, as described in Chapter 6.

5.3.4 Other analyses

Determination of soil pH, soil chloride concentration, soil C and N, moisture content, field capacity, sample preparation, and ICP-OES operation are described in Chapter 3.

5.4 Statistical analysis

Data were tested for normality before analysis. Log-normal data were log-transformed. Significant differences were determined using ANOVA with Fisher's Least Significant Difference (LSD) post-hoc test to compare means using Minitab® 17 (Minitab Inc., State College, Pennsylvania, USA). The level of significance was 0.05.

5.5 Results

Exposure of sunflower plants to 150 mg/kg AgNPs/Ag^+ for 53 days led to many morphological changes compared to the controls. The plants exposed to AgNPs/Ag^+ remained similar to controls for about 25 days (Fig. 5.1).

5.1: Sunflower seeds grown in three different media (TSL control soil, and soil mixed with 150 mg/kg AgNPs or Ag^+ at 25 days from cultivation. All the plants appeared to be in good health and there was no difference in plant morphology between the three groups.

Thereafter plants grown in soil amended with AgNPs/Ag^+ appeared stunted and unable to support their own weight (Fig. 5.2). The leaves became chlorotic and were reduced in size. The flowers were smaller and seeds were fewer in number. However, at harvest time the stem length was ~185 cm in control plants, and ~110 cm and 80 cm in plants exposed to AgNPs and Ag^+respectively. The Ag accumulated more in upper part of the stem, where the plant was most affected (Fig. 5.2).

Fig. 5.2: Sunflower plants just before harvest (53 days after sowing). Those exposed to AgNPs/Ag^+ had become weak, stunted and fallen down ~~b~~ecause the stems were too weak.

The Ag treatments from both AgNPs/Ag^+ resulted in reduced root size and root compared with the control (Fig. 5.3). The roots from the plants in soil amended with AgNPs showed a marked decrease in size with a reduced amount of root and only a few root hairs. Compared to the plants grown in AgNPs, those grown in soil mixed with Ag+ had the smallest root size with very few or no root hairs.

Fig. 5.3: Sunflower root growth at harvest 53 days after seed planting.

The Ag concentration in root hairs was 25-fold greater than in the roots (Fig. 5.4). The amounts of Ag in plants exposed to AgNPs and Ag^+ were 160- and 125-fold respectively that of the sunflowers planted in control soil.

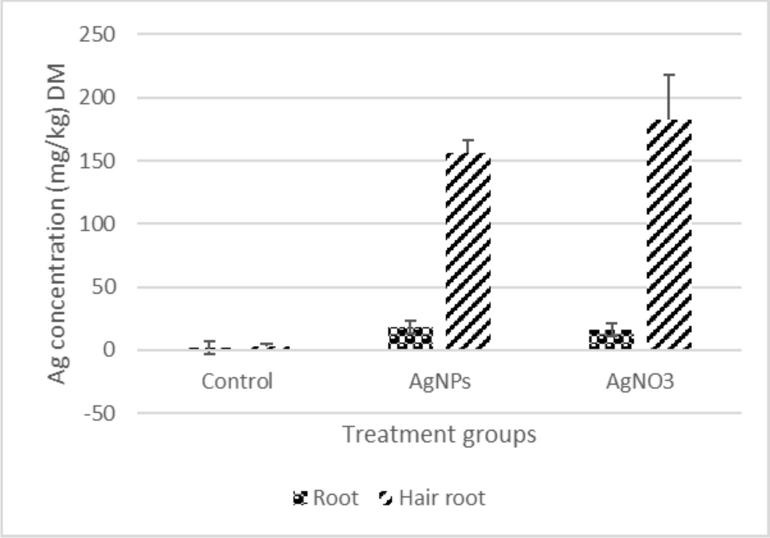

Fig. 5.4: Accumulation of silver (Ag) in roots and root hairs of sunflower plants exposed to control, AgNPs, or $AgNO_3$ amended soils.

Figure 5.5 shows the amount of Ag from AgNPs/Ag^+ in different parts of the sunflower plants, where Ag was accumulated in leaves significantly more than in the other parts. The Ag concentration in leaves of plants exposed to Ag^+ was more compared to that in plants exposed to AgNPs or the controls. All parts of sunflower plants cultivated in soil amended with AgNPs/Ag^+ showed more Ag accumulation than control plants. It is evident from Figs 5.4 and 5.5 that Ag accumulation in roots > leaves > stem, with the accumulation by plants exposed to Ag^+ > AgNPs.

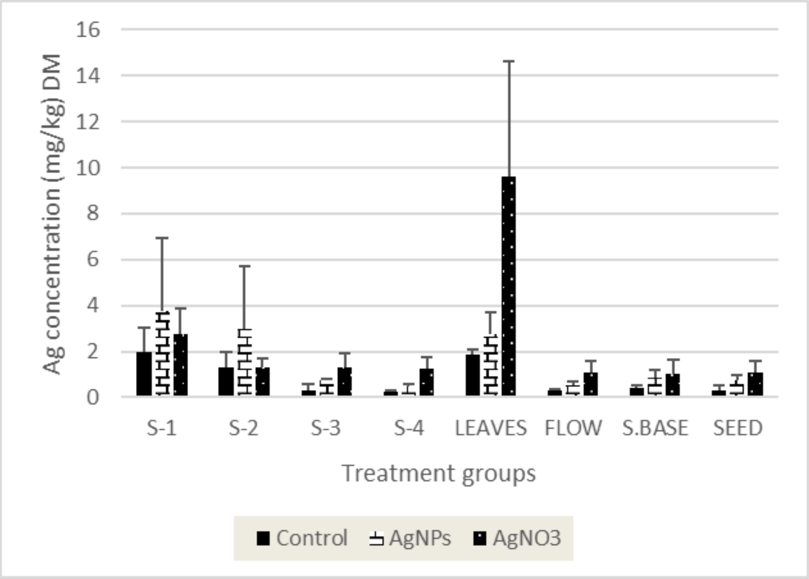

Fig. 5.5: Distribution of Ag in different parts of sunflower plants exposed to AgNPs/Ag^+ for 53 days. (S1, S2, S3, S4 refer to stem sections 1, 2, 3, and 4.)

Table 5.1 shows the effect of Ag on Ca, Cu, and K, with the concentration of Ca inhibited significantly in stem sections 2, 3, and 4, seed base and seed, but there was no significant effect on leaves. Copper was reduced significantly in all parts of the plant on exposure to AgNPs/Ag^+ but not significantly different between the plants exposed to AgNPs and Ag^+, but significant reductions in all parts of sunflower were evident when the two test treatments were compared with the control, as follows: Ag^+ > AgNPs > control. Potassium was inhibited significantly in all parts of the sunflower except in stem section 4 and seed. The amount of K found in plants was higher in those exposed to AgNPs > Ag^+ > control.

Table 5.1: Determination of calcium (Ca), copper (Cu), and potassium (K) in sunflowers exposed to 150 mg/kg AgNPs/Ag^{+}. Results expressed as mean ± SE (n = 4). Superscript letters shown for each plant segment are significantly different ($P < 0.05$).

Element	**Ca**	**Cu**	**K**
Part 1: Root			
Control	5129 ± 422 ^{a}	3.38 ± 0.18 ^{a}	2089 ± 650 ^{a}
AgNPs	4077 ± 273 ^{ab}	2.31 ± 0.22 ^{b}	13156 ± 330 ^{b}
Ag^{+}	3135± 110 ^{b}	1.58 ± 0.13 ^{c}	5903 ± 1811 ^{c}
Part 2: Root hair			
Control	10040 ± 91 ^{a}	21 ± 1.35 ^{a}	37365 ± 973 ^{a}
AgNPs	8748 ± 704 ^{a}	13 ± 0.67 ^{b}	23469 ± 4994 ^{a}
Ag^{+}	6054 ± 322 ^{a}	8 ± 0.49 ^{c}	14163 ± 3666 ^{a}
Part 3: Stem (S-1)			
Control	6974 ± 568 ^{a}	1.48 ± 0.03 ^{a}	32938 ± 9399 ^{a}
AgNPs	5789 ± 174 ^{a}	0.82 ± 0.02 ^{b}	26503 ± 2217 ^{ab}
Ag^{+}	5555 ± 301 ^{a}	0.98 ± 0.14 ^{b}	30690 ± 1521 ^{b}
Part 3: Stem (S-2)			
Control	10684 ± 177 ^{a}	1.51 ± 0.12 ^{a}	5361 ± 763 ^{a}
AgNPs	57761 ± 291 ^{b}	0.72 ± 0.05 ^{b}	23469 ± 14172 ^{ab}
Ag^{+}	7502 ± 188 ^{c}	0.9 ± 0.21 ^{b}	30690 ± 9164 ^{b}
Part 3: Stem (S-3)			
Control	9369 ± 716 ^{a}	1.45 ± 0.21 ^{a}	26597 ± 1207 ^{a}
AgNPs	8777 ± 374 ^{a}	0.81 ± 0.01 ^{b}	17704 ± 6273 ^{ab}
Ag^{+}	6041 ± 365 ^{b}	0.81 ± 0.19 ^{b}	4143 ± 670 ^{b}
Part 3: Stem (S-4)			
Control	10860 ± 117 ^{a}	2.44 ± 0.19 ^{a}	30783 ± 18486 ^{a}
AgNPs	9953 ± 722 ^{b}	0.74 ± 0.01 ^{b}	21729 ± 4229 ^{a}
Ag^{+}	8260 ± 330 ^{b}	0.95 ± 0.2 ^{c}	12974 ± 1668 ^{a}
Part 4: Leaves			
Control	40939 ± 830 ^{a}	15 ± 1.69 ^{a}	42964 ± 824 ^{a}
AgNPs	38815 ± 2001 ^{a}	2.86 ± 0.76 ^{b}	36940 ± 2987 ^{b}
Ag^{+}	37044 ± 1692 ^{a}	2.72 ± 0.2 ^{b}	27882 ± 417 ^{b}
Part 5: Flower			
Control	11080 ± 830 ^{a}	11 ± 0.75 ^{a}	30300 ± 281 ^{a}
AgNPs	8903 ± 117 ^{a}	2 ± 0.8 ^{b}	27515 ± 931 ^{ab}
Ag^{+}	4815 ± 262 ^{b}	2 ± 0.6 ^{b}	24911 ± 417 ^{b}
Part 6: Seed base			
Control	22333 ± 2113 ^{a}	13 ± 1 ^{a}	4101 ±1215 ^{a}
AgNPs	14871 ± 624 ^{b}	1.43 ± 0.15 ^{b}	20666 ± 935 ^{b}
Ag^{+}	12147 ± 849 ^{b}	1.43 ± 0.31 ^{b}	19778 ±1683 ^{b}
Part 7: Seed			
Control	15926 ± 1003 ^{a}	13 ± 0.24 ^{a}	19720 ± 2035 ^{a}
AgNPs	10274 ± 969 ^{ab}	2 ± 0.37 ^{b}	19362 ± 433 ^{a}
Ag^{+}	53041 ± 1256 ^{b}	1.4 ± 0.24 ^{b}	16232 ± 357 ^{a}

Table 5.2 shows that the concentration of Mg in the root stem sections 3 and 4 > leaves > seed base. The manganese concentration was significantly reduced in all parts of the plant, with the highest concentration in the control > AgNPs > Ag^{+}.

Table 5.2: Determination of magnesium (Mg), manganese (Mn), and sodium (Na) in sunflower exposed to 150 mg/kg AgNPs/Ag^{+}. Results expressed as mean ± SE (n = 4). Superscript letters shown for each plant segment are significantly different ($P < 0.05$).

Element	**Mg**	**Mn**	**Na**
Part 1: Root			
Control	930 ± 66 ^{a}	58 ± 9 ^{a}	20804 ±649 ^{a}
AgNPs	549 ± 18 ^{b}	22 ± 3 ^{b}	13156 ± 330 ^{b}
Ag^{+}	453 ± 11 ^{b}	19 ± 2 ^{b}	5903 ± 1810 ^{b}
Part 2: Root Hair			
Control	2124 ± 264 ^{a}	133 ± 18 ^{a}	12307 ± 1833 ^{a}
AgNPs	1963 ± 208 ^{a}	50 ± 6 ^{ab}	6818 ± 1220 ^{b}
Ag^{+}	1551 ± 129 ^{a}	13 ± 0.59 ^{b}	4655 ± 814 ^{b}
Part 3: Stem (S-1)			
Control	1551 ± 16 ^{a}	58 ± 8 ^{a}	7211 ± 2611 ^{a}
AgNPs	1401 ± 306 ^{a}	23 ± 2.5 ^{b}	2757 ± 657 ^{ab}
Ag^{+}	975 ± 31 ^{a}	13 ± 1 ^{b}	422 ± 12 ^{b}
Part 3: Stem (S-2)			
Control	2101 ± 150 ^{a}	68 ± 13 ^{a}	446 ± 136 ^{a}
AgNPs	1675 ± 161 ^{a}	28 ± 4 ^{b}	245 ± 20 ^{ab}
Ag^{+}	993 ± 73 ^{b}	14 ± 2 ^{b}	58 ± 4 ^{b}
Part 3: Stem (S-3)			
Control	2030 ± 387 ^{a}	63 ± 8 ^{a}	1266 ± 963 ^{a}
AgNPs	1447 ± 201 ^{ab}	33 ± 3 ^{b}	140 ± 42 ^{b}
Ag^{+}	984 ± 75 ^{b}	11 ± 0.7 ^{c}	27 ± 5 ^{c}
Part 3: Stem (S-4)			
Control	1865 ± 233 ^{a}	70 ± 15 ^{a}	116 ± 41 ^{a}
AgNPs	1741 ± 234 ^{ab}	28 ± 3 ^{b}	101 ± 5 ^{a}
Ag^{+}	1066 ± 110 ^{b}	14 ± 2 ^{b}	38 ± 3 ^{a}
Part 4: Leaves			
Control	4187 ± 196 ^{a}	253 ± 38 ^{a}	93 ± 7 ^{a}
AgNPs	3248 ± 133 ^{b}	155 ± 14 ^{b}	90 ± 7 ^{a}
Ag^{+}	2724 ± 117 ^{b}	59 ± 5 ^{c}	73 ± 0.2 ^{a}
Part 5: Flower			
Control	1635 ± 107 ^{a}	48 ± 8 ^{a}	283 ± 85 ^{a}
AgNPs	1463 ± 75 ^{a}	28 ± 3 ^{a}	75 ± 9 ^{b}
Ag^{+}	1385 ± 49 ^{a}	13 ± 2 ^{a}	50 ± 6 ^{b}
Part 6: Seed Base			
Control	4102 ± 245 ^{a}	118 ± 21 ^{a}	117 ± 65 ^{a}
AgNPs	2750 ± 100 ^{b}	57 ± 13 ^{b}	37 ± 4 ^{b}
Ag^{+}	2018 ± 121 ^{c}	21 ± 4 ^{b}	31 ± 1 ^{b}
Part 7: Seed			
Control	1741 ± 105 ^{a}	77 ± 11 ^{a}	94 ±10 ^{a}
AgNPs	1298 ± 122 ^{a}	30 ± 8 ^{b}	73 ± 18 ^{ab}
Ag^{+}	1291± 50 ^{a}	12 ± 0.3 ^{b}	50 ± 3 ^{b}

Table 5.3 shows that P was inhibited in all stem sections, leaves, and seeds, while the effect of Ag significantly reduced Zn content in all stem sections and seeds. Sulphur was significantly inhibited in

leaves only and it is possible that this might have played a role in green leaves turning yellow in the plants exposed to both Ag^{+} and AgNPs (Fig. 5.2).

Table 5.3: Phosphorus (P), sulphur (S), and zinc (Zn) concentrations in different parts of the sunflower plant exposed to 150 mg/kg AgNPs/Ag^{+}. Results expressed as mean ± SE (n = 4). Superscript letters shown for each plant segment are significantly different ($P < 0.05$).

Element	**P**	**S**	**Zn**
Part 1: Root			
Control	1440 ± 88 ^{a}	1646 ± 37 ^{a}	13 ± 1 ^{a}
AgNPs	641 ± 66 ^{b}	402 ± 41 ^{b}	12 ± 0.8 ^{a}
Ag^{+}	1204 ± 386 ^{a}	445 ± 9 ^{b}	17 ± 3 ^{a}
Part 2: Root hair			
Control	2664 ± 313 ^{a}	2067 ± 322 ^{a}	54 ± 9 ^{a}
AgNPs	2049 ± 249 ^{a}	1646 ± 37 ^{a}	52 ± 6 ^{a}
Ag^{+}	1392 ± 61 ^{a}	1298 ± 124 ^{a}	41 ± 2 ^{a}
Part 3: Stem (S-1)			
Control	1081 ± 66 ^{a}	2097 ± 333 ^{a}	31 ± 3 ^{a}
AgNPs	521 ± 121 ^{b}	230 ± 11 ^{b}	22 ± 2 ^{ab}
Ag^{+}	256 ± 9 ^{b}	186 ± 22 ^{b}	18 ± 4 ^{b}
Part 3: Stem (S-2)			
Control	909 ± 62 ^{a}	596 ± 84 ^{a}	26 ± 2 ^{a}
AgNPs	503 ± 79 ^{b}	256 ± 21 ^{b}	16 ± 1 ^{b}
Ag^{+}	235 ± 18 ^{c}	187 ± 3 ^{b}	11 ± 2 ^{c}
Part 3: Stem (S-3)			
Control	1150 ± 127 ^{a}	349 ± 38 ^{a}	17 ± 0.5 ^{a}
AgNPs	460 ± 67 ^{b}	295 ± 31 ^{ab}	12 ± 1 ^{b}
Ag^{+}	377 ± 40 ^{b}	190 ± 34 ^{b}	7 ± 0.7 ^{c}
Part 3: Stem (S-4)			
Control	1863 ± 100 ^{a}	439 ± 64 ^{a}	15 ± 2 ^{a}
AgNPs	1251 ± 163 ^{b}	455 ± 110 ^{a}	9 ± 0.6 ^{b}
Ag^{+}	677 ± 125 ^{c}	349 ± 38 ^{a}	7 ± 0.1 ^{b}
Part 4: Leaves			
Control	3180 ±130 ^{a}	3502 ± 180 ^{a}	45 ± 2 ^{a}
AgNPs	2664 ± 82 ^{b}	2814 ± 142 ^{b}	38 ± 0.3 ^{a}
Ag^{+}	2176 ± 42 ^{c}	710 ± 104 ^{c}	30 ± 3 ^{b}
Part 5: Flowers			
Control	3184 ±485 ^{a}	1639 ± 154 ^{a}	51 ± 6 ^{a}
AgNPs	2917 ± 138 ^{a}	1572 ± 128 ^{a}	47 ± 7 ^{a}
Ag^{+}	2143 ± 146 ^{a}	1284 ± 136 ^{a}	35 ± 6 ^{a}
Part 6: Seed base			
Control	4791 ± 499 ^{a}	2892 ± 403 ^{a}	31 ± 3 ^{a}
AgNPs	4087 ± 430 ^{a}	1951 ± 66 ^{b}	34 ± 1 ^{a}
Ag^{+}	3622 ± 222 ^{a}	1428 ± 45 ^{b}	27 ± 6 ^{a}
Part 7: Seed			
Control	3641 ± 209 ^{a}	2521 ± 461 ^{a}	66 ± 2 ^{a}
AgNPs	2508 ± 146 ^{b}	1837 ± 20 ^{a}	50 ± 1 ^{b}
Ag^{+}	2117 ±41 ^{b}	1672 ± 91 ^{a}	37 ± 3 ^{c}

5.6 Discussion

It was evident that exposure of the sunflower plant to AgNPs/Ag^+ affected a variety of parameters. There was a decrease in chlorophyll probably caused by an inhibition of chlorophyll synthesis and hence a decrease in photosynthesis. Silver nanoparticles/Ag^+ can generate ROS, which can damage chloroplasts (Lavelle, 2015) resulting in growth retardation and eventually death of the plant (Fig. 5.2). This effect was most obvious in plants grown in soil amended with Ag^+, which is consistent with the findings of Vishwakarma *et al.* (2017). Qian *et al.* (2013) exposed *Arabidopsis thaliana* to 0.2, 0.5, and 3 mg/l of AgNPs/Ag^+ and observed that AgNPs were more toxic to *A. thaliana* than Ag^+, which does not agree with my findings. Such differences are possible because of the different plants, soil and concentrations of AgNPs/Ag^+ used in the two studies.

Figure 5.3 shows the morphological changes in sunflower roots following exposure to AgNPs/Ag^+ for 53 days compared to the control. The root size in plants exposed to 150 mg/kg Ag^+ and AgNPs was about 75% and 50% respectively that of the control, and also there was root hair loss compared to the control. Krizkova *et al.* (2008) showed that exposure to Ag^+concentrations of 0, 0.1, 0.5, 1 mM results in a significant reduction in root hair and causes necrosis of the exodermis. Elevated Ag concentration in plant tissues can increase ROS formation, which can result in reduced root size, loss of root hair, disruption of many metabolic processes and DNA damage (Hassan *et al.*, 2017). The reduction in root size and lack of root hairs in my study indicated toxicity of AgNPs/Ag^+ to the roots, which is in agreement with the Krizkova *et al*. (2008) study. These changes were more predominant in plants exposed to Ag^+ than AgNPs. The exact reason for the decrease in root size is not known but Krizkova *et al*. (2008) suggested a higher metabolic activity and a change in water transport, which could alter the anatomical structure of the root.

The effect of Ag on sunflower plant roots also includes damage to the root cell wall and formation of vacuoles in the root. This damage could be due to the large particles penetrating and entering through small pores in cell walls resulting in a decline in rhizodermal cells followed by necrosis and later replacement by exodermal cells (Mazumdar, 2014). Salama (2012) exposed *Phaseolus vulgaris* L. and *Zea mays* L. plants to 20, 40, 60, 80, 100, 200 mg Ag/kg soil and observed that the lengths of shoots and roots increased at lower Ag concentrations up to 60 mg/kg soil but decreased at higher Ag concentrations. In my study, I used only one concentration of AgNPs or Ag^+ (150 mg/kg) but for a longer duration (53 days), with no morphological changes evident during the initial 25 days, but at harvest (53 days) stem length, leaf number and size, flower size and seed base size had declined compared to the control. These changes were most obvious in sunflowers exposed to Ag^+. The Salama (2012) study differed from mine in the type of plant used, dose and length of exposure, and the effect of only AgNPs concentration, with a decrease in protein concentration in the plant observed with Ag at 100 mg/kg. Pardha-Saradhi *et al.* (2018) exposed sunflowers and wheat to 10, 25, 50 and 100 mg/l of AgNPs and Ag^+ and they observed similar results to mine.

In my study, the stems of sunflowers grown in soil amended with AgNPs/Ag^+ at 150 mg/kg were reduced in size, weak and sagging (Fig. 5.2), which could be attributed to a decline in the absorption of essential nutrients and water because of the small root size and lack of root hair caused by Ag. One of the reasons that AgNPs are less toxic than Ag^+ is due to sulfidation, where AgNPs react with some ligands found in the soil such as sulphur (S), thiolate or carboxylate, forming compounds that are less toxic and less soluble such as Ag_2S-NP, and hence less AgNPs are absorbed through root cells thus minimising their toxic effects (Doolette *et al*., 2015).

5.6.1 Effect of Ag on macro- and micro-nutrients

Calcium as calcium pectate is responsible for holding together cell walls of the plant and thus stem rigidity (Demarty *et al.*, 1984). When a plant is Ca deficient (Table 5.1), new tissues such as root and shoot tips exhibit distorted growth resulting in improper cell formation. This may be one of many reasons why the stems of plants exposed to AgNPs/Ag^+ become curved initially at the upper parts of the plant, which ultimately results in drooping of the plant (Buechel, 2018). The reduction in Ca concentration in plants exposed to the two Ag forms also could be attributed to the decrease in the expression of the Ca channel protein, leading to a reduction in Ca uptake (Maathuis, 2009).

Copper is an essential element for plant growth, and is involved in electron transfer and redox reactions, a cofactor in photosynthetic mitochondrial respiration and in oxidative stress response.

Potassium is an essential element and plays an important biological role in activating enzymes and protein synthesis, in addition to transportation of proteins to the aerial parts of the plant via the xylem (Garcia *et al.*, 2006). In my study both AgNPs/Ag^+ decreased the K concentration in most parts of the sunflower plant. Both Azad *et al*. (2011) and Qian *et al.* (2013) reported that K^+ was decreased on exposure of sunflowers to $Pb(NO_3)_2$, which agrees with my findings.

Magnesium is an integral part of chlorophyll. Table 5.2 shows a marked decline in Mg concentration, with a significant difference between the control and sunflower plants exposed to AgNPs/Ag^+, with the Mg concentration in the control plants > plants exposed to AgNPs > those to Ag^+. Deficiency of Mg causes chlorosis where the old leaves of the plant turn yellow first and this extends to younger fresh leaves later. Also, Mg deficiency causes a reduction in the root and stem size (Guo *et al.*, 2016).

Those authors also found that in sunflowers there was an inverse relationship between Ca and K, and an increase in Ca and K was accompanied by a decrease in Mg concentration.

According to Table 5.3 both AgNPs and Ag^+ significantly reduced the S concentration in leaves only, where the young leaves became chlorotic first before older leaves, causing a reduction in leaf size.

Zinc is an essential micronutrient element for a variety of cellular functions and is required for plant growth. It acts as a cofactor for several enzyme reactions involved in carbohydrate and energy metabolism, energy transfer, protein synthesis, and biochemical pathways in plants containing Zn. However, Zn at high concentrations is toxic to the plant causing growth inhibition, increased root thickness and retardation of cell division (Mustafa and Komatsu, 2016). Table 5.3 shows that there was no significant difference in Zn concentration in parts of the sunflower plants except for the stem and seed, where there was a significant inhibition in Zn concentration, with the concentration in Ag^+ > AgNPs > control.

5.7 Conclusion

Silver nanoparticles and Ag^+ affected the sunflower plants markedly, by inhibiting root growth; causing weakness of the stem because of deficiency in Ca, which promotes adherence of the cell walls, resulting in upper parts of the plant having less leaves and bending especially in plants exposed to Ag^+; and colour change to yellow due to S deficiency. Plants exposed to AgNPs/Ag^+ showed significant inhibition in essential nutrients such as Ca, Cu, Zn, Mn, P. Overall, the results showed that Ag accumulates in the root > leaves > stem. The toxic effects were most pronounced in plants exposed to Ag^+ > AgNPs.

Chapter 6

Toxicity of Silver Nanoparticles / Silver Ions to Sunflower

6.1 Abstract

When plants grow in soil contaminated with Ag, the Ag becomes concentrated in roots and leaves and its effects are reflected in crop health and yield. This study focussed on the toxicity of AgNPs/$AgNO_3$ (Ag^+) to sunflowers grown in soils amended with 150 mg/kg of Ag either as AgNPs or $AgNO_3$. The basis for choosing this dose was a study carried out where a dose of 200 mg/kg was mildly toxic to ryegrass (unpublished observation).

Exposure of sunflower plants to soils containing AgNPs/$AgNO_3$ increased LPO, antioxidant enzymes (CAT, SOD, GST, GPx), peroxidases (pyrogallol peroxidase, guaiacol peroxidase), oxidases (ascorbate oxidase), urease enzymes, total phenolic compounds, antioxidant vitamins (retinols, alpha-tocopherol and L-ascorbic acid) and inhibited production of chlorophyll, total carotenoids, total soluble proteins and total soluble carbohydrates. In general, Ag+ increased the above-mentioned parameters in sunflower more than did AgNPs except for the tested vitamins, which increased and were mostly affected by AgNPs.

6.2 Introduction

Sunflower is an herbaceous annual plant belonging to the Asteraceae family. Its botanical name is *Helianthus annuus* L. Sunflower plants produce grey to white conical-shaped seeds with a smooth surface and each flower head contains hundreds of edible oil seeds. These seeds are an excellent source of health-benefiting nutrients lsuch as water- and fat-soluble vitamins; for example, 100 g of seeds contain approximately 35.17 g of alpha-tocopherol. The seeds also contain a good number of essential macro elements such as Mg, and P and micro-minerals such as Cu, Mn and Se (selenium). The seeds are packed with essential polyunsaturated fatty acids, linoleic acid and oleic acid. Sunflower seeds are also a good source of proteins and amino acids that are essential for growth of young children. Because sunflower has the ability, to some extent, to extract toxic elements from soil, it has been planted in contaminated soils to clean the soil of such elements (Vineetha, 2014).

The exposure of sunflower to AgNPs/Ag^+ causes oxidative stress and creates reactive oxygen species (ROS), and as a result activity levels of antioxidant defence enzymes and lipid peroxidation increased; in addition Ag can cause environmental damage such as soil infertility (Sairam *et al.*, 2003; Anjum *et al.*, 2013)

Treatment of sunflower with 0.5 mM Fe (II), Cu (II) or Cd (II) for 12 h increased peroxidation and lipoxygenases when exposed to sunlight, but decreased chlorophyll A & B and GSH (reduced glutathione) concentrations by 30%, 40%, and 15% respectively (Gallego *et al.*, 1996). Some free radical scavengers such as mannitol and sodium benzoate have been shown to prevent the decrease in chlorophyll and GSH, and increases of LPO and lipoxygenase. Exposure of sunflower to Fe^{2+} and Cd^{2+} ions decreased SOD while Cu^{2+} ions increased SOD. However, all these metals increased a variety of other antioxidant enzymes such as catalase, ascorbate peroxidase, glutathione reductase and dehydroascorbate reductase. Free radical scavengers such as sodium benzoate or mannitol protected many of these enzymes from inactivation, but not SOD. Excesses of Fe, Cu and Cd produce oxidative damage in sunflower leaves (Gallego *et al.*, 1996).

The impact of biocompatible magnetic nanofluid (MNF-Fe_3O_4) on sunflower chlorophyll concentration showed an interdependent relationship based on second-degree polynomial function (Pîrvulescu *et al.*, 2015). There was an average increase in chlorophyll concentration of between 1.01 and 4.58 SPAD units (chlorophyll content measurement based on leaf transmittance at 650 and 940 nm).

Sunflower plants exhibit a strong potential to form Ag^+ from AgNPs compared to *Basella alba* (Basellaccea), *Oryza sativa, Saccharum officinarum, Sorghum bicolor* and *Zea mays* (Poaceae) (Leela and Vivekanandan, 2008). When peanuts were cultivated in sandy soil amended with different doses of AgNPs (50, 500 and 2000 mg/kg) for 98 days, physiological parameters including biomass height, grain weight and yield were reduced (Rui *et al.*, 2017). Sewalem *et al*. (2014), studying the role of sunflower as a potential phytoremediator of heavy metals, found that 88.8% of Cd accumulated in roots, inducing low levels of lipid peroxidation and membrane leakage and poor root growth, while 71.4% of Pb was translocated to the shoots and hence affected photosynthesis.

AgNPs at concentrations of 20, 40, 60, 80 and 100 mg/kg negatively affect leaf surface area, chlorophyll, carbohydrate, all of which affected the growth of common bean (*Phaseolus vulgaris* L.) and corn (*Zea mays* L.), promoting plant growth at low doses and inhibition at high concentrations (Salama, 2012).

Exposure of *Bacopa monnieri* to Ag^+ and AgNPs enhanced peroxidase and catalase activity (Krishnaraj *et al.*, 2012). Qian *et al.* (2013) studied the effect of Ag on the transcription of antioxidant and aquaporin genes, and the balance between antioxidant and oxidant status and concluded that

AgNPs were more toxic than Ag^+ (in $AgNO_3$). When watermelon plants were exposed to 0, 30, 60, 90 and 200 mg/l of Ag^+ applied at intervals of 8 days throughout the crop cycle, a dose responsive increase in Ag concentration occurred in both roots and shoots and the amount of antioxidant in fruits increased by 3-fold in those exposed to 30 mg/l Ag^+ but the lycopene concentration declined (Cabrera-de la Fuente *et al.*, 2014).

The aim of this study was to investigate the effects of AgNPs and Ag^+ (in $AgNO_3$) on antioxidant defence enzymes such as SOD, CAT, GPx, GST, and antioxidant vitamins (A, E and C), ascorbate oxidase, guaiacol peroxidase, pyrogallol peroxidase, and urease. The study also investigated any decrease in protein expression, chlorophyll A and B, total carotenoids, carbohydrate and also LPO.

6.3 Materials and methods

6.3.1 Silver nanoparticle synthesis, quantification and morphology

As described in Chapter 3, sections 3.1, 3.2 and 3.3.

6.3.2 Charge measurement and particle size using zetasizer

As described in Chapter 3, section 3.4.

6.3.3 Experimental design

As described in Chapter 5, section 5.3.2.

6.3.4 Chemicals and reagents

As described in Chapter 5, section 5.3.

6.3.5 Soil pH

As described in Chapter 3, Table 3.1.

6.3.6 Soil total carbon and nitrogen

As described in Chapter 3, Table 3.1.

6.3.7 Soil chloride and moisture content in soil

As described in Chapter 3, section 3.5.2 and 3.5.4.

6.3.8 Soil field capacity measurement

As described in Chapter 3, section 3.5.5.

6.3.9 Sunflower leaf homogenisation

The frozen sunflower leaves were homogenised with liquid N_2 and the powder was stored at −20°C until analysis.

6.3.10 Leaf preparation to measure antioxidant enzymes

One gram of leaf material in liquid N_2 was homogenised with 3 ml 0.1 M phosphate buffer (pH 6.8) using a homogeniser (FJ 200, GAO SU FEN SAN JUN 2HI JI Shanghai Specimen and Model Factory homogeniser - China) in ice and centrifuged (Beckman, model J2-MI USA) at 16 000 rpm (30 390 RCF) for 20 min at 4°C and the supernatant was collected for antioxidant enzyme analysis.

Calculation of enzyme activity

This is described in Appendix G.

Catalase

Catalase enzyme activity was measured by the method described by Havir and McHale (1987). Briefly 50 µl of leaf extract was added to 3ml of a solution containing 50 mM potassium phosphate buffer (pH 7) and 20 mM hydrogen peroxide. The decrease in absorbance was measured at 240 nm wavelength every 30 s for 2 min (Ɛ = 43.6 M/cm).

Superoxide dismutase

The SOD was measured according to the method of van Rossum *et al.* (1997). Briefly, 50 µl of leaf homogenate was mixed with 2.95 ml solution of 50 mM potassium phosphate solution pH 7.8 containing 26 mM L-methionine, 75 µl nitro blue tetrazolium chloride (NBT), 100 µM EDTA and 20 µM riboflavin. The reaction was in a chamber under illumination of a 30 W fluorescent lamp at 25°C. The reaction was started by turning the fluorescent lamp on, and it was turned off after 5 min. The blue formazan produced by NBT photoreduction was measured as an increase in absorbance at 560 nm every 30 s for 2 min (Ɛ = 2640 M/ cm).

Glutathione-S-transferase

The assay was based on the method reported by Habig *et al.* (1974), a conjugation reaction between GST and 1-chloro-2,4-dinitobenzene (CDNB). Briefly, 0.1 ml of homogenised leaves was added to 2.8 ml of phosphate buffer (pH 6.5) and next 0.1 ml of CDNB was added. The increase in absorbance was recorded at 340 nm, every 30 s for 2 min (Ɛ = 9.6 M/cm).

Glutathione peroxidase

The assay used was based on the method described by Rotruck *et al.* (1973) with slight modifications. The following were mixed together: 0.4 ml of 0.4 M sodium phosphate buffer (pH 7), 0.1 ml of 10 mM sodium azide, 0.2 ml of 4 mM reduced glutathione, 0.1 ml of 2.5 mM hydrogen peroxide, 0.2 ml water and 0.5 ml leaf homogenate. Then 1 ml of 5,5-dithiobis-(2-nitro benzoic acid (DTNB) in 1% sodium citrate reagent was added. The absorbance of the colour developed at 412 nm was measured every 30 s for 2 min (Ɛ = 6422 M/cm).

Lipid peroxidation

The assay of TBARS measures MDA, which is formed by the LPO of lipids. MDA was measured based on the method of Buege and Aust (1978) with slight modifications. The reaction mixture was prepared by dissolving 3.75 g of TCA in 10 ml of 0.25 N hydrochloric acid, and 0.094 g of thiobarbituric acid in 2 ml of methanol. The two solutions were mixed and completed to 25 ml by adding 0.25 N hydrochloric acid. One millilitre of leaf homogenate was mixed with 2 ml of reaction mixture and boiled in a water bath for 15 min. The mixture was allowed to cool and then centrifuged at 4577 RCF for 5 min. The pink colour developed was measured at 532 nm (Ɛ = 163.8 M/cm).

Ascorbate oxidase activity

This was measured based on the method of Vines and Oberbacher (1965). Briefly, 8.8 mg of ascorbic acid was dissolved in 300 ml of phosphate buffer (pH 5.6) (extraction buffer). Then 100 µl of leaf homogenate was added to 3 ml of extraction buffer and the decrease in absorbance was measured at 265 nm every 30 s for 5 min (Ɛ = 7 M/cm).

Pyrogallol peroxidase activity

The assay was carried out by the method of Addy and Goodman (1972). Briefly, 0.1 ml of leaf homogenate was added to the reaction mixture composed of 0.1 M phosphate buffer (pH 6.8) containing 0.05 pyrogallol and 1% hydrogen peroxide. The increase in absorbance was measured at 430 nm every 30 s for 2 min (Ɛ = 4.5 M/cm).

Guaiacol peroxidase

In this assay 2 ml of reaction mixture consisting of 20 mM guaiacol, 20 mM hydrogen peroxide, 50 mM phosphate buffer (pH 6.8) was added to 25 ul of leaf extract, and incubated at 30°C for 10 min. The reaction was stopped by adding 0.5 ml of sulphuric acid and the absorbance was recorded at 480 nm every 30 s for 2 min (Ɛ = 26 600 M/cm) (Urbanek *et al.*, 1991).

Chlorophyll and total carotenoids

The chlorophyll and total carotenoids were measured based on the method of Sumanta *et al.* (2014). Briefly, 0.5 g of homogenised sunflower leaf was mixed with 10 ml of methanol for 15 min at 4°C and centrifuged at 4,577g RCF, 4°C and 4700 rpm for 10 min. Then 0.5 ml of supernatant was mixed with 4.5 ml of methanol. The solution mixture was analysed for chlorophyll A & B and also total carotenoids. The absorbance was measured at 470 nm for total carotenoids and at 665.2 nm for chlorophyll A (CA) and at 652.4 nm for chlorophyll B (CB).

Equations used for chlorophyll and total carotenoids calculations

A. For chlorophyll A: Absorbance at 665.2 nm x 16.72 - Absorbance at 652.4 nm x 9.16

B. For chlorophyll B: Absorbance at 652.4 nm x 34.09 - Absorbance at 665.2 nm x 15.28

C. For total carotenoids: Absorbance at 470 nm x 1000 -1.63 x CA - 104.96 x CB / 221.

Total soluble carbohydrate

The method was based on the method of Dubios *et al*. (1956). In short (from 1 g sunflower leaf was mixed with 3 ml 0.1 M phosphate buffer (pH 6.8), centrifuged as described earlier and 100 µl supernatant was mixed with 900 µl of extraction buffer (phosphate buffer pH 6.8) followed by addition of 5 ml concentrated sulphuric acid. The mixture was incubated on a hot block at 50 °C for 10 min. The red colour developed was measured at 490 nm. The concentration of total soluble carbohydrate was calculated from a calibration curve using D-glucose as the standard (within the range 0–10 mg/ml).

Total phenolic compounds

This assay was based on the method of Ainsworth and Gillespie (2007). Briefly, 0.2 g of homogenised sunflower was mixed with 0.8 ml of ice cold methanol and incubated at room temperature (RT) in the dark for 48 h, then centrifuged at 10 000 x g for 5 min. Next, 0.1 ml of the supernatant was mixed with 0.1 ml of Folin-Ciocalteu reagent to which was added 15 g of lithium sulphate and 5 ml of water, mixed and made upto 100 ml with water. The working reagent was 1 ml Folin-Ciocalteu reagent and 9 ml of water. The solution was vortexed, 0.8 ml of 700 mM sodium carbonate added and incubated at RT for 2 h. The absorbance was measured at 765 nm. Gallic acid was used as the standard within the range 0–200 ug/ml.

Total soluble protein

The Bradford (1976) method was used with minor modifications. Briefly, 950 µl water was added to a 10-µl sample (1 g homogenised sunflower leaf mixed with 3 ml of phosphate buffer (pH 6.8)) and to this was added 1 ml of diluted Bradford reagent (1 part reagent + 4 parts water). The solution was mixed and incubated at RT for 5 min. The absorbance was measured at 595 nm. The calibration curve was constructed using serum albumin within the range 0.312 to 10 µg/ml.

Urease

This assay was based on the alkaline phenol reaction (Krizkova *et al.*, 2008). Briefly, 0.25 g of leaf sample powder was homogenised with 5 ml of 30% ethanol in a 50-ml centrifuge tube. The sample was vortexed at 300 rpm for 30 min at 8°C, then centrifuged at 50 000 x g for 10 min. Next, 20 µl from the supernatant was added to 896 µl of hypochlorite solution (composed of 12% sodium hypochlorite, 0.4 M Na_2HPO_4 and 0.37 M NaOH). The pH was adjusted to 12. Next, 84 µl of phenol solution (composed of 7% phenol containing 34 mg of sodium nitroprusside) was added. The mixture was incubated at 37°C for 15 min. After an incubation period, the difference in absorbance between 630 and 670 nm was measured.

Vitamins A and E

Both vitamins A and E could be included in one extraction and measured using an isocratic HPLC with two detectors – UV and fluorescence detection – based on the method of Chotyakul *et al.* (2014) with some modifications. Briefly, 1 g of liquid-nitrogen-homogenised sunflower leaf was mixed with 5 ml of hexane for 25 s followed by centrifugation for 20 min at 4°C and 4700 rpm. Then 3 ml of the supernatant was evaporated under a gentle stream of N_2 at 45°C. The residue obtained was dissolved in 200 µl of methanol and 20 µl was injected onto an isocratic high performance liquid chromatograph (HPLC) (Aligant- 3170, Malgrave, Victoria, Australia).

High Performance Liquid Chromatography

The vitamin A and E analyses were performed on an Agilent 1100 series HPLC (Victoria, Australia), equipped with a quaternary pump LC- 1311 A, a degasser model 1322 A, and auto sampler G 1329 A (all Agilent, Victoria, Australia). The mobile phase was 96% methanol; flow rate =1 ml/min; Columns: A pre-column RP (15 x 3.2 mm; Applied Bio-system, Foster City, California, USA), particle size = 7 µm connected to analytical column RP Bio-system (220 x 4.6 mm; particle size = 5 µm). The column was maintained at 35°C. For detection, the analytical column was connected to an Agilent UV diode array detector monitoring at 325 nm and fluorescence detector (FLD) model 1321 A, operated at 292_{ex} nm and 330_{em} nm. The whole system was linked to a PC computer operated by Agilent Chemistation model LC 3 D and to an ALM thermostat model G13308.

Vitamin C

Vitamin C analysis was based on the method of Jagota and Dani (1982). Briefly 0.25 g of sunflower powder was homogenised with 2 ml of 10% trichloroacetic acid, centrifuged at 4577 g RCF for 10 min. Next, 0.5 ml of the supernatant was mixed with 1 ml of Folin-Ciocalteu reagent (diluted 10-fold with distilled water) and 0.5 ml of 20% sodium carbonate. The solution was incubated at RT for 10 min and absorbance was measured at 760 nm.

6.4 Statistical analysis

Data are presented as the mean ± SE (n = 4). Data were analysed using one-way analysis of variance (ANOVA). The Minitab v17 software statistical program was used to compare the differences among the treatment groups. Significance level was set at $P < 0.05$. Explanatory variables were nominal concentration of chemicals (Ag^+ and AgNPs) in mg/kg soil, and concentration or parameters activity in u/g homogenised leaf.

6.5 Results

6.5.1 Catalase

CAT enzyme activity in the leaves of sunflower plants grown in soil containing 150 mg/kg Ag as AgNPs or $AgNO_3$ (Ag^+) is shown in Fig. 6.1. The CAT activity was amplified 12-fold by Ag^+ and 8-fold by AgNPs compared to the control.

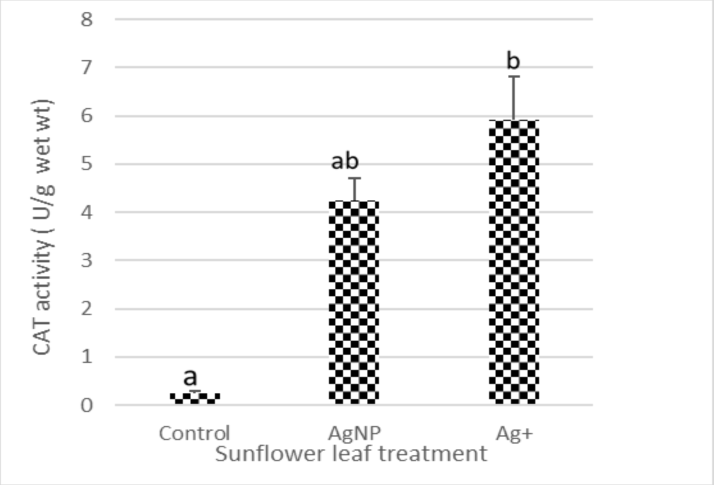

Fig. 6.1: Leaf catalase enzyme activity (CAT) in leaves of sunflower plants grown in soil containing 150 mg/kg Ag as AgNPs or Ag^+. Results are presented as mean ± SE of four replicates. Means with different letters on the bars are significantly different ($P < 0.05$).

6.5.2 Superoxide dismutase

Superoxide dismutase enzyme activity in sunflower plants grown in soil containing 150 mg/kg Ag as AgNPs or $AgNO_3$ (Ag^+) is shown in Fig. 6.2. The increase in SOD activity in sunflower leaves was approximately 2- and 3-fold respectively on exposure to AgNPs or Ag^+ compared to the control.

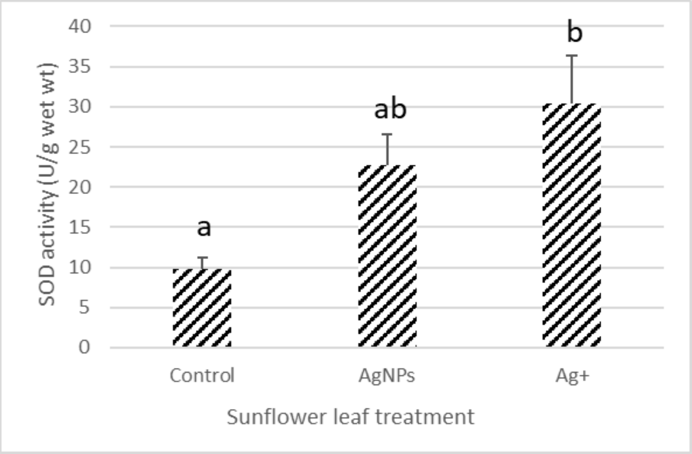

Fig. 6.2: Superoxide dismutase (SOD) enzyme activity in leaves of sunflower plants grown in soil containing 150 mg/kg Ag as AgNPs or Ag^+. Results are presented as mean ± SE of four replicates. Means with different letters on the bars are significantly different ($P < 0.05$).

6.5.3 Glutathione-S-transferase

Glutathione-S-transferase enzyme activity in sunflower plants grown in soil containing 150 mg/kg Ag as AgNPs or $AgNO_3$ (Ag^+) is shown in Fig 6.3. The GST enzyme activity in the leaves of sunflower plants exposed to Ag^+ was significantly increased about 2-fold compared to both the control and those exposed to AgNPs.

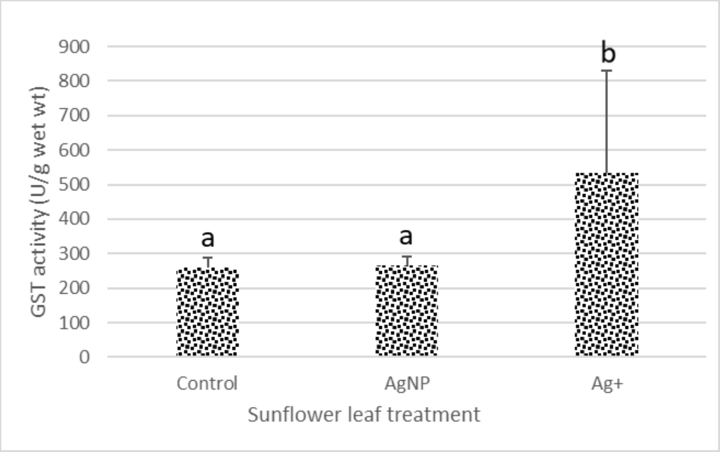

Fig. 6.3: Glutathione S-transferase (GST) enzyme activity in the leaves of sunflower plants exposed to 150 mg/kg Ag as AgNPs or Ag^+. Results are presented as mean ± SE of four replicates. Means with different letters on the bars are significantly different ($P < 0.05$).

6.5.4 Glutathione peroxidase

Sunflower leaf GPx enzyme activity in sunflower plants grown in soil containing 150 mg/kg Ag as AgNPs or $AgNO_3$ (Ag^+) are shown in Fig. 6.4. The GPx enzyme activity in the leaves of sunflower plants exposed to AgNPs or Ag^+ were approximately 2- and 4-fold respectively that of the control.

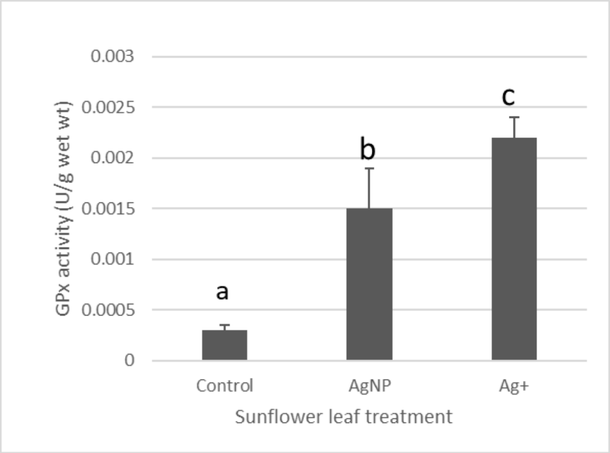

Fig. 6.4: Glutathione peroxidase (GPx) enzyme activity in leaves of sunflower plants grown in soil containing 150 mg/kg Ag as AgNPs or Ag^+. Results are presented as mean ± SE of four replicates. Means with different letters on the bars are significantly different ($P < 0.05$).

6.5.5 Lipid peroxidation

The malondialdehyde (MDA) concentration in the leaves of sunflower plants grown in soil containing 150 mg/kg of Ag as AgNPs or $AgNO_3$ (Ag^+) is shown in Fig. 6.5. The MDA concentrations in leaves of sunflower plants exposed to AgNPs or Ag^+ were significantly increased 0.3- and 0.7- fold respectively compared to the control.

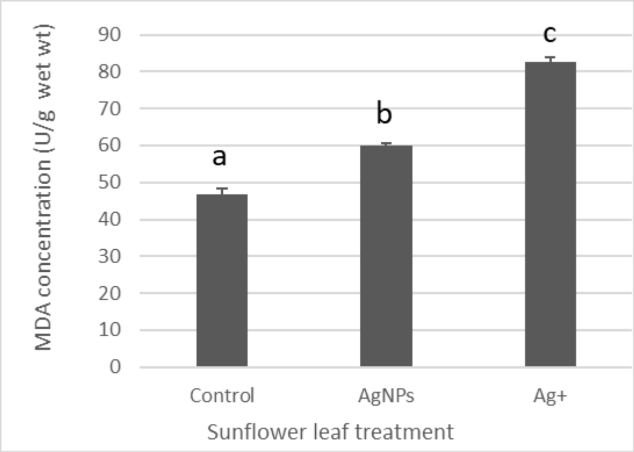

Fig.6.5: Malondialdehyde (MDA) concentration (ug/g wet wt) in leaves of sunflower plants grown in soils containing 150 mg/kg Ag as AgNPs or Ag^+. Results are presented as mean ± SE of four replicates. Means with different letters on the bars are significantly different ($P < 0.05$).

6.5.6 Ascorbate oxidase

Sunflower leaf ascorbate oxidase amounts in sunflower plants grown in soil containing 150 mg/kg Ag as AgNPs or $AgNO_3$ (Ag^+) are shown in Fig. 6.6. The ascorbate oxidase activity in sunflower leaves exposed to AgNPs or Ag^+ was increased 2- and 4-fold respectively compared to the control.

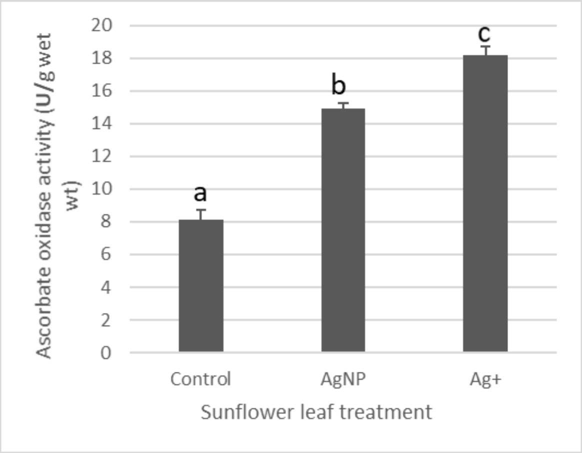

Fig. 6.6: Ascorbate oxidase activity in the leaves of sunflower plants grown in soil containing 150 mg/kg Ag as AgNPs or $AgNO_3$ (Ag^+). Results are presented as mean ± SE of four replicates. Means with different letters on the bars are significantly different ($P < 0.05$).

6.5.7 Pyrogallol peroxidase

Pyrogallol peroxidase activity in the leaves of sunflower plants grown in soil containing 150 mg/kg Ag as AgNPs or $AgNO_3$ (Ag^+) are shown in Fig. 6.7. The pyrogallol peroxidase activity in sunflower leaves exposed to AgNPs or Ag^+ was increased 6- and 11-fold respectively compared to the control.

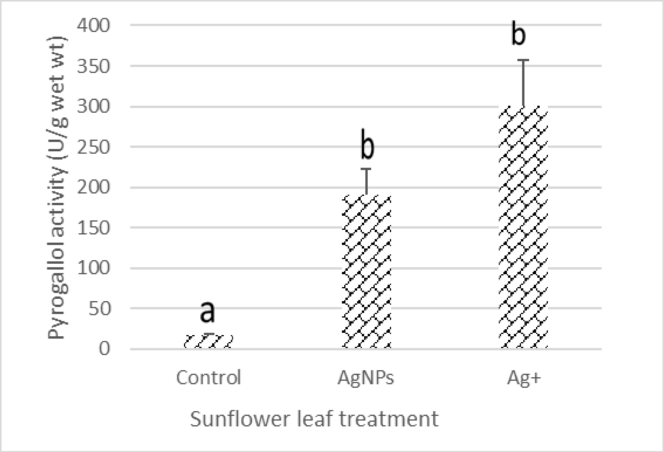

Fig. 6.7: Pyrogallol peroxidase activity in leaves of sunflower plants grown in soil containing 150 mg/kg Ag as AgNPs or $AgNO_3$ (Ag^+). Results are presented as mean ± SE of four replicates. Means with different letters on the bars are significantly different ($P < 0.05$).

6.5.8 Guaiacol peroxidase

The guaiacol peroxidase activity in leaves of sunflower plants grown in soil containing 150 mg/kg Ag as AgNPs or $AgNO_3$ (Ag^+) is shown in Fig. 6.8. The guaiacol peroxidase activity in sunflower leaves exposed to AgNPs or Ag^+ was increased 0.5- and 1.3-fold respectively compared to the control.

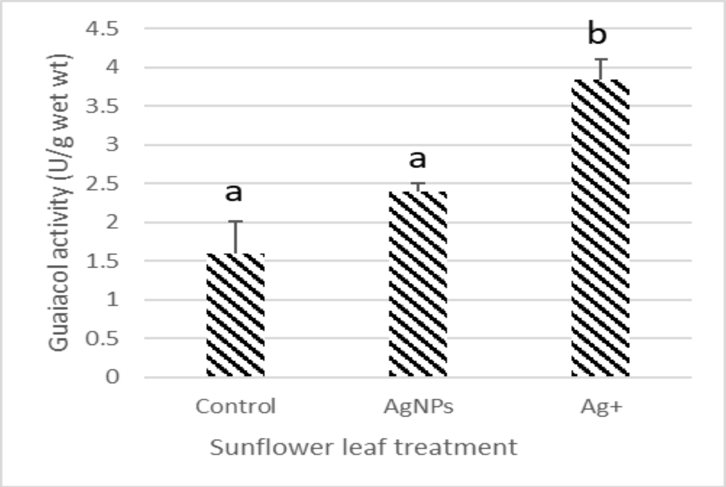

Fig. 6.8: Guaiacol peroxidase activity in the leaves of sunflower plants grown in soil containing 150 mg/kg Ag as AgNPs or $AgNO_3$ (Ag^+). Results are presented as mean ± SE of four replicates. Means with different letters on the bars are significantly different ($P < 0.05$).

6.5.9 Chlorophyll A and B and total carotenoids

Chlorophyll A and B and total carotenoid concentrations in the leaves of sunflower plants grown in soil containing 150 mg/kg Ag as AgNPs or $AgNO_3$ (Ag^+) are shown in Fig. 6.9. Chlorophyll A decreased by 30% with AgNPs and 40% with Ag^+. Chlorophyll B showed no significant difference on exposure to AgNPs/Ag^+. Total carotenoid level in sunflower leaves exposed to Ag^+ showed a 50% decrease compared to the control.

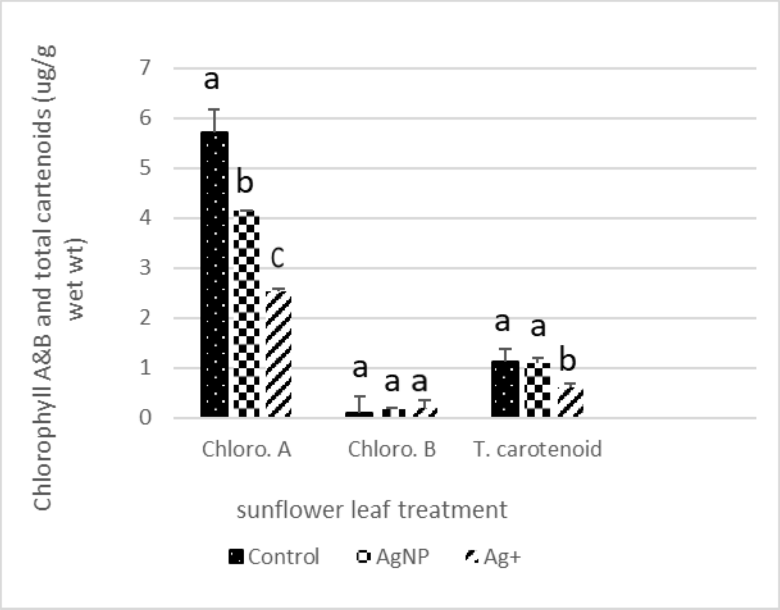

Fig. 6.9: Chlorophyll A & B and total carotenoid concentration in leaves of sunflower plants grown in soil containing 150 mg/kg Ag as AgNPs or $AgNO_3$ (Ag^+). Results are presented as mean ± SE of four replicates. Means with different letters on the bars are significantly different ($P < 0.05$).

6.5.10 Total soluble protein

Total protein concentration in the leaves of sunflower plants grown in soil containing 150 mg/kg Ag as AgNPs or Ag^+ is shown in Fig. 6.10. The total protein concentrations in sunflower leaves exposed to AgNPs or Ag^+ were 12.5% and 25% lower respectively compared to the control.

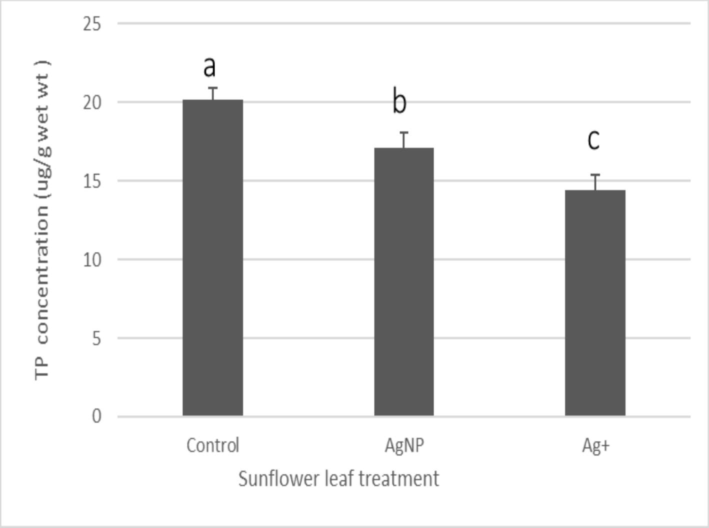

Fig. 6.10: Total protein in leaves of sunflower plants grown in soil containing 150 mg/kg Ag as AgNPs or $AgNO_3$ (Ag^+). Results are presented as mean ± SE of four replicates. Means with different letters on the bars are significantly different ($P < 0.05$).

6.5.11 Total phenolic compounds

The concentration of total phenolic compounds in theleaves of sunflower plants grown in soil containing 150 mg/kg Ag as AgNPs or $AgNO_3$ (Ag^+) are shown in Fig. 6.11. The TPC concentration in sunflower leaves exposed to AgNPs or Ag^+ were increased by 0.3- and 1-fold respectively compared to the control.

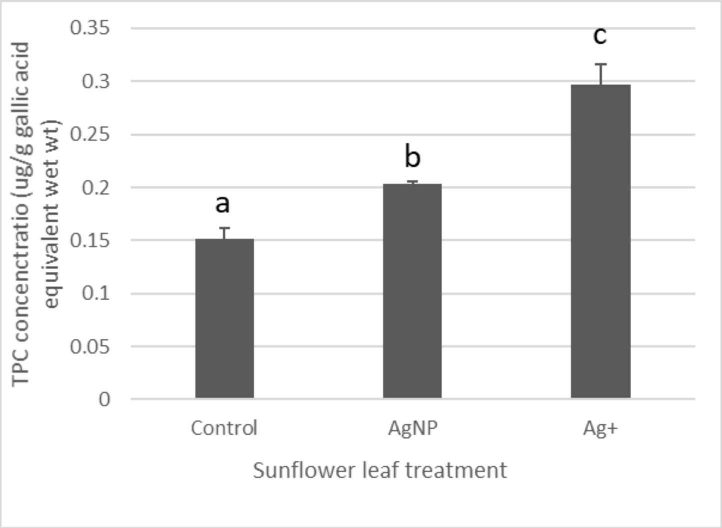

Fig. 6.11: Total phenolic compounds (TPC) in leaves of sunflower plants grown in soil containing 150 mg/kg Ag as AgNPs or $AgNO_3$ (Ag^+). Results are presented as mean ± SE of four replicates. Means with different letters on the bars are significantly different ($P < 0.05$).

6.5.12 Total soluble carbohydrates

Total soluble carbohydrate concentration (TCC) in the leaves of sunflower plants grown in soil containing 150 mg/kg Ag as AgNPs or $AgNO_3$ (Ag^+) is shown in Fig. 6.12. The TCC in sunflower leaves exposed to AgNPs or Ag^+ declined by 20% and 35% respectively compared to the control.

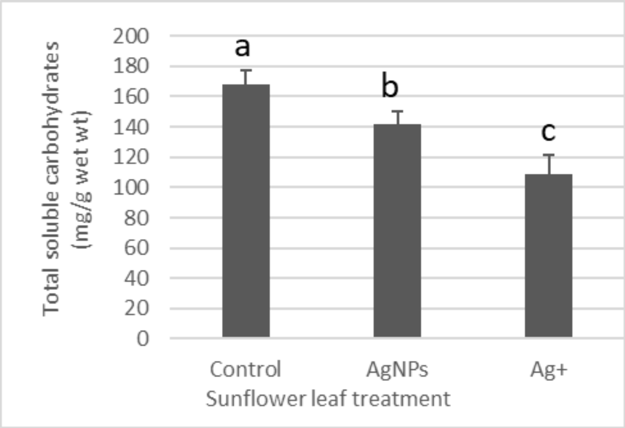

Fig. 6.12: Total soluble carbohydrate concentration in leaves of sunflower plants grown in soil containing 150 mg/kg Ag as AgNPs or $AgNO_3$ (Ag^+). Results are presented as mean ± SE of four replicates. Means with different letters on the bars are significantly different ($P < 0.05$).

6.5.13 Urease

Urease concentration in the leaves of sunflower plants grown in soil containing 150 mg/kg Ag as AgNPs or $AgNO_3$ (Ag^+) is shown in Fig. 6.13. The urease level in sunflower leaves exposed to AgNPs or Ag^+ were 0.4- and 1-fold respectively that of the control.

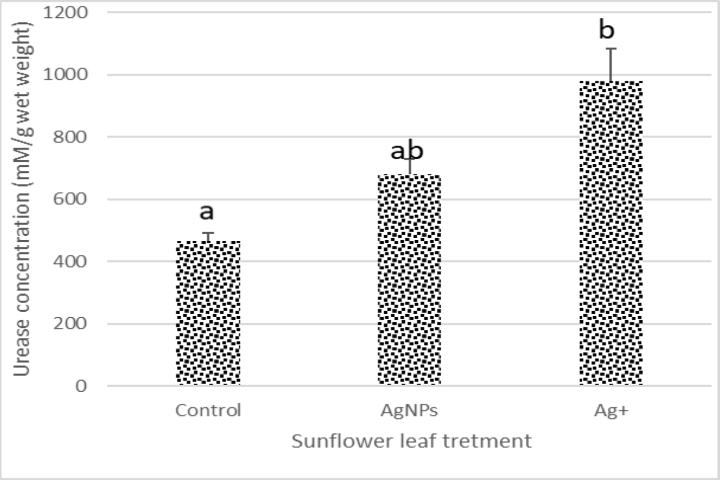

Fig. 6.13Uurease concentration in leaves of sunflower plants grown in soil containing 150 mg/kg Ag as AgNPs or $AgNO_3$ (Ag^+). Results are presented as mean ± SE of four replicates. Means with different letters on the bars are significantly different ($P < 0.05$).

6.5.14 Vitamins A and E

Vitamin A & E concentrations in the leaves of sunflower plants grown in soil containing 150 mg/kg Ag as AgNPs or $AgNO_3$ (Ag^+) are shown in Fig. 6.14. The vitamin A concentration in sunflower leaves exposed to AgNPs or Ag^+ were increased by 1- and 0.3-fold, and vitamin E concentration by 6.8- and 2.8-fold respectively, compared to the control.

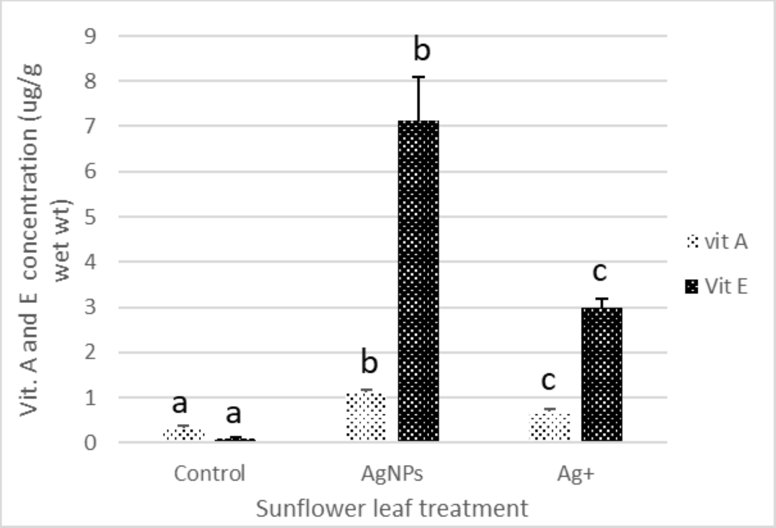

Fig. 6.14: Vitamin A and E in the leaves of sunflower plants grown in soil containing 150 mg/kg Ag as AgNPs or $AgNO_3$ (Ag^+). Results are presented as mean ± SE of four replicates. Means with different letters on the bars are significantly different ($P < 0.05$).

6.5.15 Vitamin C

Vitamin C concentration in the leaves of sunflower plants grown in soil containing 150 mg/kg Ag as AgNPs or $AgNO_3$ (Ag^+) are shown in Fig. 6.15. The vitamin C concentration in sunflower leaves exposed to AgNPs or Ag^+ increased by 25% and 21% respectively compared to the control.

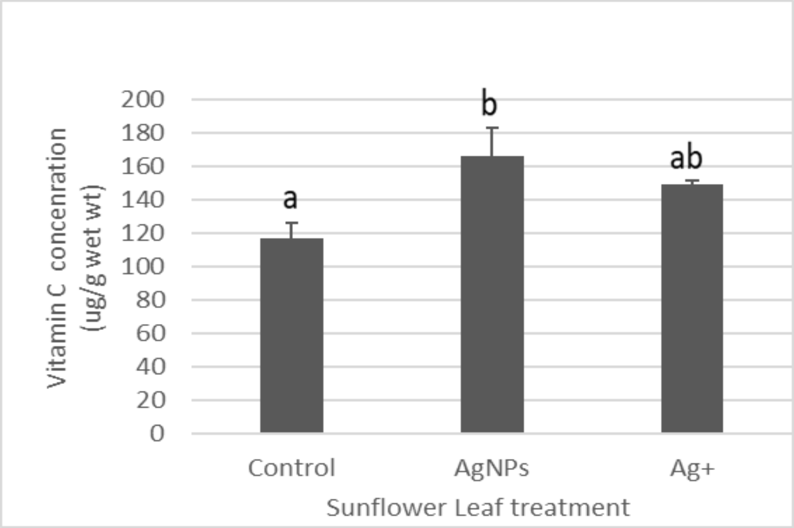

Fig. 6.15: Vitamin C in leaves of sunflower plants grown in soil containing 150 mg/kg Ag as AgNPs or $AgNO_3$ (Ag^+). Results are presented as mean ± SE of four replicates. Means with different letters on the bars are significantly different ($P < 0.05$).

6.6 Discussion

The biochemical effects of AgNPs/Ag^+ on the leaves of sunflower plants included increases in antioxidant defence enzymes, peroxidases, total phenolic compounds, urease activity and antioxidant vitamins as vitamins A, E and C. In contrast, the AgNPs/Ag^+ reduced chlorophyll A and B, total carotenoids and total protein and total soluble carbohydrate in sunflower leaves.

6.6.1 Antioxidant enzymes

I analysed the same four antioxidant enzymes (SOD, CAT, GST, GPx) and LPO that I selected for the earthworm studies to evaluate the response to ROS in sunflower leaves following exposure of sunflower seeds in soil amended with 150 mg/kg AgNPs or Ag^+. Reactive oxygen species are generated during the normal metabolism of eukaryotic cells, which involves mitochondrial electron transport, microsomal P_{-450} and other systems (Rani *et al.*, 2004). Reactive oxygen species mediate oxidative damage to macromolecules such as lipid, proteins, and DNA (Gill and Tuteja, 2010).

Metal ions like Ag cause oxidative stress in sunflower and generate toxic ROS species such as $O^{\cdot}$, OH^{-} and H_2O_2 that cause degradation of plant proteins in addition to reducing the number of chloroplasts per unit leaf tissue. Reactive oxygen species can affect a range of enzymes and activate the enzymatic antioxidant system, which responds to a series of abiotic and biotic stressors (Karuppanapandian *et al.*, 2011). The antioxidant enzymes include CAT, which causes dismutation of water; superoxide dismutase, the frontline enzyme of defence against ROS; GST, which acts as a detoxification enzyme; and GPx, which prevents damage from H_2O_2 and protects cells from oxidative stress (Das and Roychoudhury, 2014).

Sunflower plants when exposed to the two Ag forms (AgNPs and Ag^+) exhibited the activation of the antioxidant enzymes CAT, SOD, GST and GPx (Figs 6.1 to 6.4) compared with the controls. These enzymes are markedly elevated in sunflower leaves exposed to Ag^+ > AgNPs (Garcia *et al.*, 2006).

Exposure of *Bacopa monnieri* to 10 and 100 mg/kg Ag^+ increased CAT and GPx activities much higher than from exposure to the same concentration of AgNPs (Krishnaraj *et al*., 2012), which is in agreement with my findings.

Silver nanoparticles of 20-nm particle size at a concentration of 10 mg/l significantly induced oxidative stress, with an increase in ROS, in a higher aquatic plant (*Spirodela polyrhiza*) compared to the controls. On exposure of *S. polyrhiz*a to concentrations of 5 and 10 mg/l and 6-nm and 20-nm AgNPs particle size, SOD, CAT and guaiacol peroxidase were significantly increased (Jiang *et al*., 2012), which is in agreement with my sunflower study results. Jiang *et al*. (2012) also reported that 6-nm AgNPs induced a much greater increase in these enzymes compared to the 20-nm AgNPs particles, suggesting smaller sized particles are more effective probably due to their relatively larger surface area and more binding sites.

When *Arabidopsus thaliana* plants were exposed to AgNPs, anthocyanins and chloroplast (which plays a major role in photosynthesis) increased (Li *et al*., 2018). In addition, the plant tissues accumulated H_2O_2 and there was an increase in nucleic acids and proteins (which could be detected by staining plant tissues with 3,3-diaminobenzidine (DAB)). The plant leaf under stress exhibited a deep brown colour, compared with the control group whose leaves were almost transparent. In addition there was excessive accumulation of ROS and lipid peroxidation as identified by MDA measurement. Li *et al*. (2018) reported that SOD activity in *A. thaliana* on exposure to AgNPs (0.1, 0.5, 1 mg/l) significantly declined by 18.2% compared with the control. In contrast, CAT and peroxidases (POX) in the AgNPs-treated group were induced by 2.1- and 1.1-fold respectively compared to the controls, which is in agreement with my findings. But the inhibition of SOD when the plant was exposed to AgNPs (Li *et al*., 2018) did not agree with my studies. The reason for this could be the plant type and particle size differences. In my study I used 30-nm AgNPs in sunflower (Asteraceae), whereas Li *et al*. (2018) used sizes between 9 and 10 nm in *A. thaliana* (Brassicaceae). Exposure of tobacco plant to 25, 50, 75, 100 or 500 µM doses of AgNPs and Ag^+ in milli Q water in an Erlenmeyer flask resulted in greater toxicity by Ag^+ than by AgNPs (Cvjetko and Zovko (2017), which is consistent with my observations on sunflower grown in TSL soil but in that study CAT activity declined on exposure to AgNPs but increased on exposure to Ag^+.

Tomato plants exposed to 0, 25, 50, 75, and 100 mg/l of 20-nm AgNPs resulted in a linear dose-response elevation of all amino acids, but a decrease in total soluble protein and an increase in the activity of antioxidant enzymes (CAT, SOD, POX) in shoots and roots at a dose of 50 mg/l (Mehrian *et al.* (2015), which agreed with my results. However, at the AgNPs dose 100 mg/l, SOD activity declined significantly in roots probably due to excess ROS and unspecific enzyme degradation (Filek *et al.*, 2008) or due to binding of Ag to the active centre of the SOD enzyme (Stroinski and Kozlowska, 1997), the activity of which was higher in the shoot than the roots. The SOD and CAT activities in castor oil seedlings increased on exposure to AgNPs/Ag^+ (Yasur and Rani (2013), which in agreement with my data. Li *et al.* (2006) reported that heavy metals such as Cu and Zn also induced CAT, SOD, POX in castor bean (*Ricinus communis*) plants.

The effect of AgNPs on sunflower leaf GST activity was minimal, but Ag^+ increased GST compared to the control. GST is a detoxification enzyme involved in the metabolism of certain chemicals such as pesticides and heavy metals. It catalyses the conjugation of electrophilic molecules with GSH to more water soluble and less toxic metabolites (Vanhaelen *et al.*, 2001). The GSH conjugation is the first step of the mercapturic acid pathway, which is an important detoxification process (Tsuchida, 2002). GST is induced and able to detoxify chlorophenol in plants grown in polluted soil (Schroder *et al.*, 2009) including those exposed to high concentrations of Cd (Komives *et al.*, 1995).

A significant increase in the heme-containing protein GPx was observed in sunflower leaves of plants exposed to AgNPs or Ag^+ compared to the controls (Fig. 6.4). The GPx activity in plants depends on physiological and genetic status, time interval, type and concentration of exposure to pollutants (including heavy metals) and is a response to oxidative stress (Hassan *et al.*, 2017). GPx is a Se-containing enzyme that catalyses the reduction of H_2O_2 via GSH to protect plant cells from oxidative stress (Rani *et al.*, 2004) not only caused by heavy metals but also by salinity and drought conditions (Rahimizadeh *et al.*, 2007).

Nickle (Ni) is a heavy metal that has caused oxidative stress in *Amaranthus paniculatus* with resultant increase in LPO, GPx, SOD and CAT (Pietrini *et al.*, 2015). However, the authors reported that antioxidant enzymes (including GPx) in roots were progressively inhibited by increased Ni concentration in the growth solution but increased Ni also caused a marked increase in GPx and SOD activity in leaves. However, application of essential micronutrients to soil can reduce the effect of environmental stressors including drought and salinity (Wang *et al.*, 2004). There are several reports (Malan *et al.*, 1990; Bailly *et al.*, 2000; Jiang and H, 2001; Habibi *et al.*, 2004; Qian *et al.*, 2013) on oxidative stress in plants with resultant increases in ROS, LPO and GPx. The exposure of sunflower to AgNPs and Ag^+ in my work resulted not only in an increase in GPx but also in other peroxidases such as pyrogallol (Fig 6.7) and guaiacol (Fig. 6.8).

6.6.2 Lipid peroxidation (LPO) or thiobarbituric acid reactive species (TBARS)

Exposure of plants to external stress induces LPO. Fig. 6.5 showed that exposure of sunflower plants to AgNPs or Ag^+ resulted in a significant increase in MDA in the leaf with the effect by Ag^+ > AgNPs. In *A. thaliana* exposed to AgNPs or Ag^+, tissues accumulated ROS formation and LPO in the leaf, which was identified and quantified by MDA (Li *et al.*, 2018). A similar effect was observed by Karami *et al.* (2015) in the tomato plant with a concentration-dependent increase in MDA on exposure to Ag. Jiang *et al.* (2014) found that exposure of an aquatic plant *Spirodela polyrhiza* to 5 mg/l AgNPs in 10% Hoagland solution resulted in a significant increase in LPO compared to the control. MDA is also significantly increased in tobacco leaves exposed to 500-µM AgNPs and to 100-µM Ag^+ (Cvjetko and Zovko (2017). So, it appears that the changes in MDA observed in the tobacco leaves when exposed to AgNPs/Ag^+ are similar to the ones I observed in the sunflower leaf, Mostly, the effects of heavy metal ions on plants include an increase in LPO and lipoxygenase activity, and an associated decrease in chlorophyll and GSH (Gallego *et al.*, 1996). Ascorbate oxidase (Fig. 6.6) is also an antioxidant defence enzyme, which can resist ROS. It plays a major role in detoxifying H_2O_2 in plant cells. The ascorbate oxidase catalyses the conversion of hydrogen peroxide to water by acting as a specific electron donor (Caverzan *et al.*, 2012). Shimada and Ko (2008) have also reported an increase in the number of peroxidases in vegetables on exposure to AgNPs and Ag^+. The peroxidases used in my study were pyrogallol peroxidase (Fig. 6.7) and guaiacol peroxidase (Fig. 6.8).

Krishnaraj *et al.* (2012) reported that in *Bacopa monnieri* AgNPs produced more pyrogallol peroxidase than was found in plants exposed to Ag^+. In my study, the opposite was found, with the increase in pyrogallol peroxidase on exposure to Ag^+ being significantly higher than by AgNPs. The authors also observed a decrease in protein and carbohydrate of *B. monnieri* that was accompanied by an increase in the concentration of phenolics in the plant, which is in agreement with my findings.

The finding of Cvjetko and Zovko (2017) of an increase in pyrogallol peroxidase in the tobacco plant, where he observed that the effect by Ag^+ > AgNPs (because in tobacco leaves AgNPs concentrations of 100 µM and 500 µM were less toxic than Ag^+ at even a lower concentration of 50 and 75 µM) was similar to my studies but different to that reported by (Krishnaraj *et al.*, 2012) in *B. monnieri*. Guaiacol peroxidase activity on exposure of sunflower to the two silver forms showed significant increase only in the plants exposed to Ag^+ and not AgNPs, compared to the control (Fig. 6.8). Measurement of guaiacol peroxidase is based on the oxidation of guaiacol to tetraguaiacol (brown). Fig. 6.8 shows that Ag^+ significantly increasedguaiacol peroxidase activity in sunflower leaves compared to the control, with a non-significant increase in the plants exposed to AgNPs, which is in agreement with the observations of Karami *et al.* (2015) who exposed tomato plants to AgNPs (6-nm particle size) and Ag^+ and observed a significant increase in guaiacol peroxidase activity, and also the findings of Jiang *et al*. (2014), who exposed the aquatic plant *Spirodela polyrhiza* to AgNPs and observed a similar increase in guaiacol peroxidase activity.

6.6.3 Chlorophyll and total carotenoids

Leaf pigments include chlorophyll A and B and total carotenoids, which are essential for photosynthesis and hence plant growth (Costache *et al.*, 2012). The ratio between chlorophyll A and chlorophyll B indicates the response to light and shade conditions, and the ratio is used as a sensitive biomarker of pollution and environmental stress (Porra, 1991). Carotenoids are located in chloroplast and with chlorophyll are intricately involved in the photosynthetic process. In addition, carotenoids can protect chlorophyll and the thylakoid membrane (a sheet-like membrane-bound structure in chloroplast that plays a role in light-dependent photosynthesis) from peroxidative damage (Sumanta *et al.*, 2014). Carotenoids are non-polar in nature but can dissolve in non-polar and polar solvents such as diethyl ether and methanol. Hence, I selected methanol for extraction of chlorophyll and total carotenoids in a one-step extraction with good recovery; besides methanol is easier to handle. AgNPs of 20-nm size are taken up by plants into intracellular spaces and transported inside the plant through plasmodesmata of root cells, then pass through shoots and accumulate on leaves, causing inhibition of chlorophyll. Mazumdar (2014) reported that using 1000 µg/ml AgNPs in Hoagland’s nutrient solution caused significant inhibition in chlorophylls and total carotenoids in *Vigna radiata* and *Bactris campestris,* which is in agreement with my findings in the leaves of sunflower plants grown in TSL soil amended with 150 mg/kg AgNPs/Ag^+ (Fig. 6.9). Navarro *et al.* (2008b), Wang *et al.* (2011), and Atha *et al.* (2012) have all reported that AgNPs inhibit plant growth by inhibition of chlorophyll formation and total soluble protein. However, Qian *et al.* (2013) showed that AgNPs inhibited the growth of the *A. thaliana* plant by disrupting the thylakoid membrane structure and decreasing chlorophyll concentration. In my studies, I did not investigate the impact of AgNPs on thylakoid membrane structure, but I am in agreement that chlorophyll concentration is reduced on exposure to AgNPs (Fig. 6.9). In contrast Qian *et al.* (2013) found that Ag did not profoundly affect chloroplast structure as AgNPs but could alter the transcription of antioxidants and aquaporin genes, indicating that AgNPs can change the balance between oxidant and antioxidant activity thereby affecting the homoeostasis of the plant *A. thaliana.* A decline in the chlorophyll content of plants exposed to heavy metals has been reported by many studies, including a decrease in the ratio of chlorophyll A to chlorophyll B on exposure to Cu and Hg stress, with chlorophyll B responding more to Cu, while a decrease in this ratio was observed in plants exposed to other heavy metals such as Cd and Pb (Hassan *et al.*, 2017).

Carotenoids is a partner pigment in photosynthesis. Carotenoids also act as an antioxidant non-enzymatic pigment that defends chlorophyll and cell membranes against ROS produced on exposure to different heavy metals and environmental stress (Hou *et al.*, 2007; McElroy and Kopsell, 2009). The defensive role of this pigment is to reduce chlorophyll concentration to protect against chloroplast damage (Pallett *et al.,* 2000). Decline in carotenoid content indicates heavy metals toxicity, while its enhancement reflects detoxification of ROS species (Rout *et al.*, 2001; Tewari *et al.*, 2002). The studies of Gallego *et al.* (1996) and Azad *et al.* (2011) on sunflower confirmed our results that chlorophyll and total carotenoids were inhibited in sunflower leaves on exposure of sunflower plants to AgNPs and Ag^+ in soil.

6.6.4 Total soluble protein

Proteins are large biomolecules consisting of a series of amino acids. In plants, protein has five main functions: plant growth, role in hormones and enzymes, immune function, and in energy production. Exposure of sunflower plant to AgNPs and Ag^+ resulted in a reduction of protein in the leaves, with Ag^+ > AgNPs > control (Fig 6.10). Krizkova *et al.* (2008) exposed sunflower to Ag^+ cultivated in a versatile environmental test chamber (MLR- 350 H, Sanyo, Japan) to concentrations of 0 (control), 0.1, 0.5 and 1 mM, and the protein content in the shoot > root indicative of transport of proteins from roots to shoots. Garcia *et al.* (2006) showed a higher protein concentration in sunflower leaf than in roots but on exposure to heavy metals the amount of protein was reduced in both the shoot and the root. A similar decline of up to 70% protein was observed in the leaves of tomato plants exposed to 50 µM Cd in soil compared to the controls and this was accompanied by an accumulation of ammonium (Chaffei *et al.*, 2004). In contrast, in the aquatic plant *Spirodela polyrhiza*, the effect of 6-nm AgNPs at 5 mg/l increased total soluble protein content (Jiang *et al.*, 2014). However, a significant increase in total soluble protein was detected when the plant was exposed to 10 mg/l 20 nm sized AgNPs. This is in contrast to my finding of a decline in sunflower leaf protein in plants exposed to 150 mg/kg Ag, with it being most marked in the plants exposed to Ag^+ (Fig. 6.10). This could be due to the smaller particle size and the lower dose used by Jiang *et al*. (2014). However, the authors reported that exposure to a higher concentration of AgNPs decreased the shoot protein concentration probably by oxidation, and this is in agreement with my results. Heavy metals such as Pb, Cd, Mn, Co, Cr, and Co also caused significant inhibition of total soluble protein and plant growth in *Zea mays* (Abdul, 2010), which also agrees with my results. Thus, many researchers agree that exposure of plants to AgNPs and Ag^+ reduces the total soluble protein in plant leaves, and also in stem and roots. Krishnaraj *et al.* (2012) reported that during exposure of *B. monnieri* to AgNPs, the leaf protein concentration declined over time, which agrees with my study. These authors also added that the decrease in protein concentration in *B. monnieri* was accompanied by an increase in total phenolic compounds on exposure to heavy metals. The reduction in total amount of soluble protein when exposed to heavy metals could be due to an increase in the level of protease activity as reported by Palma *et al.* (2002), or because of the diverse structural alteration by denaturation of protein (John *et al.*, 2009).

6.6.5 Total phenolic compounds

Figure 6.11 showed that the amount of the TPC was significantly increased in the leaves of sunflower plants exposed to Ag^+ > AgNPs > control. Similar observations have been recorded by Krishnaraj *et al.* (2012), who also observed that heavy metal stress can also reduce protein and carbohydrates in addition to increasing TPC, and also that phenolic derivatives can act as a metal stress chelator and as an antioxidant to reduce ROS and lipid peroxidation (Krishnaraj *et al.*, 2012).

6.6.6 Total soluble carbohydrates

Total soluble carbohydrate concentration in the leaves of sunflower plants significantly declined following exposure to 150 mg/kg of AgNPs and Ag^+ in soil for 53 days and this was most marked in the plants exposed to Ag^+. Krishnaraj *et al.* (2012) exposed *B. monnieri* to 10, 100 ug/kg and 10, 100 mg/kg of AgNPs and (Ag^+) ($AgNO_3$) and observed an increase in TSC only with $AgNO_3$ during the first 10 days of cultivation and then TSC decreased sharply, which agrees with my findings. Similarly, Salama (2012) reported that the exposure of corn (*Zea mays*) and common bean (*Phaseolus vulgaris*) to doses up to 60 mg/kg of AgNPs caused an increase in TSC but at higher AgNPs concentrations such as 80, 100, 200 mg/kg, the TSC concentration decreased significantly. Yaseen *et al.* (2016) found that the application of colloidal AgNPs (1 mg/ml) as a foliar spray dose of 50 ml/l resulted in an increase in number as well as a change in the appearance of sunflower leaves.

6.6.7 Urease

Urease is an enzyme that catalyses the hydrolysis of urea to form ammonia and carbon dioxide and is a crucial plant enzyme that is very sensitive to exposure to heavy metals including Ag and Ni (Hubalek *et al.*, 2007). Also, urease has a fundamental role in recycling exogenous urea used as fertiliser (Sujoy and Aparn, 2013). In my study, there was a significant increase in urease activity in the leaves of sunflower plants exposed to 150 mg/kg AgNPs or Ag^+, with the increase being most marked in plants exposed to Ag^+ > AgNPs > control (Fig. 6.13).

6.6.8 Vitamins A, E and C

Exposure of sunflower plants to 150 mg/kg AgNPs or Ag^+ in soil resulted in a significant increase in vitamin A and E concentrations (Fig. 6.14). The greatest increase was with AgNPs > Ag^+ > Control. The exposure of sunflower plants to AgNPs and Ag^+ stimulated the production of ascorbate oxidase resulting in ROS production, which can lead to a production of L-ascorbic acid. , Vitamins A and E (alpha-tocopherol) act as a defence in addition to ascorbate oxidase, which oxidises L-ascorbic acid to dehydroascorbic acid, and therefore the amount of dehydroascorbic acid increased and total ascorbic acid decreased (Shimada and Ko, 2008). Zengin and Munzuroglu (2005) reported a significant increase in the antioxidant vitamins A and E in the bean plant (*Phaseolus vulgaris*) following exposure to heavy metals Pb (1.5, 2, 2.5 mM), Cu (0.1, 0.2, 0.3 mM), Cd (0.05, 0.06 and 0.08 mM) and Hg (0.02, 0.04 and 0.06), for 10 days, which is in agreement of my findings.

Vitamin C (Fig. 6.15) is a free radical scavenger against O_3 (Gupta *et al.*, 1991). It could also act as an antioxidant in photosynthetic organisms and reduce H_2O_2 (Pehlivan, 2017). Exposure of *Bacopa monnieri* to different Hg concentrations for 14 days resulted in a significant increase in vitamin C (Sinha *et al.*, 1996). This finding with vitamin C is in agreement with my studies on exposure of sunflower to AgNPs/Ag^+. Zengin (2013) measured the stress effect from exposure of the bean plant (*Phaseolus vulgaris L.)* to several heavy metals, namely, Ni, Co, Cr, Zn, on the concentration of vitamins A, E, and C in plant leaves. He found that the amounts of these vitamins were significantly increased in combination with carotenoids, while chlorophyll content decreased, which is consistent with our findings. Collin *et al.* (2007) reported that vitamins C and E can act as chain-breaking scavengers for proxy radicals and as a synergist with vitamin E because vitamin C can donate an H atom to vitamin E-derived phenolate radicals, thus regenerating its activity. Similar findings were observed in my studies also.

Vitamin E (alpha-tocopherol) can quench singlet oxygen ($^1O_2$) and acts as a chain-breaking antioxidant. It is found in the green parts of the plant. Vitamin E protects lipids and other membrane components by physically quenching and reacting chemically with $^1O_2$. Scavenging of $^1O_2$ oxygen by vitamin E in chloroplasts results in formation of α-tocopherol quinone, which is involved in cyclic electron transport in thylakoid membranes (Collin *et al.*, 2007).

6.7 Conclusions

Exposure of sunflower plant to AgNPs and Ag^+ (from $AgNO_3$) causes oxidative stress similar to that caused by other heavy metals such as Cd, Pb, Hg, and Ni. The stress of exposure to such heavy metals can lead to ROS and elevated activity in defence enzymes (Cat, SOD, GST, and GPx) in addition to increased activity of peroxidases (LPO, pyrogallol peroxidase and guaiacol peroxidase). The major impact of the two Ag forms, AgNPs and Ag^+, on the sunflower plant is to reduce total protein and inhibit chlorophyll synthesis in the leaf, which can result in reduced growth and yield of the crops. Overall, the responses of the parameters measured were most marked in those plants exposed to $Ag^+ >$ AgNPs.

Chapter 7

Biochemical Toxicity of Silver Nanoparticles and Ag$^+$ (AgNO$_3$) to *Aporrectodea caliginosa Earthworm,* Using Filter Paper as a Matrix

7.1 Abstract

Earthworms *A. caliginosa* were exposed to varying concentrations of AgNPs (0, 0.3, 3, 30, 300 mg/l) or Ag$^+$ (from AgNO$_3$) (0, 0.03, 0.3, 3, 10 mg/l) in moistened filter paper in Petri dishes for 24 and 48 h (n = 4). The filter paper contact test was used as a rapid screening of sub-clinical toxicity of AgNPs and Ag$^+$ toxicity to *A. caliginosa* and also as a practice run to get familiar with earthworm homogenisation and enzyme analyses for the main earthworm soil study described in Chapter 8. The sub-clinical toxicity caused by these chemicals through dermal uptake was assessed by measuring the effect on selected antioxidant enzymes, namely, superoxide dismutase, catalase, glutathione peroxidase and glutathione-S-transferase, in addition to lipid peroxidation (LPO). Based on the results, the enzyme activities and LPO were slightly higher in earthworms exposed to Ag+ than in earthworms exposed to AgNPs, and greater at 48 h than 24 h.

7.2 Introduction

Many have shown that the release of AgNPs used in different industries can have an adverse impact on the environment (McGillcuddy *et al*. 2017; Wilson 2018). Among such industries, two major ones used the most AgNPs in their products, namely, the clothing industry and the medical field. Some of these AgNPs will likely end up in sewage treatment plants and the sludge could be released into the environment as fertiliser in some plantations. The AgNPs release Ag ions that are toxic to soil microorganisms and other organisms that come in contact with soil (McShan *et al*., 2014). Another impact of AgNPs is that they are phytotoxic to some plants, such as *Phaseolus radiatus,* where seedling growth is adversely affected on exposure to AgNPs in soil (Lee *et al*., 2012).

This study was conducted to quickly screen the potential effects of AgNPs on *A. caliginosa* earthworms and to compare these with exposure to Ag$^+$ (AgNO$_3$) using filter paper as a matrix and more importantly as a trial to get familiarised with biochemical methodologies to be used in the main earthworm study described in Chapter 8. The toxicities of AgNPs and Ag$^+$ were evaluated by measuring a range of antioxidant enzyme activities prior to and after exposure to these two chemicals, using filter paper as a matrix. I used filter paper as a matrix in this short-term study to quickly scan the potential range of AgNPs/Ag^+ concentrations that could be used in the *A. caliginosa* soil study in Chapter 8. The antioxidant enzymes that were monitored (CAT, GPx, SOD, GST) are those involved in detoxification of xenobiotics to minimise the oxidative stress caused by ROS (Lionetto *et al.*, 2012). Lipid peroxidation (LPO) was also measured. Malondialdehyde (MDA), 4-hydroxy-nonenal (HNE) and the F2-isoprostane 15(S)-8-iso-prostaglandin F2α (15(S)-8-iso-PGF2α) are the most frequently measured biomarkers of lipid peroxidation (Tsikas, 2017). MDA is the prototype of the so-called thiobarbituric acid reactive substances (TBARS).

The use of biochemical markers is preferred to characterise the potential hazard of AgNPs and these could be assayed by different techniques (Ray *et al.*, 2009). The antioxidant enzymes in *A. caliginosa* homogenate were measured following exposure to 300, 30, 3, 0.3 µg/ml AgNPs and 10, 3, 0.3, 0.03 µg/ml Ag+ respectively for 24 and 48 h. The selection of these concentrations was based on the Petri dish LD_{50} studies of AgNPs and Ag+ to *A. caliginosa* carried out in our laboratory a few years ago (Zhan, 2012). As mentioned above, the objective of this study was to test the potential doses of AgNPs and Ag+ to be used and to become familiar with the earthworm homogenisation technique and also the antioxidant enzymes and LPO analyses in preparation for the main earthworm experiment in soil.

7.3 Materials and methods

7.3.1 Chemicals and reagents

Trisodium citrate and sucrose di-potassium hydrogen phosphate were purchased from BDH (UK). All the other chemicals, including $AgNO_3$, were supplied from Aldrich-Sigma (St. Louis, MO, USA).

7.3.2 Experiments

7.3.2.1 Earthworms

For this study, *A. caliginosa* earthworms were sourced from our parental stock of typed earthworms by Bates (2015). Adult earthworms (~ 1.3 – 1.5 mg) with a well-developed clitellum were used in all experiments. Prior to the experiment, the worms were removed from the stock soil, rinsed with water and blotted on filter paper to remove excess water.

7.3.2.2 AgNPs and Ag+ ($AgNO_3$) concentrations

Silver nanoparticles and $AgNO_3$ were diluted in distilled water to achieve concentrations of 0 (water), 0.3, 3, 30 and 300 mg/l for AgNPs from a stock solution was 13.45 g/l and 0 (water), 0.03, 0.3, 3, 10 mg/l for Ag^+ ($AgNO_3$). The treatment doses were selected based on a preliminary experiment conducted to determine the LD_{50} of *A. caliginosa* exposed to AgNPs (2649 mg/kg) and Ag^+ (305 mg/kg) (unpublished observation) and the highest dose employed for each of the chemicals was ~10% of the LD_{50} dose. The selected doses were based on the LD_{50} studies, which showed that Ag^+ ($AgNO_3$) was approximately 10-fold more toxic than AgNPs; hence the use of much lower doses of $AgNO_3$ in the study.

7.3.2.3 Filter paper study

Whatman no. 1 filter paper was placed in flat glass Petri dishes (2 × 9 cm diameter) and wetted with 1 ml each of the AgNPs or $AgNO_3$ solutions, or distilled water (control), with two worms per Petri dish for 24 or 48 h (n = 4 at each time point). At 24 and 48 h worms were removed, washed, dried, weighed and frozen at -20 °C pending analysis.

7.3.2.4 Homogenisation of frozen worms

Earthworms were homogenised (FJ 200, Gao Su Fen San Jun2HI JI Shanghai Specimen and Model Factory homogeniser, China) at a ratio of 1:3 (w/v) in 0.01 M phosphate saline buffer (PSB; pH 7.4) at high speed for 25 s in ice. Each 3 ml of PSB contained 175 µl of a mixture of protease inhibitors (aprotinin, leupeptin, pepstatine: 5 µg/ml; antipain 1 µg/ml; trypsin inhibitor 1 mg/ml) (Concetti *et al*., 1984; Laguerre *et al*., 2009). The homogenate was then centrifuged (Beckman J2-MI; GMI, Minnesota, USA) at 30 390 x g RCF for 20 min at 4°C. Aliquots of the supernatant for enzyme analysis were transferred to 15-ml capped plastic tubes and kept in ice. All antioxidant enzymes were measured using spectrophotometric (Shimadzu 1200, Tokyo Japan) methods

7.3.2.5 Total protein in earthworm homogenate

The method of Bradford (1976) was used with bovine serum albumin (BSA) as the standard. Briefly, a 50-µl sample was mixed with 2.5 ml of Bradford reagent and diluted 1:1 with water and the absorbance measured using a Shimadzu 1200 spectrophotometer at 595 nm. All earthworm enzyme activities reported below are expressed as a faction of the protein concentration in the earthworm homogenate supernatant.

7.3.2.6 Calculation of enzyme activity: Described in appendix G

Superoxide dismutase

SOD activity measurement was based on the inhibition of pyrogallol auto-oxidation with the extinction coefficient of pyrogallol as 2640 M/cm (Terevento *et al*., 2010). Briefly, 2.85 ml of 0.01 M phosphate buffer (pH 8), 75 µl of 10 mM pyrogallol and 75 µl of homogenate were mixed and the kinetics followed by measuring the increase in absorbance at 340 nm, every minute for 4 min.

Catalase

CAT analysis was based on determination of the kinetics of the degradation of H_2O_2 with the extinction coefficient of H_2O_2 as 43.6 M /cm (Cataldo *et al.*, 2011). Briefly, 72.5 ul of 0.01 M phosphate buffer (pH 6.5) with 2.5 ml of 0.3 M H_2O_2, and 0.5 ml of earthworm homogenate were mixed, and the kinetics followed by measuring the decrease in absorbance at 240 nm, every minute for 4 min.

Glutathione peroxidase

The assay mixture consisted of 1970 µl of assay buffer (1 mM reduced glutathione [GSH], 50 mM KH_2PO_4, 0.15 mM NADPH, 1 mM Na azide, 1.5U glutathione reductase (GR), 0.15 mM H_2O_2 and 0.0073 g EDTA). To this 30 µl of earthworm homogenate was added and the GPx activity was measured for 4 min at 22°C based on the oxidation of NADPH monitored by the decrease in absorbance of the incubation mixture at 340 nm measured every minute for 4 min. The extinction coefficient of NADPH is 6220 M/cm (Terevento *et al.*, 2010). The GPx activity was expressed as µmol oxidized NADPH min^{-1} mg^{-1}.

7.3.2.7 Glutathione-S-transferase

This measurement was based on the increase in absorbance at 340 nm due to the conjugation of GST to 1-chloro-2,4-dinitro-benzene (CDNB) and extinction coefficient of GSH as 9.6 M/cm (Cataldo *et al.*, 2011). Briefly, the reaction mixture contained 100 µl of freshly prepared GSH (40 mM) in phosphate buffer (0.01 M, pH 7.6), 100 µl of CDNB (1 mM) and 500 µl of potassium phosphate buffer (0.1 M, pH 6.5), which were mixed and incubated for 5 min at 25°C. The reaction was initiated by adding 30 µl of earthworm homogenate and the increase in absorbance at 340 nm followed every minute for 4 min

7.3.2.8 Lipid peroxidation

Malondialdehyde (MDA) concentration was used as an indicator of lipid peroxidation in the thiobarbituric acid (TBA) reactive substances (TBARS) assay as described by Cataldo *et al.* (2011). Initially, the proteins in the earthworm homogenates were removed by precipitation with trichloroacetic acid (30%), and centrifuged at 2000 × *g* for 20 min. To 1 ml of the supernatant, 1 mM EDTA and 1% TBA were added and the mixture heated in a boiling water bath for 15 min. The sample was cooled on ice and the absorbance of MDA measured at 532 nm. The concentration of MDA was calculated using the molar extinction coefficient of MDA (1.56 x 105) M^{-1} cm^{-1}) and expressed as per mg protein.

7.4 Statistical analysis

Data are presented as the mean ± SE. Data were analysed using one-way analysis of variance (ANOVA). The Minitab 17 software statistical program was used to compare differences among the treatment groups. Significance was set at $P < 0.05$. Explanatory variables were concentration of chemicals (Ag^+ and AgNPs) in (mg/kg soil, time in hours) and enzyme activity in µmol mg^{-1} min^{-1} protein.

7.5 Results

7.5.1 Superoxide dismutase

The results of *A. caligiosa* SOD analysis are shown in Fig. 7.1. There was a clear dose-dependent increase in SOD activity at 24 h (Fig. 7.1A and B) and also at 48 h (Fig. 7.1C and D). The increase in SOD by the highest dose of $AgNO_3$ (10 mg/l, Ag^+) was similar to that caused by 300 mg/l of AgNPs. The increase in SOD measured on exposure of earthworms to 48 h was slightly higher than at 24 h and again it was dose dependent.

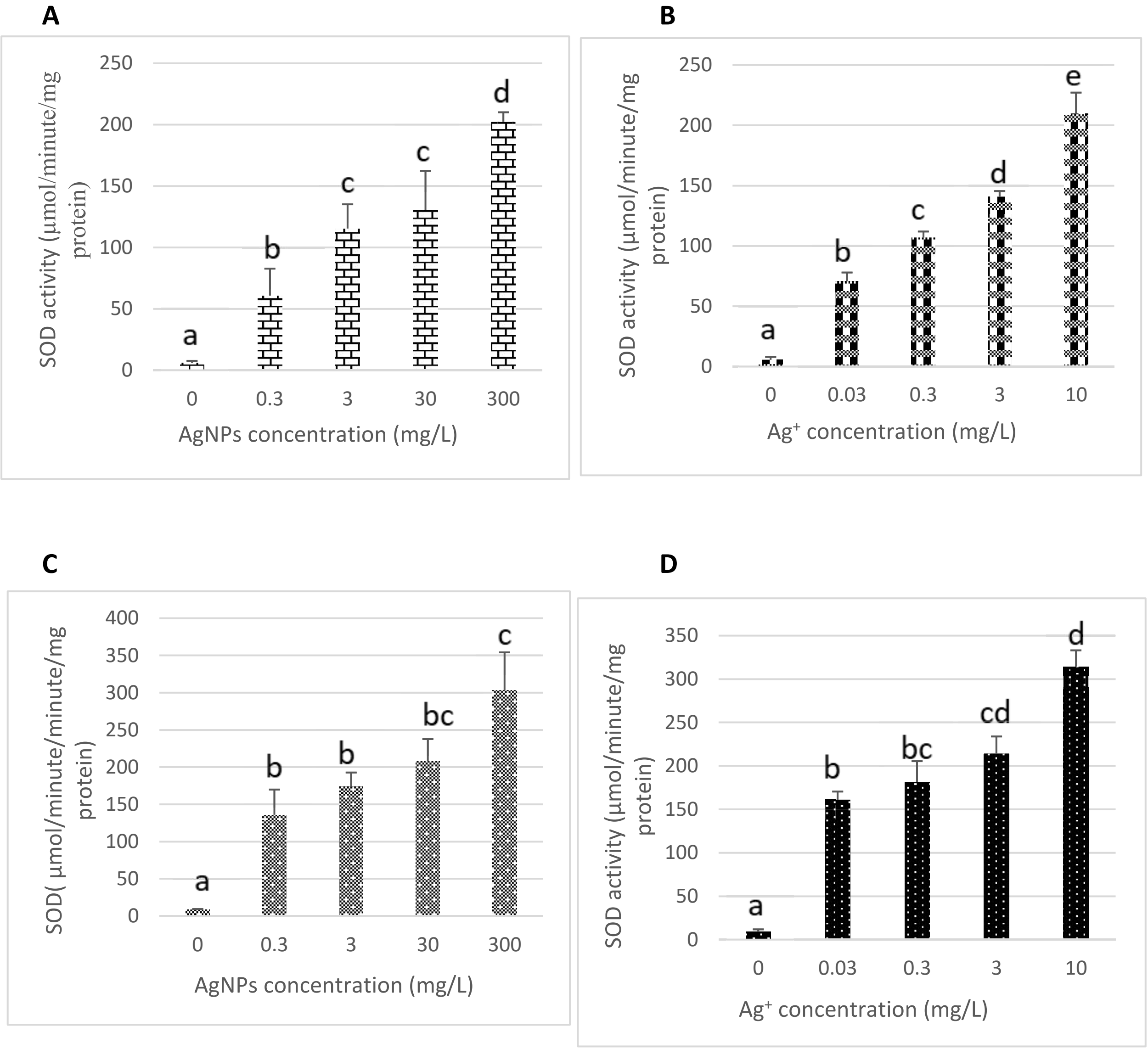

Fig. 7.1: Superoxide dismutase (SOD) enzyme activity (mean ± SE) in *A. caliginosa* exposed to AgNPs or Ag^+ ($AgNO_3$) in filter paper for 24 h (A, B) and 48 h (C, D). Means with different letters on the bars are significantly difference ($P < 0.05$).

Catalase

Catalase enzyme activity in *A. caliginosa* exposed to AgNPs or Ag^+ ($AgNO_3$) for 24 and 48 h is shown in Fig. 7.2. A dose-response was observed at 24 h on exposure to either AgNPs or Ag^+ and the effects were most marked in the earthworms exposed to Ag^+ for 48 h. The variations between earthworms exposed to AgNPs were quite high and hence the higher standard deviations in Fig 7.2C.

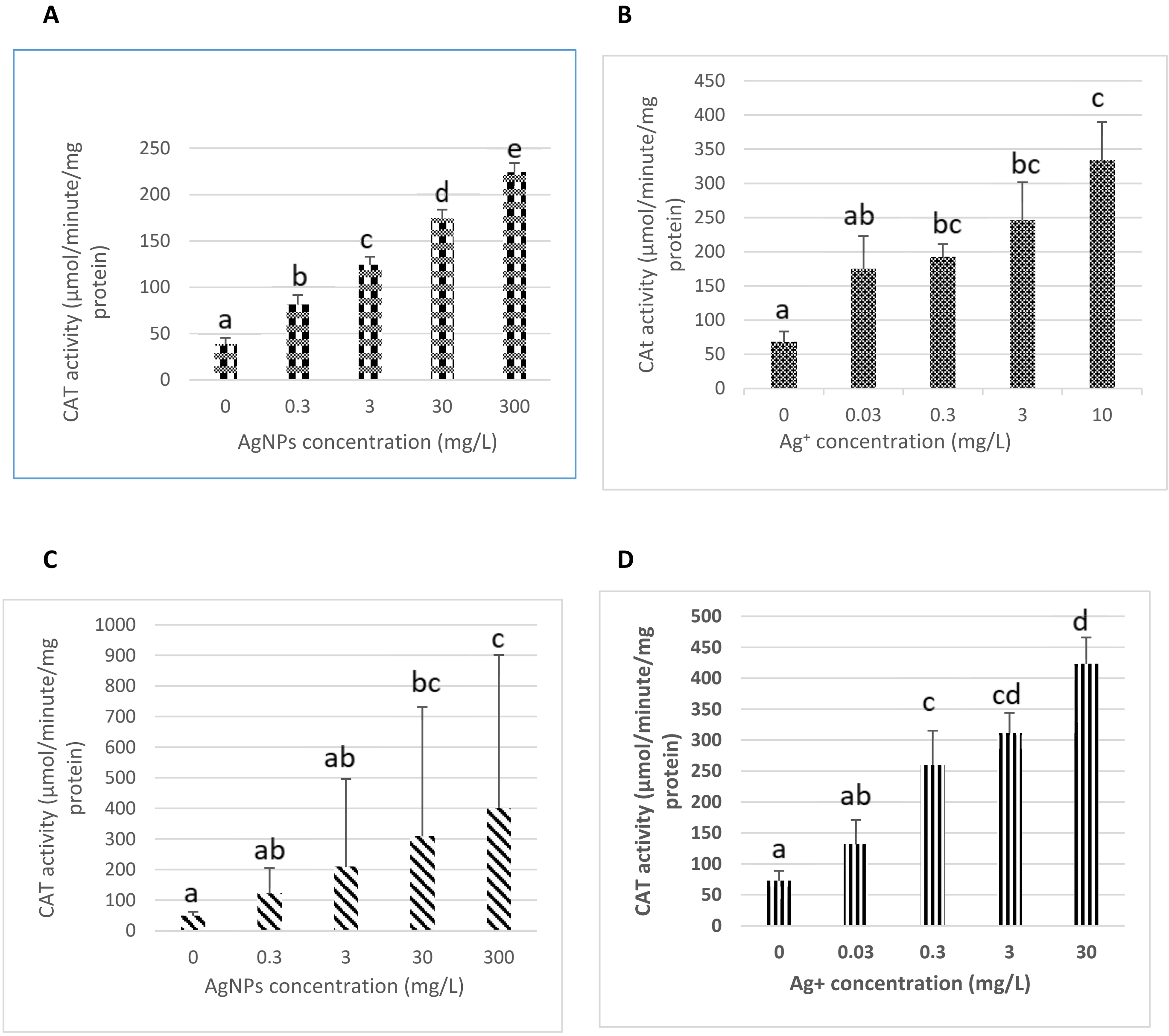

Fig.7.2: Catalase (CAT) enzyme activity (mean + SD) in *A. caliginosa* exposed to AgNPs or Ag^+ ($AgNO_3$) in filter paper for 24 h (A, B) and 48 h (C, D). Means with different letters on the bars significantly difference ($P < 0.05$).

7.5.2 Glutathione peroxidase

Glutathione peroxidase activity in *A. caliginosa* exposed to AgNPs and Ag^+ ($AgNO_3$ for 24 h and 48 h is shown in Fig 7.3. The GPx activity showed a dose-response effect with Ag^+ > AgNPs and the activity was higher in earthworms exposed for 48 h. The GPx increase on exposure to Ag^+ was approximately 1.5 to 2-fold that with AgNPs at both 24 h and 48 h.

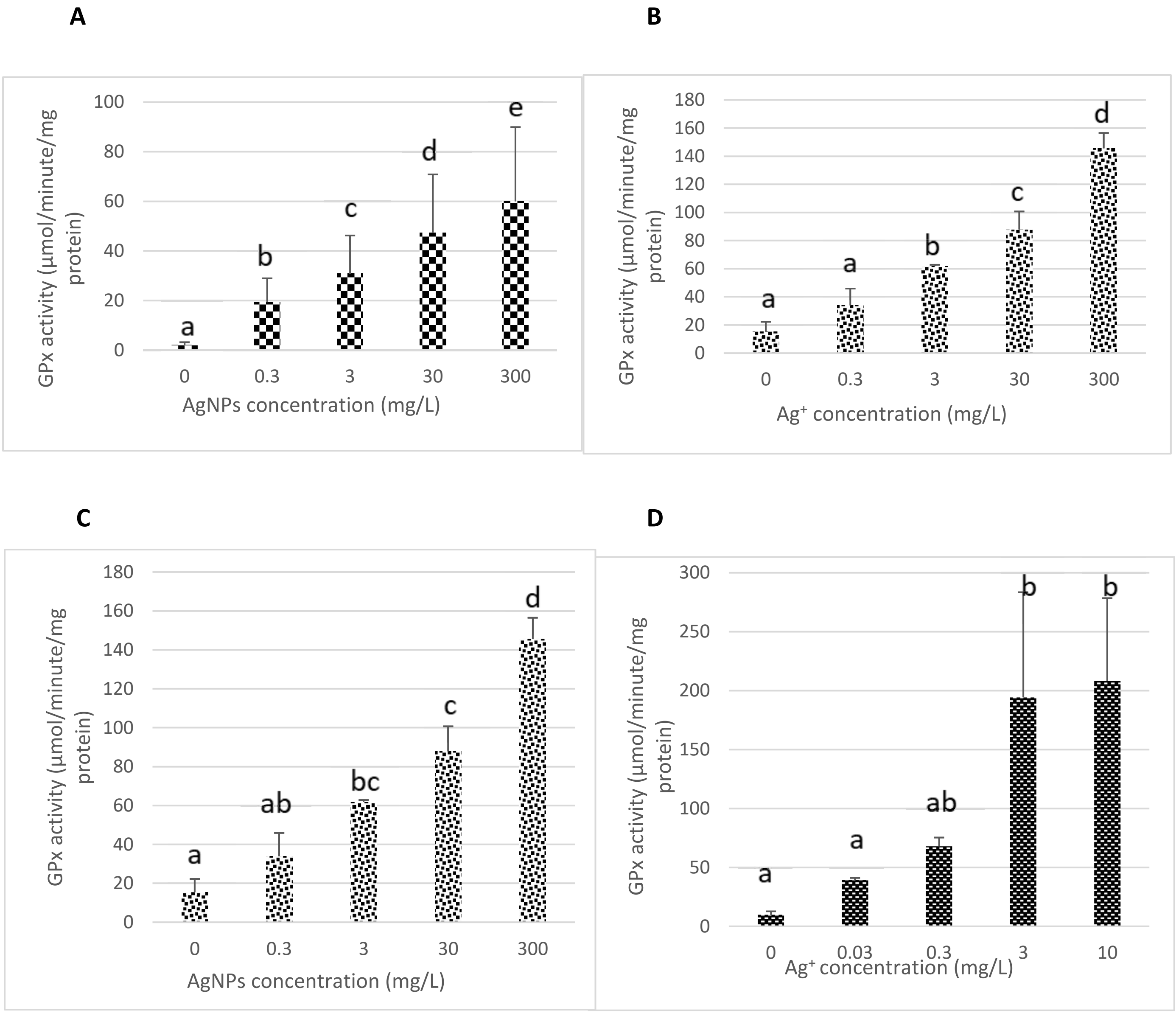

Fig. 7.3: Glutathione peroxidase enzyme activity (mean + SD) in *A. caliginosa* exposed to AgNPs or $AgNO_3$ (Ag^+) in filter paper for 24 h (A, B) and 48 h (C, D). Means with different letters on the bars are significantly different ($P < 0.05$).

7.5.3 Glutathione-S-transferase

Glutathione-S-transferase enzyme activity in earthworms exposed to either AgNPs or $AgNO_3$ (Ag^+) were generally high and produced a similar dose-response with both AgNPs and Ag^+. The increases were similar in earthworms exposed to AgNPs or Ag^+-for 24 h and 48 h (Fig. 7.4).

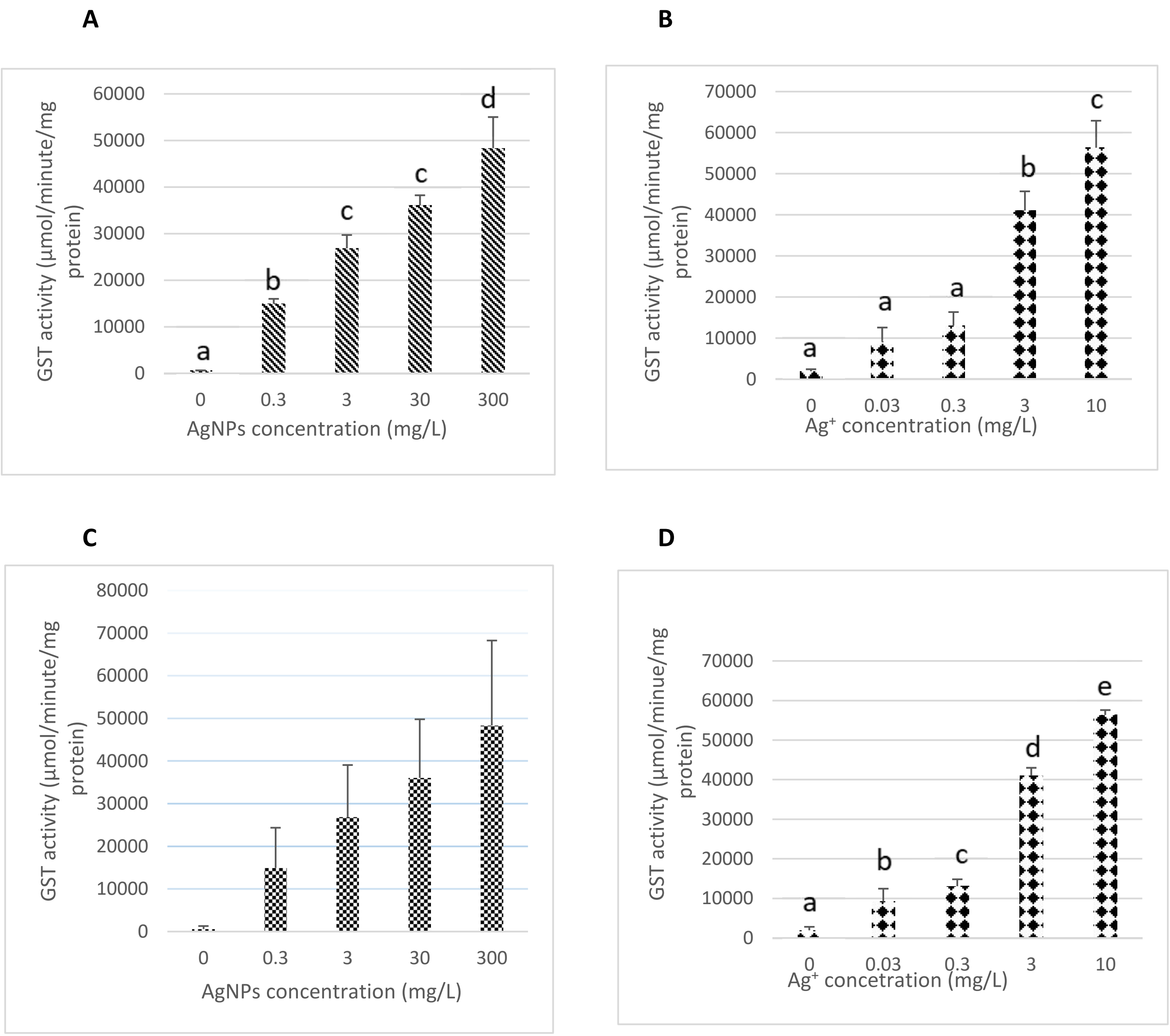

Fig. 7.4: Glutathione-S-transferase enzyme activity (mean + SD) in *A. caliginosa* exposed to AgNPs or $AgNO_3$ (Ag^+) in filter paper for 24 h (A, B) and 48 h (C, D), with no significant differences observed in graph C. Means with different letters on the bars are significantly different $p < 0.05$

.

7.5.4 Lipid peroxidation (LPO)

Malondialdehyde (MDA) concentrations, a measure of oxidative stress, were determined in *A. caliginosa* homogenates and the values are shown in Fig. 7.5. There was a similar dose response with both AgNPs and $AgNO_3$ (Ag^+) and the values were similar in earthworms exposed for either 24 or 48 h.

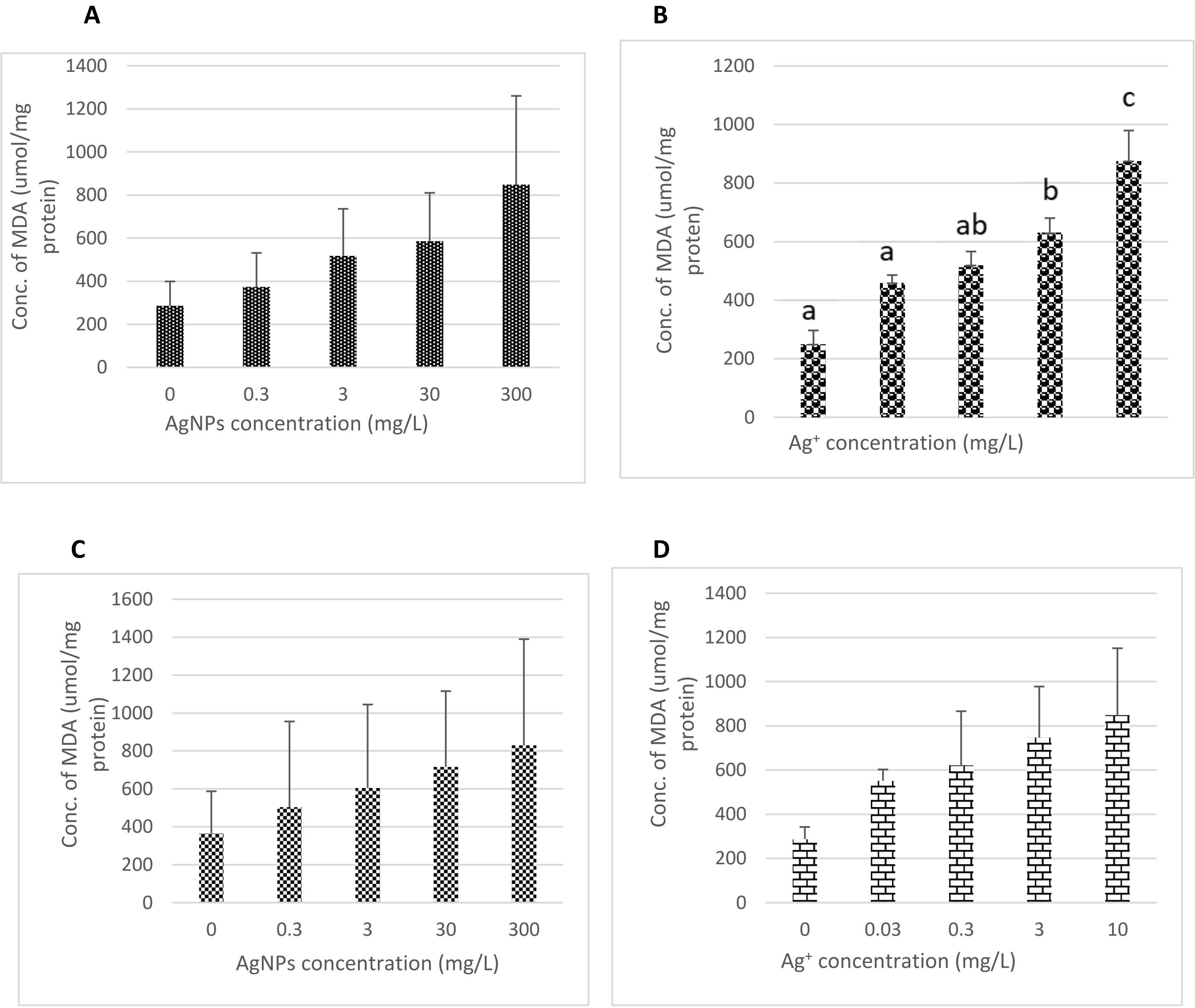

Fig. 7.5: Lipid peroxidation (as MDA) enzyme activity (mean + SD) in *A. caliginosa* exposed to AgNPs and Ag^+ in filter paper for 24 h (A, B) and 48 h (C, D). Mean with different letters on the bars (Ag^+ at 24 h) significantly different ($P < 0.05$).

7.6 Discussion

Contact filter paper bio-assay and soil toxicity studies have been conducted to compare the acute toxicity of 24 chemicals belonging to 6 chemical categories on earthworm species *Eisenia fetida* (Wang *et al*., 2012). The toxic effects of AgNPs and Ag+ to *A. caliginosa* earthworms were assessed in a short-term filter paper contact study which confirmed the potential AgNPs and Ag+ doses for a long-term study and also provided experience in the measurement of LPO and antioxidant enzyme activity analyses to be used in a sub-chronic earthworm soil study. When earthworms are exposed to polluted soil, the soil chemicals enter the body both dermally and through the gastrointestinal tract. In contrast, in the filter paper test, earthworms are exposed to chemicals via the dermal route only and also in the current study the earthworms were exposed for a maximum of 48 h only. In the current study, five concentrations of AgNPs and Ag+ were selected as exposure doses based on a preliminary study. The filter paper technique has been adopted by the EEC (European Economic Community, 1985 https://en.wikipedia.org/wiki/European_Economic_Community) and OECD (Organisation for Economic Co-operation, 1984) as an inexpensive, short-term study for screening of chemicals (Fitzpatrick *et al*. 1996) and has now been generally accepted as a laboratory test to generate preliminary toxicity data in earthworms for use in developing subsequent studies for risk assessment of agrochemicals. Earthworms may take up metals from soils by ingestion and absorption through the skin. The filter paper test can provide information about toxic effects (and in some instances even about mechanism(s) of chemical toxicity) via the dermal route only. Therefore, the short-term study in earthworms using filter paper can offer a quick and easy method of exposing earthworms to a chemical in solution that makes intimate contact with the outer body surface. This allows observation of the effect of the chemicals on earthworms, but not the overall toxicity of a chemical to earthworms. Because the filter-paper study is a short-term test done with just a few organisms, in many instances non-significant data are generated, especially if relatively low doses are used.

García-Velasco *et al*. (2016) exposed *E. fetida* earthworms to four different concentrations (0.6, 6, 8, 12 and 16 μg/cm^2) of PVP-PEI (polyvinylpyrrolidone-polyethyleneimine) coated 5-nm AgNPs particles in a filter paper study and found that the 16 μg/cm^2 concentration caused 100% mortality. The percentage of mortality decreased to about 50% at the mid-exposure doses of 6–8 μg/cm^2 (264–352 mg/l), and AgNPs concentrations higher than 0.06 μg/cm^2 caused weight loss. It was concluded that the PVP-PEI coating material may cause weight loss and also alter the bioavailability and toxicity of NPs (García-Velasco *et al.,* 2016). Therefore, to determine whether the toxicity was caused by AgNPs or by the coating agent PVP-PEI or both, the authors performed a filter paper contact test whereby *E. fetida* were exposed to PVP-PEI alone and in combination with AgNPs. The LC_{50} on exposure to PVP-PEI alone was 15.57 μg/ cm^2, equivalent to ~ 685 mg/l of AgNPs and 2-fold more than with PVP-PEI + AgNPs (LC_{50} of 7.17 μg/cm^2 equivalent to ~ 315 mg/l). The authors suggested that it is not desirable to use PVP-PEI as a NP coating, because PVP-PEI alone can be mildly toxic causing earthworm weight loss even at an exposure concentrations of ~ 290 mg/l. Weight loss and mortality of earthworms occur mostly due to a disruption of the tegument, caused by dermal absorption of

Ag^+ released from AgNPs. In my study, I exposed *A. caliginosa* up to 300 mg/l AgNPs of 30-nm particle size, which were coated with relatively non-toxic citrate to prevent NP adhesion.

It is difficult to compare toxicity in earthworms exposed to moistened filter paper with toxicity on exposure to soil, but the filter paper study can provide a general indication of the toxicity that could occur in a soil matrix. It also helped familiarise me with conducting the enzyme and LPO assays.

7.7 Conclusion

Exposure of the earthworm *A. caliginosa* in filter paper moistened with different concentrations of AgNPs or $AgNO_3$ (Ag^+) is a quick, easy, and cheap method of scanning for toxicity of chemicals and provides a general idea about dermal toxicity of such chemicals to earthworms.

Chapter 8

Antioxidant enzyme activity and lipid peroxidation in *Aporrectodea caliginosa* earthworms exposed to AgNPs and Ag+ ($AgNO_3$)

8.1 Abstract

Silver nanoparticles from industrial use and discharged via sludge application are now found in soil at increasing concentrations causing earthworms to be continually exposed to AgNPs throughout their lifespan. Excessive production of reactive oxygen species in organisms can result in lipid peroxidation, shifting the balance between oxidants and antioxidants to cause oxidative stress, which plays a role in the pathogenesis of many diseases including some caused by environmental agents. This study looked at sub-organismal biomarkers such as antioxidant responses and lipid peroxidation in *A. caliginosa* earthworms exposed to soils spiked with AgNPs or Ag+. *A. caliginosa* earthworms were exposed to Ag at 0 (control), 0.3, 3, 30, 300 mg/kg (as AgNPs) or 0, 0.03, 0.3, 3, 10 mg/kg Ag^+ (as $AgNO_3$) in soil for 4 weeks. At 1, 2, 3 and 4 weeks, the activity of the antioxidant enzymes superoxide dismutase, catalase, glutathione peroxidase, glutathione-S-transferase and lipid peroxidation increased as a function of dose and exposure time, with a much larger response for Ag^+ than AgNPs. Given the likelihood of ever-increasing AgNPs pollution of soil, where AgNPs can transform to ionic Ag (Ag^+), my findings of antioxidant response to oxidative stress in a common indicator organism even at an environmentally realistic dose of 0.03 mg/kg demonstrate that AgNPs may affect soil fertility and indirectly agricultural production. This study showed that evaluating certain biomarkers offers a meaningful assessment of AgNPs and Ag+ effects on terrestrial earthworms. To minimise such effects, regulation may be needed to prevent excessive soil contamination by the burgeoning suite of industries using Ag compounds.

8.2 Introduction

Silver nanoparticles are now increasingly used in a variety of industries (Xiong *et al*., 2013). This implies the increasing presence of AgNPs in the environment, making ecologically relevant organisms and human exposure possible (Kühnel and Nickei, 2014). In the face of rapid growth in nanotechnology, and environmental policy instruments that have not been designed to regulate the novel physical or chemical properties of substances like NPs, there is now an urgent need to understand the environmental impact of NPs, including AgNPs. Silver nanoparticles may be released into the environment, including into soil, during production and disposal of materials containing AgNPs (Stensberg *et al.,* 2011; Dobias and Bernier-Latmanic, 2013). Thus AgNPs would accumulate in the environment including soil and be transmitted indirectly to humans. Many industries release wastes into sewerage systems that end in sludge, which is sometimes spread on the land as fertiliser (Meier *et al*., 2016). Silver nanoparticles in sewage sludge when applied on soil can inhibit plant growth and impact on both terrestrial and aquatic organisms via leaching of land contaminants into waterways (Lee *et al*., 2012).

Earthworms contribute significantly to ecosystem health by modifying the physical, chemical, and biological properties of soil, recycling organic material, increasing nutrient availability, providing food for other soil organisms and improving soil structure, all of which improve soil fertility (Lemtiri *et al*., 2014). Thus, earthworms play an important role in agriculture by increasing pastoral productivity (Blouin *et al*., 2013). The earthworm *Eisenia fetida* is the most common earthworm species used to assess chemical toxicity (OECD, 1984). In New Zealand, however, the most abundant earthworm species in agricultural land is *Aporrectodea caliginosa* and this species has been shown to be equally suitable for monitoring soil toxicity (Gooneratne *et al*., 2011) and genotoxicity (Cataldo *et al*., 2011).

Silver nanoparticles have a high affinity for soil organic matter and thiol compounds, which can reduce toxicity to soil microorganisms but nevertheless still affect soil, plant and animal enzymes (Levard *et al*., 2012). Over the last decades, biomarkers at sub-organismal levels have been considered viable measures of responses to stressors (Huggett *et al*., 1992). Several biomarkers have been used at the cellular level as efficient tools due to their sensitivity, quickness, and accurate relationship between toxicant exposure and respective biological responses (Connon *et al*., 2012). Gordon *et al*. (2010) reported that Ag ions inactivate enzymes by binding to sulfhydryl (thiol) groups in amino acids and promote release of iron (Fe) with subsequent free radical formation by a variety of mechanisms, mostly mediated by ROS. Highly reactive ROS such as superoxide (O_2^-) and hydrogen peroxide (H_2O_2) are the products of univalent and bivalent reduction of oxygen (O_2) respectively. Sources of O_2^- and H_2O_2 are functionally and spatially related to the production and cellular localisation of natural antioxidant enzymes including SOD and CAT (Gobe and Crane, 2010). SODs detoxify O_2^- into H_2O_2. Hydrogen peroxide is then converted to water and molecular O_2 by CAT. Glutathione-S-transferase is a phase II enzyme that catalyses glutathionylation of xenobiotics. Glutathione peroxidase enzymes, found in a variety of intra- and extra-cellular compartments, mediate the reduction of peroxides to alcohols. The balance between ROS production and antioxidant system leads to regulated intracellular steady-state levels of ROS in aerobic organisms (Sies, 1997).

Oxidative stress (OS) is a deleterious process caused by an imbalance between oxidants and antioxidants in steady state, which plays a role in the pathogenesis of many diseases including some caused by environmental agents including metals ions (Samet and Wages, 2018). It can result in damage to proteins, DNA and also cause LPO (Wible and Bratten, 2018). It is suggested that the major AgNPs toxicity pathway in environmental organisms is via the impairment of oxidative phosphorylation, and generation of ROS, and LPO (Cataldo *et al*., 2011; Terevento *et al*., 2010).

The aim of this study was to compare several sub-organismal biomarkers, namely antioxidant enzyme activity and LPO, in *A. caliginosa* earthworms chronically exposed to AgNPs and Ag^+ (as $AgNO_3$).

8.3 Materials and methods

8.3.1 Chemicals and reagents

Tri-sodium citrate, sucrose and di-potassium hydrogen phosphate were purchased from BDH (UK). Analytical-grade $AgNO_3$ and all other chemicals were from Sigma-Aldrich (St. Louis, Missouri, USA).

8.3.2 Silver nanoparticles synthesis and quantification

Silver nanoparticles were freshly prepared on the day of the experiments as described in Chapter 3, section 3.1. The Ag concentration in AgNPs was determined by flame atomic absorption spectroscopy (FAAS) as described in Chapter 3, section 3.2.

8.3.3 Silver nanoparticles charge measurement and particle size

Zeta potential is a measure of the magnitude of the electrostatic or charge repulsion or attraction between particles and is one of the fundamental parameters known to affect NP stability. A zetasizer can measure the size distribution of a sample and this is usually performed in conjunction with dynamic light-scattering measurements to determine the accuracy between the two methods. Both zeta potential and size distribution measurements of AgNPs were performed by Dr Craig Bunt (Lincoln University).

The average mean particle size and zeta potential of AgNPs were determined using a Zetasizer Nano ZS (Malvern Instruments, Worcestershire, UK) at 25°C. The conditions employed were: He/Ne laser (wavelength = 633 nm), scattering angle 90°, refractive index 1.33, and viscosity 0.887 mPa. Prior to the measurements, the concentration of the AgNPs was diluted 200-fold with water.

Silver nanoparticle morphology and size were determined using a transmission electron microscope (TEM) (Philips CM200, Amsterdam). Silver nanoparticles were diluted with deionised water to obtain a more uniform distribution and directly transferred onto a TEM gold-carbon grid for size characterisation, using a high-resolution TEM fitted with a Gatan digital camera.

8.3.4 LD_{50} study of AgNPs and Ag^+ (Described in Appendix H)

8.3.5 Experimental design (earthworm soil studies*)*

Approximately 50 kg of Templeton Silt Loam soil were sieved and the moisture content adjusted to field capacity (Grewal *et al*., 1990). *A. caliginosa* earthworms from a colony typed to genus by Bate (2015) in my laboratory were used in the study. Adult earthworms (n = 200), 3–4 months old with a well-developed clitellum, in individual plastic containers (with small holes drilled in caps for air circulation) and containing 200 g of soil were used. Earthworms were exposed to Ag at 0, 0.3, 3, 30, or 300 mg/kg (as AgNPs) or 0, 0.03, 0.3, 3 or 10 mg/kg as Ag^+ ($AgNO_3$) with 20 earthworms per treatment dose. The treatment doses were selected based on a preliminary experiment conducted to determine the LD_{50} of *A. caliginosa* exposed to AgNPs and Ag^+ calculated using probit analysis, which were 2649 and 305 mg/kg respectively (unpublished observation). The highest dose employed in this study was ~10% of the LD_{50} dose. Thus, based on LD_{50} studies, Ag^+ was about 10-fold more toxic than AgNPs and hence relatively much lower doses of Ag+ were used in the study. At each of 1, 2, 3 and 4 weeks of exposure to the two treatments, five worms from each treatment dose were removed, rinsed, dried with filter paper, labelled and frozen at −20°C for subsequent analysis of Ag concentration, LPO and antioxidant enzyme activities (SOD, CAT, GPx, GST).

8.3.6 Earthworm homogenisation

Earthworms were homogenised (FJ 200, Gao Su Fen San Jun2HI JI Shanghai Specimen and Model Factory homogenizer, China) at a ratio of 1:3 (w/v) in 0.15 M phosphate saline buffer (PSB; pH 7.4) at high speed for 25 s in ice. Each 3 ml of PSB contained 175 µl of a mixture of protease inhibitors (aprotinin, leupeptin, pepstatine: 5 µg/ml; antipain 1 µg/ml; trypsin inhibitor 1 mg/ml) (Concetti *et al*., 1984; Laguerre *et al*., 2009). The homogenate was then centrifuged (Beckman J2-MI; GMI, Minnesota, USA) at 30 390 × g RCF for 20 min at 4°C to remove cell debris and most of the cell organelles. Aliquots of the supernatant for enzyme analysis, and Ag and protein concentration, were transferred to 15-ml capped plastic tubes and kept on ice. All antioxidant enzymes were measured using spectrophotometric (Shimadzu 1200, Tokyo Japan) methods

8.3.7 Total protein in earthworm homogenate

Total protein was determined by the method of Bradford (1976) with bovine serum albumin as the standard. All enzyme activities are expressed as a function of the protein concentration in the earthworm homogenate supernatant.

8.3.8 Silver concentration in earthworms

Earthworm homogenates were digested using concentrated nitric acid in a microwave (CEM MARS Xpress operating in selectable output of 0–1600 watts ± 15%; CEM Corporation, North Carolina, USA). The Ag concentration was determined using an inductively coupled plasma optical emission spectrophotometer (Varian 720 ICP-OES, New South Wales, Australia). The calibration internal standards were prepared by serially diluting the Merck ICP standard (Rahway, New Jersey, USA).

8.3.9 Calculation of enzymes activity (described in Appendix G)

8.3.10 Assay of antioxidant enzymes

Superoxide dismutase (SOD)

Measurement of SOD activity in earthworm homogenate was based on the inhibition of pyrogallol auto-oxidation with the extinction coefficient of pyrogallol as 2640 M/cm (Terevento *et al*., 2010). Briefly, 2.85 ml of phosphate buffer (pH 8), 75 µl of 10 mM pyrogallol and 75 µl of homogenate were mixed and the kinetics followed by measuring the increase in absorbance at 340 nm, every minute for 4 min.

Catalase (CAT)

Measurement of CAT analysis was based on determination of the kinetics of the degradation of H_2O_2 with the extinction coefficient of H_2O_2 as 43.6 M/cm (Cataldo *et al*., 2011). Briefly, 72.5 µl of 50 mM phosphate buffer (pH 6.5), 2.5 ml of 300 mM H_2O_2 (30% w/w), and 0.5 ml of earthworm homogenate were mixed, and the kinetics followed by measuring the decrease in absorbance at 240 nm, every minute for 4 min. The blank contained sodium phosphate buffer and H_2O_2

Glutathione peroxidase (GPx)

The assay mixture consisted of 1.97 ml of assay buffer (1 mM reduced glutathione [GSH], 50 mM phosphate buffer, 0.15 mM NADPH, 1 mM Na azide, 1.5U glutathione reductase (GR), 0.15 mM H_2O_2 and 0.0073 g EDTA). To this, 30 µl of earthworm homogenate was added and the GPx activity measured for 4 min at 22°C based on the oxidation of NADPH monitored by the decrease in absorbance of the incubation mixture at 340 nm measured every minute for 4 min. The extinction coefficient of NADPH was 6220 M/cm (Terevento *et al.*, 2010). The GPx activity was expressed as µmol oxidized NADPH min^{-1} mg^{-1}.

Glutathione-S-transferase (GST)

Measurement of GST in earthworm homogenates was based on the increase in absorbance at 340 nm due to the conjugation of GST to 1-chloro-2,4-dinitro-benzene (CDNB) and extinction coefficient of GSH as 9.6 M/cm (Cataldo *et al.*, 2011). Briefly, the reaction mixture contained 100 µl of freshly prepared GSH (40 mM) in phosphate buffer (0.01 M, pH 7.6), 100 µl of CDNB (1 mM) and 500 µl of potassium phosphate buffer (0.1 M, pH 6.5), which were mixed and incubated for 5 min at 25°C. The reaction was initiated by adding 30 µl of earthworm homogenate and the increase in absorbance at 340 nm followed every minute for 4 min.

Lipid peroxidation (LPO)

The assay of thiobarbituric acid (TBA) reactive substances (TBARS) measures malondialdehyde (MDA), as described by Cataldo *et al.* (2011). Initially, the proteins in the earthworm homogenates were removed by precipitation with trichloroacetic acid (30%), and centrifuged at 2000 × g for 20 min. To 1 ml of the supernatant, 1 mM EDTA and 1% TBA were added and the mixture heated in a boiling water bath for 15 min. The sample was cooled on ice and the absorbance of MDA measured at 532 nm. The concentration of MDA was calculated using the molar extinction coefficient of MDA (156 000 M/cm) and the results expressed as mg MDA equivalents normalised to total earthworm homogenate protein.

8.4 Statistical analysis

Data are presented as the mean ± SE (n = 5). Dose-response Ag accumulation in earthworms was analysed by linear regression. Minitab 17 software's statistical program was used to compare differences among treatment groups at each time point using ANOVA. Significance was set at $P < 0.05$. Explanatory variables were concentration of chemicals (Ag^+ and AgNPs) in mg/kg soil, time in weeks, and enzyme activity in µmol/mg protein.

8.5 Results

8.5.1 Silver nanoparticles

The concentration of the synthesised AgNPs used in these earthworm experiments as measured by FAAS ranged from 12 to 13 g/l. The morphology of AgNPs examined in TEM varied from circular to sometimes oval. The size distribution of the samples synthesised varied between 10 and 40 nm but most ranged from 10 to 30 nm with an average size of ~ 25 ± 8 nm. The AgNPs size measured by the zetasizer was 30 + 4 nm. Based on these 2 methods of calculation, the average size of AgNPs was taken as 30nm. The zeta potential of the synthesised AgNPs was −41 ± 6 mV indicating good stability of Ag.

8.5.2 Ag accumulation in earthworms

Following a 4-week exposure, the earthworms' accumulated Ag increased linearly as a function of exposure time (Fig. 8.1), to an average maximum of 0.84 mg/kg in the 300 mg/kg AgNPs soil treatment ($R^2 = 0.94$; $y = 0.0023x + 0.1418$) and 0.26 mg/kg in those exposed to the highest Ag$^+$ concentration of 10 mg/kg soil ($R^2 = 0.96$; $y = 0.023x + 0.0211$).

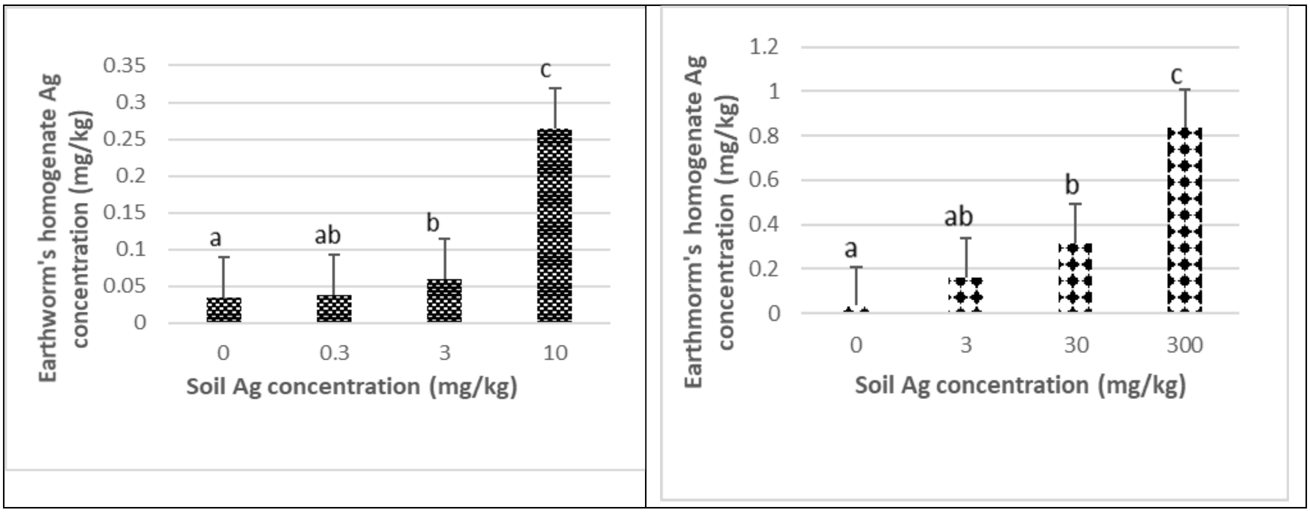

(A) Ag$^+$ (AgNO$_3$) **(B) AgNPs**

Fig. 8.1: Silver concentration (mean ± SEM) in homogenates of *A. caliginosa* (n = 5) exposed to (A) Ag$^+$ (AgNO$_3$; 0, 0.3, 3, 10 mg/kg) or (B) AgNPs (0, 3, 30, 300 mg/kg) at the end of week 4. Means with different letters on bars are significantly different ($P < 0.05$) from the controls.

8.5.3 Superoxide dismutase

The SOD enzyme activity in earthworms exposed to AgNPs or Ag$^+$ in soil is shown in Fig. 8.2. The statistical analyses of data from earthworms exposed to the two common concentrations of 3 and 0.3 mg/kg of Ag as AgNPs and AgNO$_3$ (Ag$^+$)are shown in Table 8.1. A dose-dependent significant increase ($P < 0.05$) in SOD enzyme activity in earthworms exposed to either AgNPs or Ag+ was evident at most time points (Fig. 8.2). The increase in SOD activity in earthworms exposed to Ag+ (Ag$^+$) was approximately twice that observed in the worms exposed to AgNPs (Table 8.1).

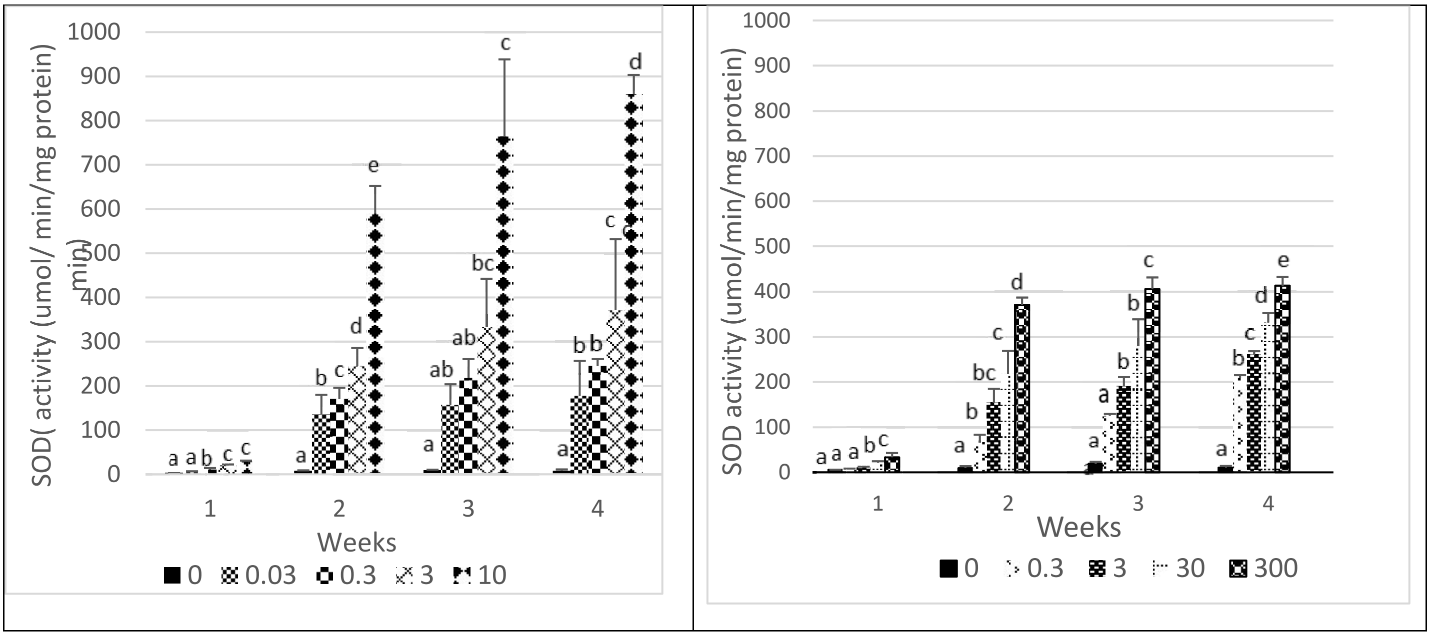

(A) AgNO₃ **(B) AgNPs**

Fig. 8.2: Superoxide dismutase (SOD) enzyme activity (mean ± SEM) in *A. caliginosa* (n = 5) exposed to (A) Ag^+ ($AgNO_3$; 0, 0.03, 0.3, 3, 10 mg/kg) or (B) AgNPs (0, 0.3, 3, 30, 300 mg/kg) for 1, 2, 3 and 4 weeks. Means with different letters on bars are significantly different ($P < 0.05$) from the controls.

Table 8.1: Comparison of mean enzyme activity, lipid peroxidation (LPO), and associated statistical data of *A. caliginosa* exposed to the two Ag concentrations (0.3, 3 mg/kg) common to both AgNPs and Ag^+ ($AgNO_3$). All enzyme results are expressed as µmol/mg protein. LPO is expressed as mg MDA / mg protein.

	$AgNO_3$ (Ag^+)	**AgNPs**	**Vr**	**SEM**	**Significance**	**LSD (5% level**
(a) 0.3 mg/kg						
SOD	199	102	23	23	P = 0.01	72
CAT	224	80	162	24	P < 0.001	76
GPx	53	33	13	10	P = 0.02	31
GST	27048	14839	7	6079	P = 0.03	19
LPO	532	291	5	126	NS (P = 0.09)	392
(b) 3 mg/kg						
SOD	263	154	11	44	P = 0.03	134
CAT	358	131	4	129	NS (P = 0.1)	401
GPx	110	54	7	23	P = 0.04	72
GST	44750	25112	5	7895	NS (P = 0.08)	19
LPO	1984	499	1	1690	NS (P = 0.28)	530

SOD: superoxide dismutase, CAT: catalase, GPx: glutathione peroxidase, GST: glutathione S transferase (all enzymes expressed as µmol min^{-1} mg $protein^{-1}$). LPO: lipid peroxidation (mg MDA per mg protein). Mean soil Ag^+ and AgNPs concentrations (mg/kg), Vr: variance ratio, SEM: standard error of the mean, LSD: least significant differences of means. This table involves comparison in enzymes activity between Ag+ and AgNPs (0.3 &3 mg/kg). Each enzyme activity consists of 5 replicants from each week over 4 weeks, the data was analysed using Genstat 17 soft ware.

8.5.4 Catalase

The CAT enzyme activity in *A. caliginosa* exposed to either AgNPs or Ag$^+$ (AgNO$_3$) over a 4-week period is shown in Fig. 8.3. A dose- and time-dependent significant increase at most time points was observed, with the elevated CAT enzyme activities most marked in the earthworms exposed to Ag$^+$ (Table 8.1)

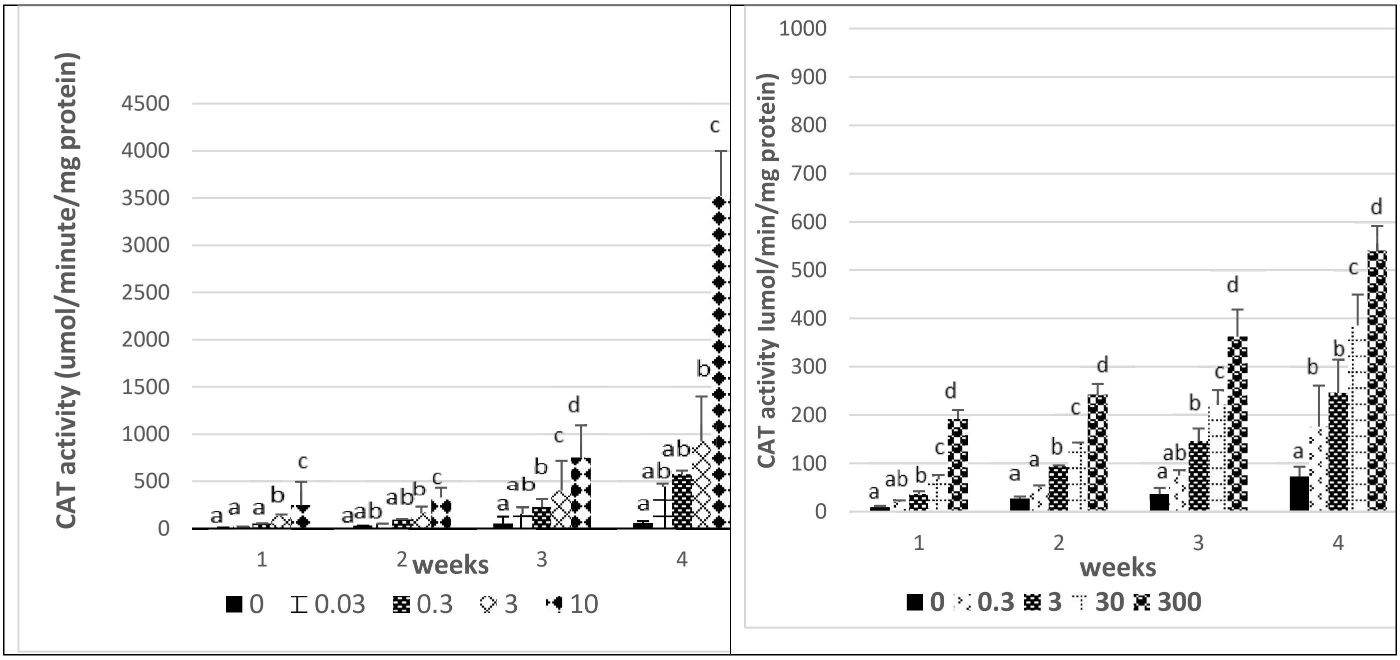

AgNO$_3$ **(B) AgNPs**

Fig. 8.3: Catalase (CAT) enzyme activity (mean ± SEM) in *A. caliginosa* (n = 5) exposed to (A) Ag$^+$ (AgNO$_3$; 0, 0.03, 0.3, 3, 10 mg/kg) or (B) AgNPs (0, 0.3, 3, 30, 300 mg/kg) for 1, 2, 3 and 4 weeks. Means with different letters on bars are significantly different ($P < 0.05$) from the controls.

8.5.5 Glutathione peroxidase

The GPx enzyme activity in *A. caliginosa* exposed to AgNPs or Ag$^+$ (AgNO$_3$) over 4-week periods is shown in Fig. 8.4. The GPx activity increased significantly ($P < 0.05$) in a dose-and time-dependent manner with the values observed on exposure to Ag$^+$ not significantly different from those observed in earthworms exposed to AgNPs (Table 8.1).

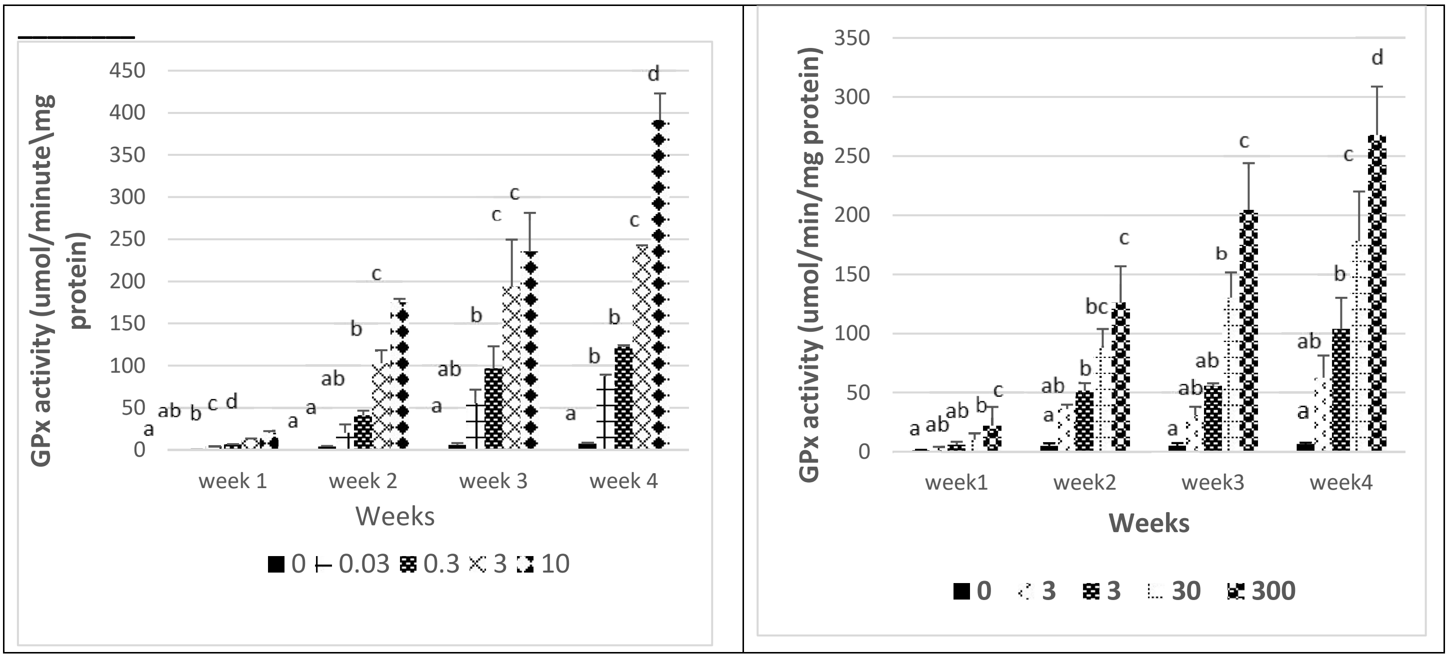

(A) AgNO3 **(B) AgNPs**

Fig. 8.4: Glutathione peroxidase (GPx) enzyme activity (mean ±SEM) in A. caliginosa (n=5) exposed To (A) Ag^+ ($AgNO_3$; 0, 0.03, 0.3, 3, 10 mg/kg) or (B) AgNPs (0, 0.3, 3, 30, 300 mg/kg) for 1, 2, 3, and 4 weeks. Means with ifferent letteras on bars are significantly different) $P < 0.05$) from the control.

8.5.6 Glutathione-S-transferase

The GSt enzyme activity wasmmarkedly elevated n earthworms exposed to both AgNPs and Ag^+ Compared to other enzyme activities (Table 8.1). There was a dose- and time- dependent increase in GSt in earthworms exposed to AgNPs or Ag^+ and this was most marked in thosed exposed to Ag^+ (Fig 8.5).

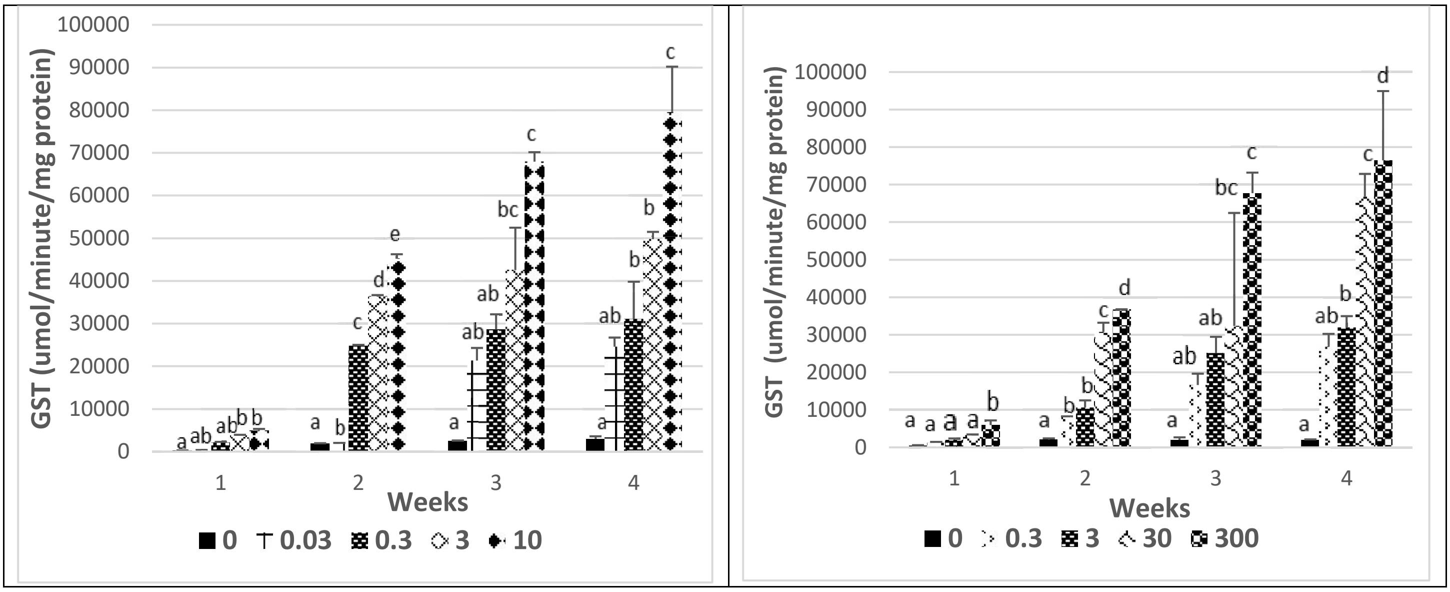

Fig. 8.5: Glutathione-S-transferase (GST) enzyme activity (mean ± SEM) in *A. caliginosa* (n = 5) exposed to (A) Ag^+ ($AgNO_3$; 0, 0.03, 0.3, 3, 10 mg/kg) or (B) AgNPs (0, 0.3, 3, 30, 300 mg/kg) for 1, 2, 3 and 4 weeks. Means with different letters on bars are significantly different ($P < 0.05$) from the controls.

8.5.6 Lipid peroxidation

The LPO activity as measured by MDA adduct formation is shown in Table 8.2, where there was a dose- and time-response increase in LPO following exposure to both AgNPs and Ag^+. The LPO activity was higher in earthworms exposed to Ag^+ > AgNPs over 4 weeks but not significantly different ($P > 0.05$)(Table 1?).

Table 8.2: Lipid peroxidation measured as malondialdehyde (MDA) equivalents normalised to total earthworm *A. caliginosa* homogenate protein (mean + SEM; n=5), following exposure to different concentrations of AgNPs or Ag^+ ($AgNO_3$) over 4 weeks. Means with different letters on bars in each column for Ag^+ and AgNPs are significantly different ($P < 0.05$) from the controls.

Ag mg/kg soil	Week 1	Week 2	Week 3	Week 4
AgNPs				
0	25.9 ± 4.97^a	51.21 ± 7.06^a	41.84 ± 11.94^a	52.25 ± 10.23^a
0.3	111.37 ± 8.91^{ab}	155.4 ± 12.2^a	222.52 ± 39.44^b	285.63 ± 29.21^b
3	179.73 ± 14.39^b	212.2 ± 25.49^b	258.4 ± 36.67^{bc}	407.46 ± 28.83^c
30	238.73 ±.33.03^c	281.5 ± 41.34^b	325.22 ± 50.52^c	438.6 ± 26.12^c
300	587.58 ± 38.82^d	608.4 ± 22.5^b	629.23 ± 7.15^d	738.31 ± 20.46^d
Ag^+				
0	46.51 ± 11.26^a	36.61 ± 4.06^a	34.09 ± 11.94^a	52.25 ± 10.23^a
0.03	119.42 ± 25.38^a	234.88 ± 21.78^{ab}	366.54 ± 62.84^{ab}	485.84 ± 128.42^b
0.3	174.32 ± 54.6^a	303.08 ± 28.21^{bc}	563.08 ± 83.76^{ab}	575.88 ± 154.88^c
3	382.24 ±.74.19^b	454.45 ± 29.2^{cd}	600.32 ± 77.74^{bc}	951 ± 302.8^c
10	546 ± 123.86^b	710.23 ± 57.7^{cd}	808.11 ± 7.15^c	1277 ± 358.34^d

8.6 Discussion

Since there are many industries that use AgNPs, there is potential for increased environmental and human exposure to occur with deleterious toxicological implications (Martirosyan *et al*., 2014). As noted in previous chapters, there is a likelihood that AgNPs will end up in soil as a result of application of sewage sludge for fertiliser, with resultant effects on soil organisms. Little is known regarding the risk posed by AgNPs and Ag^+ towards earthworms. The *A. caliginosa* earthworm was selected for this study because of its widespread occurrence in arable, pastoral, and agricultural lands in New Zealand, which makes it a good animal model to study the effects of AgNPs in the terrestrial environment of New Zealand.

One of the common mechanisms of toxicity mediated by NPs is the induction of OS (Oberdörster *et al*., 2005). This has been demonstrated with AgNPs, which induce high levels of ROS within cells (Kawata *et al*., 2009). Two modes of action have been proposed for the toxicity of AgNPs: (i) the direct induction of ROS by AgNPs (Wijnhoven *et al*., 2009) and (ii) surface oxidation leading to the release of Ag^+ ions on long-term incubation of AgNPs in soil and induction of ROS (McShan *et al*., 2014). The Ag^+ released from AgNPs can lead to LPO in earthworms *A. caliginosa* or *Eisenia fetida* (Li *et al*., 2015). ROS can stimulate the production of antioxidant molecules such as SOD, CAT, and GPx , which can minimize OS but if ROS concentration is very high, it can interact with and cause irreversible damage to proteins, lipids and nucleic acids (McShan *et al*., 2014). This study has clearly shown that the antioxidant enzymes that counteract OS and LPO were increased in a dose- and time-dependent manner in *A. caliginosa* exposed to either Ag^+ or AgNPs. Thus, over time, both mechanisms can lead to the harmful effects associated with AgNPs exposure (Durán *et al*., 2016; Wang *et al*., 2017).

Biomarkers are biological responses monitored in an organism exposed to chemicals and/or stress in the environment (Sanchez-Hernandez, 2006; Laguerre *et al*., 2009). For example, Ifemeje *et al*. (2015) exposed *E. fetida* to soil from a municipal open waste dump and observed elevated levels of ROS, CAT, SOD and LPO.The biomarkers of OS used in this study included the antioxidant enzymes SOD, CAT, GPx, and GST, and also LPO, all of which were in general significantly increased in a dose-dependent manner on exposure to both Ag^+ and AgNPs, with values in week 4 > week 3 > week 2 > week 1 (Figs 8.2–8.5). Superoxide dismutases are a ubiquitous family of metal-containing enzymes with bound Mn^{2+} (mitochondrial SOD) or Cu^{2+} or Zn^{2+} (intra- and extra-cellular SOD) as co-factors. These enzymes play a significant role in protecting cells from OS by catalysing the dismutation of O_2^- anions to H_2O_2 and O_2, and by the action of CAT this H_2O_2 is converted to water (Roubalová *et al*., 2015).

Gomes *et al*. (2015) observed that exposure of *E. fetida* to relatively high concentrations of AgNPs (uncoated, 10-nm particle size), ranging from 100 to 1500 mg/kg in OECD artificial soil (72% sand, 20% kaolin clay, 7% dried sphagnum, 0.275% $CaCO_3$) for 28 days increased LPO 2-fold. My results confirm that much lower doses can induce a much higher LPO, which is in agreement with the study of Martin *et al*. (2017), who used 30–50-nm particle-size AgNPs coated with polyvinylpyrrolidone. Among the antioxidant enzymes, CAT appears to be the most induced by AgNPs (Ribeiro *et al*., 2015). This is in agreement with my study which found a >2-fold increase in CAT activity by Ag^+. Gomes *et al*. (2015) showed that exposure of *E. fetida* to Ag^+ mixed in OECD soil spiked with from 25 to 200 mg/kg for 28 days resulted in an increase in GPx, SOD and GR by 300%, 100% and 200% respectively but reduced the activities of CAT and GST. These findings in earthworms exposed to very high concentrations are somewhat dissimilar to my much lower dose 4-week study where I observed a continued increase of all antioxidant enzymes up to 4 weeks. In addition to the doses exposed to, such differences could be attributed to several factors such as the earthworm species, soil type and also the coating agent used. Gomes *et al*. (2015) used *E. fetida* while I used *A. caliginosa* earthworms, and also Gomes *et al*. (2015) used high doses up to 200 mg/kg Ag^+ and 1500 mg/kg of uncoated AgNPs, which could be considered as unrealistic environmental concentrations. Such high doses can lead to marked irreversible enzymatic and metabolic changes. Mendes *et al*. (2015) in a similar study but with *Folsomia candida* (a member of the order Collembola, a common and widespread arthropod that occurs in soils throughout the world) found that the increases in metallothionein and GST > CAT, GR (glutathione reductase), GSH (glutathione) and LPO were more marked in those exposed to Ag^+ than to AgNPs.

One of the most important differences between my earthworm AgNPs study and those reported by others is that I used a mixture of protease inhibitors, such as aprotinin, lupeptin, pepstatine, antipain, in the homogenising buffer (Concetti *et al*., 1984; Laguerre *et al*., 2009). In a preliminary study, the protein yield of the earthworm homogenate supernatant with the use of a PSB buffer with protease inhibitors resulted in at least a 50 % higher antioxidant enzyme activity (unpublished observation). I believe that this may have prevented enzyme degradation and hence contributed to higher enzyme activities even when expressed as a fraction of the protein concentration. This is an important finding and may explain the differences in antioxidant enzyme activities and LPO between my study and those reported by others.

Exposure of the soil invertebrate *Enchytraeus crypticus* to AgNPs showed that the OS mechanism caused by AgNPs may be somewhat different to that of Ag^+, with AgNPs taking a longer time than Ag^+ to produce toxic effects (Ribeiro *et al*., 2015). A comparison of the antioxidant enzyme profiles in earthworms exposed to the same concentrations (0.3 and 3 mg/kg soil) of Ag^+ and AgNPs (Table 8. 1) showed that enzyme activity was markedly higher in earthworms exposed to Ag^+. The higher antioxidant enzyme activities in earthworms exposed to Ag^+ even at doses 10 times lower than AgNPs is probably because of the high solubility and ready absorption of Ag^+ by *A. caliginosa* (Zhan, 2012). On a molar basis, Ag^+ ions are some 5.6*10^14 times more concentrated than an equal mass of AgNPs. Given this large difference in molarity, it is likely that the toxicity of AgNPs is due in part to conversion of the AgNPs into Ag^+ ions, because such a dissociation occurs in the long-term. There are several reasons why Ag^+ may be more toxic than AgNPs. These include: (i) the solubility of Ag^+ is much higher than that of AgNPs because Ag^+ is a salt while AgNPs are considered as a base that forms a colloidal solution in water; (ii) Ag from AgNPs accumulates in the cell membranes whereas Ag^+ is localised in the cytosolic fraction (Li *et al*., 2015), and (iii) the elimination rate of Ag when exposed to as AgNPs is greater than that of Ag^+ (Ribeiro *et al*., 2015). Therefore, there is higher bioaccumulation of Ag on exposure to Ag^+, which can lead to marked oxidative damage in *Lumbricus terrestris* (Henson-Ramsey *et al*., 2009). In my study, induction of antioxidant enzymes was higher on exposure to Ag^+ > AgNPs. This finding agrees with my Ag accumulation data (~10-fold higher) and also with LPO results (2.5- to 3-fold higher) on exposure to 0.3 and 3mg/kg of Ag^+ concentration compared to AgNPs (Table 8.2). In contrast, Schlich *et al*. (2013) reported that the uptake of Ag from 15-nm AgNPs by earthworms was slightly greater than the uptake from Ag^+. When the earthworm *E. fetida* was exposed to AgNPs of two particle sizes at doses up to 500 mg/kg for 14 days, the smaller 10-nm particles were more toxic than the 80-nm (Li *et al*., 2012). Thus, it appears that AgNPs' size influences uptake and also the degree of toxicity. In addition to a greater accumulation rate of Ag^+, as described in chapter 9, some toxicokinetic parameters such as total body clearance, mean residence, half-life, bioaccumulation factor, elimination rate constant, volume of distributions and area under the curve also contribute to the greater toxicity of Ag^+ than AgNPs to *A. caliginosa* (submitted for publication).

According to Zhan (2012), the 48h LD_{50} of Ag^+ to *A. caliginosa* is 418 mg/kg, which is higher than the LD_{50} of 305 mg/kg measured by me (unpublished observation). In my 72h LD_{50} studies AgNPs (2649.2 mg/kg) were less toxic, with earthworms exposed to AgNPs taking a longer time to show toxic effects than those exposed to Ag^+, which is in agreement with Ribeiro *et al*. (2015). Choi and Park (2015) observed no mortality in *E. fetida* exposed to up to 100 mg/kg of AgNPs (citrate coated, particle size 11 nm) mixed with artificial soil and concluded that AgNPs are not acutely toxic. In contrast, Brami *et al*. (2017) observed that exposure of *Allolobophora chlorotica* earthworms to Ag^+ or AgNPs mixed in Kettering loam soil (24% clay, 18% silt, 58% sand, 6.7% organic matter, pH 6.8) at a dose of 100 mg/kg soil caused 12.5% mortality with AgNPs (uncoated spherical 80 nm particle size) compared to 66.7% with Ag^+. The highest doses of Ag^+ and AgNPs used in my study were 10 and 300 mg/kg respectively mixed in Templeton Silt Loam soil in a 4-week exposure period with *A. caliginosa*. No deaths occurred. This highlights that different earthworm species have differing sensitivities to different Ag compounds in different soil types. Wilson *et al*. (2010) mixed artificial soil with 10, 100 and 1000 mg/kg AgNPs and 10 and 100 mg/kg Ag^+ and observed that earthworms exposed to Ag^+ accumulated higher Ag concentrations than those exposed to AgNPs, which is in agreement with my results of Ag accumulation at the same Ag dose (3 mg/kg). This is also in agreement with my pharmacokinetic studies of a higher bioconcentration factor in *A. caliginosa* with Ag^+ when exposed to the same AgNPs and Ag^+ dose of 20 mg/kg (personal observation).

Pollution by heavy metals of anthropogenic origin has for some time been recognised as a serious threat to terrestrial ecosystems. Heavy metals in soil are assimilated by earthworms by soil ingestion, via ion exchange of dissolved heavy metals across the lipophilic outer membrane and/or adsorption on membrane surfaces. A range of heavy metals, especially divalent metals such as Cd^{2+}, Cu^{2+}, chromium (Cr^{2+}), Pb^{2+} and Zn^{2+}, accumulated in tissues of the earthworm *Eudrillus eugineae* exposed to 0.1 g and 1.5 g of waste (vermicomposting of municipal solid waste) (Kumar *et al*., 2008). Similarly, Ag^+ ions also accumulate in earthworms. Among the heavy metals, Cd is regarded as most toxic to earthworms and exposure of *E. andrei* to Cd^{2+} concentrations within the range 10–100 mg/kg in soil increased earthworm LPO activity in a dose-dependent manner, about 1.5- to 2-fold compared to the controls, and the accumulation of Ag in earthworm homogenate was directly related to the Ag concentration in soil (Panzarino *et al*., 2016), which is similar to my finding. However, Panzarino *et al*. (2016) showed that exposure of *E. andrei* to a higher Cd dose (100 mg/kg) in soil (composed of 70% quartz sand, 20% kaolin clay, 10% sphagnum, pH 6.1) resulted in a decline in CAT activity by 4-fold, which is in contrast to my findings, but increased LPO by 1.6-fold. However, on exposure of *E. andrei* to both AgNPs and Ag+, there was both a dose- and time-dependent increase in CAT similar to my findings. In my study, on exposure of *A. caliginosa* to AgNPs and Ag^+, CAT activity was elevated from week 1 onwards. Curieses *et al*. (2017) reported that CAT and metallothionein in coelomocytes and tissues of *E. fetida* were similarly elevated on exposure to AgNPs and Ag^+. I found that antioxidants and LPO were elevated and the increases were both dose- and time-dependent in *A. caliginosa* exposed to Ag^+ > AgNPs, and at week 4, the increases were 10-fold more than in AgNPs exposed earthworms.

It appears that different metals other than Ag vary in their effect on antioxidant enzyme activity in earthworms. In a study carried out on *A. caliginosa* at a mining site which was also contaminated with Ag in addition to Pb and Cu, the activities of CAT, GPx, and GST were elevated, and also LPO significantly lower, in earthworms sampled away from the mine site (Łaszczyca *et al*., 2004). When the earthworm *Lampito mauritii* was exposed to different doses of other mteals such as Pb and Zn separately for 28 days (Maity *et al*., 2008), the activities of GST, GPx, GSH and GR were linearly increased on exposure to Pb, but on exposure to Zn, only the activities of GPx and GR increased and that occurred only after 14 days and at concentrations > 300 mg Zn. The differences in antioxidant enzyme activity reported in these studies could be attributed also to the type of earthworms used and the exposure dose (soil concentration and exposure period).

8.7 Conclusion

The exposure of *Aporrectodea caliginosa* earthworms to AgNPs or Ag^+ resulted in accumulation of Ag. A dose- and time-dependent increase in activity of the antioxidant enzymes CAT, GPx, SOD and GST and increased LPO were exhibited in earthworms exposed to Ag^+ > AgNPs. Based on the antioxidant enzyme activities and LPO activity, in general, Ag^+ was about 2.5- to 4-fold more toxic than AgNPs to *A. caliginosa*.

Chapter 9

Comparative Pharmacokinetics Analysis of Silver in Earthworm *Aporrectodea caliginosa* Exposed to AgNPs/Ag^+

9.1 Abstract

A pharmacokinetics study was conducted in *A. caliginosa* to identify why Ag^+ is more toxic than AgNPs to the earthworm. The *A. caliginosa* earthworms were incubated in soil amended with 20 mg/kg AgNPs or Ag^+ (as $AgNO_3$) for 72 h (uptake phase), followed by transfer to clean soil for a further 72 h (elimination phase). Results showed a significant difference ($P < 0.05$) between the two treatments. Total body clearance, volume of distribution, and elimination rate constant of total body silver were significantly ($P < 0.05$) higher in earthworms exposed to AgNPs. In contrast, mean residence time, terminal half-life, maximum concentration, area under the curve to T last, and bioconcentration factor were higher in earthworms exposed to Ag^+. The pharmacokinetic observations in combination with the high solubility $AgNO_3$ (Ag^+) as reported by others and in Chapter 8 explain the greater toxicity or confirm that Ag+ is more toxic than AgNPs to terrestrial organisms such as earthworms.

9.2 Introduction

Engineered AgNPs are now widely incorporated into many consumer and industrial products. AgNPs have been imbedded in many materials during the manufacturing process and are present in finished products as wide ranging as socks to prevent odour, kitchenware to improve hardness, and have also been incorporated in toothpaste (Xiong *et al.*, 2013). Silver nanoparticles have also been used as carriers for delivering small drug molecules or large biomolecules to specific targets (Babu *et al.*, 2013).

Nanoparticles can enter waste water and end up in sewage sludge, which may be used as fertiliser but can lead to soil infertility (Lee *et al.*, 2012; Caballero-Guzman and Nowack, 2016; Meier *et al.*, 2016). When NPs are present in the soil they can be taken up by soil-dwelling organisms thus causing adverse impacts on the microbial community by generation of ROS and interfering with a range of enzymes such as those involved in energy pathways (Colman *et al.*, 2013; Garcia-Gómez *et al.*, 2014). So, there is now a strong need to understand the environmental impact of NPs such as AgNPs that may be released into the air, soil or water during production, use and disposal (Stensberg *et al*., 2011; Dobias & Bernier- Latmanic, 2013).

Pharmacokinetic models may be used to help in understanding the environmental impact of AgNPs. Accordingly, the measurement of uptake, elimination, bioaccumulation and terminal half-life, along with other pharmacokinetic parameters, could help to assess how long a chemical could reside in soil and hence how long it could potentially be toxic to an invertebrate such as the earthworm when exposed to sub-lethal doses. Many pharmacokinetic studies in earthworms assume that the movement of toxic material from soil into the earthworm is an equilibrium process between soil/soil-water and toxin absorption into the earthworm (Connell and Markwell, 1990). Schlich *et al.* (2013b) reported that the bioaccumulation factor (BAF) in earthworms exposed to AgNPs was slightly higher than for Ag^+ at similar soil Ag concentrations. In contrast, Shoults-Wilson *et al.* (2011) reported lower BAF in earthworms exposed to AgNPs with Ag accumulation not solely related to Ag^+ released from the NPs. Similarly, Waalewijin-Kool *et al.* (2014) also observed that bioaccumulation of Ag from AgNPs was lower than from Ag^+ in springtails (*Folsomia candida*) and that the dissolved Ag in water could not fully explain the total Ag uptake from AgNPs. Świątek *et al.* (2017) studied the toxicokinetics of two concentrations of Zn oxide NPs (ZnO-NPs; Zn at 500 and 1000 µg/g) compared to $ZnCl_2$ (Zn at 250 and 500 µg/g) in the *Eisenia andrei* earthworm*.* The pharmacokinetics parameters, assimilation rate constant (k_A) and elimination rate constant (k_E) were assessed using a one-compartment model for total Zn concentration in soil and soil water. The results showed that k_A was higher for soil Zn^{2+} concentration while in the water k_A was higher for ZnO-NPs. The value of k_E did not differ between the two forms of Zn in soil, but at higher concentrations, k_E related to water Zn concentration from $ZnCl_2$ was significantly higher than for ZnO-NPs.

Tourinho *et al.* (2015) found no significant difference in pharmacokinetics parameters (uptake rate constant, elimination rate constant) when woodlice (*Porcellionides pruinosus*) were exposed to AgNPs or Ag^+ ($AgNO_3$) mixed with soil at 30 and 60 mg/kg. However, when mixed in the diet, the uptake rate constant was five times higher in AgNPs with no difference in the elimination rate constant. Skip *et al.* (2014) concluded that when metal toxicokinetics follow a one-compartment model, the model allows for uptake and elimination rate constants to change between toxicokinetic stages. However, a one-compartment model did not explain toxicity when observed in terrestrial invertebrates exposed to highly contaminated feed/soil. The authors believed that the main toxicokinetic mechanism results in gut epicellular damage. Gut damage may result in a reduced metal assimilation rate and the shedding of dead cells can result in increased elimination rate (Bednarska *et al.*, 2016). Labrot *et al.* (1999), compared toxicokinetic parameters for a freshwater clam (*carbicula fluminea*) and earthworms (*E. fetida* and *Brachydani rerio)* on exposure to Pb and uranium (U). Both Pb and U were equally very toxic to the earthworm *E. fetida*. However, Pb was not toxic towards the freshwater clam whereas U was very toxic. All three-species accumulated Pb and U to varying degrees. Furthermore, in the clam Pb was not expelled by depuration.

The toxicokinetics of Cd in five species of *Artemia* (brine shrimp) was evaluated using a bicompartmental model. The BAF was inversely related to exposure concentration whilst the elimination rate was directly related to the exposure concentration. The rate of metal influx remained relatively constant with fast elimination (Sarabia *et al*., 2006). My observations on earlier studies regarding exposure of *A. caliginosa* earthworms to AgNPs or Ag^+ reported in Chapter 8 showed about a 10-fold increase in toxicity with Ag^+ compared to AgNPs based on elevated antioxidant enzyme activity. The LD_{50} values for AgNPs and Ag^+ of 2649 and 305 mg/kg respectively reported in Chapter 8, section 8.3.3, also confirm the greater toxicity of Ag^+ compared to AgNPs.

This study was performed using non-compartmental pharmacokinetics to compare AgNPs and Ag^+ toxicity to the earthworm *A. caliginosa* exposed to Templeton Silt Loam Soil (TSL) amended with AgNPs or $AgNO_3$ (Ag^+) containing the same Ag concentrations (20 mg/kg soil).

9.3 Materials and methods

9.3.1 Soil

A general description of the preparation of soil amended with AgNPs and Ag is given in Chapter 4 sections 4.3.1 and 4.3.5 and the properties of TSL soil are described in Table 4.1. All the chemicals used in this pharmacokinetics study are reported in Chapter 3 Materials and Methods.

9.3.2 Earthworms *A. caliginosa*

One hundred and eight *A. caliginosa* earthworms weighing 0.8–1.2 g were collected from the Johnston Memorial Laboratory farm and kept in moistened TSL soil with added nutrients and cow manure to feed the worms. The worms were transferred to another TSL soil without added cow manure 24 h prior to the experiment.

9.3.3 Nanoparticle preparation

As described in Chapter 3, section 3.1.

9.3.4 Silver nanoparticles characterisation

As described in Chapter 3, section 3.4.

9.3.5 Experimental design

Templeton silt loam soil (5 kg) was placed in two containers each holding 1.5 kg and covered by lids with air venting holes. Soil in each container was amended and mixed well with 20 mg/kg Ag in the form of AgNPs or Ag^+ (as $AgNO_3$) and 10 ml of water to keep the soil slightly moist. Fifty *A. caliginosa* earthworms were added to each container and left at room temperature. Samples of worms (n = 4) were collected from each container at 2, 6, 12, 24, 48, 72 h (uptake phase). At 72 h, the remaining worms from each container were transferred to another two containers each containing 1.5 kg of fresh TSL soil, and samples of worms (n = 4) were collected at 96, 120 and 144 h (elimination phase). The collected worms were washed, dried, weighed, and stored at −20°C pending acid digestion and measurement using Inductive Coupled Plasma attached to Optical Emission Spectrometry (ICP-OES), as mentioned in Chapter 3, section 3.6.2.

9.3.6 Silver analysis

This was conducted using ICP-OES as described in Chapter 3, section 3.6.2. The concentration of the Ag stock solution was 1 mg/ml. The calibration standards used were within the range from 0.1 to 1 µg/ml made by serial dilution using deionised water.

9.4 Pharmacokinetic analysis

Non-compartmental pharmacokinetic analysis of Ag in *A. caliginosa* following exposure to AgNPs and Ag^+ was performed using a Windows-based program (n-comp) as reported by Laub and Gallo (1996). The area under the curve (AUC) to T last, terminal half-life (T½) and mean residence life (MRT) were calculated according to the method of Purves (1992). The terminal elimination constant (K_e) was calculated as being 0.693/T½ (Mikov *et al.*, 2007). Total body clearance was calculated as dose/AUC. The volume of distribution was calculated according to equation: $V_d = \text{dose}/(\text{AUC}*K_e)$.

9.5 Statistical analysis

Statistical comparison between AgNPs and Ag^+ was carried out by applying Student's *t*-test (Zar, 1999; Social science statistics, n.d.). The level of significance was $P < 0.05$.

9.6 Results

The Ag concentration of the synthesised AgNPs suspension measured by flame atomic spectrometry was found to be 13.65 g/l (as described in Chapter 3, section 3.2). Based on TEM, the morphology varied from circular to oval while the size distribution of AgNPs varied between 10 and 40 nm with most particles ranging 10–30 nm with an average of ~ 25 ± 8 nm (see Chapter 3, section 3.3). The

AgNPs size measured by zetasizer was 30 ± 4 nm while the zeta potential was −41 ± 6 Mv (see Chapter 3, section 3.4).

The Ag deposition concentration curve in relation to time following incubation of *A. caliginosa* in soil amended with 20 mg/kg of Ag (as AgNPs or Ag^+) is shown in Fig. 9.1.

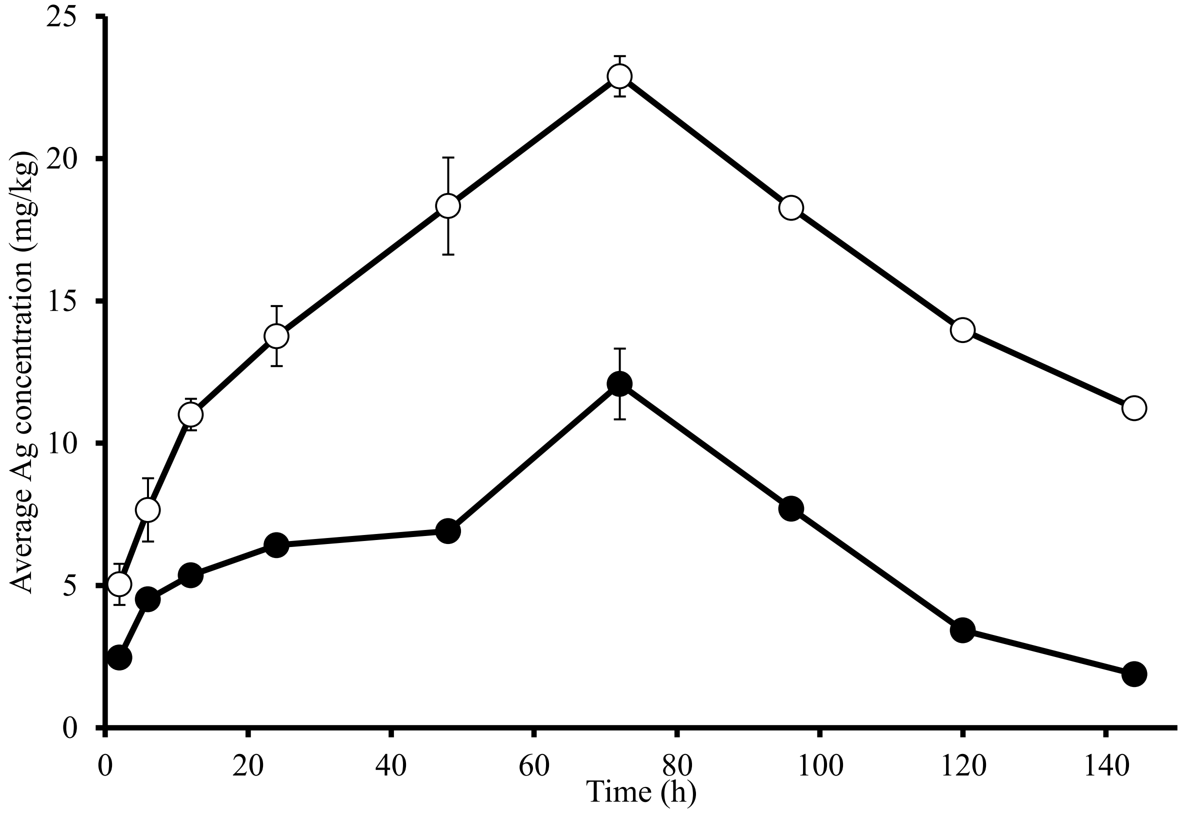

Fig. 9.1: Mean silver (Ag) concentration in *A. caliginosa* earthworm homogenate following exposure to Ag in soil at 20 mg/kg in the form of AgNP (●) or Ag^+ (○). The bars are standard error of the mean (n = 4) at each time point.

The values of the pharmacokinetic parameters are presented in Table 9.1. There was a significant difference ($P < 0.05$) in all pharmacokinetic parameters between earthworms exposed to Ag in soil amended with AgNPs and those exposed to soil amended with Ag^+.

Table 9.1: Values for pharmacokinetic parameters following exposure of *A. caliginosa* earthworms to TSL soil amended with 20 mg/kg AgNP or Ag^+. ($AgNO_3$). Results are presented as mean ± standard error of the mean (n = 4).

Pharmacokinetic parameters	AgNP	Ag^+($AgNO_3$)	P-value
Body clearance, Cl (µg ml^{-1} h^{-1})	0.02 ± 0.0	0.005 ± 0.0	<0.00001
Mean residence time, MRT	74.98 ± 0.0	130.98 ± 7.3	0.00297
Steady state volume of distribution, Vd (ml/kg)	1.47 ± 1.0	0.755 ± 0.02	<0.00001
Terminal half-life, T½ (h)	25.93 ± 0.6	70.72 ± 5.4	0.000213
Maximum concentration, C_{max} (µg/ml)	12.08 ± 3.5	22.89 ± 0.6	0.00014
Area under the curve to last time, $AUC_{0\text{-}T}$ (µg h^{-1} ml^{-1})	950.81 ± 18.4	2320.24 ± 52.2	<0.00001
Elimination rate constant, K_e	0.013 ± 0.00	0.008 ± 0.00	0.000015
Bioconcentration factor, BCF (ug/g AgNP or $AgNO_3$/ug/g metal in earthworms)	0.604 ± 0.05	1.144 ± 0.03	0.000139

9.7 Discussion

Aporrectodea caliginosa is the most widespread earthworm in New Zealand agricultural soils. Silver nanoparticles and Ag^+ induce high antioxidant enzyme activities not only in earthworms (see Chapters 7 and 8) but also in plants (Chapter 6). Many researchers have reported that Ag^+ ($AgNO_3$) is more toxic than AgNPs to earthworms and plants (Wilson *et al.*, 2010; Zhan, 2012; Schlich *et al.*, 2013b; Xiong *et al.*, 2014; Choi and Park, 2015). To the best of my knowledge, this is the first study that reports Ag pharmacokinetic parameters following exposure of *A. caliginosa* to AgNPs and Ag^+. All pharmacokinetics parameter values in *A. caliginosa* exposed to Ag^+ were much higher than those exposed to AgNPs, except V_d and K_e which were significantly lower. Volume of distribution is usually inversely related to the degree of protein binding capacity in the host (Wasfi *et al.*, 1998). Thus, it seems that Ag^+ is more protein binding than AgNP. The total body clearance of Ag in earthworms exposed to Ag^+ was less than in those exposed to AgNPs. This difference in clearance was reflected in the T½of earthworms exposed to Ag^+ which was much higher, 3-fold more than in earthworms exposed to AgNPs (70.72 h vs 25.93 h). The difference in $T_{1/2}$ could be due to a variety of factors including that Ag^+ and AgNPs are metabolised by different enzymatic systems in the body (Ji *et al.*, 2013). In my study the value of T½ of AgNPs exposure was ~ 1 day and on exposure to Ag^+ it was 3 days. The estimated T½ in different invertebrates exposed to Cd varies between 2 and 53 days (Sarabia *et al.*, 2006). For example, when exposed to Cd the T½ of the crustacean *Asellus aquaticus* was 22 days (Van Hattum *et al.*, 1989) and in gammarids it was ~ 43 h (Zauke *et al.,* 1995).The half-life of Zn in the earthworm *E. fetida* exposed to ZnO-NPs and Zn^{2+} was 30 days, and to cobalt was 35 days (Świątek *et al.*, 2017). Sarabia *et al.* (2006) reported a value of 32–139 h for Cd T½ in *Artemia.*

Tourinho *et al.* (2016) exposed *Porcellionides pruinosus* (woodlice) to AgNPs (3–8 nm particle size and alkane coating) and Ag^+ (as $AgNO_3$) in lufa soil and alder leaves (as feed). Soils were spiked with varied concentrations of Ag ranging from 50 to 800 mg/kg of AgNPs and 12.5 to 200 mg/kg of Ag^+as $AgNO_3$. The uptake and K_e via soil exposure did not differ significantly for Ag at 30 and 60 mg/kg. These authors also spiked the surface of alder leaves with the Ag concentrations used in the soil study. Tourinho *et al.* (2016) also reported an extremely high Ag accumulation in isopods exposed to Ag via application to alder leaves and believed that the isopods have an efficient heavy metal storage compartment. In my study, the K_e in AgNPs > Ag^+ ($AgNO_3$) at the exposure dose of 20 mg/kg in soil were 0.013 and 0.008 respectively. The difference in K_e could be due to the differences in the host, soil, AgNPs coating agent and particle sizes. In my study, citrate-coated AgNPs with particle size 30 nm were used in *A. caliginosa* incubated in TSL soil and the dose used was 20 mg/kg.

Following uptake through dermal contact and ingestion, AgNPs are internalised in the earthworm directly via the endocytosis pathway (Diez-Ortiz *et al*. 2015) whereas with ZnO-NPs, the intake was through dissolution (Bednarska *et al.*, 2016).

Waalewijin-Kool *et al.* (2014) reported that in the pharmacokinetics study of Ag in the springtail *Folsomia candida,* Ag^+ from $AgNO_3$ exhibited a lower K_e resulting in higher BAF and T½ values also compared with exposure to AgNPs. This observation agrees with my studies but not with the results of Tourinho *et al.* (2016), who reported no significant difference between Ag^+ and AgNPs toxicity. The difference in study results may be due to the different species used in the two experiments. Ramsey *et al.* (2009) reported that on exposure of *Anuran larvae* to Malathion, the elimination rate constant was 0.0204 ml/h, which was 2-fold higher than the K_e when earthworms are exposed to AgNPs and 3-fold higher in the case of Ag^+.

On exposure of the earthworm L*umbricus rubellus* to both Ag^+ and AgNP (Diez-Ortiz *et al.*, 2015), most if not all the Ag is taken up through the oral route and via the gut. The authors also reported that the concentration of Ag in the gut was higher from exposure to AgNPs than from Ag^+. When the mouth of the earthworm was sealed, Ag uptake was reduced by 40–70%. The X-ray analysis that shows internal distribution of Ag supported this finding. The K_e was low and was similar in both sealed and unsealed worms, when the earthworms were exposed to Ag^+ and AgNPs at 100 mg/kg soil.

Earthworms on exposure to some heavy metals such Cd, Cu, Zn, Ni exhibited damage to the mid gut cells and this damage was greater if the heavy metal stayed in the gut (Bednarska *et al.*, 2016). In my studies, Ag^+ may have caused more damage to earthworm tissues than AgNPs since it stayed in the gut for a longer time based on the pharmacokinetics analysis (Table 9.1).

On exposure of *Eisenia fetida* earthworms to aqueous solutions (40 mM) of Cd, Ni, Cu massive damage resulted to the mid-gut epithelium cells and the authors reported that Cd was the more toxic of the heavy metals since it was retained in the gut for the longest time (Bednarska *et al.*, 2016).

My studies showed that the BCF value in TSL soil was 0.6 for AgNPs and 1.44 for Ag^+. Thus Belfroid *et al.* (1995) reported a lower value for BCF for chlorobenzene in earthworms. The difference could be attributed to many reasons such as differences in the chemicals used, soil exposure time and the incubation medium. Generally, BAF value affects the partition co-efficient and there is a linear relationship between log BAF and log K_{ow} (Meylan *et al.*, 1999). Bioaccumulation could be estimated using a mechanistic model and can be described by thermodynamic partitioning between soil-solid, soil-water and the residence organism as reported by Tjalling (1998).

On exposure of the earthworm *E. andrei* to ZnO-NPs at doses between 250 and 500 µg/g for Zn^{2+} and 500 and 1000 µg/g for ZnO-NPs for 21 days followed by 21 days' elimination in clean soil, no mortality occurred and a rapid increase in internal Zn concentration was followed by a decrease to an equilibrium during the uptake phase and then a further decrease during the elimination phase (Świątek *et al.*, 2017). This was not observed in my study. Following environmental exposure of organisms such as earthworms to heavy metals, the pharmacokinetics, such as uptake and release of metal and the effect of these metals on the organism, reflect the type, nature, and concentration of the heavy metals present in that environment.

9.8 Conclusion

In a comparison of toxicity between AgNPs and Ag^+, the pharmacokinetic parameters provided an explanation as to why Ag^+ is more toxic than AgNPs when the earthworm *A. caliginosa* is exposed to both these forms of Ag at the same exposure doses. One of the major reasons for the difference was the solubility of $AgNO_3$ (Ag^+) whereby it is absorbed readily by the earthworm, whereas AgNPs, because of their particle size and the differences in pharmacokinetics parameters, is not.

Chapter 10

General Discussion, Conclusions and Future Research

10.1 General discussion

The discharge of AgNPs and dissociated Ag^+ ions in the long-term from AgNPs from industries (Tran *et al.,* 2013) via disposal of sludge from wastewater treatment plants represents a major threat to soil biota (including non-target earthworms) and plants since they are continually exposed throughout their lifespan. This project was conducted to study the fate and mobility of these Ag compounds in soil, the toxicity of Ag as AgNPs (and dissociated Ag^+ ions in the long-term) and Ag^+ (from $AgNO_3$) to an environmentally relevant earthworm in New Zealand, *Aporrectodea caliginosa*, and a plant, the sunflower *Helianthus annuus.*

Many methods have been use to synthesise AgNPs from Ag compounds, especially from $AgNO_3$, using chemical reduction, electrochemical, phytochemical, radiolytic and biological methods (Zhang *et al.*, 2016). Among these methods, chemical reduction is the most popular, where the metal ion precursors in solution are converted to zero-valent Ag atoms in the presence of reducing and coating agents, forming AgNPs. The reducing agents used are varied, and include ferrous sulphate heptahydrate, trisodium citrate, sodium borohydride, silica, polyethylene glycol, glucose, and sodium borohydride. The coating agents commonly used in AgNPs synthesis are PVP, polyvinyl alcohol and trisodium citrate. In my study I used a chemical reduction method and citrate coating because it is the easiest way to produce AgNPs with minimal aggregation and good stability (Sileikaite *et al.*, 2006; Udapudi *et al.*, 2012; I. Kim *et al.*, 2016). Both citrate and PVP coating produce a negative charge and are less toxic than uncoated NPs, with PVP coating more toxic than citrate (Nguyen *et al.*, 2013). Hence, I used citrate to coat the AgNPs. In soil, there is a high degree of repulsion between the negative charge of citrate-coated AgNPs and bacteria, which forms an electrostatic barrier that limits the interactions between cells and the particles and hence the AgNPs have reduced toxicity to organisms (El Badawy *et al.*, 2010). The size and shape of the AgNPs produced are strongly dependent on nucleation and subsequent growth, with a need to adjust reaction temperature, pH, precursors' reduction, and stabilising/coating agents to produce monodispersed AgNPs with uniform size distribution (Tran *et al.*, 2013).

The synthesised AgNPs give maximum absorbance at 400 nm, because they absorb and scatter light with extraordinary efficiency at this wavelength. The conduction electrons on the metal's surface undergo collective oscillation when they are excited by light at a specific wavelength. This oscillation is known as surface plasmon resonance (SPR) (Daghestani and Day, 2010).

The smaller AgNPs primarily absorb light near 400 nm (Fig. 3.1), while larger spheres exhibit increased light scattering and have peaks that broaden and shift towards longer wavelengths. The shift towards a longer wavelength could result from aggregation of particles (a red shift). Silver nanoparticles exhibit new properties that are not found in either molecule or bulk material, for example the presence of an absorption band at the border between ultraviolet and visible regions. This band is seeming to be present because of the surface plasmon oscillation modes of the conduction electrons, which are coupled through the surface to the external magnetic field (Sileikaite *et al.,* 2006). Udapudi *et al.* (2012) reported that the maximum absorbance of synthesised AgNPs is at 450 nm and the colour of the produced solution was pale yellow, while in my experiment the colour was reddish black, and the maximum absorbance was at 400 nm. This is despite the fact we both used the chemical reduction method of $AgNO_3$ to prepare AgNPs. This difference could be attributed to their use of boiling $AgNO_3$ solution and also not adding ferrous sulphate heptahydrate as the reducing agent with trisodium citrate.

10.2 Impact of silver nanoparticles / silver nitrate in soil on earthworms

The synthesised AgNPs and Ag^+ were used in my project to evaluate the toxicity to *A. caliginosa* when exposed to these two Ag forms, by monitoring LPO and antioxidant enzymes (Akter *et al.*, 2018). Oxidative stress occurs when these defensive antioxidants within cells fail to remove excessive ROS. The exposure of earthworms to these two Ag forms can result in elevated antioxidant defence enzymes, which can then be used as biomarkers (Vlahogianni *et al.*, 2007). In my studies, I monitored SOD, CAT, GPx and GST in addition to LPO.

Superoxide dismutase play an important role in the elimination of ROS. The superoxide anion radical (O^-_2) in cells is transformed by SOD enzymes to H_2O_2 which is then transformed into water and O_2 by CAT and other peroxidases (Livingstone *et al.*, 1990; Nordberg and Arner, 2001; Singh *et al.*, 2006). Superoxide dismutase enzyme activity varies in different organisms and plants. In my studies, SOD activity in *A. caliginosa* increased with length of exposure and Ag exposure concentration (Fig. 8.2), which is in agreement to that observed by Chao *et al.* (2017) in *E. fetida* exposed to microcystin toxin MC-LR. The activity of SOD declines if the ROS produced in cells is very high (Gomes *et al.*, 2015). Wen *et al.* (2017) exposed *E. fetida* in artificial soil (OECD, 1984) to 0.3, 0.4, 0.5, 0.6, 0.7, and 0.8

mg/kg dry weight concentration of MC-LR toxin and observed elevated activities of SOD, POX, CAT, and GPx in the earthworm in the first 21 days, but these returned back to control level at 28 days probably due to marked degradation of MC-LR in soil over time. In my experiments with *A. caliginosa*, SOD activity continually increased over the 4 weeks of the experiment, an increase that was both dose- and time-dependent.

Catalase is found in the peroxisome, mitochondria and cytosol and converts H_2O_2 into water and O_2 (Heck *et al.*, 2010). CAT activity in both *E. fetida* and *A. caliginosa* are sensitive to AgNPs/$AgNO_3$ (Ag^+) exposure. In my study, CAT activity was increased with both time of exposure and concentration of AgNPs/$AgNO_3$ (Ag^+) up to 300 and 10 mg/kg respectively. However, in a study carried by Cao *et al.* (2017) using artificial soil, CAT significantly increased initially in *E. fetida* exposed to 100 and 1000 µg/kg of MC-LR but declined after 7 days, which does not agree with my results. In other research performed by Pinho (2005) using 5.32 ug/kg MC-LR it was reported that there was an increase in CAT at 1 day and a decrease at 7 days. Otmani *et al.* (2018) exposed *E. fetida* to polluted soil collected from 0, 50, 100, 300, 1000 m from a battery-manufacturing facility and observed a significant increase in CAT activity with the highest being in the soil from 0 > 50 > 100 > 300 > 1000 m from battery plant at 1 < 3 < 7 days but declined at 14 days. Torres *et al.* (2002) suggested that the increase in antioxidant enzymes as a defence would be due to enhanced production of oxygen free radicals, which could stimulate antioxidant activity to cope with this increased oxidative stress to protect the cell from damage. A possible explanation is that the production of H_2O_2 at early stages may induce an increase in CAT activity but is then overwhelmed by OS with continued accumulation of ROS in the earthworm leading to an inhibition of CAT activity later. It is also to be recognised that *A. caliginosa* and *E. fetida* respond to different contaminants in different soils types and doses in different ways to cope with OS.

Glutathione peroxidase is a cytosolic enzyme that catalyses the reduction of H_2O_2 to H_2O and O_2 as well as catalysing the reduction of peroxide radicals to alcohols and O_2 (Mkoji *et al.*, 1988; Nair *et al.*, 2010). Thus, it acts similarly to CAT. GPx also reduces toxic LPO to corresponding less toxic hydroxy fatty acids utilising GSH. Cao *et al.* (2017) reported an increase in GPx activity in *E. fetida* exposed to 1 µg/kg of MC-LR even on 1 day after exposure, followed by a significant inhibition at 100 and 1000 µg/kg by 7–14 days. In my study, GPx activity increased in a concentration-dependent manner on exposure to AgNPs and Ag^+ up to 28 days of exposure. The difference could be due to different earthworms and different contaminants. Glutathione peroxidase activity varies according to the analytical method and substrate used. In my study, I added sodium azide (Na_3N) to inhibit CAT from competing for H_2O_2 in the assay. Otherwise, GPx activity is not detected in the absence of Na_3N.

Glutathione-S-transferase is involved in detoxification of various xenobiotic chemicals, and its activity has an important function in GSH metabolism and cellular redox (Saint-Denis *et al.*, 1998). GST catalyses the conjugation of GSH with various electrophilic substances and prevents oxidation damage by conjugating the breakdown products of LPO to GSH (Hu *et al.*, 2012). Hu *et al.* (2012) showed that AgNPs at 500 g/kg are harmful to *E. fetida* and the toxicity of the smaller 10-nm AgNPs was greater than that of the larger 80-nm particles and is in agreement with the results of Silva *et al.* (2014). In my study, I used 30-nm particles and exposed *A. caliginosa* to up to 300 mg/kg AgNPs for 28 days, which resulted in a dose-dependent increase in GST but no visible toxic effects were observed. Hu *et al.* (2012) exposed *E. fetida* to various concentrations of AgNPs (0, 20, 25, 500 mg/kg oleic-acid-coated, particle sizes of 10 nm and 80 nm, and 787 mg/kg $AgNO_3$ as positive control). The result was no changes in GST activity up to 500 mg/kg AgNPs compared with the positive control $AgNO_3$. The authors believed that AgNPs induced more stress to the earthworm than Ag+ ($AgNO_3$). Glutathione-S-transferase catalyses the conjugation of GSH with various electrophilic substances and prevents oxidative damage by conjugating the breakdown products of LPO to GSH. The determination of GST activity is dependent on two compounds, GSH and CDNB, both of which showed similar trends. GST activity is optimal at 0.7 mM CDNB and 2 mM GSH. Mendes *et al.* (2015) studied the exposure of *Folsomia candida* to AgNPs, and GST activity was continuously high to chelate radical ligands in the thiol groups in GSH, and an increase in GR was needed to balance the redox potential (GSH) recycling as a result of ROS production from AgNPs interactions.

Malondialdehyde is a product of LPO and is elevated when polyunsaturated fatty acids react with free radicals in cellular membrane and undergo changes by chain reaction to form lipid hydroperoxide, which decomposes the double bond of the polyunsaturated fatty acids and disrupt the lipid membrane (Ayala *et al.*, 2014). Malondialdehyde is frequently used as a sensitive indicator of LPO and subsequent cellular injury. Various contaminants such as heavy metals and pesticides induce LPO due to the formation of excessive ROS (Halliwell, 1991). Cao *et al*. (2017) reported that the exposure of *E. fetida* to 100 and 1000 mg/kg concentrations of MC-LR for 7 and 14 days resulted in a significantly higher MDA concentration compared to the control and induced injury to the earthworm *E. fetida*. Otmani *et al.* (2018) reported that the exposure of *Allolabophora caliginosa* to different Cd concentrations had no effect on MDA compared to the control, whereas in my study, the MDA increased markedly on exposure to both AgNPs and Ag^+.

Mendes *et al.* (2015) showed that exposure of the earthworm *Folsomia candida* to similar doses of 0, 64, 100, 130, 320, 640 mg/kg of AgNPs and $AgNO_3$ (Ag^+) for 28 days resulted in a significant increase in LPO on day 2 to 1.75 µmol/mg protein, then decreased to 1.25 µmol/mg protein at day 4 followed by a significant increase to 1.5 µmol on day 10 along with increases in MT, GST, CAT, GR, TG, and LPO. This is somewhat consistent with my studies because I observed a dose- and concentration-dependent increase in LPO, CAT, and GST during the 28-day exposure of *A. caliginosa* to both AgNPs or Ag^+.

I determined the amount of Ag from AgNPs or Ag^+ in earthworm homogenate collected from the fourth week of exposure, and the result followed a dose-response curve for 3, 30 and 300 mg/kg AgNPs and 0.3, 3, and 10 mg/kg Ag^+. The amount of Ag in the earthworms exposed to AgNPs homogenate was more than in those exposed to Ag^+ probably due to high exposure doses. However, I found Ag^+ from $AgNO_3$ to be more toxic to *A. caliginosa* than AgNPs, based on the relatively elevated levels of the monitored biomarkers, namely SOD, CAT, GPx, GST and also LPO. Similar results were obtained when I used filter paper moistened with the same concentrations of Ag as used in the contaminated soil with AgNPs/Ag^+ study. However, the changes in biomarker levels in the filter paper study were much lower because of the short exposure time and also the exposure was only via the dermal route (since earthworms do not feed on filter paper) whereas in the soil study exposure was via both the dermal and the gastrointestinal tract.

Exposure of earthworms to AgNPs/Ag^+ in both the filter paper and the soil study showed that Ag^+ was more toxic than AgNPs, which led me to examine why this would be so. To answer this question, I conducted a pharmacokinetics analysis of the data from the AgNPs/Ag^+ soil study using the same Ag dose of 20 mg/kg soil. This pharmacokinetics analysis showed that the high solubility of Ag^+ in $AgNO_3$ and other pharmacokinetics factors contributed to the greater toxicity of Ag^+ in $AgNO_3$ than AgNPs.

10.3 Impact of silver nanoparticles / silver nitrate in soil on plants

Silver nanoparticles, when released to the soil and aquatic environment, find their way into plants and excessive Ag concentrations may cause toxicity in the food chain. The exposure of plants to AgNPs/Ag^+ showed positive and negative effects depending upon the regulation of uptake and accumulation (Wang *et al.*, 2015). The uptake of AgNPs depends on cellular permeability, and the shape and size of NPs (Tripathi *et al.*, 2017a). The effects of AgNPs/Ag^+ are extended to plants, because plants take up, translocate, and accumulate AgNPs from their surrounding growth medium. Silver nanoparticles, after entering into cells and organelles, create biological alterations with the result that essential macrobiotic elements such as proteins are affected (Griffitt *et al.*, 2008; Pham *et al.*, 2012). Silver nanoparticles, after entering the root, can regulate the accumulation of proteins such as CDK-2 (cell division cycle kinase-2), 1,6-bisphosphate aldolase, protochlorophyllide, and oxidoreductase (Siddiqui *et al.*, 2015).

The mobility of AgNPs/Ag^+ in soil and the uptake of Ag in two plants (ryegrass and sunflower) and nine vegetables (carrot, radish, leek, lettuce, parsley, rocket, beetroot, silverbeet and spinach) exposed to 70 mg/kg AgNPs/Ag^+ were studied. Ryegrass was exposed to different concentrations of AgNPs/Ag^+ ranging from 1% to 0.19% to determine the lethal dose of AgNPs/Ag^+, which was determined as 200 mg/kg (Fig. 4.3A). Sunflowers were exposed to a sub-lethal concentration of 150 mg/kg AgNPs/Ag^+ and the concentrations of Ag, and Ca, Cu, P, K, Mn, Mg, Zn, in different parts of the plant were studied, along with the antioxidant enzymes CAT, SOD, GST, and LPO, chlorophyll A and B, TP, TSC, TPC, urease and vitamins A, E and C in leaves.

Silver nanoparticles enter the plant through the root with water and other solutes. The root wall consists of many pores, some smaller in size than AgNPs (Ma *et al.*, 2010), serving as a natural sieve (Navarro *et al.*, 2008a). The smaller sized AgNPs pass through the larger root pores, which acts as a semi-permeable layer that allows entry of only the smaller particles. On exposure of sunflowers to AgNPs/Ag^+, it was apparent (Fig. 5.5) that the root size and mass of the group exposed to Ag^+ ($AgNO_3$) were much smaller than for the group exposed to AgNPs, which resulted in a greater toxicity as a result of exposure to Ag^+. The reason could be due to the solubility of Ag^+, which can pass through root pores more easily, whereas for AgNPs with sizes varying from 20 to 40 nm, probably not all the particles were able to enter through the root pores. The small root pores that resulted on exposure to AgNPs/Ag^+ probably did not permit the macro and micro nutrients to pass through to the other parts of the plant, which resulted in reduced plant growth (Fig. 5.2). The two forms of Ag, which accumulated in root and leaves, can both cause phytotoxicity in the plants depending on the exposure dose (Figs 5.4 and 5.5).

The two Ag forms AgNPs/Ag^+ can damage the cell membrane, interrupting ATP production as well as DNA replication (Dakal *et al.*, 2016). The exposure of sunflower to AgNPs/Ag^+ may generate ROS that cause oxidative stress affecting gene expression and damaging DNA (Oukarroum *et al.*, 2013). Silver nanoparticles modify expression of the general proteins of primary metabolism and the cell defence system (Ma *et al.*, 2010), besides their effect on the plant's reproductive structure and damage to its DNA, creation of chromatin bridges, stickiness, disarranged metaphase and multiple chromosomal breaks (Panda *et al.*, 2011; Patlolla *et al.*, 2012; Anjum *et al.*, 2013). The main reason for AgNPs/Ag^+ toxicity to the plant is their impact on biochemistry and formation of ROS resulting in OS in plant cells (Nair *et al.*, 2010). The production of H_2O_2 in plant cells reduces growth and inhibits development of the plants (Figs 5.2 and 5.3) and could even cause plant death. The toxicity to the root is more than to other parts of the sunflower plant, because the root is the main site of interaction with AgNPs/Ag^+ (Tripathi *et al.*, 2017a).

In my studies, exposure of the sunflower plant to AgNPs/Ag^+ resulted in a decrease in chlorophyll A but chlorophyll B was not affected, and the group exposed to Ag^+ showed more inhibition compared to the control group and AgNPs. The inhibition of chlorophyll A content in both groups affected photosynthesis and this was reflected in plant growth, where stem length, number and size of the leaves and root size were much smaller in groups exposed to AgNPs/Ag^+ compared to the control (Qian *et al.*, 2013). The plant TP, TSC and TPC show a marked variation on exposure to AgNPs. My studies showed that a reduction in TSP and TSC following exposure to AgNPs was accompanied by significant increase in TPC level, which is in agreement with Krishnaraj *et al*.'s (2012) studies on the interaction of biologically synthesised AgNPs with hydroponically grown *Bacopa monnieri*. The TSP in the sunflower leaves in my study was highest in the control > AgNPs > Ag^+ which indirectly could be interpreted as a lower concentration of amino acids in the plants exposed to AgNPs/Ag^+. Mehrian *et al*. (2015) reported that all amino acids except methionine and tryptophan linearly increase in tomato plants exposed to increasing AgNPs concentrations. These authors also noted that proline accumulated in these plants, which could be an indicator of environmental stress.

The cell membrane is considered the primary site of heavy metal injury. Enhancement of oxygen $O_2^{\circ-}$ produces hydroxyl radicals, which can oxidise fatty acids into toxic LPO. In my studies, exposure of sunflower plants to 150 mg/kg AgNPs/Ag^+ resulted in a significant increase in LPO as measured by MDA in the leaf, which is consistent with the studies of Mehrian *et al.* (2015), where they exposed tomato plants to 0, 25, 50, 75, and 100 mg/kg AgNPs and observed a significant increase in MDA compared to the control.

The uptake and toxicity of AgNPs by the common grass *Lolium multiflorum* showed that the concentrations of root and shoot Ag increase on exposure to 40 mg/l gum-Arabic-coated AgNPs, with resultant inhibition of seedling growth, failure to develop root hairs and the grasses exhibited highly vacuolated and collapsed cortical cells and a damaged root epidermis. However, these changes were not observed when *L. multiflorum* was exposed to an identical concentration of Ag^+ (Yin *et al.*, 2011). In my studies on ryegrass *Lolium perenne*, I did not observe such alterations.

Li *et al.* (2017) compared the uptake, phytotoxicity and size distribution of AgNPs in soya bean and rice following root versus foliar exposure. At similar AgNPs application, the foliar spray led to an accumulation of 17–20 times more Ag concentration in the foliage especially in the cell wall and plasmalemma than the root. However, AgNPs were less toxic to the plant via foliar exposure than via root exposure. Following root exposure, the fresh biomass of both the root and shoot declined by 49–71% and 56–72% respectively for soya bean and 29–70% and 36–67% for rice (Li *et al.*, 2017).

Pappas *et al.* (2017) reported an increase in Ag concentration in *Helianthus annuus* and *Sorghum vulgare* plants as function of increasing AgNPs in soil, which agreed with the results of my ryegrass experiment, where the amount of Ag in ryegrass from AgNPs/Ag^+ was proportional to the amount in soil.

Fernandes *et al.* (2017) investigated the uptake of AgNPs by a marsh plant *Phragmites australis* and also the effects on the rhizosphere and showed that Ag accumulates mostly in below-ground plant tissue and only in the absence of rhizosediment (calcium carbonate accumulation) because sediment reduced Ag availability (Fernandes *et al.*, 2017). Plant roots accumulate Ag more when Ag exists in an NP form, which is inconsistent with my findings. Multivariate analysis of ARISA profiles showed a significant effect of absence/presence of Ag (either in ionic or NP form) on microbial community structure (Fernandes *et al.*, 2017). One of the benefits of *P. australis* is that it can be used for phytoremediation of media contaminated with Ag including AgNPs.

Potera (2010) reported that NPs are transformed into Ag_2S in the sludge from sewage treatment plant and hence there is entry of at least some AgNPs into the environment in that form. In the USA, Ag was detected in most of the sewage sludge samples collected from 74 municipal wastewater treatments, along with another 25 metal types (Venkatesan *et al.*, 2015). Energy-dispersive X-ray analysis showed that S, which is produced by microorganisms that digest sewage, can combine with Ag in a 2:1 ratio, and that the crystal structures formed confirm the formation of Ag_2SNPs. When sludge containing Ag_2SNPs is applied on agricultural land, the NPs undergo oxidation in soils and release toxic Ag ions that kill the beneficial soil microorganisms (McShan *et al.*, 2014). However, there are some bacteria, such as *Pseudomonas putida,* that can bind with Ag ions rendering them less toxic (Potera, 2010). The formed Ag_2S is highly insoluble and settles out of water, which could contribute to a lessening of Ag toxicity. By using X-ray absorption spectroscopy and X-ray fluorescence microscopy, the uptake, speciation and translocation of insoluble AgS-NPs, within two plant species, a monocot and a dicot, were characterised (Christensen *et al.*, 2003). The ICP-MS studies confirmed that Ag_2S particles within the leaves had a markedly similar size distribution to those supplied within hydroponic solution (Wang *et al.*, 2017). Following uptake of Ag_2SNPs by the plant, plant growth inhibition occurs, partially because of solubilisation of Ag^+ in plants, which causes upregulation of genes involved in the ethylene signalling pathway. This illustrates the risk accompanying AgNPs accumulation in plants and subsequent trophic transfer via the food chain (Wang *et al.*, 2017).

Kittler *et al.* (2010) revealed that the toxicity to cells of stored AgNPs is increased because of the increased presence of Ag^+ in dispersion. The authors concluded that the aged AgNPs are more toxic to the cell than freshly prepared AgNPs.

Oxidative stress caused by heavy metals could be resisted by vitamins A, E and C. Generally, vitamins are essential for humans, animals and plants because they act as co-factors and also due to their antioxidant properties (Riccioni *et al.*, 2003; Traber and Stevens, 2011). In my studies with the sunflower plant, vitamin E (α-tocopherol) in sunflower leaves was significantly increased to combat the OS associated with exposure to AgNPs/Ag^+ and these changes were most marked in the group exposed to AgNPs compared to the group exposed to Ag^+ > control. Plants exposed to both Ag forms showed significantly higher vitamin concentrations compared to the control. Vitamin E is one of the most powerful antioxidants that protects photosynthesis in plants. There is a clear correlation between degree of stress and tocopherols level (Munné-Bosch and Alegre, 2002). The increase in vitamin E confers enhanced tolerance to plants against drought and heavy metals stress. Tocopherols are also able to quench or scavenge the free radicals (Collin *et al.*, 2007; Gajewska and Skłodowska, 2007). Fryer (1992) suggested that the changes in vitamin E responses to environmental stress are characterised by two phases. In the first phase, there is tocopherol synthesis and this is followed by a second phase characterised by decline in vitamin E concentration. In the first phase vitamin E contributes by reducing ROS and inhibiting LPO to avoid cell damage. However, when the stress is severe, vitamin E degradation exceeds its synthesis and hence the concentration declines, consequently the LPO increases, followed by cellular death.

Exposure to AgNPs/Ag^+ causes an increase in vitamin C (ascorbic acid) (Sinha *et al.*, 1996). Vitamin C is the most abundant antioxidant that minimises oxidative stress (Chao *et al.*, 2010). Vitamin C participates in a variety of processes including photosynthesis, photoprotection, the cell cycle, cell wall growth and cell expansion, and synthesis of anthocyanins and hydroxy proline (Alpsoy *et al.*, 2009).

The mobility of Ag in soil solution was determined by measuring the K_D value. K_D refers to the concentration of a chemical in soil divided by the concentration of that chemical in water. Higher K_D means the chemical is strongly adsorbed onto soil and organic matter and does not move easily throughout the soil. In contrast, a low K_D value means that the mobility of the chemical is very high in soil. Both high and low K_D values affect Ag mobility (Chemsafety, 2018).

Discharged Ag accumulates and is adsorbed by soils and is a significant threat to soil structure, the bacterial community, water environment and the terrestrial ecosystem. There are some factors that affect sorption and desorption and equilibrium between solid and solution phases. These factors include pH, clay content, organic matter, cation exchange capacity and Fe/Al oxides. Chemical and physical processes occurring at different reaction sites in the soil-solution phase control the level of a heavy metal in solution and its transport, therefore influencing the release of heavy metal ions including Ag in the water phase (McIlveen and Negusanti, 1994). Silver removal from an aqueous solution by adsorption on concrete particles showed that Ag removal is favoured by low concentration and high pH. When pH declines, there is a higher concentration of H^+ to compete with Ag^+ for these anionic sites, resulting in lesser removal. Therefore, the adsorption of Ag is influenced by soil pH and the presence of organic matter. Silver can make a strong complexation with humic and fluvic acids and soluble organic matter. Silver isotherms are highly non-linear and depict strong affinities or sorption. It was found that Ag adsorption isotherms show increased sorption of Ag with time of reaction. Silver desorption shows strong time-dependent behaviour as depicted by the continued decrease of the amount sorbed with time.

10.4 Conclusions

Silver nanoparticles are used in many industries and the wastes fromf these industries reach the soil either directly or indirectly via landfill or sewage sludge. It is now known that the concentration of AgNPs in sewage sludge, which is used as land fertiliser, is increasing. Therefore, sewage sludge, in addition to improper discharge of AgNPs from factory waste, contaminates the soil.

Silver nanoparticles have a negative impact on soils, plants and soil organisms such as earthworms. Application of AgNPs/Ag^+ at low concentrations such as 60–70 mg/kg could be useful and improve plant health because the NO_3 at such concentrations could act as a fertiliser, but at high doses they can cause toxicity like other heavy metals. In my studies, the application of AgNPs/Ag^+ (nanoparticles/ions) caused toxicity to *A. caliginosa* earthworms and in plants. In my studies, I used ryegrass and the sunflower to examine the toxicity of AgNPs/$Ag^+$to plants. The results indicated that compared to AgNPs, Ag^+ is more toxic to the earthworms and plants. In earthworms, Ag^+ was more toxic because of its solubility and effects of the body (pharmacokinetics analysis), while in plants because the roots contain pores smaller than AgNPs particle size prevents passage into the plant. My study showed that AgNPs and Ag^+ in soil bind to S to form Ag_2S-NPs, which are insoluble and could be considered immobilised and hence which cause less toxicity. The research published to date concerning the negative impacts of AgNPs, including results reported here, suggests that the discharge of AgNPs from factories should be controlled and that the concentration of Ag in sewage sludge should be determined prior to soil application.

In summary, the discharge of AgNPs via industrial waste and wastewater treatment plants represents soil pollution and a major threat to non-target plants and important soil organisms such as earthworms since they are continually exposed to the AgNPs throughout their lifespan. The effects of AgNPs and Ag^+ ($AgNO_3$) on mobility in soil, plants (sunflower, ryegrass) and *A. caliginosa* earthworms were investigated by conducting a series of experiments to evaluate accumulation of Ag, and several other parameters such as LPO, antioxidant enzymes (CAT, SOD, GPx,) and also GST activity, in addition to a series of other parameters in sunflower and ryegrass, which correlated with their adverse effects. The multi-level effect approach adopted in this study, including an earthworm pharmacokinetics study, provides a better understanding of the potential risk of AgNPs to non-target plants and earthworms. This study shows that evaluating several sub-organismal biomarkers offers a meaningful and informative assessment of AgNPs effects on plants and earthworms.

10.5 Future research

Because of the ever-increasing use of AgNPs in industries there are concerns about environmental pollution, which would have a negative impact on plant growth and soil fertility directly and indirectly due to harmful effects on earthworms. Hence the need to investigate the fate of AgNPs in different soils using different methods of NPs synthesis to determine the most desirable one that lessens the impact on the environment. Studies of the long-term effects of low dose AgNPs pollution in soil need to be accompanied by studies pertaining to interactions with the microbial community, especially those involved in nutrient cycling and microbial enzymes involved in biogeochemical processes, to assess the long-term effects of NP types, taking into account the soil type and bioavailability therein. In addition, long-term field experiments where AgNPs could be applied to soil to measure the critical factors affecting the transformation of AgNPs into Ag^+.

The soil bacterial community contributes widely to soil health and function. Therefore, understanding of how enzymes function and the factors that affect microbial diversity and biogeochemical pathways require evaluation. Identification of AgNPs' metabolic pathway and metabolite formation would provide a better understanding of the toxicity and fate of AgNPs and their effect on earthworms and plants. In addition, particle size and shape should be taken into consideration in NP studies. Chemical factors to consider consist of capping/coating agent chemistry, solubility, aggregation, electrostatic forces between NPs, the dissolution of metallic ions and chemical transformations. All of these factors can determine the overall bioavailability and mobility of NPs in soil.

Silver nanoparticles in plants cause phytotoxicity. The addition of compost to the soil may reduce Ag toxicity. Determination of the stability of synthesised AgNPs would help us to determine the extent of the toxicity and the forms and toxicity of AgNPs by-products.

I

Appendix A

AgNPs stability tests

The stability tests involves:

Effect of storage at different temperatures, pHs, stability at 70°C temperature and the effect of ultraviolet radiation of AgNPs prepared as described by Carey (1889).

A.1- Effect of AgNPs storage at different temperatures

Method

First, 35 ul of AgNPs stock solution was diluted to 50 ml with water. Then 20 ml of this solution was divided into two portions, one kept in the dark at room temperature while the other was kept at 4°C. The absorbance of the two portions was recorded at zero time then weekly for 4 weeks. Results are shown in Table A.2.1.1.

Table A1.: Silver nanoparticle concentration (mg/l) in solution following incubation of fresh AgNPs for 4 weeks at different temperatures (22°C and 4°C).

Date	22°C	4°C
Zero time	1.084	1.084
Week 1	1.084	1.084
Week 2	1.0975	1.1669
Week 3	1.076	1.225
Week 4	1.1351	1.186

There was no significant difference in the concentration of prepared AgNPs kept at room temperature and at 4°C measured by AAS.

A2- Effect of pH on AgNPs spectra

Method

Three solutions of AgNPs were prepared as described by Carey (1889). The pellets formed after washing with 20% trisodium citrate were suspended in 10 ml of deionised water. A 35 µl sample of colloidal AgNPs solution was diluted to 50 ml with water and the spectrum photographed (pH 6.5). A part of the solution was rendered alkaline by adding 500 µl of borax buffer (pH 9.23) and the spectrum photographed. Finally, another part was rendered acidic by adding 500 µl of acetate buffer (pH 4.1) and the spectrum photographed. The process of acidity and alkalinity amendment was repeated using 20 µl of concentrated hydrochloric acid or 10% sodium hydroxide taking a spectral photograph in each case.

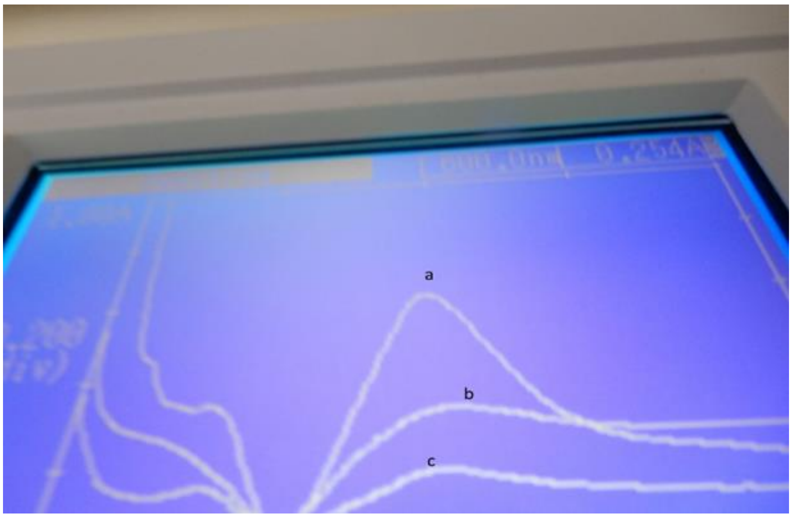

Fig. A2: Spectral changes observed at different pHs recorded at 398 nm. (a) is pH 6.5, (b) pH 9.23, and (c) pH 4.1. At pH 9.23 the spectrum became broad with a decrease in absorption intensity compared to pH 65. At pH 4.1 also the spectrum became broad with a marked decrease in absorption intensity. The concentration used was 5 µg/ml AgNPs.

A3- Effect of 70°C temperature on stability

Method

From neutral AgNPs solution (pH 6.45) five samples with concentration of 5.5 ug/ml were taken and kept in a water bath maintained at 70°C. The absorbance was recorded at 0, 1, 2 3, 4, and 5 h.

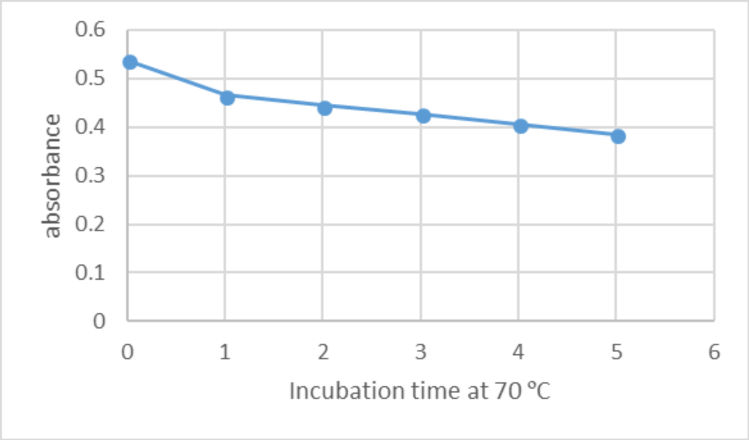

Fig. A3: Absorbance decreased 30% after incubation of AgNPs solution for 5 h at 70°C.

A4- Effect of ultraviolet radiation

Method

From AgNPs neutral solution (pH 6.45), five samples of concentration 5.5 ug/ml were prepared and kept under ultraviolet radiation of 254 nm and 30 watt power for 0, 1, 2, 3, 4 h and the spectrum at each hour was recorded.

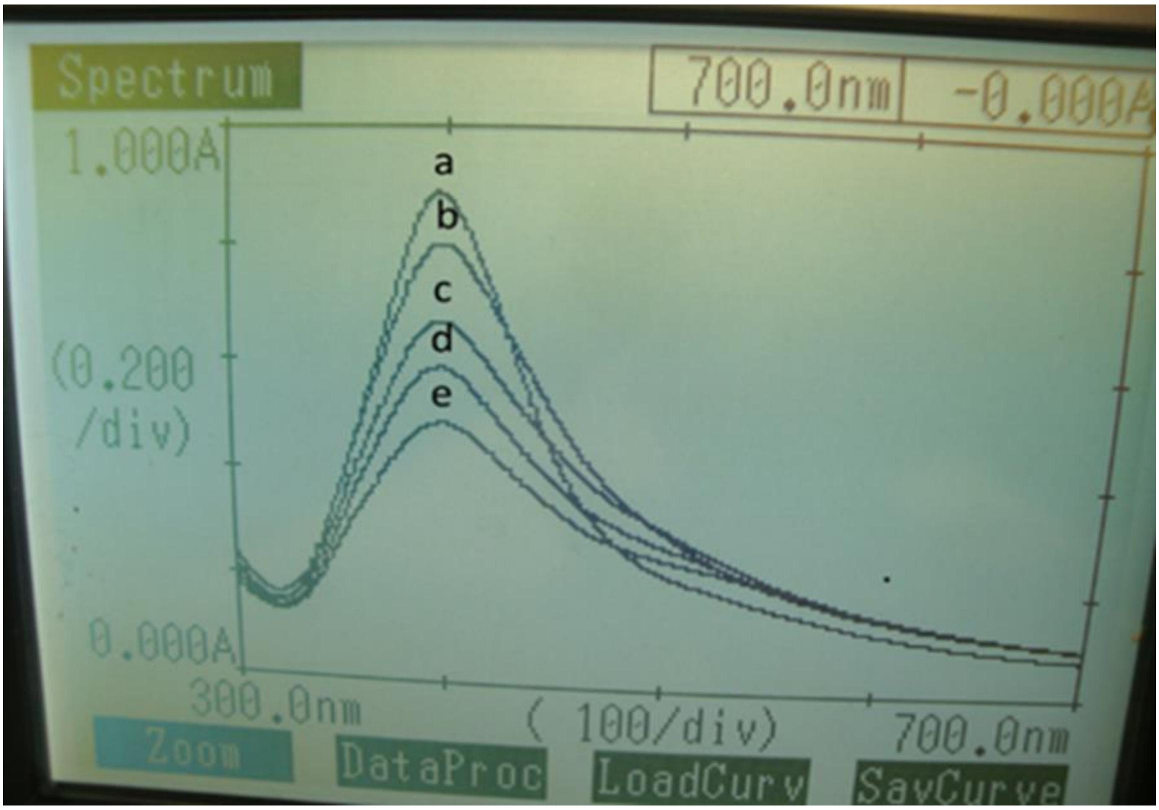

Fig. A4: Decrease in absorbance when incubated under UV light. (a) 0 h, (b) 1 h, (c) 2 h, (d) 3 h, (e) 4 h. The absorbance intensity decreased with time when exposed to UV radiation at 254 nm. The strength of ultraviolet light was 300 mW/cm^2.

Appendix B

Distribution coefficient: Comparison of different extractable solutions

Method

TSL soil (200 g) was sieved and accurately weighed. Half (100 g) was mixed with a quantity of AgNPs equivalent to1 mg/g and distributed over 36 Falcon centrifuge tubes each of 2.5 g. The other 100 g of soil were mixed with $AgNO_3$ to an amount equivalent to 1 mg/g calculated as a free base and distributed over another 36 Falcon centrifuge tubes. Solutions used for extraction were 15 ml of: 0.1 M KNO_3, 0.2 M KNO_3, 0.4 M KNO_3, 1 M KNO_3, 0.1 M KCL, 0.2 M KCL, 0.4 M KCL, 1 M KCL, 0.05 M $Ca(NO_3)_2$, 0.1 M CH3CO2NH2, 0.1 M EDTA, 0.005 M DTPA and 0.033 M NTA. Triplicate solutions from each concentration were used. The soil samples with added solutions were mixed by shaking for 2 hours, followed by centrifugation at 4700 rpm (4577 RCF) for 20 min. The supernatants were separated and recentrifuged at 13 400 rpm (9050 RCF) for 30 min using Epindorff tubes and analysed for Ag using AAS. Solutions used for the extraction of Ag from soil amended with $AgNO_3$ must be diluted 1:24 before analysis.

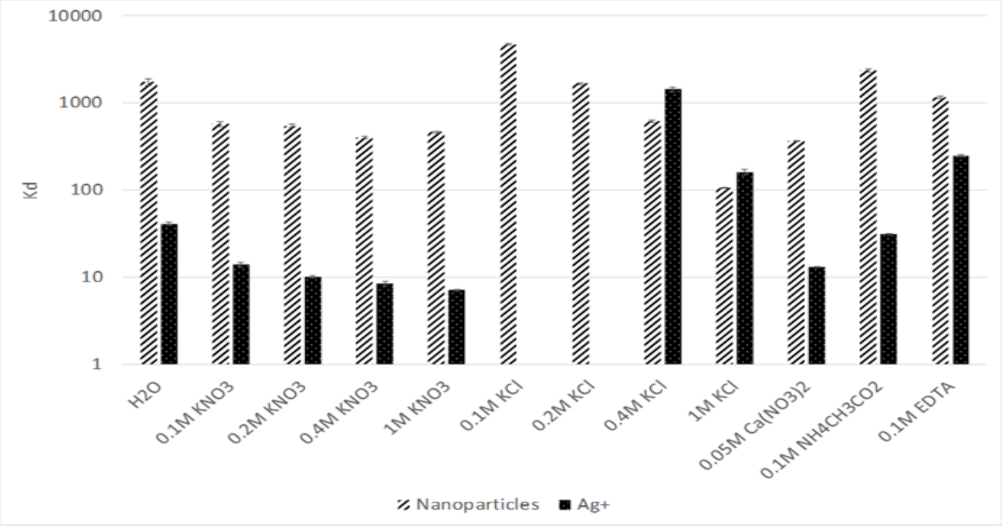

Fig. B1: Distribution coefficients (K_D = sorbed / solution concentration quotients) as a function of extractant type (*x*-axis). The soils were spiked with 1000 mg/kg Ag either as AgNPs or Ag^+. The error bars are the standard error of the mean (n = 3

Appendix C

Rate of sorption of AgNPs and Ag^+ by soil as a function of time

Method

First 30 ml of 0.1 ml KNO_3 mixed with 75 and 300 mg/l AgNP or $AgNO_3$ (Ag^+) were added to 36 Falcon centrifuge tubes containing 5 g of soil. The tubes were agitated for 0.5, 1, 2, 3, and 4 h. Three replicates per treatment were prepared. After each agitating time, the tubes were centrifuged at 4700 rpm and the supernatants were recentrifuged at 9,050 x g RCF for 30 min using Eppendorff tubes. The clear solutions were taken for analysis using AAS. Solutions spiked with $AgNO_3$ must be diluted 1:24 before analysis.

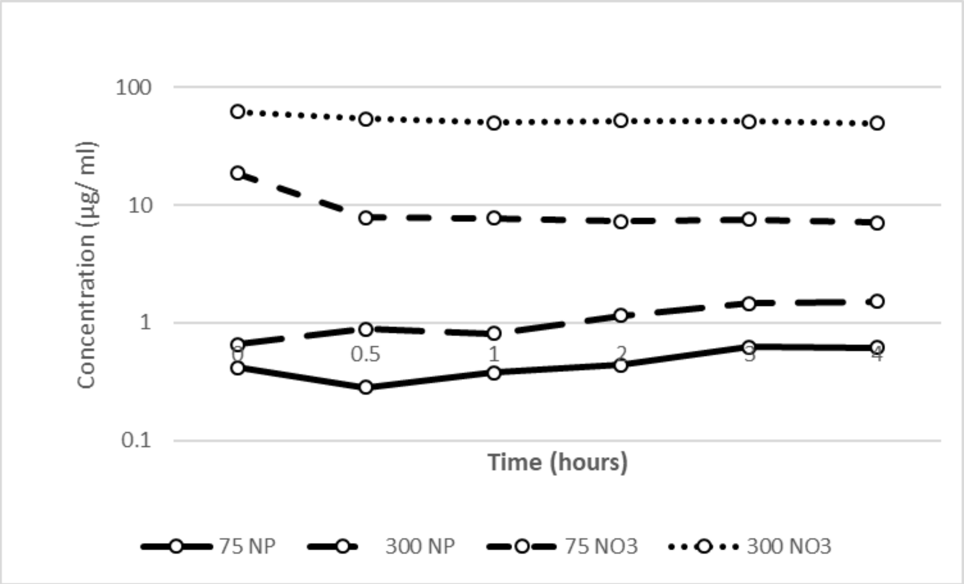

Fig. C1.1: Determination of equilibrium time of AgNPs/Ag^+ (mg/l) as a function of agitation time, 20 rpm with 0.1 M KNO_3 for AgNPs/Ag^+. Values are average of three replicates.

Two hours was most suitable for Ag extraction from soil.

Appendix D

Determination of silver (Ag) and selected elements in soil used for ryegrass cultivation, using aqua regia and 0.5-g sample (n = 3) (mg/kg)

Sample no.	Ag	Al	Ca	Cd	Cr	Cu	Fe	K	Mg	Mn	Na	Ni	P	Pb	S	Zn
1	nd	25831.77	4663.05	0.10	23.45	5.34	22273.12	6160.06	4566.89	581.7	401.84	10.21	885.10	13.30	314.60	64.33
2	nd	26184.54	4805.96	0.15	23.57	5.54	21973.44	6153.29	4620.99	572.4	453.95	10.32	902.25	12.71	361.61	65.54
3	4.6681	25376.29	4605.70	0.18	22.98	5.24	21283.43	6126.44	4429.04	573.2	396.98	9.88	849.70	11.96	309.62	63.31
4	1497.9	25356.58	4752.96	nd	23.17	5.39	21372.69	6176.86	4517.83	553.8	521.50	10.14	860.40	7.23	296.21	64.77
5	1978.1	25038.48	4665.53	nd	22.68	5.55	21308.08	6056.23	4430.53	531.17	605.42	10.01	852.55	7.47	306.80	64.48
10 000*	1853.6	25280.19	4745.28	nd	22.99	5.29	21256.09	6078.25	4403.51	538.93	535.01	9.95	877.58	7.29	298.88	63.42
7	1454.5	25071.36	4498.40	0.05	22.80	5.31	21522.84	6065.48	4338.29	540.83	476.15	10.18	861.85	15.83	296.35	63.68
8	1235.8	25564.28	4896.28	0.08	23.48	5.51	22955.66	6164.35	4623.81	601.54	575.28	10.31	928.87	11.88	328.21	65.06
5000*	1523.7	24962.67	4729.56	nd	22.76	5.36	21347.28	6054.09	4424.52	561.63	598.37	10.04	859.98	10.44	354.80	63.49
10	1546.3	24970.29	4721.08	0.10	22.73	5.31	21585.53	6064.16	4381.24	589.29	459.88	10.07	869.91	11.78	306.31	63.42
11	1025.9	26595.87	4724.20	0.10	24.23	5.43	22292.23	6422.11	4606.85	584.51	463.54	10.51	910.90	12.14	309.87	66.28
2500*	1271.6	24965.14	4775.38	0.07	22.45	5.32	22009.13	5985.96	4497.74	581.08	457.07	10.19	941.44	11.89	317.33	64.74
13	1607.3	25537.32	4427.34	0.28	23.14	5.22	27006.95	6115.62	4485.21	829.90	487.05	10.00	983.10	15.25	330.94	64.48
14	1632.2	25517.32	4656.21	0.15	23.29	5.22	21807.18	6114.46	4506.30	561.86	426.89	10.31	862.00	12.55	304.58	64.47
1250*	1909.6	24958.81	4640.35	0.16	23.08	5.26	21418.61	5919.26	4401.91	548.72	482.62	10.42	865.60	12.66	318.33	63.05
16	967.35	25039.57	4641.61	0.14	22.67	5.21	21842.27	5954.72	4376.80	597.16	419.87	9.84	879.49	12.72	305.97	62.41
17	893.75	24108.77	4420.64	0.13	21.81	4.99	20746.75	5743.50	4244.44	570.43	384.30	9.66	829.59	12.24	296.79	60.94
625*	1016.1	24574.61	4656.45	0.17	22.42	5.19	21915.60	5928.10	4427.55	619.22	413.16	10.11	917.08	12.57	315.30	63.96

19	712.59	25744.75	4116.33	0.23	25.63	5.90	21925.67	7135.30	5469.74	521.45	339.54	10.78	916.04	13.80	295.28	68.35
20	572.66	24957.06	4082.14	0.23	24.45	5.68	21353.73	6954.97	5332.69	531.33	319.22	10.21	846.43	13.91	283.39	66.83
312.5*	514.11	24772.33	3960.86	0.23	24.49	5.85	20830.25	6905.64	5132.56	527.66	342.48	10.00	832.48	13.27	284.18	65.54
22	346.96	25179.71	4217.59	0.23	24.77	6.09	21819.99	6987.12	5473.24	537.58	345.51	10.95	881.86	14.01	307.50	69.67
23	315.65	24879.08	4072.93	0.25	24.30	5.88	22041.27	6894.09	5354.12	536.98	323.54	12.07	920.98	14.30	290.24	68.46
156.75*	345.58	25999.00	4158.83	0.16	25.57	5.94	21227.33	7266.18	5483.12	503.83	378.36	10.63	862.95	13.79	303.02	68.50
25	162.1	24544.59	4081.39	0.23	24.21	5.76	21835.01	6771.70	5345.06	570.71	341.23	10.59	855.54	14.47	294.35	69.16
26	172.85	25429.01	4050.35	0.19	24.91	5.74	21467.41	7078.13	5301.34	516.61	359.25	10.28	851.97	13.78	292.20	67.14
75	163.2	25271.97	3995.12	0.21	24.74	5.77	22128.58	7078.28	5402.15	607.09	337.22	10.44	880.42	14.30	295.16	68.45
28	78.532	25065.02	4168.44	0.22	46.97	5.72	21204.98	6930.90	5603.98	505.38	366.25	13.31	847.07	13.59	280.03	67.09
29	79.456	24652.97	4241.06	0.22	24.22	5.71	21501.79	6834.78	5318.14	574.10	361.01	10.75	864.17	13.97	295.97	68.00
38	67.683	25048.02	4086.09	0.25	24.38	5.83	23075.31	6886.74	5461.75	679.79	386.19	10.86	921.19	15.02	319.35	70.00
31	32.864	24735.57	3887.75	0.21	24.67	5.56	21023.60	6880.09	5200.14	527.40	361.65	10.25	842.79	13.78	291.81	66.00
32	30.403	25588.57	4200.16	0.22	24.95	5.87	21821.36	7097.37	5409.67	513.24	364.01	10.52	870.46	13.62	291.42	68.25
33	22.159	25160.50	4048.99	0.21	24.55	5.75	21339.20	7013.03	5368.04	498.82	361.39	11.94	836.14	13.41	289.32	67.80
34	nd	24252.75	4209.75	0.26	23.74	5.74	19939.20	6731.71	5082.48	481.77	381.14	10.58	842.28	13.34	342.76	64.88
35	226.64	25151.84	4127.20	0.25	24.58	5.84	21217.35	7050.43	5226.43	636.11	395.02	10.46	859.06	13.86	311.23	66.00
36	nd	25003.82	4210.39	0.23	24.27	5.80	21848.95	7009.39	5315.76	544.21	370.04	10.60	872.31	13.50	320.83	67.59
37	1379.9	24336.02	3830.21	0.07	23.57	5.82	20907.68	6859.14	5016.16	747.65	320.69	9.98	852.39	6.94	296.50	65.30
38	2056.4	24088.49	3671.76	0.10	26.37	5.69	20576.05	6701.15	4978.46	481.27	299.27	10.64	863.14	6.31	296.84	64.97
39	2065.7	24502.14	3642.41	nd	23.61	5.78	21114.82	6851.81	5166.15	524.27	310.88	10.00	871.48	7.99	319.85	67.34
40	1560.4	24445.67	4015.61	0.10	23.70	5.69	20541.74	6891.04	5198.71	500.74	360.13	10.17	821.68	11.09	303.56	67.77
41	1996.6	24514.30	4374.87	0.13	23.78	5.53	21129.98	6967.89	5213.04	541.83	383.67	10.04	873.94	12.75	299.88	66.13
42	1722.5	24946.86	4692.92	0.11	24.16	5.72	21728.96	7038.19	5412.96	560.85	410.16	10.27	871.04	11.57	303.83	67.69
43	2677.6	24423.07	4245.34	0.19	23.79	5.61	20605.10	6855.20	5175.97	492.35	372.23	9.97	866.02	13.04	292.76	66.53
44	1383.4	24940.54	4065.63	0.17	24.20	5.54	21252.40	7052.72	5236.56	531.71	372.11	10.04	871.87	13.32	297.14	66.44
45	1466.6	24612.76	4450.62	0.22	23.89	5.53	21501.05	6965.20	5225.12	568.86	404.69	10.11	858.09	13.97	299.17	65.86
46	646.06	25922.60	4357.76	0.25	25.32	5.83	22259.39	7426.14	5629.52	569.03	455.24	11.61	880.57	14.46	313.40	69.58
47	1522.4	25208.76	4206.50	0.22	24.56	5.76	21911.94	7094.03	5451.29	578.45	388.82	10.36	869.08	13.94	298.72	68.64
48	1188.9	24777.60	3849.88	0.19	24.02	5.26	20342.55	6635.55	4894.70	489.81	343.89	9.81	810.57	12.47	279.16	63.85

49	679.61	25538.50	3969.96	0.29	24.60	5.47	22878.90	6810.05	5045.35	664.67	316.82	10.29	916.56	14.37	282.51	65.94
50	730.35	25458.37	4073.06	0.23	28.42	6.02	21483.07	6808.67	5351.64	517.94	365.51	11.17	867.47	14.04	295.32	66.41
51	629.94	25158.96	3895.80	0.21	24.38	5.56	21489.39	6696.41	5208.72	536.55	371.56	10.67	891.78	13.18	308.70	67.40
52	361.76	24271.44	3858.36	0.22	23.66	5.20	19973.70	6504.52	4907.35	496.51	304.12	9.58	799.53	12.51	260.59	64.38
53	385.91	25317.76	4036.58	0.22	24.57	5.47	20458.73	6706.98	5326.37	474.23	329.97	11.84	837.41	12.39	287.17	66.60
54	355.18	24467.50	3915.33	0.23	23.73	5.38	20528.86	6470.94	4917.96	566.49	320.03	9.82	831.18	13.46	271.61	65.20
55	190.57	24674.90	3978.10	0.21	23.61	5.38	20832.78	6522.70	4989.53	570.62	323.83	10.06	852.89	13.16	281.70	66.05
56	175.93	24397.90	3924.99	0.21	23.79	5.58	21070.23	6419.89	5103.55	507.60	347.90	10.33	835.13	13.68	292.36	68.16
57	186.08	24771.87	3884.02	0.26	23.94	5.50	21179.41	6534.99	4984.76	529.39	364.34	10.28	851.13	13.52	302.71	65.51
58	80.129	24953.58	4099.43	0.29	24.21	5.59	21141.39	6576.07	4992.64	519.69	355.50	10.31	904.74	13.19	288.72	67.06
59	96.872	25054.06	3927.64	0.25	24.25	5.60	21146.24	6584.72	5074.95	560.21	344.20	10.37	855.99	13.64	285.54	67.91
60	85.597	24673.81	4099.62	0.28	23.99	5.48	22355.50	6366.42	4924.23	933.79	361.78	10.15	879.98	14.94	293.71	67.05
61	40.774	25107.43	4100.95	0.27	24.54	5.83	22091.40	6566.79	5186.00	623.80	360.80	10.58	911.62	14.15	333.53	69.60
62	43.994	25123.43	4226.53	0.30	24.33	5.79	21280.82	6607.87	5057.45	677.95	399.09	10.31	891.26	13.03	335.45	67.27
63	42.795	24038.84	4251.78	0.27	23.47	5.71	21141.22	6367.16	5030.15	544.98	329.96	10.08	926.03	14.14	328.15	68.63
64	20.134	25161.77	4082.59	0.26	24.29	6.02	22463.75	6658.63	5168.96	792.05	357.52	10.48	961.37	15.00	338.37	69.59
65	20.199	24523.83	4088.37	0.24	23.69	5.70	21099.87	6584.88	5010.94	553.22	378.39	9.99	911.11	13.54	347.86	65.96
66	20.867	24667.27	4557.65	0.25	24.05	5.82	20969.26	6609.53	5080.14	509.65	338.90	11.41	975.44	13.25	346.77	68.84

***In bold numbers** in the first column are the concentrations silver (Ag) standards of AgNPs/Ag^+ added to the soil.

Appendix E

Determination and recovery of AgNPs and silver nitrate (Ag^+) (added to soil)

Sample	Concentration added	Concentration recovered	% recovery
AgNPs	300 mg/kg	190 mg/kg	63.33%
Silver nitrate (Ag^+)	10 mg/kg	6.34 mg/kg	63.43%

Appendix F

Determination of elements in nine vegetables exposed to 0 and 70 mg/kg AgNPs or Ag^{+}

	Ca	**Cu**	**K**	**Mg**	**Mn**	**P**	**S**	**Zn**
Carrot								
Control	4256±141 ^{a}	7.4±0.2 ^{a}	21303±1659 ^{a}	1245±57 ^{a}	17±2 ^{a}	3353±159 ^{a}	1265±73 ^{a}	64±3 ^{a}
AgNPs	3653±246 ^{a}	3.7±0.5 ^{a}	19343±909 ^{ab}	1492±185 ^{a}	17±2 ^{a}	3255±100 ^{a}	1247±83 ^{ab}	53±6 ^{a}
Ag^{+}	3934±210 ^{a}	2.8±0.3 ^{b}	16246±1258 ^{b}	2560±88 ^{b}	19±2.5 ^{a}	2863±122 ^{a}	1092±29 ^{a}	50±4 ^{a}
Radish								
Control	8436±1701 ^{a}	2±0.1 ^{a}	51968±8250 ^{a}	2144±170 ^{a}	14±2 ^{a}	2914±128 ^{a}	5156±404 ^{a}	44±3 ^{a}
AgNPs	8000±591 ^{a}	1.5±0.1 ^{b}	45840±8085 ^{a}	2240±215 ^{a}	23±3 ^{ab}	2216±80 ^{a}	3362±175 ^{b}	81±12 ^{ab}
Ag^{+}	7689±2142 ^{a}	1.8±0.1 ^{b}	58732±555 ^{a}	2115±417 ^{a}	36±11 ^{b}	2947±140 ^{a}	3945±187 ^{b}	65±11 ^{b}
Leek								
Control	7902±1172 ^{a}	7±0.4 ^{a}	28855±5364 ^{a}	1841±201 ^{a}	35±4 ^{a}	3698±210 ^{a}	3619±133 ^{a}	36±4 ^{a}
AgNPs	9154±449 ^{ab}	3±0.1 ^{b}	20969±519 ^{a}	2151±65 ^{a}	44±2 ^{a}	3499±111 ^{a}	3680±72 ^{a}	54±4 ^{b}
Ag^{+}	10392±508 ^{b}	3±0.1 ^{b}	28205±5744 ^{a}	2051±127 ^{a}	44±8 ^{a}	2588±116 ^{b}	3014±111 ^{a}	51±5 ^{b}
Lettuce								
Control	14094±1502 ^{a}	8.3±0.9 ^{a}	48747±3652 ^{a}	3682±282 ^{a}	72±7 ^{a}	4433±155 ^{a}	3139±266 a	57±6 a
AgNPs	14320±831 ^{a}	2.7±0.3 ^{b}	23788±1961 ^{b}	4495±330 ^{a}	88±9 ^{ab}	2682±259 ^{b}	3100±189 a	47±3 a
Ag^{+}	15050±1367 ^{a}	1.98±0.1 ^{b}	29943±2460	4222±510 ^{a}	125±20 ^{b}	2463±255 ^{b}	3007±200 a	45±4 a
Parsley								
Control	15157±971	7±0.5 ^{a}	5229±1582 ^{a}	2487±88 ^{a}	64±4 ^{a}	3680±276 ^{a}	3859±280 ^{a}	67±2 ^{a}
AgNPs	18965±910 ^{b}	3±0.2 ^{b}	43249±3906 ^{ab}	2982±59 ^{b}	70±6 ^{a}	2634± 171 ^{a}	5223±271 ^{b}	53±4 ^{b}
Ag^{+}	20726±669 ^{b}	3±0.2 ^{b}	48014±1267 ^{b}	3000±86 ^{b}	70±2 $^{a.5}$	3187±222 ^{a}	5276±500 ^{b}	92±1 ^{c}
Rocket								
Control	29006±1788 ^{a}	4.6±0.2 ^{a}	46698±1427 ^{a}	4493±343 ^{a}	49±3 ^{a}	3568±98 ^{a}	8885±229 ^{a}	63±3 ^{a}
AgNPs	30075±1798 ^{a}	2.5±0.2 ^{b}	35495±2998 ^{b}	5090±338 ^{a}	50±4 ^{a}	2251±235 ^{b}	8235±331 ^{a}	53±6 ^{a}
Ag^{+}	31518±1010 ^{a}	2.8±0.2 ^{b}	41258±2013 ^{ab}	4615±211 ^{a}	64±4 ^{a}	3519±102 ^{a}	7645±289 ^{a}	50±4.13 ^{a}
Beetroot								
Control	6542±844 ^{a}	11±0.4 ^{a}	19674±552 ^{a}	4362±133 ^{a}	84±3 ^{a}	3884±65 ^{a}	1764±73 ^{a}	74±5 ^{a}
AgNPs	5093±532 ^{a}	1.35±0.1 ^{b}	9499±985 ^{b}	2977±211 ^{b}	150±13 ^{b}	1565±205 ^{b}	1048±89 ^{b}	47±3 ^{b}
Ag^{+}	5105±440 ^{a}	1.8±0.1 ^{b}	11978±483 ^{c}	2892±142 ^{b}	165±9 ^{b}	1991±237 ^{b}	1075±24 ^{b}	39±1 ^{b}
Silverbeet								
Control	17670±3822 ^{a}	7±1 ^{a}	43263±9352 ^{a}	5686±997 ^{a}	186±52 ^{a}	5402±331 ^{a}	5465±941 ^{a}	90±19 ^{a}
AgNPs	30510±1860 ^{ab}	3±0.2 ^{b}	47455±1992 ^{a}	7720±426 ^{a}	485±31 ^{b}	2324±141 ^{b}	3916±1191 ^{ab}	92±10 ^{a}

Ag^+	24992±1933 ^{b}	3±0.5 ^{b}	48651±1992 ^{a}	8322±767 $_{a}$	691±79 ^{c}	3399±792 ^{b}	3540±432 ^{b}	118±36 ^{a}
Spinach								
Control	34403±48 ^{a}	4±0.2 ^{a}	36581±9467 ^{a}	9807±573 ^{a}	396±110 ^{a}	2461±219 ^{a}	4128±279 a	152±11 ^{a}
AgNPs	2219±185 ^{b}	1.98±0.3 ^{b}	55367±3987 ^{ab}	11612±779 ^{b}	192±39 ^{a}	2726±301 ^{a}	4724±349 a	144±19 ^{a}
Ag^+	21116±1147 ^{c}	1.85±0.2 ^{b}	68539±4935 ^{b}	11346±212 ^{b}	248±18 ^{a}	2908±115 ^{a}	4206±376 ^{a}	138±12 ^{a}

The table above shows the effect of AgNPs/Ag^+ (70 mg/kg) on the concentration of elements within nine vegetables. Some vegetables showed enhancement in some elements while others were reduced. For example, Ca was significantly reduced in spinach, silverbeet, and leek. Copper was significantly higher in all vegetables compared to the control. Potassium increased in spinach, and decreased in parsley, lettuce, rocket and carrot. Magnesium decreased in spinach and beetroot, but increased in parsley and carrot. Manganese increased in radish, lettuce and silverbeet. Phosphorus decreased in lettuce, silverbeet and beetroot. Sulphur increased in parsley, and reduced in radish, lettuce, rocket, silverbeet, leek, and beetroot. Zinc decreased in parsley on exposure to AgNPs but increased on exposure to Ag^+. Zinc increased in radish and leeks but decreased in beetroot. Results are presented as mean ± SE (n = 5) (mg/kg). Means with different letters are significantly different ($P < 0.05$).

Appendix G

Calculation of antioxidant enzymes activity in earthworm (μM min^{-1} mg protein^{-1}) and sunflower (U/g)

W = Weight of earthworm (g)

P = Total amount of protein in the earthworm extract

U = Unit of enzyme activity

Vs = Total volume of the earthworm extract, in litres

Ve = Volume of earthworm extract used for enzyme measurement, in litres

Vt = Total mixture of the reaction mixture

ΔA/min = Absorbance variation per minute calculated on the linear part of the curve

A = f(time) when measuring enzyme activity

ε = Extinction coefficient at specific wavelength for the enzyme (in M/cm) of the compound released by the reaction, that allows calculation of the amount of substrate hydrolysed by the enzyme according to the Beer-Lambert Law:

A = ε. 1. C. Where A is the absorbance at specific wavelength, 1 is the path length (cm), and C is the concentration of the product formed which corresponds to the concentration of substrate hydrolysed, in M/l.

Calculation in cuvette using spectrophotometry:

The path length 1 = 1 cm; (ΔA/min) / ε= C (Mol L^{-1} min^{-1}); C x Vt x 10^6 = μMol/min in the reaction mixture

(C x Vt x 10^6) x (Vs/Ve) = total amount of μMol/min in the earthworm extract corresponding to the total amount of units (U)

[(C x Vt x 10^6) x (Vs/Ve)]/ P= Specific activity in U/mg.

Appendix H

Determination of 72-h LD_{50} of AgNPs and Ag^+ in earthworm *A. caliginosa* (n = 6/dose)

A. caliginosa earthworms were exposed to different concentrations of AgNPs and $AgNO_3$ for 72 h and the LD_{50} was calculated using a polynomial curve fitted to the LD_{50} trend line.

H.1 Determination of LD_{50} of *A. caliginosa* exposed to AgNPs

Method

About 4 kg of sieved soil was weighed. To 2 kg of this soil, an equivalent amount of AgNPs (13.48 mg/ml) were added and mixed well to give a concentration of 4000 mg/kg soil. Dilutions were continued with blank sieved soil to yield 3000, 2000, 1000, 500, 100, 30, 10, 1, 0.1 and 0.01 mg/kg soil of AgNPs. From each dilution 200 g of soil were weighed in triplicate in a plastic container with holed cover. Two *A. caliginosa* worms were included in each container. The containers were checked for dead worms after 24, 48, and 72 h. Results were calculated for 72 h using a polynomial curve fitted to the LD_{50} trend line (Fig. G.1.1).

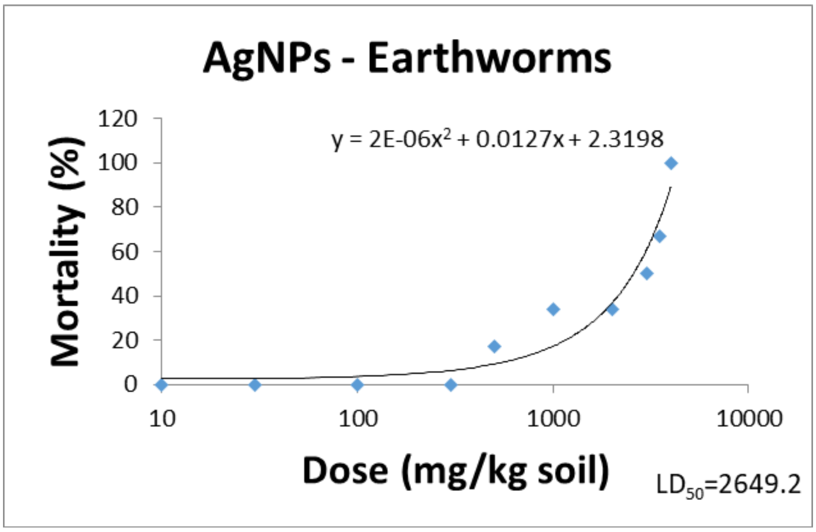

Fig. H.1: LD_{50} of AgNPs (n = 6).

H.2 Determination of LD_{50} of *A. caliginosa* exposed to $AgNO_3(Ag^+)$

Method

About 4 kg of sieved soil was weighed. To 1600 g of this soil, 2.52 g $AgNO_3$ in 48 ml of water were added and mixed well to give a concentration of 1000 mg/kg soil. Dilutions were continued with blank sieved soil to yield 500, 300, 100, 30, 10, 3, 1, 0.1 and 0.01 mg/kg soil of Ag^+ (as $AgNO_3$). The calculations used were based on Ag-free soil. From each dilution, 200 g of soil were weighed in triplicate in a plastic container with holed cover. Two *A. caliginosa* worms were included in each container. The containers were checked for dead worms after 24, 48, and 72 h. Results were calculated using a polynomial curve fitted to the LD_{50} trend line (Fig. G.2.1).

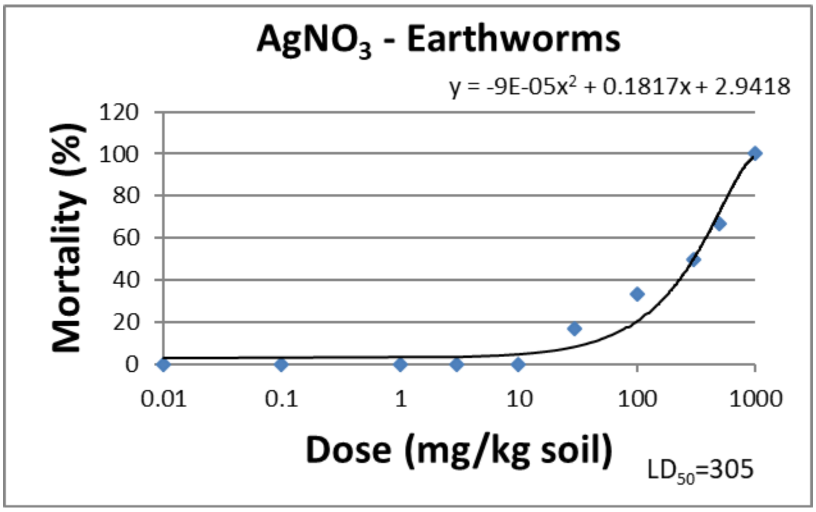

Fig. H.2: LD_{50} of $AgNO_3$ (Ag^+) (n = 6).

References

Abdallah, O., Lotfi, B., Laura, P., David, D., 2013. Silver nanoparticle toxicity effect on growth and cellular viability of the aquatic plant *Lemna gibba*. Environmental Toxicology and Chemistry 32, 902–907.

Abdul, G., 2010. Toxic effects of heavy metals on plant growth and metal accumulation in maiz *(Zea mays L.)*. Iranian Journal of Toxicology 4, 325–334.

Abraham, P.M., Barnikol, S., Baumann, T., Kuehn, M., Ivleva, N.P., Schaumann, G.E., 2013. Sorption of silver nanoparticles to environmental and model surfaces. Environmental Science & Technology 47, 5083–5091.

Addy, S.K., Goodman, R.N., 1972. Polyphenol oxidase and peroxidase in apple leaves inoculated with a virulent strain for *Ervinia amylovora*. Indian Phytopathology 25, 575–579.

Ahmed, S., Saifullah, Ahmad, M., Swami, B.L., Ikram, S., 2016. Green synthesis of silver nanoparticles using *Azadirachta indica* aqueous leaf extract. Journal of Radiation Research and Applied Sciences 9, 1–7.

Ainsworth, E.A., Gillespie, K.M., 2007. Estimation of total phenolic content and other oxidation substrates in plant tissues using Folin-Ciocalteu reagent. Nature Protocols 2, 875–877.

Akram, M.S., Ashraf, M., Shahbaz, M., Akram, N.A., 2009. Growth and photosynthesis of salt-stressed sunflower (*Helianthus annuus*) plants as affected by foliar-applied different potassium salts. Journal of Plant Nutrition and Soil Science, 172(6), 884–893.

Akter, M., Sikder, M.T., Rahman, M.M., Ullah, A.K.M.A., Hossain, K.F.B., Banik, S., Hosokawa, T., Saito, T., Kurasaki, M., 2018. A systematic review on silver nanoparticles-induced cytotoxicity: Physicochemical properties and perspectives. Journal of Advanced Research 9, 1–16.

Al Mamun, S., Chanson, G., Muliadi, Benyas, E., Aktar, M., Lehto, N., McDowell, R., Cavanagh, J., Kellermann, L., Clucas, L., Robinson, B., 2016. Municipal composts reduce the transfer of Cd from soil to vegetables. Environmental Pollution 213, 8–15.

Al Mamun, S., Lehto, N.J., Cavanagh, J., McDowell, R., Aktar, M., Benyas, E., Robinson, B.H., 2017. Effects of lime and organic amendments derived from varied source materials on cadmium uptake by potato. Journal of Environmental Quality 46, 836–844.

Alpsoy, L., Yildirim, A., Agar, G., 2009. The antioxidant effects of vitamin A, C, and E on aflatoxin B1-induced oxidative stress in human lymphocytes. Toxicology and Industrial Health 25, 121–127.

Amaral, A., Manu, S., Regina, C., Ionan, M., Armindo, R.S., 2006. Bioavailability and cellular effects of metals on *Lumbricus terrestris* inhabiting volcanic soils. Environmental Pollution 142, 103–108.

Amsh, S., 2012. Surface area to volume ratio in nanoparticles. Winner Science. https://winnerscience.com/2012/05/28/surface-area-to-volume-ratio-in-nanoparticles/

Anandalakshmi, K., Venugobal, J., Ramasamy, V., 2016. Characterization of silver nanoparticles by green synthesis method using *Pedalium murex* leaf extract and their antibacterial activity. Applied Nanoscience 6, 399–408.

Anjum, N.A., Gill, S.S., Duarte, A.C., Pereira, E., Ahmad, I., 2013. Silver nanoparticles in soil–plant systems. Journal of Nanoparticle Research 15, 1896.

Asharaf, J.M., Ansari, M., khan, H M, Alzohairy, M.A., Choi, I., 2016. Green synthesis of silver nanoparticles and characterization of their inhibitory effects on AGEs formation using biophysical techniques. Scientific Reports 6.

Atha, D.H., Wang, H., Peterson, E.J., Cleveland, D., Holbrook, R.D., Jaruga, P., 2012. Copper oxide nanoparticle mediated DNA damage in terrestrial plant models. Environmental Science & Technology 46, 189–1827.

Ayala, A., Muñoz, M.F., Argüelles, S., 2014. Lipid peroxidation: production, metabolism, and signaling mechanisms of malondialdehyde and 4-hydroxy-2-nonenal. Oxidative Medicine and Cellular Longevity 2014: 360438.

Azad, H.N., Shiva, A.H., Malekpour, R., 2011. Toxic effects of lead on growth and some biochemical and ionic parameters of sunflower (*Helianthus annuus* L.) seedling. Current Research Journal of Biological Sciences 3, 398–403.

Azevedo, H., Pinto, C.G.G., Fernades, J., Loureiro, S., Santos, C., 2005. Cadmium effects of sunflower growth and photosynthesis. Plant Nutrition 28, 2211- 2220.

Babu, A., Templeton, A.K., Munsho, A., Ramesh, R., 2013. Nanoparticles- based drug delivery for therapy of lung cancer: progress and challenges. Journal of Nanoparticles Research.
Bailly, C., Benamar, A., Corbineau, F., Come, D., 2000. Antoxidant system in sunflower seeds as affected by priming. Seed Science Research 10, 35–42.

Bate, A., 2015. *Speciation of and the effects of silver nanoparticles on the earthworm* Aporrectodea caliginosa. MApplSci thesis, Lincoln University, Lincoln, New Zealand.

Batista, C.A.S., Larson, R.G., Kotov, N.A., 2015. Nonadditivity of nanoparticle interactions. Science 350 (6257): 1242477.

Bednarska, A.J., Laskowski, R., Pyza, E., Semik, D., Swiatek, Z., Woznicka, O., 2016. Metal toxicokinetics and metal-driven damage to the gut of the ground beetle *Pterostichus oblongopunctatus*. Environmental Science and Pollution Research 23, 22047–22058.

Beer, C., Foldbjerg, R., Hayashi, Y., Sutherland, D.S., Autrup, H., 2012. Toxicity of silver nanoparticles—or silver ion? Toxicology Letters 208, 2494–2502.

Belfroid, A., Vandenberg, M., Seinen, W., Hermens, J., Vangestel, K., 1995. Uptake, bioavailability and elimination of hydrophobic compounds in earthworms (*Eisenia andrei*) in field-contaminated soil. Environmental Toxicology and Chemistry 14, 605–612.

Benoit, R., Wilkinson, K., Sauve, S., 2013. Partitioning of silver and chemical speciation of free Ag in soils amended with nanoparticles. Chemistry Central 7, 75.

Blouin, M., Hodson, M.E., Delgado E A, Baker, G., Brussaard, L., Butt, K.R., Dat, J., Dendooven, L., Peres, G., Tondoh, J.E., Cluzean, D., Brun, J.J., 2013. A review of earthworm impact on soil function and ecosystem services. European Journal of Soil Science, 161–182.

Bogart, L.K., Pourroy, G., Pellegrinol, T., 2014. Nanoparticles for imaging, Sensing and therapeutic intervention. ACS Nano 8, 3107–3122.

Booth, L.H., O'Halloran, K., 2009. A comparison of biomarker responses in the earthworm *Aporrectodea caliginosa* to the organophosphorus insecticides diazinon and chlorpyrifos. Environmental Toxicology and Chemistry 20, 2494–2502.

Boyle, E., 1968. Silver content of soils. https://www.atsdr.cdc.gov/toxprofiles/tp146-c5.pdf.

Bradford, M.M., 1976. A rapid and sensitive method for quantitation of microgram quantities of protein utilizing the principal of protein-dye binding. Analytical Biochemistry 72, 248–254.

Brami, C., Glover, A. R., Butt, K. R., Lowe, C. N. (2017). Effects of silver nanoparticles on survival, biomass change and avoidance behavimy of the endogeic earthworm *Allolobophora chlorotica*. *Ecotoxicology and Environmental Safety, 141*(Supplement C), 64–69.

Buechel, T., 2018. Role of calcium in plant culture. Promix Training Center, USA. https://www.pthorticulture.com/en/training-center/role-of-calcium-in-plant-culture/

Buege, J.A., Aust, S.D., 1978. Microsomal lipid peroxidation. Methods in Enzymology 52, 302–305.

Buhr, E., Senftleben, N., Klein, T., Bergmann, D., Gnieser, B., Frase, C.G., Bosse, H., 2009. Characterization of nanoparticles by scanning electron microscope in transmission mode. Measurment Science and Technology 20, 084025.

Caballero-Guzman, A., Nowack, B., 2016. A critical review of engineered nanomaterial release data: Are current data useful for material flow modeling? Environmental Pollution 213, 502–517.

Cabrera-de la Fuente, M., Ortega-Ortiz, H., Benavides-Mendoza, A., Sandoval-Rangel, A., 2014. Effect of application of silver nitrate on antioxidant status in watermelon plants. Pakistanian Journal of Botany 46, 1843–1846.

Cao, Q., Steinman, A.D., Yao, L., Xie, L.Q., 2017. Toxicological and biochemical responses of the earthworm *Eisenia fetida* to cyanobacteria toxins. Scientific Reports 7. Art. 15954

Carey, L.M., 1889. On allotropic forms of silver. American Journal of Science 37, 476–491.

Cataldo, J., Hidalgo, M.E., A, N., Gaete, H., 2011. Use of molecular biomarkers in *Eisenia foetida* to assess copper toxicity in agricultural soils affected by mining activities. Journal of Soil Science and Plant Nutrition 11(3), 57–70.

Caverzan, A., Passaia, G., Barcellos Rosa, S., Ribeiro, C.W., Lazzarotto, F., Margis-Pinheiro, M., 2012. Plant responses to stresses: Role of ascorbate peroxidase in the antioxidant protection. Genetics and Molecular Biology 35, 1011–1019.

CEINT, 2013. Silver nanoparticles may adversely affect environment. CEINT, Durham, N.C., USA. http://ceint.duke.edu/news/silver-nanoparticles-may-adversely-affect-en.

Chaffei, C., Pageau, K., Suzuki, A., Houda, G., Ghorbel, M.H., Masclaux daubresse, C., 2004. Cadmium toxicity induced changes in nitrogen management in *Lycopersicon esculentum* leading to a metabolic safeguard through an amino acid storage strategy. Plant Cell 45, 1681–1693.

Chao, G., Jingbo, X., Ji, L., Zhengtao, L., 2017. Biological responses in the earthworm *Eisenia fetida* exposed to soils near a typical lead acid battery plant. Soil and Sediment Contamination 25, 573–585.

Chao, Y.-Y., Hong, C.-Y., Kao, C.H., 2010. The decline in ascorbic acid content is associated with cadmium toxicity of rice seedlings. Plant Physiology and Biochemistry 48, 374–381.

Chemsafety, 2018. Soil adsorption coefficient (Kd/KOC) and chemical risk assement. http://www.chemsafetypro.com.

Chen, Y., Xianyu, Y., Jiang, X., 2017. Surface modification of gold nanoparticles with small molecules for biochemical analysis. Accounts of Chemical Research 50(2), 310–319.

Choi, J.S., Park, J.W., 2015. Molecular characterization and toxicological effects of citrate-coated silver nanoparticles in a terrestrial invertebrate, the earthworm (*Eisenia fetida)*. Molecular & Cellular Toxicology 11(4), 423–431.

Chotyakul, N., Paterio-Mour, M., Saraiva, J.A., Torres, J.A., Perez-lameia, C, 2014. Simultaneous HPLC quatification of vitamins A and E content in raw, pasteurized and UHT cow's milk and their changes during storage. European Food Research and Technology 238, 535–547.

Christensen, T.M., Vejlupkova, Z., Sharma, Y.K., Arthur, K.M., Spatafora, J.W., Albright, C.A., Meeley, R.B., Duvick, J.P., Quatrano, R.S., Fowler, J.E., 2003. Conserved subgroups and developmental regulation in the monocot rop gene family. Plant Physiology 133, 1791–1808.

Collin, V.C., Eymery, F., Gent, B., Rey, P., Havaux, M., 2007. Vitamin E is esential for the tolerance of *Arbidopsis thaliana* to metal-induced oxidative stress. Plant, Cell & Environment 31, 244–257.

Colman, B.P., Armount, C.L., Anciaux, S., Gunsch, C.K., Hochella, M.F., Kim, B., Lowry, G., McGill, B.M., Reinsch, B.C., Richardson, C.J., Unrine, J.M., Wright, J.P., Yin, L., Bernhards, E.S., 2013. Low concentration of silver nanoparticles in biosolids cause adverse ecosystem responses under realistic field scenario. PLoS One 8, 57189.

Concetti, A., Fioretti, E., Barra, D., Ascoli, F., 1984. Protease inhibitors from the parasitic worm *Parascaris equorum*. European Journal of Biochemistry 145(2), 417–421.

Connell, D., Markwell, R., 1990. Bioaccumulation in the soil to earthworm system. Chemosphere 20, 91–100.

Connon, R.E., Geist, J., Werner, I., 2012. Effect-based tools for monitoring and predicting the ecotoxicological effects of chemicals in the aquatic environment: Review. Sensors 12: 12741–12771.

Costache, M.A., Campeanu, Neata, G., 2012. Studies concening the extraction of chlorophyll and total carotenoids from vegetables. Romanian Biotechnology Letters 17, 7702–7708.

Coutris, C., Joner, E.J., Oughton, D.H., 2012. Aging and soil organic matter affect the fate of silver nanoparticles in soil. Science of the Total Environment 15, 420–427.

Cox, A., Venkatachalam, P., Sahi, S., Sharma, N., 2016. Silver and titanium dooxide nanoparticle toxicity in plants: A review of current research. Plant Physiology and Biochemistry 107, 147–163.

Cunningham, P., Foot, J., Reed, K., 1993. Perennial ryegrass (*Lolium perenne*) endophyte (*Acremonium lolii*) relationships: the Australian experience. Agriculture, Ecosystems & Environment 44, 157–168.

Curieses, S.P., García-Velasco, N., Urionabarrenetxea, E., Sáenz, M.E., Bilbao, E., Di Marzio, W.D., Soto, M., 2017. Responses to silver nanoparticles and silver nitrate in a battery of biomarkers measured in coelomocytes and in target tissues of *Eisenia fetida* earthworms. Ecotoxicology and Environmental Safety 141, 57–63.

Cvjetko, P., Zovko, M., 2017. Phytotoxic effects of silver nanoparticles in tobacco plants. In: Chen, Y.-P. (Ed.), Environmental Science and Pollution Research. Springer Berlin Hiedelberg.

Daghestani, H.N., Day, B.W., 2010. Theory and applications of surface plasmon resonance, resonant mirror, resonant waveguide grating, and dual polarization interferometry biosensors. Sensors 10, 9630–9646.

Dakal, T.C., Kumar, A., Majumdar, R.S., Yadav, V., 2016. Mechanistic basis of antimicrobial actions of silver nanoparticles. Frontiers in Microbiology 7, 1831.

Das, K., Roychoudhury, A., 2014. Reactive oxygen species (ROS) and response of antioxidants as ROS-scavengers during environmental stress in plants. Frontiers in Environmental Science 2, 53.

de Kanter, M., Meyer-Kirschner, J., Viell, J., Mitsos, A., Kather, M., Pich, A., Janzen, C., 2016. Enabling the measurement of particle sizes in stirred colloidal suspensions by embedding dynamic light scattering into an automated probe head. Measurement 80, 92–98.

de la Fuente, M.C., Ortiz, H., Mendoza, A., Rangel, A., 2014. Effect of the application of silver nitrate on antioxidant status in watermelon plants. Pakistan Journal of Botany 46, 1843–1846.

Deepa, M.K., Suryaprakash, T.N.K., Kumar, R, 2016. Green synthesized silver nanoparticles. Chemical and Pharmaceutical Research 8, 411–419.

Demarty, M., Morvan, C., Thellier, M., 1984. Calcium and the cell wall. Plant, Cell & Environment 7, 441–448.

Deschamps, J.R., 2010. X-ray crystallography of chemical compounds. Life Sciences 86, 585–589.

Diez-Ortiz, M., E, L., Killl, p., Powel, K., John, M., Kerstin, J., Cornelis, A.M., Van Gestel, J., Fred, W., Mosselmans, J.F.W., Claus, S., David, J.S., 2015. Uptake routes and toxicokinetics of silver nanoparticles and silver ions in the earthworm *Lumbricus rubellus*. Environmental Toxicology and Chemistry 34, 2263–2270.

Dobias, J., Bernier- Latmanic, R., 2013. Silver release from silver nanoparticles in natural waters. Environmental Science & Technology 47(9), 4140–4146.

Dong, X., Ji, X., Wu, H., Zhao, L., Li, J., Yang, W., 2009. Shape control of silver nanoparticles by stepwise citrate reduction. The Journal of Physical Chemistry C 113, 6573–6576.

Doolette, C.L., Mcaughlin, M.J., Kirby, J.K., Navarro, D.A., 2015. Bioavailability of silver and silver sulfide nanoparticles to lettuce (*Lactuca sativa*): Effect of agricultural amendments on plant up take. Journal of Hazardous Materials 300, 788–795.

Dubios, M., Gilles, K.A., Hamilton, J.K., Rebers, P.A., Smith, F., 1956. Colorimetric method for determination of sugars and related substances. Analytical Chemistry 28, 350–356.

Durán, N., Durán, M., de Jesus, M.B., Seabra, A.B., Fávaro, W.J., Nakazato, G., 2016. Silver nanoparticles: a new view on mechanistic aspects on antimicrobial activity. Nanomedicine: Nanotechnology, Biology and Medicine 12(3), 789–799.

Dushenkov, V., Kumar, P.N., Motto, H., Raskin, I., 1995. Rhizofiltration: the use of plants to remove heavy metals from aqueous streams. Environmental Science & Technology 29, 1239–1245.

El-Temsah, Y.S., Joner, E.J., 2010. Impact of Fe and Ag nanoparticles on seed germination and differences in bioavailabilty during exposure in aqueous suspension and soil. Environmental Toxicology 27, 42–49.

El Badawy, A.M., Silva, R.G., Morris, B., Scheckel, K.G., Suidan, M.T., Tolaymat, T.M., 2010. Surface charge-dependent toxicity of silver nanoparticles. Environmental Science & Technology 45, 283–287.

Faghihi, R., Larijani, K., Abdossi, V., Moradi, P., 2017. Green synthesis of silver nanoparticles by grapefruit's peel and effect of these nanoparticles on superoxide dismutase enzyme activity and growth of cucumber inoculated with *Rhizoctonia solani.* Oriental Journal of Chemistry 33(6):2810-2820.

Fernandes, J.P., Mucha, A.P., Francisco, T., Gomes, C.R., Almeida, C.M.R., 2017. Silver nanoparticles uptake by salt marsh plants – Implications for phytoremediation processes and effects in microbial community dynamics. Marine Pollution Bulletin 119, 176–183.

Filek, M., Keskinen, R., Hartikainen, H., Szarejko, I., Janiak, A., Miszalski, Z., Golda, A., 2008. The protective role of selenium in rape seedlings subjected to cadmium stress. Plant Physiology 165, 833–844.

Fitzpatrick, L.C., Muratti-Ortiz, J.F., Venables, B.J., 1996. Comparative toxicity in earthworm *Eisenia fetida* and *Lumbricus terrestris* exposed to cadmium nitrate using artificial soil and filter paper protocols. Bulletin of Enviromental Contamination and Toxicology 57, 63–68.

Fryer, M., 1992. The antioxidant effects of thylakoid Vitamin E (α-tocopherol). Plant, Cell & Environment 15, 381–392.

Gajewska, E., Skłodowska, M., 2007. Relations between tocopherol, chlorophyll and lipid peroxides contents in shoots of Ni-treated wheat. Journal of Plant Physiology 164, 364–366.

Gallego, S.M., Benavídes, M.P., Tomaro, M.L., 1996. Effect of heavy metal ion excess on sunflower leaves: evidence for involvement of oxidative stress. Plant Science 121, 151–159.

Gandhi, H., Khan, S., 2016. Biological synthesis of silver nanoparticles and its antibacterial activity. Journal of Nanomedicine & Nanotechnology 7, 2.

Garcia, J.S., Gratao, P.I., Azevedo, R.A., Arruda, M.A., 2006. Metal contamination effects on sunflower (*Helianthus annuus L.*) growth and protein expression in leaves during development. Journal of Agricultural and Food Chemistry 54, 8623–8630.

Garcia-Gómez, C., Fernandez, M.D., Babin, M., 2014. Ecotoxicological evaluation of sewage sludge contaminated with zinc oxide nanoparticles. Archives of Environmental Contamination and Toxicology 67, 494–506.

García-Velasco, N., Gandariasbeitia, M., Irizar, A., Soto, M., 2016. Uptake route and resulting toxicity of silver nanoparticles in *Eisenia fetida* earthworm exposed through Standard OECD Tests. Ecotoxicology 25, 1543–1555.

Gauthami, M., Srinivasan, N., Goud, N.M., Boopala, K., Thirumurugan, K., 2015. Synthesis of silver nanoparticles using *Cinnamomum zeylanicum* bark extractand its antioxidant activity. Nanoscience & Nanotechnology-Asia 5(1), 2–7.

Geisler-Lee, J., Brooks, M., Gerfen, J.R., Wang, Q., Fotis, C., Sparer, A., Ma, X.M., Berg, R.H., Geisler, M., 2014. Reproductive toxicity and life history study of silver nanoparticle effect, uptake and transport in *Arabidopsis thaliana*. Nanomaterials 4, 301–318.

Gill, S.S., Tuteja, N., 2010. Reactive oxygen species and antioxidant machinery in abiotic stress tolerance in crop plants. Plant Physiology and Biochemistry 48, 909–930.

Gobe, G., Crane, D., 2010. Mitochondria, reactive oxygen species and cadmium toxicity in the kidney. Toxicology Letters 15(198), 49–55.

Gomes, S.I.L., Hansen, D., Scott-Fordsmand, J.J., Amorim, M.J.B., 2015. Effects of silver nanoparticles to soil invertebrates: oxidative stress biomarkers in *Eisenia fetida*. Environmental Pollution 199C, 49–55.

Gooneratne, S.R., Buser, A., Landsay, P., Welby, M., 2011. Ecotoxicological assessment of acid mine draingage: Electrophysiological changes in an earthworm *(Aporrectodea caliginosa)* and aquatic oligochaete *(Lumbriculus variegatus)*. Journal of Environmental Monitoring 13, 1360–1365.

Gordon, O., Sienters, T.V., Brunetto, P.S., Sturdevant, D.E., Otto, M., Landmann, R., Fromm, K.M. 2010. Silver coordination polymers for prevention of implant thiol interaction, impact onrespiratory chain enzymes and hydroxyl radical induction. Antimicrobial Agents and Chemotherapy 54(10), 4208–4218.

Goudarzi, M., Mir, N., Mousavi-kamazani, M., Bagheri, S., Salavat-Niasari, M., 2016. Biosynthesisand characterization of silver nanoparticles prepared from two novel natural prercursors by facile thermal decomposition methods. Scientific Reports 6.

Graf, C., Vossen, D.L., Imhof, A., van Blaaderen, A., 2003. A general method to coat colloidal particles with silica. Langmuir 19, 6693–6700.

Grewal, K.S., Buchan, G.D., Tonkin, P.J., 1990. Estimation of field capacity and wilting point of some New Zealand soils from their saturation percentages. New Zealand Journal of Crop and Horticultural Science 18, 241–246.

Griffitt, R.J., Hyndman, K., Denslow, N.D., Barber, D.S., 2008. Comparison of molecular and histological changes in zebrafish gills exposed to metallic nanoparticles. Toxicological Sciences 107, 404–415.

Gruyer, N., Dorais, M., Bastien, C., Dassylva, N., Triffault-Bouchet, G., 2014. Interaction between silver nanoparticles and plant growth. Acta Horticulturae 1037, 795–800.

Gudikandula, K., Maringanti, S.C., 2016. Synthesis of silver nanoparticles by chemical and biological methods and their antimicrobial properties. Journal of Experimental Nanosciences 11, 714–721.

Guo, W., Nazim, H., Liang, Z., Yang, D., 2016. Magnesium deficiency in plants: An urgent problem. The Crop Journal 4, 83–91.

Gupta, A.S., Alscher, R.G., McCune, D., 1991. Response of photosynthesis and cellular antioxidants to ozone in *Populus* leaves. Plant Physiology 96, 650–655.

Gusman, M.G., Dille, J., Godet, S., 2009. Synthesis of silver nanoparticles by chemical reduction. International Journal of Chemical and BiomolecularEngineering 2, 104.

Habibi, D., Boojar, M.M., Mahmoudi, A., Ardakani, M.R., Taleghani, D., 2004. Antoxidative enzymes in sunflower subjected to drought stress. 4th International Crop Science Congress, Australia.

Habig, W.H., Pabst, M., WE, J., 1974. Glutathione-S-Transferase: The first enzymatic step in mercapturic acid formation. Journal of Biological Chemistry 249, 7130–7139.

Halliwell, B., 1991. Reactive oxygen species in living systems: Source, biochemistry, and role in human disease. The American Journal of Medicine 91, S14–S22.

Hassan, Z., Ali, S., Ahmed, R., Iqbal, M., 2017. Biochemical and molecular response of oilseed crops to heavy metal stress: Yield and adaptations under environmental stress. Research Gate, Pakistan.

Havir, E.A., McHale, N.A., 1987. Biochemical and developmental charcterization of multiple forms of catalase in tobacco leaves. Plant Physiology and Biochemistry 84, 450–455.

He, Y., Li, X., Zheng, Y., Wang, Z.Y., Ma, Z., Yang, Q., Yao, B., Zhao, Y., Hao, Z., 2018. A green approach for synthesizing nanoparticles, and their antibacterial and cytotoxic activities. New Journal of Chemistry 42, 2882–2888.

Heck, D.E., Shakarjian, M., Kim, H.D., Laskin, J.D., Vetrano, A.M., 2010. Mechanisms of oxidant generation by catalase. Annals of the New York Academy of Sciences 1203, 120–125.

Hedberg, J., Kleja, D.B., Wallinder, I.O., 2015. Sorption and dissolution of bare and coated silver nanoparticles in soil suspensions-Influence of soil and particle characteristics. Journal of Environmental Science and Health Part A-Toxic/Hazardous Substances & Environmental Engineering 50, 891–900.

Henson-Ramsey, H., Levine, J., Kennedy-Stoskopf, S., Taylor, S.K., Shea, D., Stoskopf, M.K., 2009. Development of a dynamic pharmacokinetic model to estimate bioconcentration of xenobiotics in earthworms. Environmental Modeling & Assessment 14(3): 411–418.

Hoke, R., Huggett, D., Brasfield, S., Brown, B., Embry, M., Fairbrother, A., Kivi, M., Paumen, M.L., Prosser, R., Salvito, D., Scroggin, R, 2015. Review of laboratory based terrestrial bioaccumulation assessment approaches for organic chemicals: current status and future possibilities. Integrated Environmental Assessment and Management 12(1), 109–122.

Hou, W., Chen, X., Song, G., Wang, Q., Chang, C., 2007. Effect of copper and cadmium on heavy metal polluted waterbody restorationtion by duckweed *(Lemma minor)*. Plant Physiology and Biochemistry 45, 62–69.

Howe, P.D., Dobson, S., 2002. Silver and silver compounds: environmental aspects. Concise International Chemical Assessment Document 44, World Health Organization, Geneva.http://www.inchem.org/documents/cidads/cicads44.htm

Hu, C., Li, M., Wang, W., Cui, Y., Chen, J., Yang, L., 2012. Ecotoxicity of silver nanoparticles on earthworm *Eisenia fetida*: responses of the antioxidant system, acid phosphatase and ATPase. Toxicological & Environmental Chemistry 94, 732–741.

Hubalek, J., Hradecky, J., Adam, V., Krystova, O., Huska, D., Masarik, M., Trunkova, L., Horna, A., Klosova, K., Adamek, M., Zehnalek, J., Kizek, R., 2007. Spectrometric and voltammetric analysis of urease- nickel. Sensors 7(7), 1238–1255.

Huggett, R.J., Kimerly, R.A., Mehrle, P.M., Bergman, H.L. Jr., 1992. Biomarkers: Biochemical, Physiological and Histological Markers of Anthropogenic Stress. Lewis: Chelsea, MI, USA.

Ifemeje, J., Udedi, S., Okechukwu, A.U., Nwaka, A.C., Lukong, C.B., Anene, I.N., Egbuna, C., Ezeude, I.C., 2015. Determination of total protein, superoxide dismutase, catalase activity and lipid peroxidation in soil macro-fauna (earthworm) from Onitsha municipal open waste dump. Journal of Scientific Research and Reports 6, 394–403.

Jacobson, A.R., McBride, M.B., Baveye, P., Steenhuis, T.S., 2005. Environmental factors determining the trace-level sorption of silver and thallium to soils. Science of the Total Environment 345, 191–205.

Jagota, K.S., Dani, H.M., 1982. A new colorimetric technique for the estimation of Vitamin C using folin phenol reagent. Analytical Biochemistry 127, 178–182.

Jesmer, A.H., Velicogna, J.R., Schwertfeger, D.M., Scroggins, R.P., Princz, J.I., 2017. The toxicity of silver to soil organisms exposed to silver nanoparticles and silver nitrate in biosolids-amended field soil. Environmental Toxicology and Chemistry 36, 2756–2765.

Ji, C., Wu, H., Wei, L., Zhao, J., Lu, H., Yu, J., 2013. Proteomic and metabolomic analysis of earthworm *Eisenia fetida* exposed to different concentrations of 2,2′,4,4′-tetrabromodiphenyl ether. Journal of Proteomics 91, 405–416.

Jiang, H.S., Qiu, X.N., Li, G.B., Li, W., Yin, L.Y., 2014. Silver nanoparticles induced accumulation of reactive oxygen species and alteration of antioxidant system in the aquatic plant *Spirodela polyrhiza*. Environmental Toxicology and Chemistry 33, 1398–1405.

Jiang, Y., H, H., 2001. Drought and heat stress injury to two cool-season turf grasses in relation to antioxidant metabolism and lipid peroxidation. Crop Science 41, 436–442.

Jiang, Z.J., Liu, C.Y., Sun, L.w., 2005. Catalytic properties of silver nanoparticles supported on silica spheres. The Journal of Physical Chemistry 109, 1730–1735.

Jiang, H.S., Li, M., Chang, F.Y., Li, W., Yin, L.Y., 2012. Physiological analysis of silver nanoparticles and $AgNO_3$ toxicity to *Spirodela polyrhiza*. Environmental Toxicology and Chemistry 31, 1880–1886.

Johari, S.A., Kalbassi, M.R., Soltani, M., Yu I, J., 2012. Toxicity comparison ofcolloidal silver nanoparticles in various life stages of rainbow trout (*Oncorhynchus mykiss*). Iranian Journal of Fisheries Sciences 12, 76–95.

John, R., Ahmad, P., Gadil, K., Sharma, S., 2009. Heavy metal toxicity: effect on the plant growth, biochemical parameters and metal accumulation by *Brassica juncea* L. International Journal of Plant Production 3, 65–76.

Juarez-Maldonado, A., Rosales-Velazquez, J.L., Ortega-Ortiz, H., Cabrera-De-la-Fuente, M., Ramirez, H., Benavides-Mendoza, A., 2013. Accumulation of silver nanoparticles and its effect on the antioxidant capacity in *Allium cepa* L. International Journal of Experimental Botany 82, 91–97.

Kalbassi, M.R., 2011. Toxicity of silver nanoparticles in aquatic ecosystem: Salinity as the main cause in reducing toxicity. Irianian Journal of Toxicoloy 3, 136–143.

Kandarp, M., Mihir, S., 2013. Synthesis of silver nanoparticles by using sodium borohydride as a reducing agent. International Journal of Engineering Research & Technology 2, 1–5.

Karami, S., Heidare, R., Rahmani, F., 2015. Effect of silver nanoparticles on free amino acids content and antioxidant defense system of tomato plants. Indian Journal of Plant Physiology 20, 257–263.

Karuppanapandian, T., Moon, J.-C., Kim, C., Manoharan, K., Kim, W., 2011. Reactive oxygen species in plants: their generation, signal transduction, and scavenging mechanisms. Australian Journal of Crop Science 5, 709.

Kawata, K., Osawa, M., Okabe, S., 2009. In vitro toxicity of silver nanoparticles at non-cytotoxic doses to HepG2 human hepatoma cells. Environmental Science & Technology *43*(15), 6046–6051.

Khalil, A.M., 2016. Physiological and genotoxic responses of the earthworm *Aporrecodea caliginosa* exposed to sublethal concentrations of AgNPs. The Journal of Basic & Applied Zoology 74, 8–15.

Khan, I., Saeed, K., Khan, I., 2017. Nanoparticles: Properties, applications and toxicities. Arabian Journal of Chemistry. https://doi.org/10.1016/j.arabjc.2017.05.011

Khan, M.Z.H., Tareq, F.K., Hossen, M.A., Roki, M.N.A.M., 2018. Green synthesis and characterization of silver nano particles using *Coriandrum stivum* leaf extract. Journal of Engineering Science and Technology 13, 158–166.

Kim, I., Lee, B.-T., Kim, H.-A., Kim, K.-W., Kim, S.D., Hwang, Y.-S., 2016. Citrate coated silver nanoparticles change heavy metal toxicities and bioaccumulation of *Daphnia magna*. Chemosphere 143, 99–105.

Kim, J.H., Lee, S.H., Cha, Y.J., Hong, S.J., Chung, S.K., Park, T.H., Choi, S.S., 2016. *C. elegans*-on-a-chip for in situ and in vivo Ag nanoparticles uptake and toxicity assay. Scientific Reports 7.

Kim, K.-J., Sung, W.S., Suh, B.K., Moon, S.-K., Choi, J.-S., Kim, J.G., Lee, D.G., 2009. Antifungal activity and mode of action of silver nano-particles on *Candida albicans*. Biometals 22, 235–242.

Kittler, S., Greulich, C., Diendorf, J., Koller, M., Epple, M., 2010. Toxicity of silver nanoparticles increases during storage because of slow dissolution under release of silver ions. Chemistry of Materials 22, 4548–4554.

Kladivko, E.J., Mackay, A., Bradford, J.M., 1986. Earthworms as a factor in the reduction of soil crusting. Soil Science Society of America Journal of 50, 191–196.

Klein, D.H., 1972. Mercury and other metals in urban soils. Environmental Science & Technology 6, 560–562.

Kleja, D., Nakata, S., Persson, I., Gustafsson, 2016. Silver (I) Binding properties of organic soil materials are different from those of isolated humic substances. Environmental Science & Technology 50, 7453–7460.

Klitzke, S., Metreveli, G., Peters, A., Schaumann, G.E., Lang, F., 2015. The fate of silver nanoparticles in soil solution — Sorption of solutes and aggregation. Science of the Total Environment 535, 54–60.

Komives, T., Aioub, A.A.A., Gullner, G., 1995. Effect of chemicals stress caused by heavy metals on the glutathione-S-transferase enzyme activity in maize *(Zea mays L.)*. Acta Phytopathologica et Entamologica Hungarica 30, 215–220.

Krajczewski, J., Kotatal, K., Kudelski, A., 2017. Plasmonic nanoparticles in chemical analysis. Royal Society of Chemistry 7, 17559–17576.

Krishnaraj, C., Jagan, E.G., Ramachandran, R., Abirami, S.M., Mohan, N., Kalaichelvan, P.T., 2012. Effect of biologically synthesized silver nanoparticles on *Bacopa monnieri* (Linn.) Wettst. plant growth metabolism. Process Biochemistry 47, 651–658.

Krizkova, S., Ryani, P., Adam, V., Galiova, M., Beklova, M., Babula, P., Kaiser, J., Novotny, J., Liska, M., Malina, R., Zrhnalek, J., Hubalek, J., Havel, L., Kizek, R., 2008. Mult-instrumental analysis of tissues of sunflower plants treated with silver(I) ions – plants as bioindicators of environmental pollution. Sensors (Basel) 8.

Kühnel, D., Nickei, C., 2014. The OECD meeting on ecotoxicology and environmental fate – Towards the development of improved OECD guidelines for the testing of nanomaterials. Science of the Total Environment, 472, 347–353.

Kumar, S., 2010. Infrared spectroscopy: Method development and ligand binding studies. Licentiate thesis, Department of Biochemistry and Biophysics Stockholm University, Stockholm, Sweden. http://www.diva-portal.org/smash/get/diva2:327876/FULLTEXT01.pdf

Kumar, S., Sharma, V., Bhoyar, R.V., Bhattacharyya, J.K., Chakrabarti, T., 2008. Effect of heavy metals on earthworm activities during vermicomposting of municipal waste. Water Environmental Research 80(2), 154–161.

Kumari, M., Mukherjee, A., Chandrasekaran, N., 2009. Genotoxicity of silver nanoparticles in *Allium cepa*. Science of the Total Environment 407, 5243–5246.

Labrot, F., Narbonne, J.F., Ville, P., Saint Denis, M., Ribera, D., 1999. Acute toxicity, toxicokinetics, and tissue target of lead and uranium in the clam Corbicula fluminea and the worm *Eisenia fetida*: Comparison with the fish *Brachydanio rerio*. Archives of Environmental Contamination and Toxicology 36, 167–178.

Laguerre, C., .Sanchez-Hernandez, J.C., Kohler, H.R., Triebskorn, R., Capowiez, Y., Rault, M., Mazzia, C., 2009. B-type esetrases in the snail *Xeropicta derbentina*: An enzymological analysis to evaluate their use as biomarkers of pesticides exposure. Environmental Pollution 157(1), 199–207.

Lakshmanan, G., Sathiyaseelan, A., Kalaichelvan, P., Murugesan, K., 2018. Plant-mediated synthesis of silver nanoparticles using fruit extract of *Cleome viscosa* L.: Assessment of their antibacterial and anticancer activity. Karbala International Journal of Modern Science 4, 61–68.

Łaszczyca, P., Augustyniak, M., Babczyńska, A., Bednarska, K., Kafel, A., Migula, P., Wilczek, G., Witas, I., 2004. Profiles of enzymatic activity in earthworms from zinc, lead and cadmium polluted areas near Olkusz (Poland). Environment International 30(7), 901–910.

Laub, P.B., Gallo, J., 1996. Ncomp – A windows- based computer programe for non compartmental analysis of pharmacokinetic data. Journal of Pharmaceutical Science 85, 393–395.

Lavelle, J., 2015. Stressed plants destroy damaged chloroplasts. Science & Technology Concentrates 93(2), 23.

Lee, W.L., Kwak, J.I., An, Y.J., 2012. Effect of silver nanopartciles in crop plants *Phaseolus radiatus* and *Sorghum bicolor*. Media effect on phytotoxicity. Chemosphere 86(5), 491–499.

Leela, A., Vivekanandan, M., 2008. Tapping the unexploited plant resources for the synthesis of silver nanoparticles. African Journal of Biotechnology 7(17), 3162-3165.

Lemtiri, A., Colinet, G., Alabi, T., Cluzeau, D., Zirbes, L., Haubruge, É., Francis, F., 2014. Impacts of earthworms on soil components and dynamic. A review. Biotechnologie, Agronomie, Société et Environnement 18(1), 121–133.

Levard, Hotze, E.M., Lowry, G.V., Brown, G. E. Jr., 2012. Environmental transformations of silver nanoparticles: impact on stability and toxicity. Environmental Science & Technology 46(13), 6900–6914.

Li, C.-C., Dang, F., Li, M., Zhu, M., Zhong, H., Hintelmann, H., Zhou, D.-M., 2017. Effects of exposure pathways on the accumulation and phytotoxicity of silver nanoparticles in soybean and rice. Nanotoxicology 11, 699–709.

Li, C.H.M., Wang, W., Cui, Y., Chen, J., Yang, L., 2012. Ecotoxicity of silver nanoparticles on earthworm *Eisenia fetida:* responses of the antioxidant sytem, acid phosphatase and ATPase. Toxicological & Environmental Chemistry 94(4), 732–741.

Li, L., Wu, H., Peijnenburg, W.J., van Gestel, C.A., 2015. Both released silver ions and particulate Ag contribute to the toxicity of AgNPs to earthworm *Eisenia fetida*. Nanotoxicology 9(6), 792–801.

Li, M., Hu, C.W., Zhu, Q., Chen, I., Kong, Z.M., Liu, Z.L., 2006. Copper and zinc induction of lipid peroxidation and effect on antioxidant enzyme activities in the microalga *Pavlova ciridis* (Prymnesiiphyceae). Chemosphere 62, 565–572.

Li, X., Ke, M., Zhang, M., Peijnenburg, W.J.G.M., Fan, X., Xu, J., Zhang, Z., Lu, T., Fu, Z., Qian, H., 2018. The interctive effects of diclofop-methyl and silver nanoparticles on *Arabidopsis thaliana*: Growth, photosynthesis and antioxidant system. Environmental Pollution 232, 212–219.

Linares, M.G., 2016. Ecotoxicological effect of silver nanoparticles in biosolid amended soils to the earthworm *Eisenia fetida* and the crop *Hordeum vulgare*. Department of Natural Resource Science. McGill University, Montreal- Canada, P. 104

Lionetto, M.G., Calisi, A., Schettino, T., 2012. Earthworm biomarkers as tools for soil pollution assessment. In: Hernandez Soriano M.C. (Ed.) Soil Health and Land Use Management. InTech. Pp. 305–322.

Liu, J., Hurt, R.H., 2010. Ion release kinetics and particle persistence in aqueous nano-silver colloids. Environmental Science & Technology 44, 2169–2175.

Livingstone, D.R., Martinez, P.G., Michel, X., Narbonne, J., O'hara, S., Ribera, D., Winston, G., 1990. Oxyradical production as a pollution-mediated mechanism of toxicity in the common mussel, *Mytilus edulis* L., and other molluscs. Functional Ecology 4(3), 415–424.

Ma, X., Geiser-Lee, J., Deng, Y., Kolmakov, A., 2010. Interactions between engineered nanoparticles (ENPs) and plants: phytotoxicity, uptake and accumulation. Science of the Total Environment 408, 3053–3061.

Maathuis, F.J.M., 2009. Physiological functions of mineral macronutrients. Plant Biology 12, 250–258.

Maity, S., Roy, S., Chaudhury, S., Bhattacharya, S., 2008. Antioxidant responses of the earthworm *Lampito mauritii* exposed to Pb and Zn contaminated soil. Environmental Pollution 151(1), 1–7.

Makama, S., Piella, J., Undas, A., Dimmers, W.J., Peters, R., Puntes, V.F., van den Brink, N.W., 2016. Properties of silver nanoparticles influencing their uptake in and toxicity of the earthworm *Lumbricus rubellus* following exposure in soil. Environmental Pollution 218, 870–878.

Malan, C., Greyling, M.M., Gressel, J., 1990. Correlation between Cu.Zn suoeroxide dismutase and xenobiotic stress tolerance in maize inbreds. Plant Science 69, 157–166.

Martin, J.D., Colson, T.L.L., Langglois, V.S., Metcalfe, C.D., 2017. Biomarkers of exposure to nanosilver and silver accumulation in yellow perch (*Perca flavescens*). Environmental Toxicology and Chemistry 36(5), 1211–1220.

Martirosyan, A., Bazes, A., Schnuder, Y.J., 2014. In vitro toxicity assessment of silver nanoparticles in the presence of phenolic compounds—preventive agents against the harmful effect? Nanotoxicology 8(5), 573–582.

Mattson, M.P., Calabrese, E.J., 2009. Hormesis: A Revolution in Biology, Toxicology and Medicine. Springer Science & Business Media.

Mazumdar, H., 2014. The impact of silver nano particles on plant biomass and chlorophyll content. International Journal of Engineering and Science 4, 12–20.

Mazumdar, H., Ahmed, G.U., 2011. Phytotoxicity effect of silver nanoparticles on *Oryza sativa*. International Journal of ChemTech Research 3, 1494–1500.

McDaniel, J.P., Butters, G., Barbarick, K.A., Stromgerger, M.E., 2015. Effect of *Aporrectodea Caliginosa* on soil hydraulic properties and solute dispersivity. Soil Science Society of Americal Journal 79, 838–847.

McElroy, J.S., Kopsell, D.A., 2009. Physiological role of carotenoids and other antioxidants in plants and application to turfgrass stress management. New Zealand Journal of Crop and Horticultural Science 37, 327–333.

McGillicuddy, E., Murray, I., Kavanagh, S., Morrison, L., Fogarty, A., Cormican, M., Dockery, P., Prendergast, M., Rowan, N., Morris, D., 2017. Silver nanoparticles in the environment: Sources, detection and ecotoxicology. Science of the Total Environment 575, 231–246.

McIlveen, W., Negusanti, J., 1994. Nickel in the terrestrial environment. Science of the Total Environment 148, 109–138.

McLaughlin, M.J., Tiller, K.G., Naidu, R., Stevens, D.P., 1996. Review: The behaviour and environmental impact of contaminants in fertilizers. Australian Journal of Soil Research 34, 1–54.

McLennan, S.M., 1998. Geochemical classification of the elementsclassification of the elements. In: Geochemistry. Springer: Dordrecht, The Netherlands. Pp. 263–266.

McShan, D., Ray, P.C., Yu, H., 2014. Molecular toxicity mechanism of nanosilver. Journal of Food and Drug Analysis 22(1), 116–127.

Mehrian, S.K., Heidare, R., Rahmani, F., 2015a. Effect of silver nanoparticles on free amino acids content and antioxidant defense system of tomato plants. Indian Journal of Plant Physiology 20, 257–263.

Meier, C., Voegelin, A., Pradas del Real, A., Sarret, G., Mueller, C.R., and Kaegi, R., 2016. Transformation of silver nanoparticles in sewage skudge during incineration. Environmental Science & Technology 50(7), 3503–3510.

Mendes, L.A., Maria, V.L., Scott-Fordsmand, J.J., Amorim, M.J., 2015. Ag nanoparticles (Ag NM300K) in the terrestrial environment: effects at population and cellular level in *Folsomia candida* (Collembola). International Journal of Environmental Research and Public Health 12(10), 12530–12542.

Meyer, J.N., Lord, C.A., Yang, X.Y., Turner, E.A., Badireddy, A.R., Marinakos, S.M., Chilkoti, A., Wiesner, M.R., Auffan, M., 2010. Intracellular uptake and associated toxicity of silver nanoparticles in *Caenorhabditis elegans*. Aquatic Toxicology 100, 140–150.

Meylan, W.M., Howard, H.P., Boethling, R.S., Aronson, D., Printup, H., Gouchie, B., 1999. Improved method for estimating bioconcentration/bioaccumulation factor from octanol/water partition coefficient. Environmental Toxicology and Chemistry 18, 664–672.

Mikov, M., Boni, N., Al-Salami, H., Kuhajda, K., Kevresan, S., Golocorbin-Kon, S., Fawcett, J., 2007. Bioavailability and hypoglycemic activity of the semisynthetic bile acid salt, sodium 3α, 7α-dihydroxy-12-0X0-5β-cholanate, in healthy and diabetic rats. European Journal of Drug Metabolism and Pharmacokinetics 32, 7–12.

Miralles, P., Tamara, L., 2012. Toxicity, uptake, and translocation of engineered nanomaterials in vascular plant. Environmental Science & Technology 46, 9224–9224.

Mishra, P.P., 2015. Properties of Nano-materials. Science. https://www.slideshare.net/ParthaPMishra/properties-of-nanomaterials

Mkoji, G., Smith, J., Prichard, R., 1988. Antioxidant systems in *Schistosoma mansoni*: evidence for their role in protection of the adult worms against oxidant killing. International Journal for Parasitology 18, 667–673.

Mody, V.V., Siwale, R., Singh, A., Mody, H.R., 2010. Introduction to metallic nanoparticles. Journal of Pharmacy and BioAllied Sciences 2(4), 282–289.

Munné-Bosch, S., Alegre, L., 2002. The function of tocopherols and tocotrienols in plants. Critical Reviews in Plant Sciences 21, 31–57.

Murthy, V.S., Seshaiah, K.R., 1974. Sunflower (*Helianthus annuus*), a promising oil seed crop. Andhra Agricultural Journal.

Mustafa, G., Komatsu, S., 2016. Toxicity of heavy metals and metal-containing nanoparticles on plants. Biochimica et Biophysica Acta - Proteins and Proteomics 1864, 932–944.

Nair, R., Varghese, S.H., Nair, B.G., Maekawa, T., Yoshida, Y., Kumar, D.S., 2010. Nanoparticulate material delivery to plants. Plant Science 179, 154–163.

Navarro, E., Baun, A., Behra, R., Hartmann, N.B., Filser, J., Miao, A.-J., Quigg, A., Santschi, P.H., Sigg, L., 2008a. Environmental behavior and ecotoxicity of engineered nanoparticles to algae, plants, and fungi. Ecotoxicology 17, 372–386.

Navarro, E., Piccapieta, F., Wagner, B., Marconi, F., Kaegi, R., Odzak, N., 2008b. Toxicity of silver nanoparticles to *Chalmydomonas reinhardtii*. Environmental Science & Technology 42, 8959–8964.

Nguyen, K.C., Seligy, V.L., Massarsky, A., Moon, T.W., Rippstein, P., Tan, J., Tayabali, A.F., 2013. Comparison of toxicity of uncoated and coated silver nanoparticles. Journal of Physics: Conference Series. IOP. P. 012025.

Nogueira, A., Ricardo, Machado, A. F., de Souza, A. Z., Martinello, F., Franco, C.V. and Dutra, G.B 2014. Synthesis and characterisation of silver nanoparticles produced with a bifunctional stabilizing agent. Indstrial and Enginering. Chemistry Research. 53, 3426–3434.

Nordberg, J., Arner, E.S., 2001. Reactive oxygen species, antioxidants, and the mammalian thioredoxin system1. Free Radical Biology and Medicine 31, 1287–1312.

Oberdörster, G., Oberdörster, E., Oberdörster, J., 2005. Nanotoxicology: an emerging discipline evolving from studies of ultra fine particles. Environmental Health Perspectives 113(7), 823–839.

OECD. 1984. *OECD Guidelines for testing of chemicals, Section 2: Effects on biotic systems. Test No. 207. Earthworm: acute toxicity tests.* www.oecd.org/chemicalsafetytesting/444098118.pdf.

Olchowik, J., Mariusz Bzdyk, R., Studnicki, M., Bederska-Błaszczyk, M., Urban, A., Aleksandrowicz-Trzcińska, M., 2017. The effect of silver and copper nanoparticles on the condition of English oak (*Quercus robur* L.) seedlings in a container nursery experiment. Forests 8, 310.

Olivieri, C., Parry, k.M., Powell, C.J., Tobias, D.J., Brown, M.A., 2016. Quantitative interpretation of molecular dynamics stimulation for X- ray photoelectron spectroscopy of aqueous solutions. The Journal of Chemical Physics 144(15), 154704.

Oromieh, A.G., 2011. Evaluating solubility, aggregation and sorption of nanosilver particles and silver ions in soils. Masters Thesis in Environmental Science. Department of Soil and Environment, Swedish University of Agricultural Sciences, Sweden.

Otmani, H., Tadjine, A., Moumeni, O., Zeriri, I., Amamra, R., Samira, D.B., Djebar, M.R., Berrebbah, H., 2018. Biochemical responses of the earthworm *Allolobophora caliginosa* exposed to cadmium contaminated soil in the Northeast of Algeria. Bulletin de la Société Royale des Sciences de Liège.

Oukarroum, A., Barhoumi, L., Pirastru, L., Dewez, D., 2013. Silver nanoparticle toxicity effect on growth and cellular viability of the aquatic plant *Lemna gibba.* Environmental Toxicology and Chemistry 32, 902–907.

Paliwal, H.B., Gupta, N., James, A., 2013. Study on accumulation of lead in sunflower (*Helianthus annuus*). http://icontrolpollution.com.

Pallavicini, P., Dacarro, G., Diaz-Fernandez, Y.A., Taglietti, A., 2014. Coordination chemistry of surface-grafted ligands for antibacterial materials. Coordination Chemistry Reviews 275, 37–53.

Pallett, K.E., Young, A.J., 2000. Antioxidants in higher plants.CRC Press: Boca Raton, FL, USA.

Palma, J., Sandalio, L., Corpas, F., 2002. Plant protease, protein degradation and oxidative stress: role of peroxisomers. Plant Physiology and BIochemistry 40, 521–530.

Panda, K.K., Achary, V.M.M., Krishnaveni, R., Padhi, B.K., Sarangi, S.N., Sahu, S.N., Panda, B.B., 2011. In vitro biosynthesis and genotoxicity bioassay of silver nanoparticles using plants. Toxicology in vitro 25, 1097–1105.

Panzarino, O., Hyrsl, P., P, D., Vojte, L., Vernile, P., Bari, G., Terzano, R., Spagnuolo, M., De Lillo, E., 2016. Rank-based biomarker index to assess cadmium ecotoxicity on the earthworm *Eisenia andrei*. Chemosphere 145, 480–486.

Pappas, S., Patakfalvi, R., Dekany, I., 2007. Formation and stabilization of noble metal nanoparticles. Croatica Chemica Acta 80, 493–502.

Pappas, S., Turaga, U., Kumar, N., Ramkumar, S., Kendall, R.J., 2017. Effect of concentration of silver nanoparticles on the uptake of silver from silver nanoparticles in soil. International Journal of Environmental and Agriculture Research 3(5). DOI: 10.25125/agriculture-journal-IJOEAR-MAY-2017-12

Pardha-Saradhi, P., Shabnam, N., Sharmila, P., Ganguli, A.K., Kim, H., 2018. Differential sensitivity of light-harnessing photosynthetic events in wheat and sunflower to exogenously applied ionic and nanoparticulate silver. Chemosphere 194, 340–351.

Patlolla, A.K., Berry, A., May, L., Tchounwou, P.B., 2012. Genotoxicity of silver nanoparticles in *Vicia faba*: a pilot study on the environmental monitoring of nanoparticles. International Journal of Environmental Research and Public Health 9, 1649–1662.

Pehlivan, F.E., 2017. Vitamin C: An antioxidant agent. Open Access book chapter: doi:10.5772/intechopen.69660

Peng, S., McMahon, J.M., Schatz, G.C., Gray, S.K., Sun, Y., 2010. Reversing the size-dependence of surface plasmon resonances. Proceedings of the National Academy of Sciences USA 107(33), 14530–14534.

Perkin, V.P., Colin, S., Pair and Robert, W., 2001. Lycopen content differ among red-fleshed watermelon cultivars. Journal of the Science of Food and Agriculture 18, 983–987.

Peyrot, C., Wilkinson, K.J., Desrosiers, M., Sauve, S., 2014. Effects of silver nanoparticles on soil enzyme activities with and without added organic matter. Environmental Toxicology and Chemistry 33, 115–125.

Pham, C.H., Yi, J., Gu, M.B., 2012. Biomarker gene response in male Medaka (*Oryzias latipes*) chronically exposed to silver nanoparticle. Ecotoxicology and Environmental Safety 78, 239–245.

Phanjom, P., Ahmed, G., 2017. Effect of different physicochemical conditions on the synthesis of silver nanoparticles using fungal cell filtrate of *Aspergillus oryzae* (MTCC No. 1846) and their antibacterial effect. Advances in Natural Sciences: Nanoscience and Nanotechnology 8, 045016.

Pietrini, F., Iori, V., Cheremisina, A., Shevyakova, N.I., Radyukina, N., Kuznetsov, V.V., Zacchini, M., 2015. Evaluation of nickel tolerance in *Amaranthus paniculatus* L by measuring photosynthesis, oxidative status, antioxidative response and metal-binding molecule content. Environmental Science and Pollution Research 22, 482–494.

Pinho, G.L.L., 2005. Antioxidant responses and oxidative stress after microcystin exposure in the hepatopancreas of an estuarine crab species. Ecotoxicological and Enviromental Safety 61, 353–360.

Pîrvulescu, A., Sala, F., Boldea, M., 2015. Variation of chlorophyll content in sunflower under the influence of magnetic nanofluids. AIP Conference Proceedings. AIP, P. 670009.

Pletikapić, G., Žutić, V., Vinković Vrček, I., Svetličić, V., 2012. Atomic force microscopy characterization of silver nanoparticles interactions with marine diatom cells and extracellular polymeric substance. Journal of Molecular Recognition 25, 309–317.

Porra, R.J., 1991. Recent advances and re-assessments in chlorophyll extraction and assay procedures for terrestrial, aquatic, and marine organisms, including recalcitrant algae. In: Chlorophylls, Scheer, H. (Ed.) Pp. 31–57.

Potera, C., 2010. Nanomaterials: transformation of silver nanoparticles in sewage sludge. Environmental Health Perspectives 118, A526.

Purves, R.D., 1992. Optimum numerical integration methods for estimation of area-under-the-curve (AUC) and area-under-the-moment-curve (AUMC). Pharmacokinetics and Biopharmaceutics 20, 211–226.

Putt, E.D., 1997. Early history of sunflower. Sunflower Technology and Production, 1–19.

Qian, H., Peng, X., Han, X., Ren, J., Sun, L., Fu, Z., 2013. Comparison of the toxicity of silver nanoparticles and silver ions on the growth of terrestrial plant model *Arabidopsis thaliana*. Journal of Environmental Sciences 25, 1947–1956.

Rahimizadeh, M., Habibi, D., Madani, H., Sabet, A.M., 2007. The effect of micronutrients on antioxidant enzymes metabolism in sunflower (*Helianthus annuus* L.). Helia 30, 167–174.

Rahmatpour, S., Shirvani, M., Mosaddeghi, M.R., Bazarganipour, M., 2017. Retention of silver nano-particles and silver ions in calcareous soils: Influence of soil properties. Journal of Environmental Management 193, 136–145.

Ramsey, H., Levine, H., Kennedy, J., 2009. Development of a dynamic pharmacokinetic model to estimate bioconcentration of xenobiotics in earthworms. Environmental Modeling & Assessment 14(3), 411–418.

Rani, P., Unni, M., Karthikeyan, J., 2004. Evaluation of antioxidant properties of berries. Indian Journal of Clinocal Biochemistry 19, 103–110.

Rani, P.V., Low kah Mun, G., Hande, M.P., Valiyaveettil, S., 2009. Cytotoxicity and genotoxicity of silver nanoparticles in human cells. AcS Nano 3, 279–290.

Ray, P.C., Yu, H., Fu, P.P., 2009. Toxicity and environmental risks of nanomaterials: challenges and future needs. Journal of Environmental Science and Health Part C 27, 1–35.

Ribeiro, M.J., Maria, V.L., Scott-Fordsmann, J.J., Amorim, M.J.B., 2015. Oxidative stress mechanisms caused by Ag nanoparticles (NM300K) are different from those of $AgNO_3$: Effects in the soil invertebrate *Enchytraeus crypticus.* International Journal of Environmental Research and Public Health 12(8), 9589–9602.

Riccioni, G., D'Orazio, N., Menna, V., De Lorenzo, A., 2003. Fat soluble vitamins and immune system: an overview. European Journal of Inflammation 1, 59–64.

Robinson, B.H., Bañuelos, G., Conesa, H.M., Evangelou, M.W.H., Schulin, R., 2009. The phytomanagement of trace elements in soil. Critical Reviews in Plant Sciences 28, 240–266.

Roh, Y., Sang, J.S., Jongheop, Y.I., Kwangsik, P., 2009. Ecotoxicity of silver nanoparticles on the soil nematode *Caenorhabdditis elegans* using functional ecotoxicogenomics. Environmental Science & Technology 43, 3933–3940.

Rotruck, J.A., Pope, A.L., Ganther, H.E., Hoekstra, W.G., 1973. Selenium biochemical role in citrus mitochondria to arsenate. Nature 206, 319–320.

Roubalova, R., Prochazkova, P., Dvofak, J., Skant, F., Bilies, F., 2015. The role of earthworm defense mechanisms in ecotoxicity studies. ISJ 12, 203–213.

Rout, G., Samantaray, S., Das, P., 2001. Aluminium toxicity in plants: A review. Argonomie 21, 3–21.

Rui, M., Ma, C., Tang, X., Yang, J., Jiang, F., Pan, Y., Xiang, Z., Hao, Y., Rui, Y., Cao, W., 2017. Phytotoxicity of silver nanoparticles to peanut (*Arachis hypogaea* L.): physiological responses and food safety. ACS Sustainable Chemistry & Engineering 5, 6557–6567.

Saba, A., Seyed, A., Johari, J.L., Yong, S.K., 2012. Toxicity of various silver nanoparticles compared to sliver ions in *Daphnia magna*. Journal of Nanobiotechnology 10, 6–11.

Sagee, O., Dror I., Berkowitz, B., 2012. Transport of silver nanoparticles (AgNPs) in soil. Chemosphere 88, 670–675.

Saint-Denis, M., Labrot, F., Narbonne, J., Ribera, D., 1998. Glutathione, glutathione-related enzymes, and catalase activities in the earthworm *Eisenia fetida andrei*. Archives of Environmental Contamination and Toxicology 35, 602–614.

Sairam, R., Singh, D., Srivastava, G., 2003. Changes in activities of antioxidant enzymes in sunflower leaves of different ages. Biologia Plantarum 47, 61.

Salama, H.M.H., 2012. Effects of silver nanoparticles in some crop plants, common bean (*Phaseolus vulgaris* L.) and corn (*Zea mays* L.). International Research Journal of Biotechnology 3, 190–197.

Samet, J., Wages, P.A., 2018. Oxidative stress from environmental exposure. Current Opinion in Toxicology 7, 60–66.

San, C.Y., Don, M.M., 2013. Biosynthesis of silver nanoparticles from *Schizophyllum commune* and in-vitro antibacterial and antifungal activity studies. Journal of Physical Science 24(2), 83–96.

Sanchez-Hernandez, J. C., 2006. Earthworm biomarkers in ecological risk assessment. Reviews of Environmental Contamination and Toxicology, 188, 85–126.

Sarabia, R., Varo, I., Amet, F., Pastor, A., Del-ramo, J., Diaz-Mayan, I., Torrebalance, A., 2006. Comparative toxicokinetics of cadmium in *Artemia*. Environmental Contamination and Toxicology 50, 111–120.

Scherer, M.D., Sposito, J.C.V., Falco, W.F., Grisolia, A.B., Andrade, L.H.C., Lima, S.M., Machado, G., Nascimento, V.A., Gonçalves, D.A., Wender, H., Oliveira, S.L., Caires, A.R.L., 2019. Cytotoxic and genotoxic effects of silver nanoparticles on meristematic cells of *Allium cepa* roots: A close analysis of particle size dependence. Science of the Total Environment 660, 459–467.

Schlich, K., Klawonn, T., Terytze, K., Hund-Rinke, K., 2013a. Hazard assessment of a silver nanoparticle in soil applied via sewage sludge. Environmental Sciences Europe 25, 17.

Schlich, K., Klawood, T., Terytze, K., Hand-Rinke, 2013b. Effects of silver nanoparticles and silver nitrate on earthworm reproduction test. Environmental Toxicology and Chemistry 32, 181–188.

Schroder, P., Lyubenova, L., Huber, C., 2009. Do heavy metals and metalloids influence the detoxification of organic xenobiotics in plants? Environmental Science and Pollution Research 16, 795.

Schwirn, K., Tietjen, L., Beer, I., 2014. Why are nanomaterials different and how can they be appropriately regulated under REACH? Environmental Sciences Europe 26, 4.

Sekine, R., Brunetti, G., Donner, E., Khaksar, M., Vasilev, K., Jamting, A.K., Scheckal, K., Kappen, P., Zhang, H., Lombi, E., 2015. Speciation and lability of Ag-, AgCl-, Ag_2S nanoparticles in soil determined by X-ray absorption spectroscopy and diffusive gradients in thin films. Environmental Science & Technology 49(2), 897–905.

Sepúlvida, V.V., 2014. Fate of silver nanoparticles in treatment wetlands. Master of Science in Environmental Sanitation Dissertation, Faculty of Bioscience Engineering. Gent University.

Settimio, L., McLaughlin, M.J., Kirby, J.K., Langdon, K.A., Lombi, E., Donner, E., Scheckel, K.G., 2014. Fate and lability of silver in soils: Effect of ageing. Environmental Pollution 191, 151–157.

Sewalem, N., Elfeky, S., El-Shintinawy, F., 2014. Phytoremediation of lead and cadmium contaminated soils using sunflower plants. Journal of Stress Physiology & Biochemistry 10, 123–134.

Sharma, P., Bhatt, D., Zaidi, M.G.H., Saradhi, P.P., Khanna, P.K., Arora, S., 2012a. Silver nanoparticle-mediated enhancement in growth and antioxidant status of *Brassica juncea*. Applied Biochemistry and Biotechnology 167, 2225–2233.

Sharma, P., Jha, A.B., Dubey, R.S., Pessarakli, M., 2012b. Reactive oxygen species, oxidative damage, and antioxidative defense mechanism in plants under stressful conditions. Journal of Botany 2012, Article ID 217037.

Shimada, Y., Ko, S., 2008. Ascorbic acid and ascorbate oxidase in vegetables. Chugokugakuen Journal 7, 7–10.

Shin, Y.J., Kwak, J.I., An, Y.J., 2012. Evidence for the inhibitory effects of silver nanoparticles on the activities of soil exoenzymes. Chemosphere 88, 524–529.

Shoults-Wilson, W.A., Reinsch, B.C., Tsyusko, O.V., Bertsch, P.M., Lowry, G.V., Unrine, J.M., 2011. Effect of silver nanoparticle surface coating on bioaccumulation and reproductive toxicity in earthworms (*Eisenia fetida*). Nanotoxicology 5, 432–444.

Siddiqui, M.H., Al-Whaiby, M.H., Firoz, M., Al-Khaishany, M.Y. 2015. Role of nanoparticles in plants. In: Nanotechnology and Plant Sciences: Nanoparticles and Their Impact on Plants, M.H. Siddiqui, M.H. Al-Whaibi, F. Mohammad (Eds). Springer. Pp. 19–35.

Sies, H. 1997. Oxidative stress: oxidants and antioxidants. Experimental Physiology*, 82*, 291–295.

Sileikaite, A., Prosycevas, I., Puiso, J., Juraitis, A., Guobiene, A., 2006. Analysis of silver nanoparticles produced by chemical reduction of silver salt solution. Materials Science 12, 287–291.

Silva, T., Pokhrel, L.R., Dubey, B., Tolaymat, T.M., Maier, K.J., Liu, X., 2014. Particle size, surface charge and concentration dependent ecotoxicity of three organo-coated silver nanoparticles: Comparison between general linear model-predicted and observed toxicity. Science of the Total Environment 468–469, 968–976.

Simmler, M., Ciadamidaro, L., Schulin, R., Madejon, P., Reiser, R., Clucas, L., Weber, P., Robinson, B., 2013. Lignite reduces the solubility and plant uptake of cadmium in pasturelands. Environmental Science & Technology 47, 4497–4504.

Singh, S., Eapen, S., D'souza, S., 2006. Cadmium accumulation and its influence on lipid peroxidation and antioxidative system in an aquatic plant, *Bacopa monnieri* L. Chemosphere 62, 233–246.

Singh, S., Singh, D., 2010. Biodiesel production through the use of different sources and characterization of oils and their esters as the substitute of diesel: a review. Renewable and Sustainable Energy Reviews 14, 200–216.

Sinha, S., Gupta, M., Chandra, P., 1996. Bioaccumulation and biochemical effects of mercury in the plant *Bacopa monnieri* L. Environmental Toxicology 11(2), 105–112.

Skip, B, Bednarska, A.J., Laskowski, R., 2014. Toxicokinetics of metals in terrestrial invertebrates: making things straight with the one-compartment principle. PLoS ONE 9(9): e108740.

Smith, I., Carson, B., 1977. Trace element in the environment. Ann Arbor Science Publishers.

Social science statistics, ND. T-Test Calculator for 2 Independent Means. www.socscistatistics.com/tests/studentttest/Default.aspx.

Solomon, S.D., Mozghan, B., Aravindan, V.J., 2007. Synthesis and Study of Silver Nanoparticles. Journal of Chemical Education, 84, 322–325.

Somasundaram, S., Abraham, J.S., Maurya, S., Makhija, S., Gupta, R., Toteja, R., 2018. Cellular and molecular basis of heavy metal-induced stress in ciliates. Current Science 114, 1858–1865.

Stensberg, M. C., Wei, Q., McLamore, E. S., Porterfield, D. M., Wei, A., Sepúlveda, M. S., 2011. Toxicological studies on silver nanoparticles: challenges and opportunities in assessment, monitoring and imaging. Nanomedicine 6(5), 879–898.

Stroinski, A., Kozlowska, M., 1997. Cadmium induced oxidative stress in potato tuber. Acta Societatis Botanicorum Poloniae 66, 189–195.

Su, D., 2017. Advanced electron microscopy characterization of nanomaterials for catalysis. Green Energy & Environment 2, 70–83.

Su, S.S., Chang, I., 2018. Review of Production Routes of Nanomaterials. Commercialization of Nanotechnologies–A Case Study Approach. Springer, Pp. 15–29.

Sujoy, B., Aparna, A., 2013. Potential clinical significance of urease enzyme. European Scientific Journal, ESJ 9.

Sumanta, N., Haque, C.I., Nishika, J., Suprakash, R., 2014. Spectrophotometric analysis of chlorophylls and carotenoids from commonly grown fern species by using various extracting solvents. Research Journal of Chemical Sciences 4, 63–69.

Suriati, G., Mariatti, M., Azizan, A., 2014. Synthesis of silver nanoparticles by chemical reduction method: Effect of reducing agent and surfactant concentration. International Journal of Automotive and Mechanical Engineering 10, 1920–1927.

Świątek, Z.M., Van Gestel, M, C.A., Bednarska, A.J., 2017. Toxicokinetics of zinc-oxide nanoparticles and zinc ions in the earthworm *Eisenia andrei*. Ecotoxicology and Environmental Safety 143, 151–158.

Terevento, A.R.A., Castroman, G.M.C., Saadoum, A., 2010. Oxidative status in vitro iron-induced lipid oxidation and speroxide dismutase, catalase and glutathions peroxidase activities in rhea meat. Meat Science 84(4), 706–710.

Tewari, R., Kumar, P., Sharma, P., Bishi, S., 2002. Modulation of oxidative stress responsive enzymes by excess cobalt. Plant Science 162, 381–388.

Théoret, T., Wilkinson, K.J., 2017. Evaluation of enhanced darkfield microscopy and hyperspectral analysis to analyse the fate of silver nanoparticles in wastewaters. Analytical Methods 9, 3920–3928.

Thuesombat, P., Hannongbua, S., Akasit, S., Chadchawan, S., 2014. Effect of silver nanoparticles on rice (*Oryza sativa* L. cv. KDML 105) seed germination and seedling growth. Ecotoxicology and Environmental Safety 104, 302–309.

Tjalling, 1998. Mechanistic approach for estimating bioconcentration of organic chemicals in earthworms (Oligochaeta). Environmental Toxicology and Chemistry 17, 2080–2090.

Torres, M.A.S., Testa, C.P., Gáspari, C., Masutti, M.B., Panitz, C.M.N., Curi-Pedrosa, R., de Almeida, E.A., Di Mascio, P., Wilhelm Filho, D., 2002. Oxidative stress in the mussel *Mytella guyanensis* from polluted mangroves on Santa Catarina Island, Brazil. Marine Pollution Bulletin 44, 923–932.

Tourinho, P.S., Van Gestel, C.A.M., Jurkschat, K., Soares, A., Loureiro, S., 2015. Effects of soil and dietary exposures to Ag nanoparticles and $AgNO_3$ in the terrestrial isopod *Porcellionides pruinosus*. Environmental Pollution 205, 170–177.

Tourinho, P.S., Van Gestel, C.A.M., Morgan, A.J., Kille, P., Svendsen, C., Jurkschat, K., Mosselmans, J.F.W., Soares, A., Loureiro, S., 2016. Toxicokinetics of Ag in the terrestrial isopod *Porcellionides pruinosus* exposed to Ag NPs and AgNO3 via soil and food. Ecotoxicology 25, 267–278.

Traber, M.G., Stevens, J.F., 2011. Vitamins C and E: beneficial effects from a mechanistic perspective. Free Radical Biology and Medicine 51, 1000–1013.

Tran, Q.H., Nguyen, V.Q., Tuan Le, A., 2013. Silver nanoparticles: Synthesis, properties, toxicology, applications and perspectives. Advances in Natural Sciences: Nanoscience and Nanotechnology 4, Article ID: 033001.

Tripathi, D.K., Singh, S., Singh, S., Srivastava, P.K., Singh, V.P., Singh, S., Prasad, S.M., Singh, P.K., Dubey, N.K., Pandey, A.C., 2017a. Nitric oxide alleviates silver nanoparticles (AgNPs)-induced phytotoxicity in *Pisum sativum* seedlings. Plant Physiology and Biochemistry 110, 167–177.

Tripathi, D.K., Tripathi, A., Singh, S., Singh, Y., Vishwakarma, K., Yadav, G., Sharma, S., Singh, V.K., Mishra, R.K., Upadhyay, R., 2017b. Uptake, accumulation and toxicity of silver nanoparticle in autotrophic plants, and heterotrophic microbes: a concentric review. Frontiers in Microbiology 8, 7.

Tsikas, D., 2017. Assessment of lipid peroxidation by measuring malondialdehyde (MDA) and relatives in biological samples: Analytical and biological challenges. Analytical Biochemistry 524, 13–30.

Tsuchida, S., 2002. Glutathione transferase. Encyclopedia of Cancer (Second Edition).

Udapudi, B., Naik, P., Savadatti, S.T., Sharma, R., Balgi, S., 2012. Synthesis and characterization of silver nanoparticles. International Journal of Pharmacy and Biological Science 2, 10–14.

Urbanek, H., Kuzniak-Gebarowska, E., Herka, H., 1991. Elicitation of defense responses in bean leaves by *Botrytis cinerea* polygalacturonase. Acta Physiologia Plantarum 43, 43–50.

USEPA, 2018. Non-Carcinogen Tolerable Daily Intake (TDI) values from USE EPA. United States Environmental Protection Agency http://www.popstoolkit.com/tools/HHRA/TDI_USEPA.aspx. (accessed 22 Jan 2019).

Van Aerle, R., Lange, A., Moorhouse, A., Paszkiewicz, K., Ball, K., Johnston, B.D., de- Bastos, E., Booth, T., Tyler, C.R., Santos, E.M., 2013. Molecular mechanism of toxicity of silver nanoparticles in zebrafish embryos. Environmental Science & Technology 47(14), 8005–8014.

van der Ploeg, M.J., Handy, R.D., Waalewijin-Kool, P.L., van den Berg, J.H., Herrera Rivera, Z.E., Bovenschen, J., Molleman, B., Baveco, J.M., Tromp, P., Peters, R.J., Koopmans, G.F., Rietjens, I.M., van den Brink, N.W., 2014. Effects of silver nanoparticles (NM-300K) on *Lumbricus rubellus* earthworms and particle characterization in relevant tests matrices including soil. Environmental Toxicology and Chemistry 33(4), 743–752.

Van Hattum, B., De Vooge, P., Van Den Bosch, L., 1989. Bioaccumulation of cadmium by the fresh water isopod *Asellus aquaticus* (L.) from aqueous and diettary sources. Environmental Pollution 62, 129–152.

Van Koetsem, F., Woldetsadik, G.S., Folens, K., Rinklebe, J., Du Laing, G., 2018. Partitioning of Ag and CeO_2 nanoparticles versus Ag and Ce ions in soil suspensions and effect of natural organic matter on CeO_2 nanoparticles stability. Chemosphere 200, 471–480.

van Rossum, M., Alberda, M., van der Plas, L.H.W., 1997. Role of oxidative damage in tulip bulb scale micropropagation. Plant Science 130, 207–216.

VandeVoort, A.R., Arai, Y., 2012. Environmental chemistry of silver in soil: current and historic perspective. Advances in Agronomy 114, 59–90.

Vanhaelen, N., Haubruge, E., Lognay, G., Francis, F., 2001. Hoverfly glutathione S-transferase and effect of Brassicaceae secondary metabolite. Pesticide Biochemistry and Physiology 71, 170–177.

Vannini, C., Domingo, G., Onelli, E., Prinsi, B., Marsoni, M., Espen, L., Bracale, M., 2013. Morphological and proteomic responses of *Eruca sativa* exposed to silver nanoparticles or silver nitrate. PLoS One 8, e68752.

Venkatesan, A.K., Done, H.Y., Halden, R.U., 2015. United States National Sewage Sludge Repository at Arizona State University—a new resource and research tool for environmental scientists, engineers, and epidemiologists. Environmental Science and Pollution Research 22, 1577–1586.

Vines, H.M., Oberbacher, M.F., 1965. Response of oxidation and phosphorylation in citrus mitochondria to arsenate. Nature 206, 319–320.

Vineetha, 2014. 8 amazing benefits & uses of sunflower seeds. http://www.healthbeckon.com/benefits-of-sunflower-seeds

Vishwakarma, K., Upadhyay, N., Singh, J., Liu, S., Singh, V.P., Prasad, S.M., Chauhan, D.K., Tripathi, D.K., Sharma, S., 2017. Differential phytotoxic impact of plant mediated silver nanoparticles (AgNPs) and silver nitrate (AgNO3) on *Brassica* sp. Frontiers in Plant Science 8, 1501.

Vlahogianni, T., Dassenakis, M., Scoullos, M.J., Valavanidis, A., 2007. Integrated use of biomarkers (superoxide dismutase, catalase and lipid peroxidation) in mussels *Mytilus galloprovincialis* for assessing heavy metals' pollution in coastal areas from the Saronikos Gulf of Greece. Marine Pollution Bulletin 54, 1361–1371.

Waalewijin-Kool, P., Klein, K., Fornies, R.M., Van Gestel, C., 2014. Bioaccumulation and toxicity of silver nanoparticles and silver nitrate to the soil arthropod *Folsomia candida*. Ecotoxicology 23, 1–9.

Wang, B., Che, B., Zhang, L.W., Dong, G., Luo, Q., Xin, L., 2017. Comparative genotoxicity of silver nanoparticles in human liver HepG2 and lung epithelial A549 cells. Journal of Applied Toxicology 37(4), 495–501.

Wang, J., Koo, Y., Alexander, A., Yang, Y., Westerhof, S., Zhang, Q., Schnoor, J.L., Colvin, V.L., Braam, J., Alvarez, P.J., 2013. Phytostimulation of poplars and *Arabidopsis* exposed to silver nanoparticles and Ag^+ at sublethal concentrations. Environmental Science & Technology 47, 5442–5449.

Wang, P., Lombi, E., Sun, S., Scheckel, K.G., Malysheva, A., McKenna, B.A., Menzies, N.W., Zhao, F.-J., Kopittke, P.M., 2017b. Characterizing the uptake, accumulation and toxicity of silver sulfide nanoparticles in plants. Environmental Science: Nano 4, 448–460.

Wang, P., Menzies, N.W., Lombi, E., Sekine, R., Blamey, F.P.C., Hernandez-Soriano, M.C., Cheng, M., Kappen, P., Peijnenburg, W.J., Tang, C., 2015. Silver sulfide nanoparticles (Ag2S-NPs) are taken up by plants and are phytotoxic. Nanotoxicology 9, 1041–1049.

Wang, R., Du, H., Wang, Y.J., Wang, D.J., Sun, Q., Zhou, D.M., 2018. Retention of silver nanoparticles and silver ion to natural soils: effects of soil physicochemical properties. Journal of Soils and Sediments 18, 2491–2499.

Wang, S.H., Yang, Z.M., Yang, H., Lu, B., Li, S.O., Lu, Y.P., 2004. Copper-induced stress and antioxidative responses in roots of *Brassica juncea*. Botanical Bulletin of Academia Sinica 45, 203–212.

Wang, Y., Cang, T., Zanao, X., Yu, R., Chen, L., Wu, C.C., Wang, Q., 2012. Comparative acute toxicity of twenty-four insecticides to earthworm, *Eisenia fetida*. Ecotoxicology and Enviromental Safety 79, 122–128.

Wang, Z.Y., Li, J., Zhao, J., Xing, B., 2011. Toxicity and internalization of CuO nanoparticles to prokaryotic alga *Microcystis aeruginnosa* as affected by dissolved organic matter. Environmental Science & Technology 45, 6032–6040.

Wasfi, I.A., Eighazali, M., Hadi, A.A.A., Zorob, O., Boni, N.S., Alkatheeri, N.A., Barezaiq, I.M., 1998. Pharmacokinetics of tolfenamic acid and its detection time in urine after intravenous administration of the drug in camels (*Camelus dromedarius*). American Journal of Veterinary Research 59, 1451–1458.

Wen, H.F., Li, Y.W., Xiang, L., Zhao, H.M., Chen, L., Cai, Q.Y., Li, H., Mo, C.H., Zhou, D.M., Wong, M.H., 2017. Toxicological effects of microcystin-LR on earthworm (*Eisenia fetida*) in soil. Biology and Fertility of Soils 53, 849–860.

Wible, D.J., Bratten, S.B., 2018. Reciprocity in ROS and autophagic signaling. Current Opinion in Toxicology 7, 28–36.

Wijnhoven, S.W.P., Peijnenburg, W.J.G.M., Herverts, C.A., Van De Meent, P., Gosens, I., Dekkers, D., De Jong, W.H., van Zijverden, M., Sips, A.J.A.M., Geertsma, R., 2009. Nano-silver -a review of available data and knowledge gaps in human and environmental risk assessment. Nanotoxicology 3, 109–138.

William, A., Shoults-Wilson, W.A., Brian, c., Reinsch, O.V., Paul, M.B., Gregory, V.L., Jason, M.U., 2011. Effect of silver nanoparticle surface coating on bioaccumulation and reproductive toxicity in earthworms (*Eisenia fetida*). Nanotoxicology 5, 412–444.

Wilson, A.S., Reinsch, B.C., Tsyusko, O.V., Bertsch, P.M., Lowry, G., unrine, J.M., 2010. Role of particle size and soil type in toxicity of silver nanoparticles to earthworms. Soil Science Society of America Journal 75(2), 365–377.

Wilson, N., 2018. Nanoparticles: environmental problems or problem solvers? BioScience 68, 241–246.

Xiong, J., Xue, Q., Wu, X., 2013. Synthesis of stable dispersions of water-soluble and SERS-active silver nanoparticles using PAM. Nano *8*(5), 1350046.

Xiong, W., Ding, X., Zhang, Y., Sun, Y., 2014. Ecotoxicological effects of a veterinary food additive, copper sulphate, on antioxidant enzymes and mRNA expression in earthworms. Environmental Toxicology and Pharmacology 37(1), 134–140.

Yaseen, A.A.M., Khaqlidah, M.S., Basim, S., Wasan, M.H., 2016. Effect of foliar spray of nanosilver silver and organic fertilizer (Agastar) and salicyclic acid on some morphological characteristics and carbohydrate content in (*Helianthus annuus* L.). Journal of Agriculture and Ecology Research International 9(3), 1–7.

Yasur, J., Rani, P.U., 2013. Environmental effects of nanosilver impact on castor seed germination, seedling growth, and plant physiology. Environmental Science and Pollution Research 20, 8636–8648.

Yin, L., Cheng, Y., Espinase, B., Colman, B.P., Auffan, M., Wiesner, M., Rose, j., Liu, L., Bernhardi, E.S., 2011. More than the ions: the effect of silver nanoparticles on *Lolium multiflorum*. Environmental Science & Technology 45, 2360–2367.

Yin, L., Colman, B.P., McGill, B.M., Wright, J.P., Bernhardt, E.S., 2012. Effects of silver nanoparticle exposure on germination and early growth of eleven wetland plants. PLoS One 7, e47674.

Yokel, R.A., MacPhail, R.C., 2011. Engineered nanomaterials: exposures, hazards, and risk prevention. Journal of Occupational Medicine and Toxicology 6, 7.

Zar, J.H., 1999. Biostatistical analysis. Pearson Education: India.

Zengin, F.K., 2013. Physiological behaviour of bean (*Phaseolus vulgaris* L.) seedlings under metal stress. Biological Research 46, 79–85.

Zengin, F.K., Munzuroglu, O., 2005. Effects of some heavy metal on content of chlorophyll, proline and some antioxidant chemicals in bean (*Phaseolus vulgaris* L.) seedlings. Acta Biologica Cracoviensia 47, 157–164.

Zhan, Y., 2012. *Effect of silver nanoparticles on bacteria and earthworms*. MSc thesis, Lincoln University, Lincoln, New Zealand.

Zhang, L., 2012. Silver transport and adsorption-desorption in soils: influence of zinc. The School of Plant, Environmental, and Soil Science. Louisiana State University and Agricultural and Mechanical College, Louisiana.

Zhang, X.F., Liu, Z.G., Shen, V., Gurunathan, S., 2016. Silver nanoparticles: Synthesis, characterization, properties, applications and therapeutic approach. International Journal of Molecular Sciences 19, 1534.

Zuverza-Mena, N., Armendariz, R., Peralta-Videa, J.R., Gardea-Torresdey, J.L., 2016. Effects of silver nanoparticles on radish sprouts: root growth reduction and modifications in the nutritional value. Frontiers in Plant Science 7, 90.